Downloaded from orbit.dtu.dk on: Apr 19, 2024

DTU Library

Milling and Physical Properties of Wood Pellets for Suspension-Fired Power Plants

Masche, Marvin

Publication date:
2019

Document Version
Publisher's PDF, also known as Version of record

Link back to DTU Orbit

Citation (APA):
Masche, M. (2019). *Milling and Physical Properties of Wood Pellets for Suspension-Fired Power Plants*. Technical University of Denmark.

General rights
Copyright and moral rights for the publications made accessible in the public portal are retained by the authors and/or other copyright owners and it is a condition of accessing publications that users recognise and abide by the legal requirements associated with these rights.

- Users may download and print one copy of any publication from the public portal for the purpose of private study or research.
- You may not further distribute the material or use it for any profit-making activity or commercial gain
- You may freely distribute the URL identifying the publication in the public portal

If you believe that this document breaches copyright please contact us providing details, and we will remove access to the work immediately and investigate your claim.

DTU Chemical Engineering
Department of Chemical and Biochemical Engineering

Milling and Physical Properties of Wood Pellets for Suspension-Fired Power Plants

Marvin Masche

Milling and Physical Properties of Wood Pellets for Suspension-Fired Power Plants

Marvin Masche

Ph.D. Thesis

January 2019

Department of Chemical and Biochemical Engineering

Technical University of Denmark

DTU Chemical Engineering
Department of Chemical and Biochemical Engineering

Copyright 2019 [Masche]

Preface and acknowledgements

This dissertation is submitted to fulfill the partial requirements of obtaining the degree of Doctor of Philosophy (Ph.D.) at the Department of Chemical and Biochemical Engineering (CHEC) at the Technical University of Denmark (DTU). The Ph.D. study is part of the Energiteknologiske Udviklings- og Demonstrationsprogram (EUDP) project 12325 "AUWP – Advanced Utilization of Wood Pellets" (2015-2019). The project is funded by EUDP in collaboration with DTU, Ørsted, and HOFOR to whom I would like to express my gratitude for their financial support.

The Ph.D. study was conducted in the Biomass Gasification Group (BGG) as part of CHEC at DTU Campus Risø. I hereby want to acknowledge the BGG for providing me the opportunity to conduct my Ph.D. research in an inspiring and stimulating work environment with a fjord view. Experimental work was performed in the BGG laboratories (DTU/Risø), at the Department of Energy Conversion and Storage (DTU/Risø), at CHEC (DTU/Lygnby), at Dansk Teknologisk Institut (DTI) in Sønder Stenderup, at HOFOR's biomass-converted suspension-fired power plant Amagerværket unit 1 (AMV1) in Copenhagen, and at the Thermal Energy Department at SINTEF Energy Research in Trondheim (Norway).

A great number of people have in many ways contributed to this work, and their support is gratefully acknowledged. First of all, I would like to express my sincere gratitude to my supervisors Jesper Ahrenfeldt (Senior Scientist), Maria Puig Arnavat (Researcher), Peter Arendt Jensen (Associate Professor), Sønnik Clausen (Senior Scientist), Ulrik Birk Henriksen (Senior Researcher) from CHEC at DTU, and Jens Kai Holm (Senior Specialist) from the Department of Bioenergy & Thermal Power at Ørsted. Thank you for your valuable comments, thoughtful ideas, and constructive suggestions for my research project. Special thanks to Maria, who provided patient advice and guidance throughout my whole research work, especially in view of writing scientific articles. Sincere thanks to Jens, who provided us with insights into the industrial utilization of wood pellets in power plants and with samples from the wood pellet producer Enviva. Thanks also to Peter and Jens for attending (almost) every supervisor meeting in the past three years despite crossing North Zealand.

Next, I want to thank my roomie Giulia for the many hours we have shared the same office. Thank you to my scientific colleagues in the group Tobias, Rasmus, Zsuzsa, and Alexander for creating a friendly and enjoyable working atmosphere. Special thanks to Rasmus, who introduced me to the Danish food and ice hockey culture in Esbjerg. I am also grateful to the CHEC technical staff, especially Kristian, Erik, and Peter at DTU/Risø for their unlimited support and providing creative solutions to technical problems when needed, and to Nikolaj at DTU/Lyngby for his valuable assistance in the single particle combustion reactor. Sincere thanks to Peter, who is the heart of the BGG, with his social event-planning and sweets-bringing skills.

Special thanks to my collaborators Johan Wadenbäck (HOFOR) for a very valuable and successful cooperation and your help when correcting my article, Lasse Eckerdal Jessen (DTI) for his assistance and helpful knowledge regarding biomass milling and pelletization, and Adam Kofoed Månsson (Bregentved) for assisting in harvesting and chipping of beech and pine trees. Moreover, I want to acknowledge Per Lang Sørensen from DTI, Birte Asmussen and Bjarne Rasmussen from SkanLab ApS, Pernille Hedemark Nielsen and Kurt Engelbrecht from DTU Energy, Susanne Finderup from HOFOR, Kai Düffels from Retsch Technology (Germany), Liang Wang from Sintef (Norway), Bachelor student Benjamin Ekstrøm Clausen, and Associate Professor Zhimin Lu from South China University of Technology (China). Their guidance and help were essential for the completion of my work.

I sincerely thank my girlfriend for her support and patience, for bringing joy and happiness in my life daily, and for doing the best risalamande in the world. Thank you to my beloved family for all the unwavering support and encouragement throughout the whole process. I also want to thank my friends in Copenhagen for bringing a lot of fun to my new life in Denmark. Last but not least, I would like to thank all those I have not mentioned, but who deserve a thank you.

Roskilde, 31st of January 2019

Marvin Masche

Abstract

The utilization of sustainably produced wood pellets in the existing coal suspension-fired power plants can offer a cost-efficient option of mitigating greenhouse gas emissions. However, the fibrous and non-brittle structure of wood poses challenges with regard to the size reduction process of wood pellets in the existing coal mills. There is a lack of understanding of the pellet grinding behavior and morphology (i.e., size and shape) of milled pellet particles, and how the particle morphology can be related to the wood pellet processing history. New knowledge in this area has the potential to promote efficient and fast conversion of coal-fired power plants to the firing of milled pellets.

For this purpose, the study investigated the pellet grinding behavior in lab- and industrial-scale mills. The grinding behavior was determined by measuring the specific grinding energy and analyzing the morphology of milled and internal pellet particles. New methods were introduced to characterize the grinding behavior of wood pellets by laboratory testing, and to investigate if it is possible to predict grinding results in power plant coal mills. The study used two industrial pellet qualities, and two pellet types made from Austrian pine (softwood) and European beech (hardwood) stem wood. Pellets were characterized according to standardized methods.

The study has found that the industrial pellet production process has a larger impact on modifying the pre-densified wood particle shape than the pellet grinding process. The pellet grinding behavior can be related to the mill type and pellet processing history (including feedstock type and internal pellet particle size distribution). It was shown that grinding of raw and pelletized beech produces finer, rounder and less elongated particles, and requires a lower grinding energy than pine. The proposed laboratory roller mill-classifier system has the potential to assess the grinding properties of different pellet qualities. The comparison with grinding results from industrial mills showed that similar particle size reduction ratios can be achieved.

This work presents relevant experimental data that provide an understanding of the morphology changes occurring during the industrial pelletization process. It also has great value for power plant operators to maximize the pellet grinding capacity in the existing coal mills.

Danish abstract/ dansk resumé

Titel: Formaling og fysiske egenskaber af træpiller for støvfyrede kraftværker

Træpiller produceret af bæredygtige skovbrug kan være en økonomisk attraktiv løsning til at reducere drivhuseffekten ved erstatning af kul med biomasse i støvfyrede kraftværker. Det er dog ikke uden problemer at neddele træets fiberagtige og seje struktur til fint støv ved formaling af træpillerne i eksisterende kulmøller. Der mangler viden og forståelse af træpillernes formalingsegenskaber og morfologi, f.eks. partikelstørrelse og form, af formalede træpiller partikler, og hvorledes partikel morfologien kan relateres til træpillernes fremstillingshistorik. Ny indsigt i dette område har potentiale til en mere effektiv brug af møllerne.

I dette studie ses på træpillernes formaling i møller på dels laboratorieskala, dels i fuldskala på et kraftværk. Formalingsegenskaberne blev bestemt ved måling af den specifikke energi brugt til formaling af træpillerne og ved analyse af partikelstørrelsesfordeling, partikelform, mv. af det formalede træstøv og træpillernes oprindelige partikler. I dette arbejde introduceres nye metoder for karakterisering af pillernes formalingsegenskaber målt ved formaling af træpiller i mindre laboratoriemøller og resultater herfra sammenholdes med formalingsegenskaber af pillerne fundet på store kulmøller. I studiet anvendes to forskellige industrielle træpiller kvaliteter, og to type piller fremstillet af dels østrigsk fyr (nåletræ) og dels europæisk bøge (løvtræ) stammer. Pillerne blev karakteriseret ud fra standard metoder.

Studiet viser at produktionsprocessen af træpillerne har en større indvirkning på ændringer af træpartiklernes form end formalingen af piller. Pillernes formalingsopførsel afhænger af mølletype og pillernes fremstillingshistorik. Det vises, at formaling af rå og pelleteret bøg resulterer i finere, mere runde og mindre aflange træpartikler, og at der skal anvendes mindre energi til formaling end for nåletræ. Den foreslåede laboratoriemølle med luftklassifikationssystem viser bedre formalingsegenskaber for piller med finere interne partikler, f.eks. et lavere energiforbrug til formaling, end for piller bestående af mere grove partikler.

Dette arbejder indeholder relevante eksperimentelle data mht forståelse af de morfologiske ændringer som sker under den industrielle pilletering. Dette kan have stor værdi for operatører af træstøvsfyrede kraftværker mht. at maksimere møllekapaciteten.

Publication list

This Ph.D. thesis is based upon the work contained in the following papers, referred to by Roman numerals in the text.

I. From wood chips to pellets to milled pellets: the mechanical processing pathway of Austrian pine and European beech

Marvin Masche*, Maria Puig-Arnavat, Jens K. Holm, Sønnik Clausen, Peter A. Jensen, Jesper Ahrenfeldt, Ulrik B. Henriksen

Published[1] in: Powder Technology, 2019, 350: 134-145 (see Appendix II)

II. Wood pellet milling tests in a suspension-fired power plant

Marvin Masche*, Maria Puig-Arnavat, Johan Wadenbäck, Sønnik Clausen, Peter A. Jensen, Jesper Ahrenfeldt, Ulrik B. Henriksen

Published[1] in: Fuel Processing Technology, 2018, 173: 89-102 (see Appendix III)

III. Grinding performance of wood pellets in laboratory-scale mills

Marvin Masche*, Maria Puig-Arnavat, Peter A. Jensen, Jens K. Holm, Sønnik Clausen, Jesper Ahrenfeldt, Ulrik B. Henriksen

In review: Biomass & Bioenergy (see Appendix IV)

IV. An investigation of the grindability of wood pellets in a lab-scale roller mill with classifier

Marvin Masche*, Maria Puig-Arnavat, Peter A. Jensen, Jens K. Holm, Sønnik Clausen, Jesper Ahrenfeldt, Ulrik B. Henriksen

In review: Biomass & Bioenergy (see Appendix V)

V. Combustion behavior of single particles of raw and pelletized wood

Marvin Masche*, Benjamin E. Clausen, Zhimin Lu, Maria Puig-Arnavat, Peter A. Jensen, Jens K. Holm, Sønnik Clausen, Jesper Ahrenfeldt, Ulrik B. Henriksen

Individual chapter of the Ph.D. thesis (see Appendix VI)

* Corresponding author

[1]Journal papers are reprinted with kind permission of the publisher.

Conferences and workshop contributions

This study has also contributed to the following conferences and workshops:

Masche M[*], Puig-Arnavat M, Wadenbäck J, Clausen S, Jensen PA, Ahrenfeldt J, Henriksen UB. *Full-Scale Milling Tests of Wood Pellets for Combustion in a Suspension-Fired Power Plant Boiler*. Oral presentation at the Nordic Flame Days, Stockholm, Sweden, 10-11 October, 2017

Masche M[*], Puig-Arnavat M, Wadenbäck J, Clausen S, Jensen PA, Ahrenfeldt J, Henriksen UB. *Wood Pellet Milling Performance in a Suspension-Fired Power Plant"*. Poster presentation at the 26th European Biomass Conference & Exhibition (EUBCE), Copenhagen, Denmark, 14-17 May, 2018

Masche M[*], Puig-Arnavat M, Holm JK, Jensen PA, Ahrenfeldt J, Clausen S, Henriksen UB. *Combustion Behavior of Single Particles of Raw Wood and Pelletized Wood*. Poster presentation at the 8th Workshop on Cofiring Biomass with Coal, Copenhagen, Denmark, 11-13 September, 2018

Masche M[*], Puig-Arnavat M, Wadenbäck J, Clausen S, Jensen PA, Ahrenfeldt J, Henriksen UB. *From Wood Chips to Pellets to Milled Pellets: the Mechanical Processing Pathway of Wood*. Poster presentation at the 2nd International Conference on Bioresource Technology for Bioenergy, Bioproducts & Environmental Sustainability, Sitges, Spain, 16-19 September, 2018

[*] Corresponding author

Table of contents

Preface and acknowledgements i

Abstract iii

Danish abstract/ dansk resumé iv

Publication list v

Conferences and workshop contributions vi

Table of contents vii

List of tables x

List of figures xi

Nomenclature xii

Chapter I Introduction to the thesis 1

1.1 Research objectives 3

1.2 Thesis outline 4

Chapter II Theoretical background 6

2.1 Suspension-fired power plants 6

2.1.1 General 6

2.1.2 Industrial milling equipment 7

2.1.3 Milling circuit 8

2.1.4 Size classification 8

2.1.5 Modifications of coal mills for wood pellet milling 10

2.1.6 Wood suspension-firing 11

2.2 Wood pellets for heat and power production 12

2.2.1 Sustainability criteria 12

2.2.2 Feedstock selection 13
2.2.3 Feedstock structure and chemistry 15
2.2.4 Feedstock mechanical properties 19
2.3 Importance of feedstock properties 20
2.3.1 Wood species 20
2.3.2 Moisture content 21
2.3.3 Wood density 22
2.3.4 Particle size 23
2.4 Wood pellet production process 25
2.4.1 General 25
2.4.2 Pelletizing process conditions parameters 26
2.4.3 Pellet quality standards 28
2.5 Wood and pellet grindability 30
2.5.1 Wood pellet processing history 30
2.5.2 Wood fracture behavior 31
2.5.3 Grindability and grindability methods 32
2.5.4 Model predicting grinding energy and product size 33
2.6 Wood particle characterization 34
2.6.1 Particle size distributions 35
2.6.2 Particle size distributions methods 37
2.7 Concluding remarks 38
Chapter III Experimental methods and materials 40
3.1 Biomass samples 40
3.2 Wood pellet characterization 42
3.2.1 Chemical characterization 42

3.2.2 Physical and mechanical characterization 42
3.3 Milling equipment 44
3.4 Pelletizing equipment 46
3.5 Combustion equipment 47
3.6 Wood particle characterization methods 48
3.6.1 Sample preparation from bulk samples 49
3.6.2 Sieve analysis 49
3.6.3 Image analysis 49
3.7 Statistical analysis of experimental data 51
Chapter IV Summary of the appended papers 52
Chapter V Concluding remarks 60
5.1 Introductory restatement of the research problem 60
5.2 Summary of findings and main conclusions 60
5.3 Recommendations for future work 64
References 66
Appendix I 88
Appendix II 89
Appendix III 106
Appendix IV 123
Appendix V 161
Appendix VI 191

List of tables

Table 2-1: Industrial milling circuits. 9

Table 2-2: Chemical makeup of dry wood (wt.%) [54]. 18

Table 2-3: Young's modulus of selected woods along their main directions [73]. 19

Table 2-4: Important specifications of graded wood pellets for industrial use. 29

Table 2-5: Operating conditions for three mills that can affect the mill performance. 32

Table 3-1: Pellet samples and their chemical composition. 41

Table 3-2: Mill setups used in the experimental studies. 45

Table 3-3: Pelletizing setups used in the experimental studies. 47

Table 3-4: SPC reactor at suspension-firing conditions. 48

Table A-1: Size and shape descriptors to characterize the wood particles. 88

List of figures

Figure 1-1: Summary of the experimental studies performed. 5

Figure 2-1: Schematic representation of the key elements of AMV1. 7

Figure 2-2:Woody biomass feedstock for pellet production [42–47].....13

Figure 2-3: Schematic view of a section from a tree [52].....15

Figure 2-4: Microstructure of hardwood (right) and softwood (left) [55].....16

Figure 2-5: Schematic drawing of a a) ring die and b) flat die pellet mill [136,137]..25

Figure 2-6: The three fracture modes in wood.....31

Figure 2-7: Irregular shapes and sizes of wood particles retained on a sieve screen...35

Figure 2-8: Example of a typical cumulative PSD analyzed by image analysis. 36

Figure 2-9: 3D representation of wood particles by X-ray computed tomography.....38

Figure 3-1: Wood pellet samples used in the experimental studies.....40

Figure 3-2: Working principle of a disc mill, roller mill, and a hammer mill.....44

Figure 3-3: Working principle of the cubic pellet die (a), and ring die pellet mill (b) 46

Figure 3-4: Schematic drawing (a) and picture (b) of the SPC reactor 48

Figure 3-5: Principle of the X-Jet mode of the Camsizer® X2. Adapted from [218]..50

Nomenclature

$A_{particle}$	particle projection area (mm^2)
$P_{particle}$	particle perimeter (mm)
Ar	as received
C	circularity (dimensionless)
D	particle size (mm)
D	pellet diameter (mm)
d*	RRBS characteristic particle size (mm)
d.b.	dry basis
D90	particle size at 90th percentile of the cumulative undersize distribution (mm)
$d_{c,min}$	shortest maximum chord (mm)
d_f	RRBS characteristic particle size (mm) of the feed
$d_{Fe,max}$	maximum Feret diameter (mm)
d_p	RRBS characteristic particle size (mm) of the product
DW	dry wood basis
ER	particle elongation ratio (dimensionless)
K_R	Von Rittinger's material characteristic parameter (kWh mm t^{-1})
N	RRBS uniformity constant (dimensionless)
N_2	nitrogen
O_2	oxygen
P	absorbed mill power (kW)
PSD	particle size distribution
R(d)	cumulative undersize distribution (%)
RRBS	Rosin-Rammler-Bennet-Sperling
SEC	specific energy consumption (kWh/t)
SEM	scanning electron microscope
SPC	single particle combustion
T_g	glass transition temperature
TGA	thermogravimetric analysis
w.b.	wet basis
wt.%	weight percent

Chapter I

Introduction to the thesis

Denmark has a long history of encouraging the use of solid biomass. In 1993, a binding biomass agreement initiated by the Danish government mandated that large-scale combined heat and power (CHP) plants co-fire solid biomass [1]. Today, Denmark is committed to reaching the binding renewable targets set by the EU's Renewable Energy Directive, and solid biomass plays a significant role in it. The conversion of existing coal-fired CHP plants into the operation of 100% biomass is part of Denmark's strategy to reduce greenhouse gas (GHG) emissions and phase out fossil fuels from its electricity and heating sector. For instance, the largest Danish energy company, Ørsted, is striving to stop all use of coal at its power stations by 2023 [2]. Utilizing the existing milling equipment and auxiliary plant infrastructure offers a cost-efficient and practical option with low capital investment [3]. The converted plants also preserve grid reliability compared to intermittent renewable energies like wind and solar [4]. Furthermore, the use of solid biomass for heating purposes in Denmark is promoted by tax exemptions [5].

Wood pellets play a substantial role to replace coal in Danish suspension-fired boilers. Since 2000, the pellet consumption in Denmark has increased significantly for both large-scale CHP plants and private households reaching ca. 1.7 million metric tons (MMT) in 2010. However, at the same time, the national pellet production capacity was only 0.4 MMT, representing less than 25% of the Danish pellet demand [6]. Due to the lack of raw materials in Denmark, the production of pellets from local forests is not able to fulfill the growing demand for wood pellets. Denmark has hence become a country trading pellets globally in increasing numbers [7] and importing over 90% of the annual demand [8]. Imports of wood pellets are expected to increase from about 2 MMT in 2014 [9] to over 3 MMT in 2020 [8]. Most of the wood pellets consumed in Danish CHP plants come from the Baltic region, Russia, Canada, and USA [7].

Driven by European policies, the Southeastern part of the United States has responded to the increasing demand of pellets by enhancing pellet production, with

many large-scale pellet plants being constructed for export to the European market [10]. For instance, Enviva LP, which is one of the largest pellet producers in the world, operates many pellet plants in the Southeast United States with a total production capacity of 2.9 MMT of pellets a year. Some of these plants also supply wood pellets to Danish CHP plants [11]. Looking ahead, the challenge for Denmark is to secure a reliable supply of pellets that are produced sustainably from woody biomass.

The growing interest in utilizing wood pellets in the existing infrastructure of coal suspension-fired power plants in Denmark and other European countries requires a better understanding of the processing of pellets as a fuel source and the combustion of the milled pellet particles at suspension-fired conditions. Traditionally, existing power plant mills are designed based on the grinding properties of brittle coal. The grinding of coal to the required size accounts for about 1% of the power generated by these power plants [12]. However, due to the fibrous and non-brittle nature of wood, pellet comminution is more energy intensive than coal [13], increasing the cost of fuel preparation in the power plants. In addition, the milled product has different morphology (e.g., size and shape), leading to different combustion characteristics. Understanding the milling behavior of wood pellets with different physical properties and the accurate characterization of the physical properties of milled pellet particles are extremely important for power plants. The purpose is to ensure an efficient grinding process and milled pellet particles with desirable properties for suspension-firing, thus achieving a high fuel burnout.

The results of this Ph.D. thesis support an efficient and fast conversion of coal suspension-fired power plants to operate on sustainable wood pellets. Avoiding pellets with undesired properties has economic and practical motivation for power plants. Examples include higher combustion efficiencies, reduced boiler downtime, lower levels of unburned carbon in the ash, and lower NOx emissions. The results of this research work may also encourage other countries to invest in biomass for heating and power purposes, as suspension-fired systems are the most common power plant technology worldwide.

1.1 Research objectives

The main objective of this research project is to address important issues regarding wood pellet milling, physical properties of milled pellet particles, and wood particle combustion. Thus, the following research questions will be answered throughout the Ph.D. study:

1. How can milled wood pellet particles be characterized with respect to their physical properties (e.g., size and shape)? Traditionally, the sieve analysis characterizes the size of milled spherical coal particles. However, due to the fibrous nature of wood, the geometrical description of wood particles by only one parameter is inaccurate for combustion modeling.
2. How can the grindability of wood pellets be tested? Is it possible to predict the milling results obtained at the power plant by applying laboratory-scale mills? The existing grindability tests developed for coal are not applicable to wood pellets due to their different fracture properties. There is hence a need for a new grindability method to provide quantitative data on the grinding behavior of wood pellets prior to their use in power plant mills.
3. How do comminution and pelletization affect the physical properties of wood particles? An understanding of the mechanical processing pathway of wood is important to relate the properties of the milled wood pellet particles to the properties of the original pre-densified material. These results allow pellet producers to optimize their process to fulfill the requirements about the desired particle properties of material within pellets for suspension-fired power plants.
4. How does the wood species affect the grinding and combustion characteristics? Chemically, hardwood and softwood show distinct structural differences. An understanding of how wood pellets of different origin fractures is important for power plant operators to accommodate the milling of wood pellets of different properties.

5. Can the physical and mechanical properties of wood pellets be related to their grinding characteristics (e.g., specific grinding energy and milled product fineness) in a mill? The aim is to review current pellet specifications and establish new measurable parameters that can be incorporated to analyze wood pellets for industrial use.
6. How does pelletization affect the combustion behavior of wood at suspension-firing conditions? Pelletization increases the density compared to raw wood. It is hence of interest to study if particles from the same wood type, but with different apparent densities affect the combustion behavior.

1.2 Thesis outline

The Ph.D. thesis includes a collection of five scientific papers (**Papers I-V**) published/submitted or in preparation for publication in relevant peer reviewed journals. These papers present the core of the experimental work performed in this thesis. Figure 1-1 illustrates the different focus areas of these papers. **Paper I** investigates the mechanical processing pathway of European beech (hardwood) and Austrian pine (softwood), from wood chips to pellets and then to milled pellets, to assess how pelletization and comminution alter the physical properties of wood particles. **Paper II** studies the grinding behavior of two industrial wood pellet qualities in vertical coal roller mills in closed-circuit with dynamic classifiers at the suspension-fired CHP plant AMV1 (Copenhagen, Denmark). **Paper III** investigates the influence of wood pellet properties, including wood type, moisture content, internal pellet particle size distribution (PSD), and three mechanical properties (density, durability, diametral compressive strength) on the pellet grindability characteristics (e.g., grinding energy and milled product fineness) in two lab-scale, open-circuit compression mills. A simple milling procedure is suggested to determine the relative grindability of wood pellets. **Paper IV** investigates the grinding process of wood pellets in a lab-scale roller mill in closed-circuit with a zigzag classifier to simulate a continuous grinding operation similar to an industrial mill classifier system. The results from this study are compared with those from field experiments (**Paper II**) and open-circuit grinding (**Paper III**). **Paper V** examines the combustion characteristics of raw and pelletized beech and pine in a single particle combustion (SPC) reactor.

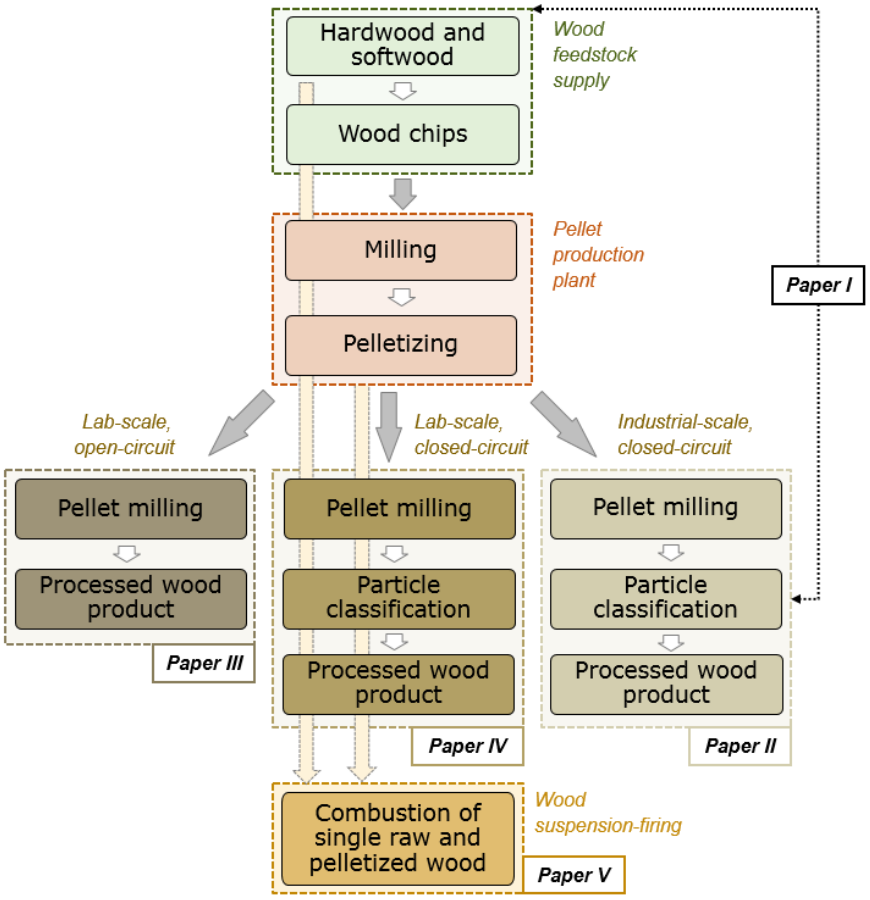

Figure 1-1: Summary of the experimental studies performed.

Overall, the thesis is organized into four main chapters. Chapter II presents selected literature that may be informative and useful for understanding the process of size reduction and pelletization of sustainable woody biomass. In this context, the influence of important parameters on the processing of wood is discussed. The chapter also presents technical aspects that need to be considered to utilize wood pellets in the existing coal mills of suspension-fired power plants. Chapter III presents the materials and experimental methods employed in this thesis. Chapter IV summarizes the appended scientific papers (**Papers I-V**). Chapter V presents the concluding remarks of the present research work and provides recommendations for future work.

Chapter II

Theoretical background

This chapter describes the theoretical background information for this Ph.D. thesis. It provides fundamental basis to understand the complex chemistry, properties, and structure of wood, which affect the energy requirements for grinding and pelletizing, the properties of milled wood particles, and the quality of wood pellets. This chapter also covers how wood particles and wood pellets can be characterized. Comprehensive knowledge of these topics is necessary to understand the milling behavior of wood pellets and determine their suitability as fuels in existing coal suspension-fired systems.

2.1 Suspension-fired power plants

2.1.1 General

Coal suspension-firing has been the dominant technology for generating heat and power in industrial boilers for almost a century [14]. In suspension-firing, the milled fuel particles are suspended as a cloud in the primary (combustion) air. The functional principle of a typical coal suspension-fired boiler is explained in the following for the CHP plant AMV1 (Figure 2-1) located in Copenhagen (Denmark). AMV1 has a capacity of 80 MW electricity and 250 MW heat. Originally designed for coal, it was converted in 2010 to operate 100% on biomass, mainly wood pellets. AMV1 is also part of the grinding study included in the present thesis (**Paper II**).

For suspension-firing, wood pellets need to be milled to dust-like particles to permit fast and efficient combustion. Fed by a silo, wood pellets travel via conveyor belts to the coal roller mills. The mills perform various functions, including fuel drying using a hot primary air stream, pellet comminution, and fuel particle classification (and circulation). The hot air stream, coming from the bottom of the mill table, not only dries the fuel but also lifts the milled product to the classifying unit, from which coarser

particles are returned to the milling table for further grinding. The particles smaller than the classifier cut size move pneumatically through burner pipes to four low nitrogen oxide (NO_x) front wall burners, each fed by a separate burner pipe distributed in three different levels (Figure 2-1). Thus, the suspension-fired boiler has 12 burners. The boiler then completes the heat and power production.

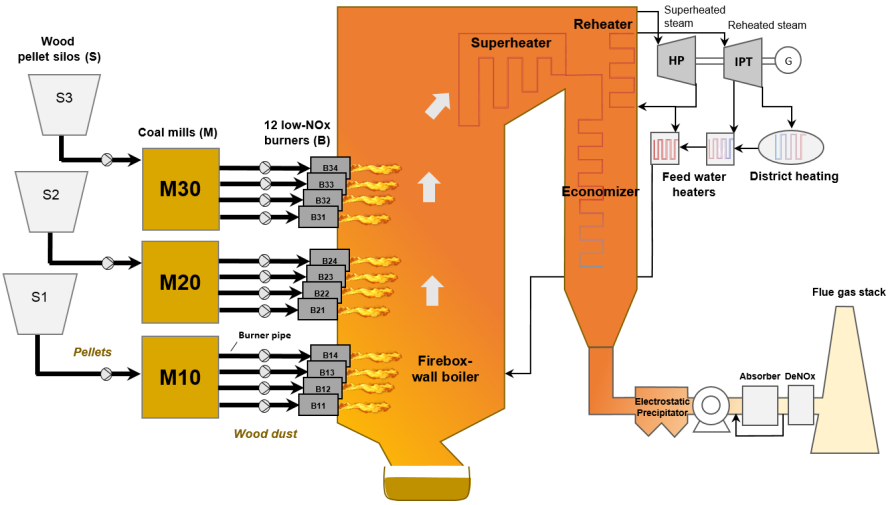

Figure 2-1: Schematic representation of the key elements of AMV1.

2.1.2 Industrial milling equipment

Industrial coal mills, designed to process brittle coal, can be divided into three types [15]: slow-speed mills (e.g., tube-ball mills), medium-speed mills (e.g., vertical roller mills, VRM), and high-speed mills (e.g., hammer mills and disc mills). Tube-ball mills and vertical roller mills (or vertical spindle mills) are one of most common mill types in existing power plants for coal pulverization [16], while sometimes also disc mills are used [17]. Although suitable for biomass, cutting mills are typically not used for pulverizing coal [15]. Hammer mills are the most common mill type in biomass-converted power plants and new plants [18], as well as in pelletizing plants [3]. The conversion of hammer and rollers mills to process 100% wood pellets has been successfully demonstrated in several power stations in Sweden, Denmark, UK, Netherlands, Belgium, and Canada [3,18]. Trials with tube-ball mills using biomass pellets have been shown to be unsuccessful, thus requiring new milling capacity to be

installed [19]. Generally, the choice of milling equipment depends on the following parameters [20,21]:

- material properties (e.g., hardness, brittleness, abrasiveness, fibrous nature);
- size of feed and product;
- mill capacity;
- breakage mode (e.g., compression, abrasion, or impact);

Roller mills offer low operating and maintenance (O&M) costs along with improved availability and safety [19]. In contrast, hammer mills are very sensitive to fuel ash and foreign bodies, such as stones and metals, which can cause severe damage to the hammers and classifying screens. Hence, hammer mills require higher O&M costs, such as for hammer and screen replacements. These result in higher plant downtimes. In addition, sparks, e.g., from stones represent a high ignition and explosion risk in the high-speed rotating mill, especially sparks leaving the classifying screen that can ignite the finely-ground product. Overall, roller mills are the preferred option for conversion to biomass, as the utilization of the existing milling equipment can offer a safe, cost-efficient and practical option at low capital investment [3].

2.1.3 Milling circuit

Industrial milling circuits are either open-circuit or closed-circuit (Table 2-1). In open-circuit milling, the fuel passes only once through the mill without recycling or classification [20]. Mills operated in closed-circuit are additionally equipped with classifying equipment to have better control of the product particle size. The milled product leaving the mill is subjected to a classifier, which returns the coarse particles (or recirculating load) to the mill for further grinding along with the new feed material.

2.1.4 Size classification

For the optimal conversion of fuel particles in suspension-fired boilers, classifiers need to control the milled product fineness. The finer and more uniform the product is, the higher the chance to achieve complete combustion in the available residence time in the boiler [15]. On the other hand, a poor distribution of primary air and coarse wood dust particles lead to unstable flames, accelerated erosion of

pulverized fuel system components, and dust deposition in the pipeline that increase the risk of fires and dust explosions [16].

Table 2-1: Industrial milling circuits.

	Description
Open-circuit milling	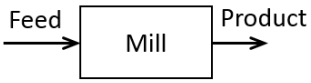
Closed-circuit milling	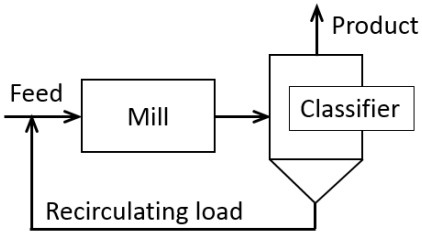

For coal, the target product fineness is about 75% of particles passing 75 µm sieve screen [22]. Equivalent limits for biomass have not been established. Generally, particle sizes as fine as coal are not needed because of the higher reactivity of biomass. Esteban and Carrasco [23] recommended that ca. 95 % of particles (dry matter) shall pass a 1 mm screen to achieve optimal combustion of woody biomass, which implies adjustments of the current coal mill classifier settings. Due to the lower energy density of biomass, the mill capacity for grinding wood pellets is reduced compared to coal [3]. Thus, understanding the classification process is even more important for biomass, as efficient classification technologies can reduce the recirculating load and increase the production of fine material (final product), which increases the grinding capacity [24]. Proper particle size classification also results in reduced NOx emissions and lower levels of unburned carbon [18].

The design of classifiers is constantly changing in an effort to develop more efficient and cleaner power plants. Traditionally, vertical roller mills in coal-fired power plants were equipped with static classifiers, which have no moving parts in the separation chamber. Nowadays, they are often upgraded with modern dynamic classifiers, which employ a rotor cage to exert a radial forced centrifugal field [25]. The

classifier cut size is then controlled by adjusting the rotor speed and airflow rate. Dynamic classifiers result in a much sharper classification operation [18], indicating a higher efficiency in rejecting oversized fuel particles (i.e., better fuel fineness), which will reach the boiler bottom before complete burnout.

2.1.5 Modifications of coal mills for wood pellet milling

The modifications of coal mills depend on factors, such as the type of mill installed and their suitability to process wood pellets, the available mill capacity, and the combustion system requirements (e.g., milled product fineness) [19]. This section primarily focuses on vertical roller mills, as they are the most common mills in coal suspension-fired boilers [26].

For comminuting wood pellets in a roller mill, a larger relative movement between the milling table and the rollers that causes higher shear forces was found to be beneficial [18]. To improve shearing inside the milling gap between milling table and rollers, e.g., blind holes can be drilled into the milling table, as it was done at AMV1 [27]. A similar approach was undergone at the power station Avedøre unit 2 (Denmark). Optionally, the roller orientation can be adjusted [3]. Taking into account the different flowability and bulk density of wood pellets compared to coal, the fuel feeder systems to the mill require recalibration. Typically, the pellet flow to the mill is adjusted to the needs of the boiler.

The temperature of the hot primary airflow entering the mill has to be much lower for wood pellets than for coal due to their higher volatile matter content and higher reactivity. While it can be up to 350°C for coal, for wood pellets, it has to be tempered by a cooler to between 125 and 130°C [3,27] to prevent the release of volatile matter and avoid pellet pre-ignition and mill fires. Mill inlet air temperatures of 80-90°C are also reported [28,29]. The reduction of the inlet air temperature also reduces the outlet air temperature (ca. 60°C for biomass compared to 80°C for coal) [27]. Generally, the maximum temperature inside the mill has to be kept well below the minimum ignition temperature of biomass [18]. Many mill systems and the associated pipework have been equipped with explosion suppression systems to detect sparks and explosions [3].

The lower density and different size and shape of wood particles imply that optimal air velocities in the mill differ from those of coal particles [18]. A common approach is to install fixed baffle plates in the upper part of the mill body to maintain correct air velocities and to reduce the tendency of partially-milled wood pellets to accumulate in the mill [30]. For combustion systems that are sensitive to coarse particles, such as front-wall-fired furnaces, dynamic classifiers are the preferred solution to ensure the required comminuted product quality [27]. Other furnace configurations, including corner-fired (tangentially-fired) and opposite-wall-fired furnaces, are more tolerant of a coarser comminuted product. While the requirement for a fine comminuted product for front-wall-fired furnaces suggests a significant unit output de-rating, it is between 0 and 10% for other furnace configurations. Another common measure to accept a coarser comminuted product is the injection of dry coal pulverized fuel ash through existing boiler ports to mitigate the negative characteristics of white wood pellet ash [19].

2.1.6 Wood suspension-firing

Fuel particles entering suspension-fired boilers are rapidly heated at high heating rates (> 10,000 K/s) and peak temperatures of up to 1600°C [31]. Generally, the different chemical composition between coal and wood affect the conversion rate and combustion process [32]. Ballester et al. [33] found that a higher amount of volatiles in wood produces a more intense flame close to the burner compared to coal under similar conditions indicated by high concentrations of unburnt gases. Furthermore, they distinguished two distinct combustion stages in the wood flame: an intense combustion zone of a larger amount of volatiles released from small particles close to the burner, and a second zone further downstream, linked to the devolatilization of coarser particles and char combustion.

Generally, the char combustion is the most time-consuming step of the total conversion process. Therefore, wood particles with rapid char combustion are desired for suspension-firing. Studies have shown that coarse particles increase the char yield [34], and particles with a higher length-to-diameter ratio heat more rapidly due to their larger surface area, resulting in faster conversion rates [35]. Momeni [35] observed similar conversion behaviors for hammer-and roller-milled wood pellet particles,

although the latter ones were much larger, which they attributed to the different specific particle surface areas. Furthermore, an increased oxygen concentration and increased temperature speed up the particle conversion process, thus shortening the devolatilization and char combustion times.

Several studies on single biomass particle combustion at suspension-fired conditions have been conducted [34,36,37] to understand the key parameters that influence the particle conversion process. Linear relationships between devolatilization time and particle mass were reported for wood particles of various sizes and torrefaction degrees [34] and various wood species with different apparent densities [37]. Lighter particles have a lower thermal capacity, and thus heat up and devolatilize faster [34]. Lu et al. [34] also showed that the char burnout time of raw and torrefied wood particles was strongly influenced by the char particle mass, and thereby by the char yield.

2.2 Wood pellets for heat and power production

2.2.1 Sustainability criteria

When replacing coal with wood pellets for thermal heat and power generation, it is essential that the woody biomass for pellet production is sourced from sustainably managed forests. In 2013, a number of European energy utilities, including Vattenfall, Ørsted, and E.ON had hence formed a certification scheme for the production and purchase of wood pellets. Through this so-called Sustainable Biomass Partnership (SBP) program, it can be assured that biomass is sourced from legal and sustainable forests [38]. The SBP framework provides a number of strict sustainability criteria, e.g., that forestry ensures conservation of biodiversity and that the carbon sequestration capability of the forests is preserved [39]. The timberland is typically reforested by planting seedlings, direct seeding, or (natural) regrowth. Ørsted, for example, has increased its sourcing of certified sustainable biomass from 678,000 metric tons in 2016 to 2.1 MMT in 2017, which is a share of 72% of its total sourced volume. By 2020, the target is to have 100% of the sourced biomass being certified as sustainable [2].

2.2.2 Feedstock selection

In the past, pellet plants most commonly relied on sawmill residues, such as sawdust and wood shavings. However, both a decrease in wood harvest and an increased demand for wood pellets in the EU outpaced the supply of these traditional raw materials. Therefore, pellet producers started to broaden their feedstock portfolio of woody biomass (Figure 2-2). To ensure a stable and secure supply of feedstock, wood pellet producers have long-term supply agreements with forest owners [6]. Common pellet feedstock sources include [40,41]:

- By-products from the wood processing industry, e.g., wood chips and sawdust.
- Logging residues, such as treetops, tree stumps, branches with needles or leaves that cannot be processed into lumber.
- Low-grade wood fiber and round wood that would otherwise be rejected from lumber and sawmilling industries because of diseases, small size, defects (e.g., crooked stem, tree knots, rotten core), or lightning damage.
- Thinning weak or damaged trees, typically, from commercial softwood plantations to reduce competition for nutrients, water, and sunlight, enabling the growth of higher value timber for other markets.
- 'Whole-tree' wood chips made by in the forest out of low-grade wood and logging residues.

Figure 2-2:Woody biomass feedstock for pellet production [42–47].

Depending on the pellet mill and its location, the ratio of hardwood to softwood, species mix, and particle sizes (branches vs. wood chips vs. sawdust, etc.) vary [48]. For example, the Enviva pellet mill Southampton located in Virginia (USA) sources 100% hardwood species, while the Enviva pellet mill Cottondale located in Florida (USA) uses mostly softwood species for the production of wood pellets. Pellet plants that are close to each other geographically show a relatively comparable ratio of hardwood and softwood [49]. In 2018, from the total volume of wood sourced by Enviva, about 58% was hardwood, and 42% was softwood, with hardwood species being predominantly harvested [50].

Tree species used for pelletization in the Southeastern US include red maple, black tupelo, and water oak categorized as broad-leaved trees, and pond pine, bald cypress, and longleaf pine, which are conifers [49]. In the literature, conifers are commonly referred to as softwoods and broad-leaved trees as hardwoods, alternatively. However, these terms may be misleading, as there are relatively hard conifers, such as longleaf pine that has a higher bulk density (ca. 650 kg/m^3 air-dried wood) than some hardwoods such as black tupelo (ca. 545 kg/m^3 air-dried wood). Therefore, softwoods and hardwoods are primarily referred to the origin of the wood and only indirectly to the wood properties.

As stated, the suitable feedstock for wood pellet production includes all types of natural and untreated lignocellulosic biomass. Any treated wood (e.g., painted, glued, lacquered) or contaminated wood by foreign matter is excluded for the pellet production because of halogenated organic compounds or heavy metals [30]. Feedstock containing bark needs to be considered carefully due to its higher ash content, which tends to produce clinker in the boiler. Bark also has higher levels of chlorine and sulfur, which can cause harmful emissions in addition to corrosion in the boiler. The diversity of woody biomass sources and sizes implies that the size reduction is an important but complex pre-processing operation prior to pelletization, and careful selection of feedstock for pelletization is required.

2.2.3 Feedstock structure and chemistry

Wood macrostructure

The structural features of wood visible with the naked eye are shown in Figure 2-3. In the center, there is the pith. The tree grows in thickness by adding a layer of new wood cells each year around the pith. Stemwood consists of two distinct areas: heartwood and sapwood. The heartwood is the older central wood made of inactive cells, while in the newly-formed sapwood made of living cells all conduction and storage take place. The outer layer of wood comprises an inner bark (or phloem) transporting the sap and an outer bark (periderm), which protects the tree. Between the inner bark and sapwood, there is the cambium, which forms new wood cells. The wood rays are composed of parenchyma cells, which run radially from the pith towards the bark [51].

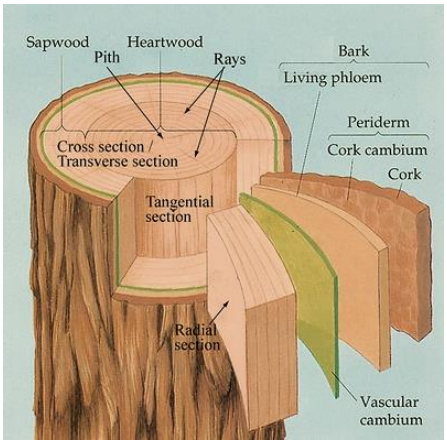

Figure 2-3: Schematic view of a section from a tree [52].

Wood microstructure

The microstructure of wood shows features that are visible under a microscope, including the types of cells and their properties. Wood can be classified into two groups, softwoods (i.e., trees with needle-like or scale-like leaves) and hardwoods (i.e., broad-leaved trees). In general, softwoods have a simpler and more uniform distinct internal structure than hardwoods (see Figure 2-4). Softwoods comprise mostly longitudinal, thin-walled cells (ca. 90–95% of wood volume), which are called tracheids. These cells

have an open channel used for conducting water and nutrients throughout the tree [53]. Tracheids are ca. 3-4 mm long and 30 µm in diameter, leading to length-to-diameter ratios of 100. The remaining 5-10% is made up of radially-orientated storage cells (parenchyma ray cells), which are similar in diameter, but much shorter (0.2 mm) [54].

In comparison, the hardwood anatomy shows a wider variety of cell types, resulting in a greater variation in their physical properties than softwoods. About half of the wood volume or more is made of thick-walled fibers, which are 1-2 mm long and 15 µm wide. An essential characteristic of hardwoods is the presence of thin-walled vessels (pores), which make about 25% of the wood volume. These vessels are short (0.3-0.6 mm) and wide (up to 300 µm). As the hardwood fibers have a very narrow channel, only the vessels conduct water and nutrients throughout the length of the tree. Hardwoods can be divided into diffuse-porous wood with vessels evenly distributed throughout the wood (e.g., aspen) or ring-porous wood with more larger vessels in the spring wood (e.g., oak). The remaining wood volume (ca. 25%) consists of storage parenchyma ray cells, which are more numerous than in softwoods [54].

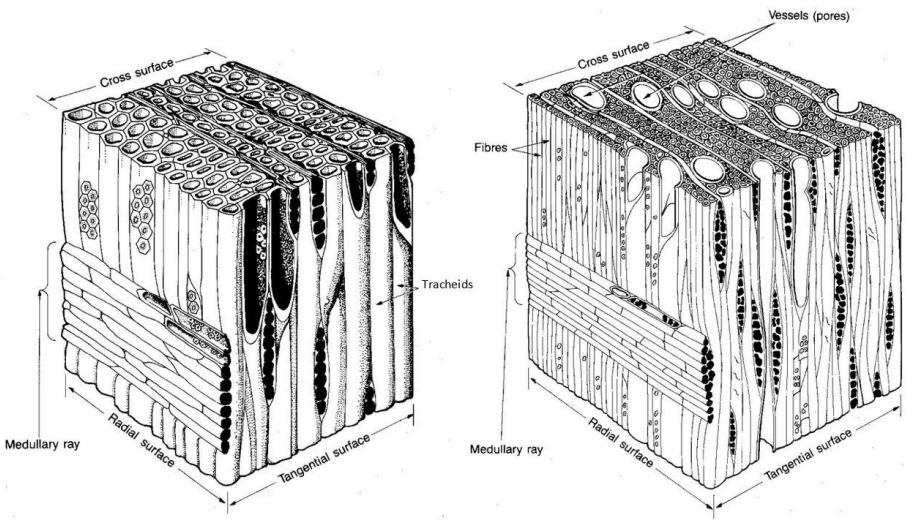

Figure 2-4: Microstructure of wood showing the presence of vessels (pores) in hardwood (right) and absence in softwood (left). Adapted from [55].

Wood chemistry

Woody biomass with regard to the dry matter is mainly made up of three biopolymers: cellulose, hemicelluloses, and lignin. These biopolymers form a complex three-dimensional polymeric composite that provides a rigid structural framework of the plant cell wall [56]. The remaining components in woody biomass include inorganics (ash), structural proteins, pectins, and extractives (such as resins). The share of these components in biomass can vary greatly between different parts of the tree (e.g., stem, bark, branches), between wood species, and even within one species (e.g., due to different soil type and growing location). The different chemical make-up of hardwoods, softwoods, and bark is shown in Table 2-2.

Cellulose is the major structural component of wood and provides the mechanical strength of the plant cell wall. It is a long linear polymer chain of glucose units with oxygen linkages between them. Cellulose is composed of several hundred to thousands of molecules, which are linked together by strong inter-and intramolecular hydrogen bonds. These bonds are responsible for forming the fibrous wood structure. Cellulose molecules are aggregated together in bundles of microfibrils. The angle between the cellulose microfibrils and the wood fiber axis, which is referred to as the microfibril angle (MFA), plays a critical role on the physical and mechanical properties of wood [57]. Generally, softwoods were found to have a larger MFA compared to hardwoods [58], and larger MFA are linked to a low tensile strength [59]. About 65% of the cellulose in wood is crystalline, and the rest amorphous [60]. Crystalline cellulose is insensitive to water. Thus, water adsorption occurs only in the amorphous area of cellulose [61]. Wood comminution can reduce the degree of cellulose crystallinity, depending on the milling principle applied and milling conditions [62,63].

Hemicelluloses are found in the matrix between cellulose microfibrils in the wood cell wall. They contribute to the structural component of the tree. Unlike cellulose, they have side groups, which are less ordered and more amorphous [64]. Thus, they are more susceptible to chemical and thermal degradation than cellulose [65]. Hemicelluloses are carbohydrates, consisting of multiple sugars, including hexoses (e.g., mannose, glucose, galactose), pentoses (e.g., xylose, arabinose), and sugar acids (e.g., uronic acids) [66]. Softwoods contain predominantly mannan, which is a polysaccharide made from mannose monomers. In hardwoods, the most common

hemicellulose component is xylan, which is made up of xylose monomers. The xylan to mannan ratio in hemicellulose (similar to the syringyl to (syringyl + guaiacyl) ratio in lignin) can then be used as an indicator of the plant origin and to distinguish between hardwood and softwood [67].

Lignin is a highly branched polymer that fills the space between cellulose and hemicellulose, providing structural strength and rigidity of plant tissue. Unlike the two polysaccharides, lignin is a three-dimensional aromatic and amorphous polymer composed of phenylpropane units [66]. Generally, lignin consists of three basis phenolic monomers: guaiacyl monomer (G type), syringyl monomer (S type), and p-phenyl monomer (P type). The quantities of these monomers in lignin vary for different wood species [68]. For softwoods, the ratio of G-S-P is 94:1:5, while the ratio in hardwoods is 56:40:4 [69]. Intense milling in a vibratory mill can facilitate the breakdown of the wood cell wall structure, e.g., indicated by depolymerization of lignin [70].

Table 2-2: Chemical makeup of dry wood (wt.%) [54].

	Softwood	Hardwood	Bark
Cellulose	40-45	45-50	20-33
Hemicelluloses	25-30	25-35	<10
Lignin	26-34	22-30	15-30
Extractives	0-5	0-10	20-40
Inorganics (ash)	0-1	0-1	2-5

The composition of woody biomass also influences its thermal decomposition (or devolatilization behavior). Each biopolymer component decomposes at a different temperature range. The random and amorphous structure of hemicellulose favors its quick degradation, which occurs at 220-315°C. Cellulose decomposes at 315-400°C. The decomposition of lignin occurs over a wide temperature range (from 160-900°C) due to the presence of aromatic phenyl units [71]. Lignin hence has a higher thermal stability than cellulose and hemicellulose.

2.2.4 Feedstock mechanical properties

Naturally, wood is highly anisotropic, as its properties depend greatly on the wood grain direction. Up to 95% of all wood cells are aligned parallel to the stem. The remaining percentage of cells is arranged radially to the stem, with no cells at all arranged tangentially [52]. Wood can also be considered as orthotropic with three mutually perpendicular axes, a longitudinal axis parallel to the grain direction, a radial axis normal to the perpendicular to the growth rings, and a tangential axis perpendicular to the grain, but tangential to the growth rings. The anisotropic and orthotropic nature of wood affect its mechanical properties, e.g., toughness, strength, and stiffness [72–74]. For instance, wood has a very high Young's modulus (is much stiffer) in grain direction, whereas it is smaller across the grain, as shown for spruce, oak, and ash trees in Table 1-2. This behavior is due to binding energies of the chemical wood constituents. When stress is applied, covalent bonds are more active in grain direction, while weaker hydrogen bonds are more active across the grain [73]. In compression and tension, woody biomass is stronger parallel to the grain than across the grain.

Table 2-3: Young's modulus of selected woods along their main directions [73].

Wood species	Axial (MPa)	Radial (MPa)	Tangential (MPa)
Spruce	13650	789	289
Oak	15789	1875	1269
Ash	11778	2046	1029

Generally, the strength properties of wood are affected by many variables [74,75]: variations in macrostructure (e.g., density of compression or tension wood, tree age of juvenile or mature wood); mode of stress applied (e.g., tension, shear, axial or diametral compression); wood anisotropy; variations in microstructure (e.g., MFA); environmental conditions (e.g., temperature, moisture content); and duration of stress. The wood toughness, defined as the energy required to propagate a crack [54], strongly depends on the density. Thus, the toughness increases with increasing density [76]. Generally, wood has good toughness across the grain but is relatively brittle along the grain [77].

2.3 Importance of feedstock properties

Understanding the properties of woody feedstock is important for the design and operation of downstream processes, including size reduction and pelletization. They are also relevant for the thermochemical conversion of the fuel, and the design and operation of handling, storage, and transportation systems. In the following, important feedstock properties are reviewed.

2.3.1 Wood species

Different tree species and different parts of the tree have different structures and chemical makeups, which will affect their processing accordingly. Thus, the energy input for milling and pelletizing will vary. Several studies reflect the different grinding energy input required by different raw wood species and parts of the tree [23,54,59,78–83]. However, there is no clear trend in the literature regarding the energy requirement for grinding softwood and hardwood species. Nati et al. [82] reported that chips produced from pine were smaller than those produced from poplar, and no difference in specific energy consumption for chipping was detected. Esteban and Carrasco [23] obtained 120 kWh/t oven-dried wood (ODW) for poplar chips and 150 kWh/t ODW for pine chips using the same hammer mill screen size, which resulted in similar product particle sizes. Repellin et al. [78] reported that fine grinding spruce chips using an ultracentrifugal mill equipped with a 500 µm screen required less energy (750 kWh/t) than beech chips (850 kWh/t). Temmerman et al. [81] noted that the energy for grinding hardwood chips (oak, beech) and softwood chips (pine, spruce) varied more within a wood species than between species. He obtained the following grinding data: for beech 5-307 kWh/t, oak 6-172 kWh/t, pine 5-199 kWh/t, and spruce 5-252 kWh/t. In comparison, grinding coal requires between 7-36 kWh/t [78].

Wood species with high lignin content are generally preferred for pelletization, as it allows milder pelletization conditions [84]. Lignin shows thermosetting properties if heated and acts as intrinsic resin [85]. The transition of lignin from a glassy into a rubbery state (i.e., the lignin glass transition), improves the inter-particle bonding, formed by solid bridges [86]. The lignin glass transition varies between wood species [87] and for different moisture contents [88]. The subsequent flow and hardening of

lignin improve the pellet quality (e.g., density, durability) without adding chemical binders. The pellet durability can steadily be increased with increasing feedstock lignin content [89,90]. However, above a threshold of 34% (sum of lignin and extractives), the quality of wood pellets decreases [91].

Structural differences between hardwood and softwood should be given attention, as they require different pelletizing pressures to produce pellets with desirable quality. Holm et al. [92] found that beech is more difficult to pelletize than pine, as beech particles caused the blockage of the pellet die. High extractives in wood species act as lubricants and lower the friction in the die channels, leading to lower energy demand for pelletizing and higher production capacity [93]. Regarding the role of extractives in the pellet quality, there has been some disagreement. Several studies found that species with more extractives decreased the pellet strength [94–96] and pellet durability [97]. In contrast, Filbakk et al. [93] established a positive relationship between extractives and pellet durability. Pellets made of bark with high extractives showed excellent durability [89]. However, Ahn et al. [90] observed that blending bark to the pelletization process significantly reduced the durability of larch pellets and slightly improved the durability of tulip pellets.

2.3.2 Moisture content

Several studies have been conducted to determine the effect of moisture on the grinding energy and physical properties of the milled product [23,59,78,80,81,98–101]. All studies report that biomasses with higher moisture levels significantly increase the grinding energy input, especially for the production of fine particles [80]. For similar moisture levels, pellets require less grinding energy than wood chips [81]. The increasing energy input is attributed to water acting as a plasticizer in wood. The bound water (below the fiber saturation point), which is accumulated in the structure of wood cell walls, triggers the viscoelastic behavior [102]. As wood dries, irreversible cell wall damage is formed, causing severe failure mechanisms. As a result, a more brittle fracture process is induced [103], resulting in lower grinding energy [54] and smaller particles at similar mill settings [104]. Thus, the mechanical behavior of dry wood is different from green wood due to the ‘damaged’ microstructure.

The moisture content also has an essential role in the pelletizing process and pellet quality. Water acts as a friction-reducing lubricant in the die channel, which reduces the pelletizing pressure [105]. In pellets, water also plays an active role as a binder due to hydrogen bonds between adjacent particles, leading to more durable pellets [89,90,97]. However, increasing the moisture content above an optimum level has an adverse effect on the pellet durability [93,106] and pellet density [107,108]. The moisture content also affects the glass transition point of lignin, hemicellulose, and amorphous cellulose [63]. Generally, the optimum moisture content for pelletization depends on the wood species [109]. For industrial wood pellets, the moisture content is limited to 10 wt.% [110].

It is well known in the literature that the feedstock moisture content influences the thermochemical conversion of biomass. Feedstock with high moisture content will lower the heating value, cause ignition and combustion problems, prolong the burnout times, and extend the particle residence time in the boiler.

2.3.3 Wood density

Generally, the density of biomass fuel can be categorized as particle density and bulk density. The bulk density is important for handling, storage and transportation, and hence influences directly the costs for these operations [111]. The particle density (or apparent density) refers to the specific density of the biomass, defined as the mass of the material over its volume excluding the pore space volume. The commonly accepted value for the oven-dry specific cell wall density is 1.53 g/cm3 [112]. Variations in density between wood species and between different parts of the tree reflect the different relative volume of cell wall material and cell cavities [54].

A number of studies have shown that woods with higher particle density increased the specific fracture energy demand [54,59,78,100,113]. However, some studies lack information about the initial particle size. Naturally, the wood density varies with the moisture content and specific gravity, which is affected by the weight and volume of wood [114]. Naimi [59] reported that disks of hardwoods (poplar and aspen) with lower particle density required more energy to be milled to a specific particle size than softwoods (pine and Douglas fir). However, severe weakness of this statement is that these hardwoods are much softer than other common hardwoods, e.g., beech and oak. Naimi [59] further

observed coarser milled particle sizes for softwood compared to hardwood. He stated that the presence of vessels (pores) in hardwoods promotes the fragmentation into smaller particles.

The density of woody biomass affects its mechanical and physical properties, and hence the mechanical processing of wood in the pellet mill. Krizan [73] stated that hardwood species are stronger, harder, and more resistant to mechanical processing than softwoods. Pelletizing hardwood particles is a challenge due to their higher frictional forces in the pellet die channels compared to softwood [115]. Consequently, the blockage of the pellet matrix is more likely to occur when hardwood species are used [92].

The fuel density is also relevant for the thermochemical conversion. Biomass particles too dense can enter the bottom ash stream with little or no conversion, posing fuel conversion challenges. Generally, the biomass particle density is significantly lower than for coal, commonly half that of coal. Biomass bulk densities are about one fifth that of coal. This results in an overall fuel density roughly one-tenth that of coal [116].

2.3.4 Particle size

Commonly, the initial particle size of biomass feedstock is not considered as a variable in grinding studies. However, because woody biomass varies significant in shapes and sizes, information about the initial biomass size is necessary. This information is also useful in evaluating the efficiency of the size reduction process in relation to the grinding energy requirements. Gil et al. [117] reported that larger particle sizes increase the probability of internal flaws where cracks initiate, while smaller particles have a higher fracture resistance. Jiang et al. [118] added to this that initial particles with larger sizes required more energy for milling than finer particles. Shaw et al. [108] observed that grinding poplar chips in a hammer mill (3.2 mm screen) required considerable more energy than wheat straw (190 kWh/t and 11 kWh/t respectively), which they mainly attributed to the higher initial size of poplar chips. Contrary to the previous study, Rosentrater [119] concluded that the initial size of corn stover had no significant effect on the specific grinding energy, suggesting to reduce the unnecessary coarse grinding step before fine grinding.

Considerable research has been conducted on the effect of particle size on the pelletization process and pellet quality [107,108,120–123]. Generally, the friction in

the pellet die channel increases for biomasses with smaller particle sizes due to a higher surface contact area between the pellet and die walls, causing higher pelletizing pressures [115,121]. Several studies using single pelletizer units [107,108,122,123] concluded that the pellet feedstock should have reduced particle size to improve the pellet quality (e.g., density, durability, strength, diametral compression). However, studies using industrial pellet mill equipment showed that decreasing the particle size had no effect [120], a minor effect [124], or even an adverse effect [125] on the pelletization process and pellet quality. The latter study observed an improved quality of pellets (more durable and denser) for feedstock with coarser particles (6.5 mm) instead of finer ones (3.2 mm) [125]. To produce good quality pellets, it is recommended that the feedstock particle size is between 0.5 and 0.7 mm [105]. Furthermore, the amount of fines (particles below 0.5 mm) shall be below max. 20% [109].

The target particle size for biomass is relevant for suspension-firing, as the coarser size of biomass particles compared to coal will imply changes in the particle conversion behavior. The coarser particle size results in large temperature gradients inside the biomass particle, causing overlap of particle drying, devolatilization, and char oxidation processes [35], longer devolatilization times [33], and thus longer particle burnout times [32]. The typical average size of milled coal particles is about 65 μm [32], while it is not uncommon to see characteristic particle sizes of milled wood of up to 900 μm [126]. However, particle sizes as fine as coal are not needed due to the higher volatile content and reactivity of biomass in combustion systems [127]. Hence, a reduction to the same size as coal is unnecessary and wasteful of mill power [128]. When modeling the combustion zones inside boilers, it is typically assumed that particles are spherical. However, the elongated shape of wood particles makes this assumption invalid.

2.4 Wood pellet production process

2.4.1 General

In its original form, woody biomass has low bulk and energy densities, irregular shapes and sizes, and high moisture contents. These properties pose challenges for handling, storage, feeding, and transportation processes for the utilization of biomass for renewable energy production [129,130]. Densifying woody biomass into a uniformly solid material in the form of pellets (i.e., pelletization) can address those problems by producing a denser fuel with more homogeneous properties compared to the woody biomass feedstock [129,131]. Pelletization can enhance the bulk density of sawdust and wood chips from 320 kg/m3 (moisture content of 50 wt.%) [132] to about 650 kg/m3 (moisture content of 8 wt.%) [133] by removing inter-and intraparticle voids [134], thereby increasing transport efficiency [135], simplifying storage and handling infrastructure [129], and achieving a higher energy density biofuel [30].

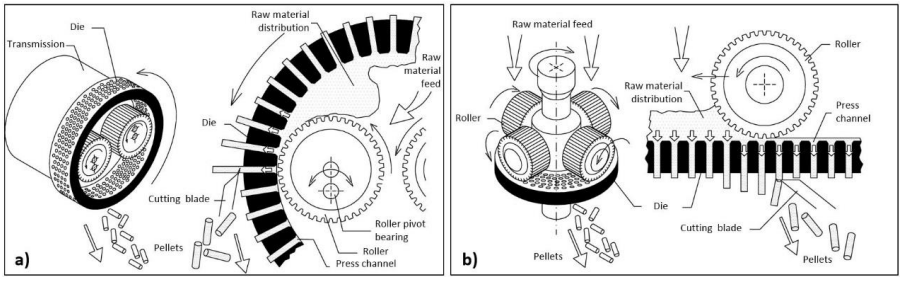

Figure 2-5: Schematic drawing of the pelletization process in a a) ring die and b) flat die pellet mill [136,137].

Generally, before densification, woody biomass undergoes some pretreatment, both mechanical, like particle size reduction (e.g., chipping, hammer milling), and thermal, like drying (e.g., belt or drum drying). The main feature of the pellet production process is the pellet mill, which can be designed as a ring die or a flat die with cylindrical press channels and two to four rollers (Fig. 3.2a and b, respectively). As the die and/or the rollers rotate, the feedstock is pressed through the opening of the channels every time the rollers pass the channels. Due to friction between wood particles and the die channel walls, a layered structure of densified solid biofuel (i.e.,

the pellet) is formed, which is cut by a blade to the desired length. The die channel diameter determines the pellet diameter.

Attempts have been made to understand the physical forces acting on the pellet in the press channel of a pellet mill [92,94,121,138,139], which are important for optimizing the pelletizing process. Holm et al. [92] reported that the ability to produce pellets with desired quality depends on several parameters, including the sliding friction coefficient (i.e., the friction with the die channel walls), the pellet die aspect ratio (i.e., the ratio of press channel length to channel diameter), and the material-specific parameters (e.g., elastic modulus and Poisson's ratio). These parameters also affect the pressure build-up in the die channel, which is caused by friction between the die channel walls and the biomass [138]. The friction generates heat that can heat the material to 130°C [94], which is why cooling is required after pelletization and before storage. It is assumed that biomass particles align perpendicular to the press channel direction, causing longitudinal strain of the particles when subjected to a radial pressure [92].

2.4.2 Pelletizing process conditions parameters

The important role of feedstock characteristics (e.g., composition, moisture content, particle size) on the pelletization process and pellet quality has already been discussed in a previous section (cf. 2.3 Importance of feedstock properties). The following pellet mill specific parameters and process conditions have also been identified to affect both the pellet quality and/or the pelletization process.

Pellet mill specifications

Pellet mill specifications that influence the pelletization process and/or the pellet quality include metallurgy, which can influence friction and temperature build-up, as well as channel design, channel pattern, and channel numbers that affect pellet throughput and pellet ejection [140]. However, most of the published literature focuses on the effects of die aspect ratio, die speed, and clearance (gap) between the roller and die. The die aspect ratio has a major influence on the pelletizing pressure. In general, increasing the die channel length increases the pressure needed to press the pellet through the die [92]. This was found to enhance significantly the durability of various agricultural residue pellets [125]. However, a too large die aspect ratio will clog the die

and choke the pellet mill [135]. Other studies reported that increasing the die channel length had only a negligible effect on the density and compressive strength of compost pellets [141–143] and an inverse effect on the durability of garden waste pellets [144]. Hence, it is concluded that the optimal die dimensions depend on the individual feedstock and pelletizing conditions. Commonly, hardwood pellets are produced using a lower die aspect ratio compared to softwoods [92,135].

The die speed is decisive for how the material is compacted in the press channels. The optimal die speed varies with the pellet diameter and with the feedstock bulk density [145]. Increasing the die speed for pelletizing wheat was found to increase the specific pelletizing energy, while no clear trend was observed on the pellet durability or pellet production rate [146]. The pellet hardness and durability can vary with the clearance (gap) between the roller and die. Too large a gap will decrease the pellet quality due to large amounts of lateral material leaking [145].

Pelletizing process conditions

The temperature and pelletizing pressure are key factors in the densification process, affecting both pellet quality and specific energy required to produce pellets. Pressing biomass through the die channels produces frictional heat that is important for the thermal softening of lignin. The subsequent flow and hardening of lignin result in improved pellet quality [147]. For the processing temperature, the general trend observed is that increasing the temperature reduces the pelletizing pressure [148,149] and the friction in the die channels, and thus the specific energy for pelletizing [94]. The decrease in specific energy requirement allows higher production capacity with the installed motor [150]. Increasing the processing temperature also enhanced the densified product quality (e.g. density, durability, strength, hardness) for pine and beech [94], spruce [151], sugar maple [115], bamboo [148], olive tree [123], torrefied pine [152], birch and spruce [153], and pine, beech, oak, and spruce [154,155]. However, high temperatures may increase the risk of fires [152]. Some studies [115,155] concluded that the interaction of temperature and pelletizing pressure is very important.

The pelletizing pressure directly affects the density of the final densified product and the specific pelletizing energy consumption. Too low pressures are disadvantageous, as biomass cannot be densified [156]. With increasing pressure,

porosity decreases, enhancing the densified product quality (e.g., density, strength, durability) for pine, beech, oak, and spruce [154,155], sugar maple [115], spruce and beech [121], spruce [151], and birch and spruce [153]. It can be expected that the product density will reach a maximum close to the density of the plant cell wall (ca. 1.53 g/cm3 [112]). Hence, there is a limit on how much biomass can be densified. Stelte et al. [121] concluded that pressures above 200 MPa affected only slightly the pellet density for beech and spruce. Under high pressure, the natural binders (e.g., organic extractives and lignin) are pressed out of the particles, which enhances bonding between adjacent particles [105], resulting in larger adhesive strengths [147]. Stronger adhesion between particles reduces the risk of pellet expansion (i.e., spring-back) [96].

2.4.3 Pellet quality standards

In order to ensure reliable high qualities for wood pellets, the development of national and especially international standards is a key factor, as trade between countries becomes more global. It is important that the final pellet product satisfies the permissible threshold values for fuel-specific parameters stated in these standards, as variations in pellet quality would affect its thermal utilization. Typically, the pellet quality is agreed primarily with pellet producers so that the fuel requirements of the combustion application and the demands of the end user can be met [157].

The European Committee for Standardization (CEN/TC 335 Solid Biofuels) has developed a list of uniform characterization methods to harmonize and better compare pellet qualities on a European basis [158]. In 2014, the International Organization for Standardization (ISO/TC 238) published about 60 standards in the ISO 17225 series, which are largely based on CEN standards. The objective of the ISO 17225 is to create consistent sustainability and quality standards for solid biofuels worldwide to enable efficient trading and good understanding between the seller and buyer [159]. The new ISO standards have replaced all European standards. In general, the characterization of a solid biofuel has to be performed according to the latest test standards [157].

ISO 17225-2:2014 (Table 2-4) determines fuel quality classes and fuel specifications of graded pellets made from non-thermally treated woody biomass for industrial use [110]. If pellets fulfill the requirements outlined for I1, they are referred

to as I1. Wood pellets graded as I1 are the best quality pellets (but most expensive), while I3 pellets are pellets of the lowest quality (but cheaper).

Table 2-4: Important specifications of graded wood pellets for industrial use (I1, I2, I3) based on ISO 17225-2:2014 [110].

Wood parameters	Unit	I1 pellets	I2 pellets	I3 pellets
Diameter	mm	6 ± 1; 8 ± 1;	6 ± 1; 8 ± 1;	6 ± 1; 8 ± 1;
			10 ± 1;	10 ± 1; 12 ± 1;
Length	mm	3.15 - 40	3.15 - 40	3.15 - 40
Moisture	wt.% a.r.	≤ 10	≤ 10	≤ 10
Ash	wt.% DW	≤ 1.0	≤ 1.5	≤ 3.0
Mechanical durability	wt.% a.r.	97.5 - 99.0	97.0 - 99.0	96.5 - 99.0
Additives[a]	wt.% a.r.	< 3	< 3	< 3
Bulk density	kg/m3	600 - 750	600 - 750	600 - 750
Net calorific value	MJ/kg a.r.	≥ 16.5	≥ 16.5	≥ 16.5
PSD of disintegrated pellets	wt.% DW	≥ 99 % (<3.15 mm)	≥ 98 % (<3.15 mm)	≥ 97 % (<3.15 mm)
		≥ 95 % (<2.0 mm)	≥ 90 % (<2.0 mm)	≥ 85 % (<2.0 mm)
		≥ 60 % (<1.0 mm)	≥ 50 % (<1.0 mm)	≥ 40 % (<1.0 mm)

[a]Type and amount has to be stated.

Important specifications include the mechanical durability (or abrasive resistance) of pellets measured using a tumbling device according to ISO 17831-1:2015 [160]. This method predicts the fines production during storage, handling, and shipping. During these operations, the high amount of fines (i.e., lower durability) may increase the risk of fires and explosions [161]. The PSD of disintegrated pellets (or internal pellet PSD [162]) is another important fuel specification. For example, I3 pellets have coarser internal particles (≥ 40 % < 1 mm) than I1 pellets (≥ 60 % < 1 mm). The internal pellet

PSD is intended for operators of suspension-fired power plants, who mill wood pellets before combustion, to optimize the fuel particle burnout during suspension-firing. It is often believed that wood pellets, after comminution in the existing coal mills, will be broken down to the original feedstock PSD before pelletizing [157,163,164]. Hence, to obtain information about the pre-densified PSD of material within fuel pellets, pellets are disintegrated into their constituents in hot water according to ISO 17830:2016 [163]. The internal pellet PSD is hence an important fuel specification for industrial end users with respect to the particle combustion properties.

To aid the production of durable industrial wood pellets, several additives (up to 3 wt.%) can be added to the pelletization process. These include corn flour, potato flour, starch, vegetable oil, and lignin. Sometimes also pressing aids (e.g., oils and waxes) are used to reduce the die wall friction and pelletizing pressure, hence improving the production process [110].

2.5 Wood and pellet grindability

2.5.1 Wood pellet processing history

Pelletized wood for suspension-fired power plants undergoes multiple size reduction processes over its processing cycle. For example, if logwood is used as a feedstock for pelletization (**Paper I**), then the logistics of wood chip production has to be considered. In this scenario, chipping is the first size reduction step to turn the logwood into smaller pieces that can be handled easier by downstream milling operations. One of the most common chipping equipment is the drum chipper, consisting of a horizontally rotating drum with knives mounted on its surface [30]. Further size reduction of the fresh wood chips often occurs in a series of hammer mills (i.e., coarse and fine milling) with a drying step in between to enable easier control. After fine milling, pellets are produced. At the power plant, pellets undergo a final size reduction operation in the existing mills before combustion in the boiler. Pelletization and combustion processes have their specific particle size requirements to operate efficiently. Therefore, size reduction is important to modify the physical properties (e.g., particle size, shape, bulk density) of wood to fulfill the requirements of the

different conversion processes. Size reduction is also one of the most energy-intensive and expensive operations in fuel processing.

2.5.2 Wood fracture behavior

During wood processing, the size reduction equipment applies stress that causes deformation and fractures in wood. Wood fracturing happens in two steps: crack initiation and crack propagation, which are described in more detail in [76]. Generally, crack propagation in wood proceeds in opening mode (mode I) and sliding modes (mode II and mode III) [76], as shown in Figure 2-6. Theoretically, six propagation directions exist in wood due to the orthotropic nature of wood.

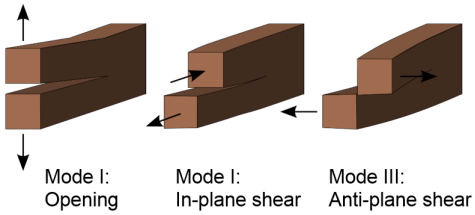

Figure 2-6: The three fracture modes in wood.

The main issue in all size reduction processes is the creation of a stress field inside the particles that is intense enough to cause fracturing. The stress provides the energy necessary for the crack growth process inside the particle and on the particle surface. The particle reaction (e.g., deformation, fracturing) to the state of stress depends on the physical and mechanical properties of the material, the state of stress itself, as well as the presence of flaws [21].

Influence of mill operating conditions and mill type

The applied stress required to fracture wood varies depending on the mill operating conditions and across mills due to different breakage modes [21], hence leading to fluctuations of the mill performance (i.e., grinding energy, throughput capacity, and milled product fineness). Different mills apply forces in different ways, which make them more suited to a particular material type [21]. For instance, hammer mills apply impact and shearing forces, while roller mills accomplish size reduction through a combination of compression and shearing. For a given mill breakage mechanism, there

exists a size reduction limit upon which comminution below a certain particle size is not possible [165]. Moreover, the mill performance depends on the grinding feedstock properties (cf. 2.3 Importance of feedstock properties).

Numerous parametric studies have been performed to investigate the effect of different mill operating conditions on the mill performance for different mill types [99,166–174]. The mill performance is significantly affected by the change in operating conditions. For example, decreasing the classifying screen size in a hammer mill and knife mill produces smaller biomass particles [171]. It is intuitive that grinding biomass to smaller particle sizes requires more energy. The milled particle size is inversely proportional to the new specific surface area created, i.e., the finer the particles, the higher the specific surface area. Therefore, the mill power consumption increases with an increase in the specific surface area [175]. Some studies [168,170] reported that increasing the mill feed rate decreased the specific grinding energy and had some effect on the average product particle size.

Table 2-5: Operating conditions for three mills that can affect the mill performance.

	Disc mill	Roller mill with dynamic classifier	Hammer mill
Breakage mode	Compression and shearing	Compression and shearing	Impact and shearing
Machine operating conditions	▪ feed rate ▪ disc distance ▪ disc speed ▪ disc structure	▪ feed rate ▪ number of rollers ▪ grinding pressure ▪ milling table speed ▪ roller angle ▪ structure of roller or table ▪ classifier rotor speed ▪ airflow to classifier	▪ feed rate ▪ rotor speed ▪ hammer-screen gap ▪ screen size ▪ fixed or free swinging hammers ▪ hammer shape

2.5.3 Grindability and grindability methods

Grindability

Different materials show a greater or lesser grindability, which is a measure of the material resistance to grinding. Materials that have the least grinding energy

requirement to reach fine sizes are classified as brittle (such as coal) [176], while those that require the largest grinding energy are referred to as non-brittle and fibrous (such as wood [177,178]). Unlike coal, which fractures explosively into many fragments when strained sufficiently, wood fractures progressively, resulting from the growth of cracks over the course of stressing events [176]. Almost all size reduction devices are designed for brittle materials and have some problems with non-brittle or ductile materials. Especially, mills that apply compression forces are likely to have major difficulties with these materials, as they tend to flatten and flake them. As a result, particle agglomeration may take place instead of size reduction [21].

Grindability methods

A grindability test allows comparing the relative grindability of different fuels before their utilization in power plant mills. The experimental data may also be used to model the comminution process in different mills. Over the years, standard grindability tests have been developed for coal to estimate its grinding behavior in industrial-scale mills: the Hardgrove Grindability Index (HGI) for ball, ring, and roller mills [179], the Bond Work Index for tube and ball mills [180], and the Hybrid Working Index for planetary ball mills [181]. Alternative grindability measures of coal include counting the number of mill rotations to reach a specified fineness [182] and methods based on its proximate analysis [183]. Currently, there is a lack of reliable standard grindability tests for lignocellulosic biomass. Recent studies [180,184] suggest that the classical HGI method is insufficient for determining the grindability of non-thermally treated biomass. The wood pellet industry and large-scale CHP plant operators are thus in need of a standardized grindability test to provide quantitative data on the grinding behavior of wood pellets in an industrial-scale mill.

2.5.4 Model predicting grinding energy and product size

The performance of a size reduction device can be evaluated in terms of grinding energy requirements and particle size achieved for a given material. It is hence of interest to predict the PSD after milling and the energy required to break the particles of a given size, shape, and material. Three well-known comminution theories, developed for the mineral processing industry, have been proposed by Von Rittinger, Kick, and Bond to predict the energy requirements for particle size reduction [20]. Kick

proposed the theory that the energy required to produce any given size reduction ratio in the volume is constant. Bond's theory is based on the assumption that the grinding energy is proportional to the length of the new crack formed. Von Rittinger proposed a theory stating that the grinding energy is proportional to the newly generated surface area [185].

Traditionally, for biomass, the relationship between the grinding energy and the obtained product size for a given feed size has been studied thoroughly without applying the above comminution theories [23,80,99,186,187]. Recently, several studies [81,101,188,189] have been aimed at finding ways to predict the energy requirements for wood chips and wood pellets with respect to the application of existing comminution laws. In all studies, among the three theories, the application of Von Rittinger's theory resulted in the best fit to the experimental data for hammer mills [81,188] and knife mills [101,189]. Therefore, Von Rittinger's comminution law is suited to predict the grinding energy requirement of wood chips and wood pellets. An advantage of this law is the application of the size reduction ratio to normalize the effect of the initial feed particle size. Von Rittinger's theory is defined as follows [165]:

$$SGEC = K_R \left(\frac{1}{d_p} - \frac{1}{d_f}\right) \quad (1)$$

Where *SGEC* is the specific grinding energy consumption (in kWh/t), d_p (in mm) is the characteristic particle size of the milled product, and d_f (in mm) is the characteristic particle size of the feed material. K_R (in kWh mm t^{-1}) is the Von Rittinger's constant, which is a measure of the wood grindability.

2.6 Wood particle characterization

The specific morphology (including size, size distribution, and shape) of particles is the result of their processing history. For many processing operations, morphology information is important for determining the physical material properties. The particle morphology typically varies with the size reduction equipment, milling conditions, and feedstock properties [162]. The particle size and shape also provide information about the overall performance of the size reduction operation. Characterizing particles by a single number is only accurate for monodisperse materials

containing spherical particles [20]. However, wood particles vary largely in size and appear irregular with elongated and/or flat shapes (Figure 2-7). The elongated particle shape is attributed to the anisotropic structure of wood [190]. Hence, it is better practice to describe the population of wood particles by a PSD and range of particle shapes.

Figure 2-7: Irregular shapes and sizes of wood particles retained on a sieve screen.

2.6.1 Particle size distributions

Commonly, PSDs are expressed as cumulative curves, which represent the fraction smaller (undersize) or larger (oversize) than the specified sizes [191]. Depending on the size analysis method, distributions can be by mass (sieve analysis) or volume (image analysis). An example of a cumulative undersize PSD analyzed by image analysis is presented in Figure 2-8. The 10th percentile (D10), the 50th percentile (D50), and the 90th percentile (D90) are important characteristics of the PSD. For example, the D50 is defined as the median particle size where half of the population lies. The absolute distribution span, defined as D90-D10, gives information about how narrow or wide a distribution is [192]. Analyzing the PSD (and its statistical parameters) of wood particles is useful to understand the influence of different processing operations on the PSD. The PSD data shown in this thesis is mostly presented in this form. Hence, a basic understanding of how to interpret these cumulative distributions is important.

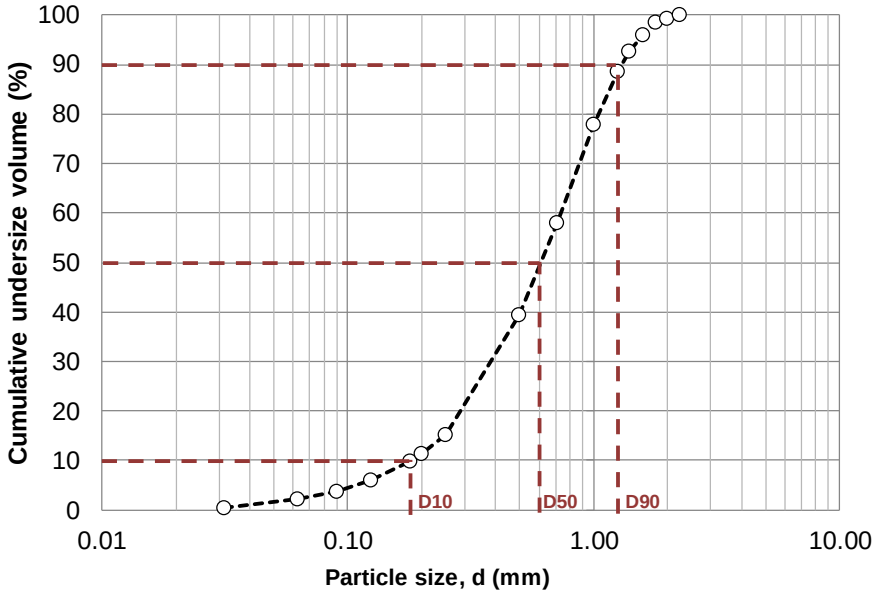

Figure 2-8: Example of a typical cumulative (%, undersize) PSD analyzed by image analysis. The important characteristics of the PSD are: D10=0.18 mm, D50=0.62 mm, D90=1.30 mm, and (D90-D10)=1.12 mm.

Prediction of particle size distributions

The Rosin-Rammler-Bennet-Sperling (RRBS) model distribution (also called Rosin-Rammler or Weibull distribution), originally used to represent the sieve analysis results of crushed coal [191], has been found to fit well with the PSD of milled biomass particles [167,174,193,194]. The RRBS model is a two-parameter distribution function expressed as follows [195]:

$$R(d) = 100 - 100 \cdot e^{-\left(\frac{d}{d^*}\right)^n} \quad (2)$$

Where *R(d)* is the cumulative (%, undersize) distribution of material finer than the particle size *d*, d^* is the characteristic particle size defined as the size at which 63.21 % of the PSD lies below, and *n* is the distribution parameter. A plot of ln[ln[100/(100-R(d)]] against ln(d) on the double logarithmic scale will give a straight line of slope *n*, if the PSD fits the RRBS model equation. The d^* also characterizes the material fineness.

2.6.2 Particle size distributions methods

Sieve analysis

Sieve analysis (or mechanical screening) is the most common, simple, and cheap method to determine the PSD of powdered materials [191]. It classifies large sample quantities physically into size fractions using wire mesh sieves, which commonly have square holes. The characteristic sieve size, $d_{sieving}$ (in mm), is then defined based on the square-hole sieves as the minimum aperture size through which each wood particle can pass. The individual size fractions are weighed. The sieve aperture size above and below the fraction governs the size range of each fraction. This information is converted into a mass-based cumulative (undersize) distribution related to the $d_{sieving}$. Sieve analysis is also the standard method to determine the PSD of solid biofuels (e.g., sawdust) [196].

Digital 2D image analysis

Dynamic image analyzers, such as the Camsizer® system (Retsch Technology GmbH, Germany) have been recently used to characterize the morphology of biomass particles [13,101,197–202]. The use of 2D images has the advantages that both size and shape information can be collected. Low concentrations are required to avoid misinterpretation due to particles overlapping. Particles are individually detected as projected areas, digitalized, and the images processed. Based on the 2D particle image, a quantitative description of the size and shape can be given. The PSD can be represented by different particle size descriptors (e.g., Feret diameter). Compared to sieve analysis, the PSD is presented as a cumulative volume distribution.

Alternative methods

Many studies have been conducted to characterize the morphology of biomass particles using alternative methods [187,199,203–207], including laser diffraction, focused-beam reflectance measurement (FBRM), flow cytometry analysis (FCM), static image analysis, and scanning electron microscopy (SEM). Measuring non-spherical biomass particles with laser diffraction was found to be inaccurate, as laser diffraction assumes that measured particles are spheres [187,199]. Moreover, laser diffraction provides no shape information. Visualizing biomass particles with SEM or static image analysis (e.g., optical microscope) has some drawbacks due to the time-

consuming analysis, particles overlapping, small sample size (low particle statistic), and the need for proper sample preparation (e.g., sputter-coating for SEM) [204]. Particle size measurements using FBRM only take place in wet media (e.g., water, ethanol), which may result in particle swelling [208]. FCM is not able to recognize particles larger than 0.1 mm [204]. Another method is 3D X-ray computed tomography (Figure 2-9), which allows the precise representation of all three particle dimensions, thus enabling calculations of the particle volume. However, the analysis of particles in bulk is very difficult, samples require proper preparation, and particle scans are very time-consuming.

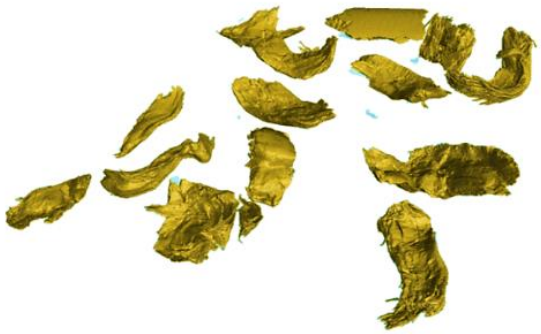

Figure 2-9: 3D representation of wood particles by X-ray computed tomography.

2.7 Concluding remarks

After reviewing the literature, one can conclude that wood size reduction and pelletization are complex processes affected by the chemical, physical, and mechanical properties of wood and the equipment used. Numerous material properties and machine variables have been reviewed that influence the performance of both the size reduction process (including grinding energy, milling capacity, and milled product fineness) and the pelletization process (including pelletizing energy, pelletizing capacity, and pellet quality).

Most of the pelletization studies available do not focus on the complete mechanical processing pathway of wood, but only on the optimization of the pelletization step. However, qualitative information about the particle morphology after

grinding and pelletizing are important to understand the transformations that occur during wood processing. This information can be used to optimize the processing steps that are crucial in determining the internal pellet particle size (and shape), which is expected to be close to the pre-densified PSD after pellet comminution in the existing coal mills.

Large-scale pellet production plants source their woody biomass locally and with different ratios of hardwood and softwood species. Understanding the structural differences between hardwood and softwood is important to evaluate the size reduction performance (e.g., grinding energy requirement) for pellets of different origin, and hence to relate the properties of the milled wood pellet PSD to the pre-densified wood PSD. Moreover, the different structure (e.g., density) of hardwood and softwood particles may affect their thermochemical conversion.

The major drawbacks of woody biomass compared to coal are its non-brittle fracture behavior and higher ignition sensitivity that complicate the size reduction process in the existing coal mills. Hence, there is a need to modify the existing power plant infrastructure to allow wood pellet operation. The published studies show no comparison of pellet grinding data between laboratory-and industrial-scale mills. It is therefore important to work on the correlation between lab-scale tests and industrial-scale tests to develop methods for wood pellets that can be used by power plant operators. The lack of test methods to predict the grindability of non-thermally treated wood pellets at the power plant urges the development of alternative methods.

Moreover, characterizing the physical and mechanical material properties may advance the understanding of the performance of the size reduction process. The applicability of Von Rittinger's comminution theory for wood pellets has been shown for the hammer mill and knife mill. It is hence of interest to extend this theory for other mill types, such as disc mill and roller mill. The advantage of applying this theory lies in characterizing the pellet grindability by a single parameter.

Chapter III

Experimental methods and materials

This section briefly introduces the biomass samples, experimental and material characterization methods used throughout the Ph.D. study. It describes the different wood pellet samples, and milling equipment used, as well as a list of characterization methods for wood pellets and wood particles. For a more detailed description of the experiments, references to the respective papers are given.

3.1 Biomass samples

In the following, the four wood pellet types (Figure 3-1a-d) used in the experimental studies (**Papers I-V**) are briefly described. The origin of the pellets and the chemical composition are summarized in Table 3-2.

Figure 3-1: Wood pellets used in the experimental studies: I1 pellets (a), I2 pellets (b), beech pellets (c), and pine pellets (d).

Table 3-1: Pellet samples and their chemical composition.

		Beech pellets	Pine pellets	I1 pellets	I2 pellets
Source		Denmark	Denmark	Baltic states[a]	Southeastern US[a]
Wood species		European beech (*Fagus sylvatica*)	Austrian pine (*Pinus nigra*)	Norway spruce[a] (*Picea abies*), Scots pine[a] (*Pinus sylvestris*)	Loblolly pine[a] (*Pinus taeda*)
Wood type		Hardwood	Softwood	Mainly softwood[a]	ca. 93% softwood[a]
Debarked		Yes	Yes	n/a	n/a
Experimental studies		**Paper I, Papers III-V**	**Paper I, Papers III-V**	**Papers II-IV**	**Papers II-IV**
Composition					
Carbohydrates					
Glucan	%, DW	39.2	38.1	40.0	39.5
Xylan	%, DW	18.0	4.3	12.7	6.7
Mannan	%, DW	1.7	11.3	4.0	9.3
Others	%, DW	4.9	5.8	4.1	5.0
Total	%, DW	63.8	59.4	60.8	60.5
Lignin					
Klason lignin	%, DW	23.4	24.8	22.4	27.2
ASL	%, DW	2.9	0.6	1.8	0.9
Extractives					
Water-soluble	%, DW	0.9	4.5	4.6	3.6
Ethanol-soluble	%, DW	0.9	10.6	5.7	6.4
Ash content	%, DW	0.5	0.6	0.9	0.9
Total	%, DW	92.4	100.6	96.2	99.5

[a]Information obtained from the power plant AMV1.

[b]Acid soluble lignin.

3.2 Wood pellet characterization

Pellets are characterized regarding their chemical, physical, and mechanical properties to relate their properties to the performance of the size reduction process in the mills.

3.2.1 Chemical characterization

The analysis of the composition of the raw lignocellulosic materials was carried out in the analytical laboratory at Celignis Biomass (County Limerick, Ireland) according to the standard analytical procedures provided by the National Renewable Energy Laboratory [209,210].

3.2.2 Physical and mechanical characterization

Pellets are characterized in triplicate according to international standardized methods, and their quality is assessed according to ISO 17225-2:2014 [110]. In the following, the main characterization methods are briefly described

Moisture content

The pellet moisture content is determined by drying a wood sample up to 16 h in a drying oven at 105±2°C according to ISO 18134-1:2015 [211]. The moisture content is calculated based on the mass decrease during drying.

Internal pellet particle size distribution

Pellets are disintegrated in hot deionized water and subsequently dried in an oven according to ISO 17830:2016 [163] to determine their internal PSD.

Specific density

The pellet ends are flattened with sandpaper to make them exact cylinders. The diameter and length of individual pellets are then measured using a caliper according to ISO 17829: 2015. The pellet weight is measured on an electronic balance (type EW-N, KERN & SOHN GmbH, Germany) to nearest 0.01 g. The specific density of a pellet is then simply calculated based on its known mass and volume.

Mechanical durability

The mechanical durability of pellets is measured using a tumbling device according to EN ISO 17831-1:2015 [160], which predicts the fine production during storage, handling, and shipping. Generally, pellets with low durability have a high amount of fines.

Diametral compressive strength

The diametral compression strength of single pellets is tested to assess their mechanical strength. The test may be appropriate to resemble how pellets break in compression mills, such as a roller or disc mill. The compressive strength is measured using a universal testing machine (type Z030, Zwick Roell GmbH & Co, Germany) with an Xforce K load cell of maximum 30 kN. A single pellet is radially compressed at a constant rate of 10 mm/min between two flat metal platens. Commonly, compression tests are applied for brittle materials to measure the maximum compressive load that a material can bear before cracking. However, an ideal point of failure cannot be expected for the non-brittle wood pellets. Thus, the compressive strength is defined as the maximum force (F_{max}) in N required to deform (strain) a pellet by 4 mm. As the maximum force is expected to depend on the pellet dimensions, the force is normalized by division with the pellet dimensions. The diametral compressive strength (in MPa) is calculated as follows [212]:

$$\sigma_c = \frac{F_{max}}{\pi LB} \quad (3)$$

Where L is the pellet length (mm), and B is 50 % contact width of the pellet diameter (mm). Pellets are sanded to produce smooth ends for length measurements. Force-deformation data for each pellet is recorded using testXpert II testing software V3.61.

3.3 Milling equipment

In the following, the three mill types used in the experimental studies (**Papers I–IV**) are briefly explained. These types include a disc mill, a vertical roller mill, and a hammer mill (Figure 3-2a-c).

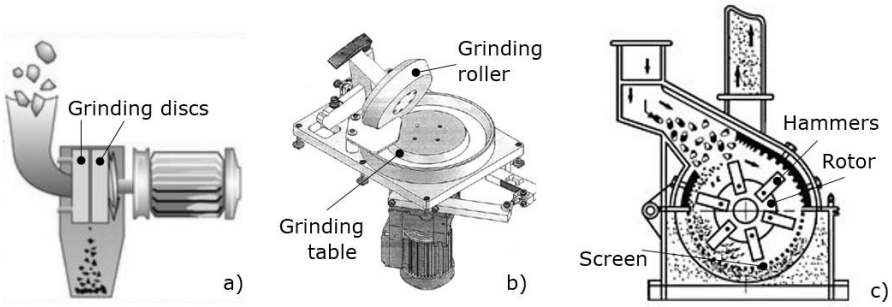

Figure 3-2: Illustration of the working principle of a disc mill adapted from [213] (a), a vertical roller mill adapted from [214] (b), and a hammer mill adapted from [215] (c).

The disc mill comminutes pellets in the gap between two grinding burr discs, one stationary and one rotating. The product fineness is controlled by changing the gap size. The vertical roller mill comprises one grinding roller and a grinding table. The roller moves due to the movement of the table, which is driven by an electric motor. Pellets fed onto the rotating table pass under the roller, which crushes the pellets. For better control of the product fineness, air classifiers (e.g., zigzag classifier or dynamic classifier) are used. The hammer mill comprises a rotating shaft mounted with hammers and an interchangeable classifying screen to control the particle top size. The rotating hammers apply impact forces and shearing between hammers and screen to break the pellets down in size. The screen prevents all oversized material from exiting the milling chamber, while the milled product, small enough to pass through the screen openings, leaves the mill. The finer the screen, the higher the recirculating load and hence less material can be handled by the mill. It is obvious that each mill design has a different mechanism to break the pellets. The different mill setups used in this thesis are summarized in Table 3-2.

Table 3-2: Mill setups used in the experimental studies.

	Disc mill	Vertical roller mill			Hammer mill
Breakage mechanism	Compression and shearing	Compression and shearing			Impact and shearing
Application	Laboratory	Laboratory	Laboratory	Industrial	Semi-industrial
Classifier	No	No	Zigzag classifier	Dynamic classifier	Internal screen classification
Milling-circuit	Open-circuit	Open-circuit	Closed-circuit	Closed-circuit	Closed-circuit
Mill type	Kenia, Mahlkönig, (Germany)	CMT mill	CMT mill	LM 19.2 D, Loesche GmbH (Germany)	Multimill 450 and Optimill 500, Andritz AG (Austria)
Motor drive power	0.60 kW	0.12 kW	0.12 kW	315 kW	90 and 110 kW
Feeder system	Vibrating feeder	Dosing feeder	Dosing feeder	Conveyor belt	Screw feeder
Wattmeter	Available	Available	Available	Available	Available
Mill operating conditions	**Paper III**	**Paper III**	**Paper IV**	**Paper II**	**Paper I**

3.4 Pelletizing equipment

In the following, the two pelletizing devices used in the experimental studies (**Paper I and Paper V**) are briefly explained. For the combustion experiments (**Paper V**), cubic beech and pine pellets are produced using a cubic metal die with a square-hole cross-section of 3.2x3.2 mm^2, equipped with a heating cast (Figure 3-3a). Temperature is controlled by two thermocouples connected to a controller. A removable bottom part functions as a backstop, and a removable top part is used to compress the raw material inside the cubic die via a hydraulic press. The compression force is measured using a 50 kN load cell. A semi-industrial ring die pellet mill, as illustrated in Figure 3-3b, produced beech and pine pellets from the fine grinds, i.e., the product from fine hammer milling (**Paper I**). The pellet mill is equipped with a control panel to control feeder frequency, and a continuous data logger to record throughput and mill power consumption. Pellets are produced using a warmed up die, as the pellet quality produced during start-up was not acceptable due to the cold die. Cooled and screened pellet samples are taken at steady-state conditions. The two pelletizing setups used in this thesis are summarized in Table 3-2.

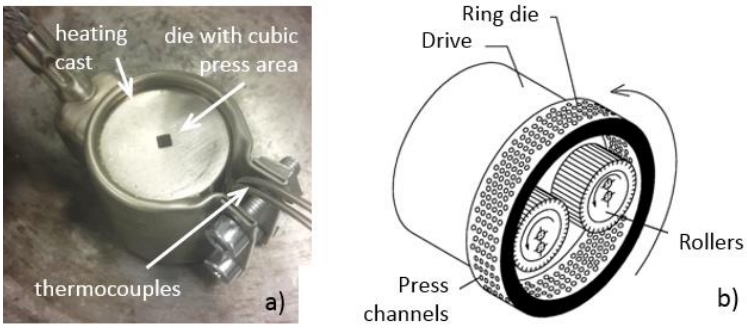

Figure 3-3: Illustration of the working principle of the cubic pellet die for producing single cubic pellets (a), and a ring die pellet mill adapted from [137] (b).

Table 3-3: Pelletizing setups used in the experimental studies.

	Single pellet press	Ring die pellet mill
Application	Laboratory	Semi-industrial
Type	Designed in-house	PM615W, Andritz AG (Austria)
Motor drive power	no motor	160 kW
Press channel cross-section	3.2x3.2 mm^2	π/4x6 mm^2
Press channel length	2 mm	35 and 50 mm
Pelletizing experiments	**Paper V**	**Paper I**

3.5 Combustion equipment

A lab-scale single particle combustion (SPC) reactor consisting of a hydrogen-fired burner and a gas supply system (Figure 3-4) is used in the combustion experiments (**Paper V**). The gas temperature, gas velocity, and oxygen concentration are adjusted to simulate an industrial suspension-fired boiler. The reactor conditions for the combustion tests are selected by regulating the flow rate of the inlet gases (i.e., H_2, O_2, N_2) to the metal burner. A suction pyrometer and gas analyzer (type Rosemount™ NGA 2000, Emerson, USA) measured the temperature and oxygen concentration (d.b.) at the center of the reactor, where the samples are combusted. A protection tube is inserted into the reactor to prevent particle conversion before reaching the reactor center position. Wood samples held by a thin thermocouple wire are then inserted from the opposite side of the reactor through the protection tube to the reactor center. The protection tube is then rapidly withdrawn from the reactor, and the particle conversion process is initiated. A high-quality camera (Stingray F-033B/F-033C, Allied Vision Technology GmbH, Germany) records the entire combustion process. Table 3-4 summarizes the SPC reactor conditions.

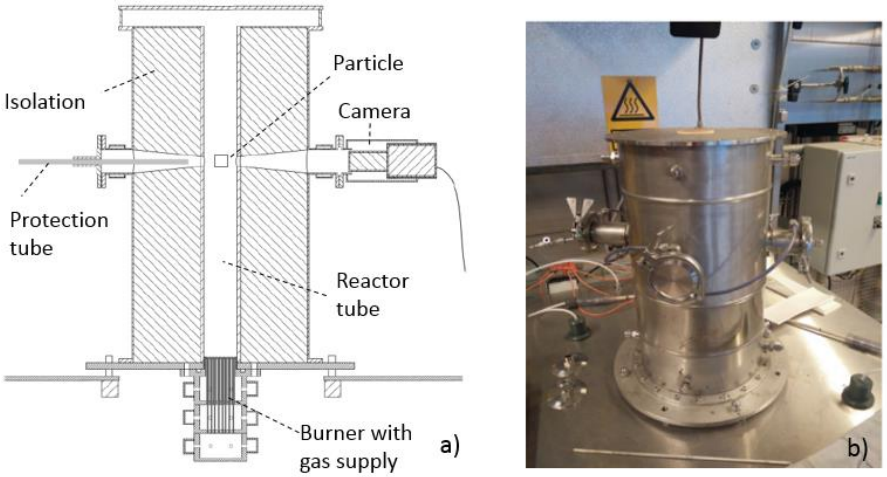

Figure 3-4: Schematic drawing of the SPC reactor (a). Adapted from [216]. Picture of the SPC reactor (b).

Table 3-4: SPC reactor at suspension-firing conditions.

	SPC reactor
Application	Laboratory
Temperature at reactor center	1260°C
Oxygen at reactor center	5.0 vol.%
Gas velocity around sample	1.52 m/s
Gas flow rates	8.4 Nl/min for H_2, 5.4 Nl/min for O_2, 22.3 Nl/min for N_2.

3.6 Wood particle characterization methods

The morphology characterization of wood powder particles has been done in many ways, including sieve analysis and dynamic image analysis.

3.6.1 Sample preparation from bulk samples

For particle size and shape analysis in the laboratory, proper sample sizes are necessary. Hence, the collected gross wood sample needs to be reduced to a laboratory sample size. The sample size reduction is done by mixing the gross sample thoroughly and splitting it into representative subsamples using a rotating sample divider (type PT100, Retsch Technology GmbH, Germany), which conforms to ISO 14780:2017 [217]. Wood products from the industrial and semi-industrial milling processes (**Papers I-II**) are sampled in motion and for many short time increments to ensure a true representation of the main bulk.

3.6.2 Sieve analysis

A vibrating sieve shaker (AS 200 control, Retsch Technology GmbH, Germany) is used to analyze the PSD of different wood samples. The sieve shaker consists of a base and a stack comprising square-hole sieves with a diameter of 200 mm. The number and aperture sizes of sieves held in the shaker are adjusted to the different wood types. For wood chips, sieves with aperture sizes of 1.4, 2.8, 5.6, 7.1, 10, 12.5, 16, 20 and 25 mm mounted on a collecting pan are used. For coarse grinds, aperture sizes of 0.5, 1.0, 1.4, 2.0, 2.8, 4.0, 5.6, 7.1, and 10 mm are used. For fine grinds, disintegrated wood pellets, and milled wood pellets, the sieve stack includes sieves with aperture sizes of 0.25, 0.5, 1.0, 1.4, 2.0, 2.8, and 3.15 mm. Samples of about 50-150 g were tested. The individual sieves and pan before and after sieving are weighed to nearest 0.01 g using an electronic balance (EW-N, KERN & SOHN GmbH, Germany). Following pre-tests on milled wood particles, sieve analysis run at 10 min and 1 mm amplitude was found to show acceptable repeatability.

3.6.3 Image analysis

Dynamic 2D image analysis

A dynamic 2D image analyzer (type Camsizer® X2, Retsch Technology GmbH, Germany) is used to record the shape and size of wood particles. The method conforms to the ISO 13322-2:2006 standard. The analyzer features two linked CCD cameras (a basic and a zoom camera) with a resolution of 4.2 megapixels per image. The zoom

camera zooms in on a region of the field of view to analyze smaller particles with higher resolution, whereas the basic camera records larger particles. The zoom camera provides a distribution of the smallest particles that are not captured by the basic camera. The 2D images are analyzed by the Camsizer® X2 software for size descriptors and shape parameters (see Table A-1 in Appendix I for definitions used in this thesis). Following pre-tests on milled wood particles, the maximum covered area of the two cameras was adjusted to discard images with too many particles to avoid misinterpretation due to particles overlapping.

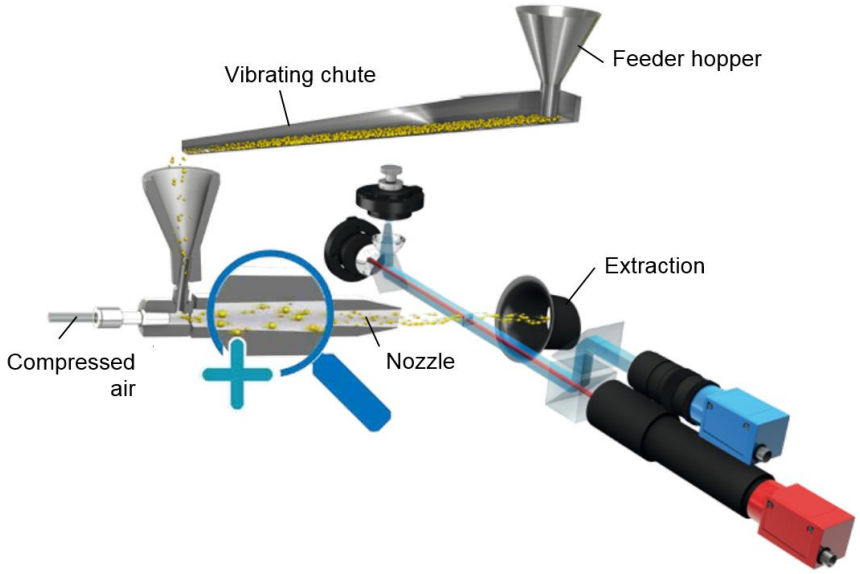

Figure 3-5: Principle of the X-Jet mode of the Camsizer® X2. Adapted from [218].

The analyzer offers three dispersion options: X-Fall for free fall dispersion (similar to the Camsizer P4), X-Jet for air pressure dispersion, and X-Flow for liquid dispersion. In the present thesis, the X-Jet mode (measuring range from 0.8 µm to 5 mm) of the Camsizer® X2 was used to disperse the wood particles falling from a vibrating feeder by a compressed air-driven venturi nozzle (Figure 3-5). When passing through the nozzle, particles are accelerated by the compressed air and subjected to shear forces, which break up agglomerates [218]. After the measurement, samples are collected in a vacuum cleaner. Pre-tests on wood particles were run to estimate the optimal compressed air pressure (30 kPa) and sample size (15-20 g). Velocity adaption

was performed using the Camsizer® X2. This function is required, as larger particles travel more slowly through the field of view of the cameras, which increases their probability to be detected by the camera. The X-Flow mode was not used due to swelling of wood particles in organic liquids [208] and its lower measuring range (0.8 µm to 1 mm). Trials on wood particles using the X-Fall mode, where particles fall between the field of view of the two cameras only by gravity, showed one major drawback. The wood particles tend to agglomerate and entangle with each other during free fall, which leads to a shifted PSD. Instead, the X-Jet mode resulted in better particle dispersion.

Scanning electron microscopy

The morphology of selected wood samples are analyzed by SEM (type TM3000, Hitachi High Technologies America, USA). The wood samples are prepared for SEM analysis by sputter-coating with gold using an ion coater.

3.7 Statistical analysis of experimental data

Statistical analysis of the experimental data was performed using R Studio (version 1.0.143, R Studio Inc., Boston, USA). The analysis includes calculating the mean and standard deviation of a data set, and the Pearson's correlation coefficients (r) to study the strength of linear relationships between two parameters. In some cases, multiple comparisons using one-way analysis of variance (ANOVA) followed by a Tukey's HSD test for post-hoc analysis was conducted to determine if there are significant differences between the means of independent groups. All results are considered statistically significant at the 95% confidence level ($p < 0.05$). On graphical presentation of results, error bars represent one standard deviation from the mean. In some cases, errors bars represent a 95% confidence interval to determine the reliability of a sample mean.

Chapter IV

Summary of the appended papers

Paper I

This Ph.D. thesis is intended to solve some of the remaining key challenges in relation to wood pellet conversion of coal CHP plants. One of these challenges is the understanding of the physical properties (size, shape, density) of the milled pellet particles and how these properties can be related to the process history of wood pellets. The first study (**Paper I**) contributes to the understanding of the processing pathway of wood pellets, as they are mechanically processed from wood chips to pellets and then to milled pellets. One hardwood (beech) and one softwood (pine) species are used to understand how the wood type affects the performance of the size reduction and pelletization process. The study quantifies how each of the processing steps, including fine feedstock milling, pelletization, and pellet comminution affect the morphology (size, shape) of wood.

The results show that pelletization does not modify the particle width, but reduces the particle length. This indicates a directional particle breakage behavior in the process of pellet formation, probably due shearing of wood particles in the ring die pellet mill. The particle breaking effect is more dominant for beech than pine. Fewer extractives in beech may cause greater friction in the roller-pellet die contact area, thus favoring a more brittle fracture behavior. The change in particle length inevitably influences the particle shape, resulting in particles with higher circularity and elongation ratio. Overall, beech and pine particles become rounder and less elongated along their processing pathway. Pelletization modifies the particle shape more than pellet milling, which only has a negligible effect on the particle shape. Pellet milling leads to higher bulk densities, narrower PSDs and reduces the particle lengths and widths compared to the fine grinds and disintegrated pellets. Final characteristic particle widths and lengths of 0.68 mm and 1.47 mm for milled beech pellets and 0.90 mm and 1.94 mm for milled pine pellets, respectively, are determined. The general trend in all milling steps is that milling pine produces longer and wider particles than beech.

Beech pellets, which have lower quality (e.g., durability and density) than pine pellets, are more difficult to disintegrate in hot water according to ISO 17830:2016, which causes beech particles to agglomerate. Adding, again, hot water to the dried disintegrated beech pellet particles results in better particle separation. In that case, it is suggested to perform the disintegration procedure twice. Disintegrated pine pellets contain longer and wider particles than disintegrated beech pellets. The study also shows that traditional sieve analysis represents well the wood particles width, but not the particle length and thickness. Caliper measurements show that all three dimensions of wood chips linearly increase with increasing sieve fraction.

This study also investigates the grinding and pelletizing energy requirement for pine and beech. Generally, milling pine requires more energy and leads to a lower Von Rittinger's size reduction ratio than beech, indicating a lower grindability for pine. A strong power law relationship (R^2=1.00 for pine and R^2=0.90 for beech) exists between the specific grinding energy and Von Rittinger's size reduction ratio, indicating that Von Rittinger's comminution law fits well the experimental data. The specific energy for grinding pine pellets is about 10 kWh/t DW for a characteristic product particle size of 0.8 mm, while grinding beech pellets requires about 7 kWh/t DW for a characteristic product particle size of 0.6 mm. For the same hammer mill screen size, milling pellets requires significantly less energy (ca. 80 %) than fine milling. Furthermore, pelletizing beech requires more energy than pine due to fewer extractives in beech.

Paper II

For suspension firing, the morphology (size and shape) of fuel particles is important, as it influences particle ignition and the unburned carbon content in the bottom ash and fly ash. The particle morphology depends on the mill type, milling conditions, and feedstock properties. Hence, comminution in the coal mills is crucial for the production of fuel particles with sufficient morphology to achieve complete combustion. For wood pellets, there is limited experience and knowledge regarding their grinding behavior in the existing power plant coal mills and the milled particle morphology. The second study (**Paper II**) aids to assess the grinding behavior of two industrial wood pellet qualities (designated I1 and I2 as per ISO 17225-2:2014) in coal roller mills in closed circuit with dynamic classifiers at the suspension-fired CHP plant AMV1 (Denmark). The study quantifies how the internal pellet PSD and milling

conditions influence both the mill performance (with respect to specific grinding energy and differential mill pressure) and the milled product morphology. During steady-state operation, average values for the mill operating conditions are recorded.

The results show that the mill classifier system significantly reduces the size of the internal pellet particles. At a mill load (i.e., the feed rate to the mill) of ca. 21 t/h, the milling of I1 and I2 pellets reduces the characteristic internal pellet particle size from 0.83 to 0.50 mm and from 1.09 to 0.56 mm, respectively. About 76 % of milled I2 pellets are below 1 mm compared to 84 % of milled I1 pellets. The difference in the largest particles can probably be linked to the internal pellet PSD, because I2 pellets are composed of a 20 % lower fraction of particles below 1 mm than I1 pellets. Hence, milled I1 pellets are more likely to achieve complete combustion in the available boiler residence time. Shape factors of milled pellet particles are similar to those of internal pellet particles, indicating that the roller mill only has little impact on the wood particle shape. Thus, observed shape factors are probably related to the upstream pelletization process and the original pellet feedstock material (**Paper I**). At similar milling conditions, milling I1 pellets to a particle size of 0.50 mm requires about 10 kWh/t, while milling I2 pellets to a particle size of 0.56 mm requires about 14 kWh/t, indicating a higher grindability for I1 pellets. The higher grinding energy for I2 pellets may be explained by their coarser internal pellet particles. Milling I2 pellets also leads to a 29 % higher differential mill pressure compared to I1 pellets, which increases the risk of mill choking (i.e., a situation that occurs when the mill pressure exceeds a threshold).

Reducing the primary airflow rate and increasing the classifier rotor speed result in a finer milled product PSD and thus larger Von Rittinger's size reduction ratios. However, this is at the expense of higher grinding energy and higher differential mill pressure, as more particles are returned to the milling table (i.e., higher circulation load). The mill operated at lower loads decreases the power consumption, the differential mill pressure, and increases the milled product fineness. However, this is at the expense of higher grinding energy. Hence, the larger the difference between the internal pellet PSD and the milled product PSD, the higher the grinding energy, which is in line with Von Rittinger's comminution theory. Mill load changes have a negligible effect on the wood particle shape. The study also shows that the RRBS model fits well the milled pellet PSD determined by sieve analysis (R^2>0.998) and dynamic image

analysis (R^2>0.988). However, sieving appears to be less accurate to describe the width of fine particles, possibly due to particle agglomerations on sieves with small apertures.

Paper III

There is a lack of standard grindability tests for non-thermally treated wood pellets. The most widely used grindability test for coal, the Hardgrove Grindability Index (HGI) test, works poorly to evaluate the grindability of wood due to its fibrous and non-brittle nature. Furthermore, the HGI test provides no information about the specific grinding energy. The third study (**Paper III**) aims to investigate the grindability characteristics (e.g., specific milling energy and milled product fineness) of as-received and oven-dried pellets in two lab-scale open-circuit compression mills (i.e., disc mill and roller mill). The study also characterizes the chemical, physical, and mechanical properties of pellets with the aim to predict the grinding energy requirement in a mill.

The initial fuel characterization shows that the xylan to mannan ratio may be used to distinguish between hardwood and softwood. Hence, I1 pellets probably comprise a higher proportion of hardwood, while I2 pellets contain more softwood. Disintegrated pine pellet particles have the largest characteristic size (1.16 mm), followed by I2 pellets (1.09 mm), beech pellets (0.99 mm), and I1 pellets (0.83 mm). Disintegrated beech and I1 pellet particles are rounder and less elongated than disintegrated pine and I2 pellet particles. The different particle morphologies are a result of the different pellet process history. Drying reduces the durability of pellets and hence their brittleness. The durability of dried pellets is in the order: I1 pellets (98.5 %) > I2 pellets (98.4 %) > pine pellets (97.3 %) > beech pellets (96.6 %). The study shows that the number of pellets present in a sample has a negative effect on the durability, indicating that most of the fines originate from the pellet end parts. The trend for the specific density of dried pellets is as follows: beech pellets (1219 kg/m^3) > I1 pellets (1174 kg/m^3) > pine pellets (1140 kg/m^3) > I2 pellets (1111 kg/m^3). The diametral compressive strength test shows that pellets have a non-linear (ductile) stress-strain behavior, which is well represented by a third-degree polynomial (R^2=0.986-0.997). The stress-strain curve indicates three distinct regions: a) an elastic part due to pellet distortion, b) a long plateau, and c) a region of final densification. This strength test may hence provide an understanding of how pellets will fracture in a compression mill. The maximum compressive strength for dried pellets is in the following order: pine

pellets (47 MPa) > I2 pellets (33 MPa) > beech pellets (30 MPa) > I1 pellets (13 MPa). The characteristic internal pellet particle size has a large effect on the maximum compressive strength.

The milling results show that drying improves the pellet grindability due to an increased material brittleness, resulting in a finer milled product, higher Von Rittinger's size reduction ratios, and grinding energy savings. The average grinding energy from the disc mill decreases from 8.0 to 4.3 kWh/t and from 0.7 to 0.6 kWh/t in the roller mill. Moisture acts as a plasticizer, which induces a more ductile fracture behavior and hence higher grinding energy. The disc mill produces a higher product fineness and achieves a higher Von Rittinger's size reduction ratio than the roller mill, which is at the expense of higher grinding energy. The pellet grindability depends on the mill type. For instance, milling beech pellets in the disc mill exhibits high grindability (i.e., favorable grinding characteristics), while milling beech pellets in the roller mill results in negative Von Rittinger's size reduction ratios, indicating that the grinding action under the roller is insufficient to disintegrate the pellets into their constituent particles. Hence, Von Rittinger's comminution theory can be applied to evaluate the breakage of pellets during milling. Milled beech pellet particles are rounder and less elongated than milled pine pellet particles, which is a similar trend for the disintegrated beech and pine pellet particles. Thus, pellet properties have a more dominant impact on the particle shape than the size reduction method applied.

The study also shows that the maximum diametral compressive strength and the characteristic internal pellet particle size have a large effect on the grinding energies from the disc mill and the roller mill. Hence, pellets with coarser internal pellet particles require a higher grinding energy effort in compression mills (**Paper II**). In operating a milling circuit, it is crucial to control variables (e.g., pellet moisture content, flow rate) that influence the size reduction performance. Under controlled conditions, the disc mill is suitable to compare the relative pellet grindability, i.e., whether they are easy or difficult to grind. The negative Von Rittinger's size reduction ratios obtained by the roller mill in open-circuit suggest investigating the pellet grindability in a closed-circuit operation, with the aim to achieve higher size reduction ratios (**Paper IV**).

Paper IV

Industrial coal mills with dynamic classifiers can be considered as a black box, where only the input (i.e., wood pellets) and output characteristics (i.e., suspended wood dust) of the milling circuit are known (**Paper II**). The classifier feed and reject cannot be known without proper sampling inside the mill, which makes it difficult to describe the milling and classification process accurately. The fourth study (**Paper IV**) hence aims to investigate the grindability of wood pellets in a lab-scale roller mill in closed-circuit with a zigzag classifier, which simulates a continuous milling operation similar to an industrial mill. It allows collecting samples around the zigzag classifier. Varying the air velocity in the classifier affects the final classifier product similar to changes in the feed (and airflow) rate in the industrial mill. The zigzag classifier provides information about the material circulation load and circulation factor, which are important measures for the mill capacity and the specific grinding energy with respect to the fine classifier fraction (SGE_{ff}). The study determines whether it is possible to predict the milling results obtained at the power plant (**Paper II**) by laboratory testing. It also compares lab-scale open- and closed-circuit milling (**Paper III**).

The comparison with the open-circuit mill shows that after reaching steady-state conditions, the closed-circuit system significantly reduces the grinding energy and produces a finer and narrower milled product, indicating a greater size reduction of the internal pellet particles. Decreasing the air velocity in the zigzag classifier produces a finer and narrower milled product, but increases the material circulation factor and the SGE_{ff}. The characteristic internal pellet particle size has a large effect on the SGE_{ff} from the roller mill in closed-circuit. Particles from the classifier product show an increasing circularity with decreasing particle size, which may indicate that the zigzag classifier follows Stokes' law to select the product particle sizes. The separation process in the zigzag classifier is based on both size and shape. The characteristic parameters of the separation efficiency curve (Tromp curve) from the zigzag classifier show that the particle separation process is very effective with moderate sharpness of separation.

The study shows a strong power-law relationship (R^2 between 0.961 and 0.999) between the SGE_{ff} from the lab-scale closed-circuit and the Von Rittinger's size reduction ratio and the characteristic product particle size. To grind pellets to a specific product particle size, beech pellets require the lowest SGE_{ff} followed by I1 pellets, I2

pellets, and pine pellets. At a fixed value of SGE_{ff} = 5 kWh/t FF, beech pellets achieve the highest Von Rittinger's size reduction ratio followed by I1 pellets, I2 pellets, and pine pellets. Thus, beech pellets have a higher grindability than pine pellets, and pellets with a finer internal PSD reach the target product size at lower grinding energy. The energy-size relationship for I2 pellets and pine pellets is very similar. This demonstrates a similar breakage behavior, probably due to their similar internal pellet PSD and origin.

The comparison with the industrial-scale mill shows that the proposed lab-scale system produces similar characteristic product particle sizes and Von Rittinger's size reduction ratios than the wood dust produced from industrial mills. However, the specific grinding energy from the lab-scale mill is lower. In the industrial mill, the energy-size and energy-size reduction relationships between I1 and I2 pellets based on the characteristic product particle size are relatively similar. The lab-scale mill confirms a similar energy-size reduction relationship between I1 and I2 pellets. However, I1 pellets require less energy than I2 pellets to be reduced to the same product fineness. The milled product PSD curves from the industrial mill are shallower and have a lower inclination than the product PSD obtained from the lab-scale mill. Hence, the zigzag classifier performs better than the industrial dynamic classifier, which broadens the milled product PSD.

Paper V

This study is motivated by previous research work [34,37], which have shown that the particle mass has a large influence on the devolatilization and char combustion time of raw and torrefied Schima hardwood particles of various sizes [34], and on the devolatilization time of raw and torrefied wood species with different apparent densities [37]. It is hence of interest to investigate if particles originating from the same wood species, but with different apparent densities influence the combustion process. The fifth study (**Paper V**) contributes to the research gap by investigating the combustion behavior of single particles of raw and pelletized beech and pine cubes at suspension-firing conditions (ca. 1260°C and 5 vol.% oxygen). The study aims to investigate the influence of pelletizing conditions on the combustion characteristics.

The results show that under similar pelletizing conditions, pelletizing pine particles leads to higher apparent pellet densities (980-1060 kg/m3) than beech (810-

1020 kg/m3). Pelletizing pine has a better pellet quality indicated by stronger inter-particle bonds that show higher dimensional stability (i.e., lower spring-back). Increasing the pelletizing pressure from 100 to 200 MPa has a stronger effect on the apparent pellet density than increasing the pelletizing temperature from 75 to 125°C. The combustion behavior of pelletized wood is very different from that of raw wood. During devolatilization, raw wood shrinks more in tangential direction than in longitudinal direction. Raw pine shows larger shrinking in both directions than beech, probably due to different hemicellulose content between pine and beech. During devolatilization, pellets largely expand in the longitudinal press direction (ca. 40-80%), while the expansion in the tangential direction is rather small (ca. 0-15%), indicating a stronger bonding between adjacent pellet particles in tangential direction than in longitudinal press direction. The rapid release of volatiles that causes high stress on the longitudinal direction can explain the expansion of the pellet structure. As a result, the bonds between adjacent pellet particles break. During devolatilization, pine pellets show better dimensional stability than beech pellets, which confirms weaker inter-particle bonding strengths produced during beech pellet production (possible due to the lack of extractives). Moreover, pelletizing conditions influence the pellet expansion during devolatilization, as pellets produced at least severe conditions result in larger expansion compared to pellets produced at the most severe conditions.

The study shows that the apparent density of raw and pelletized wood has a strong influence on the devolatilization time. During char combustion, the wood pellets fragment into their constituent particles, while no fragmentation takes place of the raw wood cubes. The combining effect of pellet fragmentation, different char yields, and different material properties may influence the different char burnout times. Pellet fragmentation is more pronounced for beech pellets indicating weaker inter-particle bonds in beech pellets. Different pelletizing conditions lead to different degrees of fragmentation. The char combustion time is the most time-consuming step of the total particle conversion process.

Chapter V

Concluding remarks

5.1 Introductory restatement of the research problem

This Ph.D. study completed experimental research on the characterization of wood pellets and milled pellet particles with the aim to contribute to the limited experience and knowledge about the pellet grindability in lab-and industrial-scale mills. The research was based on the hypothesis that the pellet grinding properties (e.g., specific grinding energy and milled product fineness) result from the combined effect of pellet processing history, wood properties, mill type, and milling conditions. The Ph.D. study attempted to accomplish the following objectives:

1. How can the milled wood pellet particle morphology be characterized?
2. How can the wood pellet grinding properties be tested? Can lab-scale mills predict the milling results obtained at power plants?
3. Is it possible to relate the wood pellet properties to the pellet grinding characteristics in a mill?
4. How do comminution and pelletization affect the physical properties (e.g., size, shape, and density) of wood particles?
5. How does the wood species affect the grinding and combustion characteristics?
6. How does pelletization influence the combustion process of wood particles?

5.2 Summary of findings and main conclusions

Only a few researchers have addressed the grindability of wood pellets and the characterization of the milled pellet particles in the existing power plant mills. This study provides a new understanding of the grindability of pellets with well-defined properties and new knowledge of the milled particle morphology to ensure an efficient grinding process.

Considerable insight has been gained with regard to the morphology changes of wood along its processing pathway from chips to pellets and to milled pellet particles. The study has highlighted that the industrial pelletization process has a larger impact on modifying the (original) pre-densified wood particle shape than the pellet milling step. Hardwood (beech) particles became rounder and less elongated along their processing pathway compared to softwood (pine) particles. This work has great value for power plant operators, as the milled pellet particle shapes obtained by roller or hammer mills are a result of the pellet processing history and origin. In view of these findings, this study represents an excellent initial step towards the understanding of the morphology changes occurring during the industrial pellet production process. This finding potentially allows pellet producers to control the shape (aerodynamic) properties of particles for suspension-firing.

The study has been able to demonstrate the different grinding behavior of pellets with a different origin. At the pellet plant, the milling of similarly sized hardwood (beech) and softwood (pine) chips has shown that pine produced coarser particles, led to a lower Von Rittinger's size reduction ratio, and required higher grinding energy. In the process of pellet formation, hence, pine pellets comprised coarser pre-densified particles compared to beech pellets, which, milled to a specific target size, required less grinding energy than pine pellets. The pellet grinding behavior can thus be ascribed to the pellet processing history, including both feedstock origin and internal pellet particle size distribution. Therefore, pellets with similar internal pellet particle sizes and origin are likely to demonstrate a similar grinding behavior.

Promising results have been found to predict the grinding behavior of wood pellets with a different origin by laboratory testing. The proposed roller mill equipped with a zigzag classifier was aimed to simulate a continuous grinding operation similar to an industrial vertical roller mill. It was shown that the lab-scale mill is useful to assess the grinding properties (milled product fineness and grinding energy) of the different pellet qualities. Beech pellets required the lowest grinding energy to achieve a specific size reduction ratio than the other three pellet samples. The comparison with the grinding results obtained at the power plant showed similar trends with regard to the pellet type and size reduction ratio on grinding energy. Hence, the proposed lab-scale mill with classifier has a great potential to be applied as a standard method to predict

the pellet grindability at industrial scale. Accurate prediction of the pellet grindability prior to the industrial-scale operation has economic and practical motivation for power plant operators, as there is no need for costly pilot-or industrial-scale experiments.

While some researchers believe that mills only break the pellets down into the pre-densified particle sizes, the study has demonstrated that mills not only break the weak interparticle bonds in pellets, but also achieve a size reduction of the particle length and width compared to the pre-densified (and disintegrated pellet) particles. The degree of particle size reduction achieved by the mill is thereby dependent upon the mill (i.e., type, conditions, circuit) and the material properties. Von Rittinger's comminution theory described well the relationship between size reduction ratio and grinding energy, suggesting that the milling of fibrous and non-brittle wood is likely dominated by the creation of new surface areas. Thus, Von Rittinger's comminution theory is a promising approach to evaluate the pellet breakage behavior during milling.

Considerable understanding regarding the grinding behavior of industrial wood pellets in the existing coal roller mills with classification equipment at the suspension-fired power plant Amagerværket (Denmark) has been gained. Milling of pellets with coarser internal particle sizes resulted in higher specific grinding energy, differential mill pressure, and larger fraction of milled coarse particles. The study has underlined that the internal (disintegrated) particle size distribution is an important specification to determine the pellet grindability. Information about the pellet grindability has great value for power plant operators. Thus, utilizing pellets made of finer particles can help to maximize the mill capacity, reduce the risk of mill choking (and mill wear), and facilitate complete combustion of particles in the available boiler residence time. However, those pellets are typically more expensive to produce, resulting in additional fuel costs.

The study has also reviewed current pellet specifications and established new measurable parameters that might be incorporated to characterize the chemical, physical, and mechanical properties of wood pellets for industrial use. Among these are biopolymer analysis, number of pellets present in a given sample, and diametral compressive strength. The number of pellets had a large effect on the pellet durability. The diametral compressive strength test has shown that pellets had a non-linear

(ductile) stress-strain behavior, which may predict how pellets will fracture in a compression mill (e.g., disc or roller mill).

The moisture content of pellets affects their grinding characteristics. Drying increased the pellet brittleness, milled product fineness, and reduced the grinding energy requirement. Thus, drying has the potential to maximize the mill capacity and improve the boiler efficiency. This finding highlights the importance of fuel drying, especially in biomass power plants that feature mill types with no integrated drying step, such as the disc or hammer mill, where new drying concepts may be installed to enhance the milling performance and reduce mill wear. The additional energy input for drying may be reduced by utilizing the waste heat contained in flue gases.

The pellet disintegration method in hot water (ISO 17830:2016), developed to determine the internal pellet particle size distribution, has great practical utility for the evaluation of the size reduction ratio achieved by the mill, especially when the pre-densified particle size distribution is unknown. However, beech pellets were more difficult to disintegrate into individual particles than pine pellets. Higher attractive forces between the smaller beech particles may explain their tendency to form agglomerates. Adding hot water again to the dried disintegrated beech pellets resulted in a better separation of all particles. The study hence suggests to perform the procedure twice, if particle agglomerates are observed after the first disintegration.

For the characterization of the milled particle morphology, traditional sieve analysis has shown to suffer from some limitations. These include the determination of only one particle dimension (i.e., width) and lower accuracy to describe the width of fine particles due to clogging of smaller sieve openings. Dynamic image analysis has shown the great importance of determining the length and shape of wood particles and hence has the potential to replace sieve analysis in the laboratory.

Finally, the study has been able to investigate the influence of wood pelletization on the combustion behavior at suspension-firing conditions. The study has shown that the wood type and pelletizing conditions affect the pellet swelling during devolatilization and the pellet fragmentation during char combustion, as well as that the apparent pellet density influences the devolatilization time. The findings implicate that fragmentation has some effect on the char combustion times.

5.3 Recommendations for future work

As a result of the above conclusions, it is recommended that further research should be undertaken in the following areas:

- *Characterization of milled wood particles*

  Future work should be done on the analysis of the flow properties and particle density, e.g., it would be interesting to determine how pelletization and comminution operation influence the wood particle density. Characterizing the flow properties (e.g., cohesiveness or stickiness) of milled wood particles could help to understand and optimize the milling process. For example, very cohesive wood particles may clog the classifying screen of a hammer mill.

- *Pellet disintegration in hot water*

  A more detailed understanding of the different disintegration mechanism between softwood and hardwood pellets would be desirable. The results shown for beech pellets should be validated by a larger sample size of pellets produced from well-defined hardwood.

- *Industrial pelletization process*

  Further research is needed to investigate the actual cause of the breakage of the longest wood particle dimension during the process of industrial pellet formation, and why beech particles are more likely to break than pine particles.

- *Pilot-and industrial-scale pellet milling*

  The promising grinding characteristics for beech pellets compared to pine pellets in the lab-scale closed-circuit roller mill should be validated by further experimental grinding studies in a pilot-or industrial-scale mill. Reproducing the results from the laboratory has the potential to apply this mill system as a standardized method to predict the pellet grindability in industrial roller mills.

- *Grindability testing*

  The current grindability procedure of the lab-scale closed-circuit roller mill is time-consuming due to the separate milling and separation operation. It is suggested to automate the mill to continuous operation from start to finish, which will reduce experimental error and analysis time. Moreover, replacing the zigzag classifier by a dynamic classifier may resemble more closely the classification operation in industrial roller mills.

- *Wood suspension-firing*

  Additional work on the combustion behavior of milled wood pellet particles obtained from different mills (e.g., roller mill and hammer mill) would help to relate the milled particle morphology to the combustion characteristics. In that way, critical sizes required for thermal conversion can be communicated with the size reduction process.

- *Effect of bark*

  Grinding tests may be extended on wood pellets containing bark. The industrial wood pellets (I1 and I2) in the present study probably contained bark particles, while beech and pine pellets comprised mainly stem wood. Generally, bark has a better grindability than stem wood. Further studies should investigate the grindability of pellets made from bark and wood blends.

References

[1] J.S. Gregg, S. Bolwig, O. Solér, L. Vejlgaard, S.H. Gundersen, P.E. Grohnheit, I.T. Herrmann, K.B. Karlsson, Report on experiences with biomass in Denmark, DTU. (2014).

[2] The Ørsted Way - let's create a world that runs entirely on green energy, Ørsted. (2017). https://orsted.com/-/media/Aarsrapport2017/Orsted_report_Summary_2017_Final_EN (accessed June 1, 2018).

[3] W.R. Livingston, The status of large scale biomass firing: The milling and combustion of biomass materials in large pulverised coal boilers, IEA Bioenergy Task 32: Biomass Combustion and Co-Firing. (2016) 21–23. http://www.ieabcc.nl/publications/IEA_Bioenergy_T32_cofiring_2016.pdf (accessed August 13, 2017).

[4] M. Odenberger, The role of combustion in the future energy system, Keynote Presentation at the Nordic Flame Days, in: Stockholm, Sweden, 2017.

[5] D. Level, P. Name, W. Package, Report on bioenergy framework for selected countries, (2015).

[6] M. Cocchi, L. Nikolaisen, M. Junginger, C.S. Goh, R. Hess, J. Jacobson, L.P. Ovard, D. Thrän, C. Hennig, M. Deutmeyer, P.P. Schouwenberg, Global wood pellet industry market and trade study, IEA Bioenergy Task. (2011) 190pp.

[7] C. Verhoest, Y. Ryckmans, Industrial Wood Pellets Report, (2014) 29. doi:IEE/10/463/SI2.592427.

[8] Usda Staff, The Market for Wood Pellets in Denmark, (2013) 3–5. http://gain.fas.usda.gov/Recent GAIN Publications/The Market for Wood Pellets in Denmark_The Hague_Denmark_11-5-2013.pdf.

[9] S. Korea, Sector Snapshot : Biomass Wood Pellets, (2015) 2012–2015.

[10] J. Joudrey, W. McDow, T. Smith, B. Larson, European Power from U . S .

Forests: How evolving EU Policy is Shaping the Transatlantic Trade in Wood Biomass, (2012) 44.

[11] Enviva Partners (LP), Business overview, (2018). https://www.envivapartners.com/sites/envivabiomass.investorhq.businesswire.com/files/doc_library/file/EVA_Investor_Presentation_June_2018_vFinal.pdf (accessed May 14, 2017).

[12] T. Napier-Munn, Is progress in energy-efficient comminution doomed ?, Minerals Engineering. 73 (2015) 1–6. doi:10.1016/j.mineng.2014.06.009.

[13] O. Williams, G. Newbolt, C. Eastwick, S. Kingman, D. Giddings, S. Lormor, E. Lester, Influence of mill type on densified biomass comminution, Applied Energy. 182 (2016) 219–231. doi:10.1016/j.apenergy.2016.08.111.

[14] D.I. Barnes, Understanding pulverised coal, biomass and waste combustion – A brief overview, Applied Thermal Engineering. 74 (2015) 89–95. doi:10.1016/j.applthermaleng.2014.01.057.

[15] N.S. Harding, Biomass cofiring in utility boilers, University of Utah, USA. (2012). https://utahbiomassresources.org/files-ou/15Presentation-Final.pdf (accessed May 20, 2018).

[16] M. Colechin, A. Malmgren, Best Practice Brochure: Co-Firing of Biomass (Main Report), Crown. (2005). http://webarchive.nationalarchives.gov.uk/tna/+/http:/www.dti.gov.uk/files/file20737.pdf (accessed February 15, 2017).

[17] C.B. Petersen, Conversion of a traditional coal fired boiler to a multi fuel biomass unit, Burmeister & Wain Energy A/S – BWE. (2011) 1–18. http://www.bwe.dk/download/articles_pdf/art-pge2011.pdf (accessed May 1, 2018).

[18] A. Malmgren, Talking about the revolution, World Coal. (2015) 1–4. http://www.bioc-ltd.com/images/Talking_about_the_revolution-World_Coal-Nov_2015.pdf (accessed June 8, 2017).

[19] H. Lechner, The Future of Biomass in the Renewables Portfolio, (2017). https://www.drax.com/wp-content/uploads/2017/12/Future-biomass-renewables-portfolio-Poyry-Drax.pdf (accessed April 2, 2018).

[20] M. Rhodes, Introduction to Particle Technology, 2nd ed., John Wiley & Sons, Ltd, Chichester, UK, 2008. doi:10.1002/9780470727102.

[21] D.W. Green, R.H. Perry, Perry's Chemical Engineers' Handbook, 8th ed., McGraw-Hill Education, 2007.

[22] J.L. Afolabi, The performance of a static coal classifier and its controlling parameters. PhD thesis, University of Leicester, UK. (2012).

[23] L.S. Esteban, J.E. Carrasco, Evaluation of different strategies for pulverization of forest biomasses, 166 (2006) 139–151. doi:10.1016/j.powtec.2006.05.018.

[24] A. Jankovic, W. Valery, Closed circuit ball mill-Basics revisited, Minerals Engineering. 43–44 (2013) 148–153. doi:10.1016/j.mineng.2012.11.006.

[25] N.M. Isa, Performance enhancement of a coal classifier (PhD thesis), University of Leicester, UK, (2012).

[26] B.G. Miller, Clean Coal Engineering Technology, 2nd ed., Butterworth-Heinemann, 2016.

[27] M. Masche, M. Puig-Arnavat, J. Wadenbäck, S. Clausen, P.A. Jensen, J. Ahrenfeldt, U.B. Henriksen, Wood pellet milling tests in a suspension-fired power plant, Fuel Processing Technology. 173 (2018) 89–102. doi:10.1016/j.fuproc.2018.01.009.

[28] I. Obernberger, G. Thek, The Pellet Handbook: The Production and Thermal Utilization of Biomass Pellets, Routledge, London, UK, 2010. http://bios-bioenergy.at/uploads/media/The-Pellet-Handbook-Flyer.pdf (accessed August 8, 2017).

[29] M. Tamura, S. Watanabe, N. Kotake, M. Hasegawa, Grinding and combustion characteristics of woody biomass for co-firing with coal in pulverised coal boilers, Fuel. 134 (2014) 544–553. doi:10.1016/j.fuel.2014.05.083.

[30] I. Obernberger, G. Thek, The Pellet Handbook : The Production and Thermal Utilization of Biomass Pellets, Earthscan Ltd, 2010.

[31] J.R. Gibbins, J. Williamson, Advances in laboratory tests for predicting coal-related combustion problems, Proceedings of the Institution of Mechanical Engineers, Part A: Journal of Power and Energy. 212 (1998) 13–26.

doi:10.1243/0957650981536709.

[32] S. Caillat, E. Vakkilainen, Biomass Combustion Science, Technology and Engineering, 1st ed., Woodhead Publishing Limited, 2013. doi:10.1533/9780857097439.3.189.

[33] J. Ballester, J. Barroso, L.M. Cerecedo, R. Ichaso, Comparative study of semi-industrial-scale flames of pulverized coals and biomass, 141 (2005) 204–215. doi:10.1016/j.combustflame.2005.01.005.

[34] Z. Lu, J. Jian, P.A. Jensen, H. Wu, P. Glarborg, Influence of Torrefaction on Single Particle Combustion of Wood, Energy and Fuels. 30 (2016) 5772–5778. doi:10.1021/acs.energyfuels.6b00806.

[35] M. Momeni, Fundamental study of single biomass particle combustion (PhD thesis), Aalborg University, Denmark, (2012).

[36] Z. Lu, J. Jian, P. Arendt Jensen, H. Wu, P. Glarborg, Impact of KCl impregnation on single particle combustion of wood and torrefied wood, Fuel. 206 (2017) 684–689. doi:10.1016/j.fuel.2017.05.082.

[37] H. Luo, Z. Lu, J. Jian, H. Wu, P.A. Jensen, P. Glarborg, Devolatilization of wood and torrefied wood with different apparent density: Experimental and modelling study, in: The Joint Meeting of the Polish and Scandinavian-Nordic Sections of the Combustion Institute, 2018.

[38] From sustainable biomass to competititve bioenergy, State of Green. (2015). https://stateofgreen.com/en/uploads/2015/11/From-Sustainable-Biomass-to-Competitive-Bioenergy.pdf (accessed May 24, 2018).

[39] Biomass for energy: Why coal and gas should be replaced by wood pellets and wood chips, Danish Energy Association. (2018). https://www.danskenergi.dk/sites/danskenergi.dk/files/media/dokumenter/2017-09/BiomassForEnergy.pdf (accessed October 18, 2018).

[40] T. Meth, Wood Pellet Production and Resource Potential (Report), Enviva. (2016).

[41] E. Sontag, The Wood Pellet Industry and its Supply Chain (Report), Enviva. (2016).

[42] Peer-Span GmbH, Wood shavings, (n.d.). http://peer-span.de/produkte/hobelspaene/ (accessed June 24, 2016).

[43] Peer-Span GmbH, Sawdust, (n.d.). http://peer-span.de/produkte/saegemehl/ (accessed June 24, 2016).

[44] Wood chips, (n.d.). http://www.drevozavod-prazan.cz/editor/filestore/Image/PilinyStepka/Stepka.jpg (accessed June 24, 2016).

[45] Logwood, (n.d.). http://images.nymag.com/realestate/features/realestate130121_log_560.jpg (accessed June 24, 2016).

[46] Stump, (n.d.). http://pre02.deviantart.net/4395/th/pre/i/2013/178/e/4/tree_stump_002___hb593200_by_hb593200-d6avfgk.png (accessed June 24, 2016).

[47] Bark, (2015). http://epsomsandandsoil.com.au/wp-content/uploads/2014/03/Coarse-Pine-Bark-e1394581555507.jpg.

[48] Enviva, Enviva biomass, (2016). http://www.envivabiomass.com/.

[49] South Environmental Law Center, New Study Shows Drax/Enviva Reliance on Southeast U.S. Hardwoods for Pellets Will Result in Greater Carbon Emissions Than Continued Reliance on Coal, (2014) 1–5. doi:10.1007/s13398-014-0173-7.2.

[50] Enviva Partners, Enviva track and trace, (2018). http://www.envivabiomass.com/sustainability/track-and-trace/ (accessed August 26, 2018).

[51] P. Technology, 2 . WOOD STRUCTURE AND FIBERS Table of content Kaj Henricson, (2004).

[52] University of Cambridge, The structure of wood, (n.d.). http://www.doitpoms.ac.uk/tlplib/wood/structure_wood_pt2.php.

[53] E. Sjöström, Wood Chemistry. Fundamentals and Applications, Academic Press Inc, 1981.

[54] R.J. Gravelsins, Studies of grinding of wood and bark-wood mixtures with the

Szego mill (PhD thesis), University of Toronto, Canada, 1998.

[55] Hardwood vs Softwood Timber, Timber Queensland. (n.d.). http://www.buyqldtimber.com.au/news-3/Hardwood-vs-Softwood-Timber.aspx (accessed September 18, 2016).

[56] J.W. Lee, Advanced Biofuels and Bioproducts, Springer, 2012.

[57] I.D. Cave, Modelling the structure of the softwood cell wall for computation of mechanical properties, Wood Science and Technology. 10 (1976) 19–28. doi:10.1007/BF00376381.

[58] H. Lichtenegger, A. Reiterer, S.E. Stanzl-Tschegg, P. Fratzl, Variation of Cellulose Microfibril Angles in Softwoods and Hardwoods - A Possible Strategy of Mechanical Optimization, Journal of Structural Biology. 128 (1999) 257–269. doi:10.1006/jsbi.1999.4194.

[59] L.J. Naimi, A Study of Cellulosic Biomass Size Reduction (PhD thesis), The University of British Columbia, Canada, 2016.

[60] R. Rowell, R. Pettersen, M. Tshabalala, Cell Wall Chemistry, in: Handbook of Wood Chemistry and Wood Composites, Second Edition, CRC Press, 2012: pp. 33–72. doi:10.1201/b12487-5.

[61] E.L. Back, L. Salmen, Glass transitions of wood components hold implications for molding and pulping processes, Tappi. 65 (1982) 107–110.

[62] P. Karinkanta, M. Illikainen, Effect of grinding conditions in oscillatory ball milling on the morphology of particles and cellulose crystallinity of Norway spruce (Picea abies), 67 (2013) 277–283. doi:10.1515/hf-2012-0098.

[63] P. Karinkanta, A. Ämmälä, M. Illikainen, J. Niinimäki, Fine grinding of wood – Overview from wood breakage to applications, Biomass and Bioenergy. 113 (2018) 31–44. doi:10.1016/j.biombioe.2018.03.007.

[64] S.-T. Yang, H. El-Ensashy, N. Thongchul, Bioprocessing Technologies in Biorefinery for Sustainable Production of Fuels, Chemicals, and Polymers, 1st ed., Wiley-AIChE, 2013.

[65] M. Ek, G. Gellerstedt, G. Henriksson, Wood Chemistry and Biotechnology, 1st ed., De Gruyter, 2009.

[66] J. Yan, Handbook of Clean Energy Systems, 1st ed., Wiley, 2015.

[67] Y. Huang, L. Wang, Y. Chao, D.S. Nawawi, T. Akiyama, T. Yokoyama, Y. Matsumoto, Relationships between Hemicellulose Composition and Lignin Structure in Woods, Journal of Wood Chemistry and Technology. 36 (2016) 9–15. doi:10.1080/02773813.2015.1039543.

[68] H. Chen, Biotechnology of lignocellulose: Theory and practice, 2014. doi:10.1007/978-94-007-6898-7.

[69] R.W. Kessler, Grundlagen wichtiger prozessanalytischer Methoden, Wiley, 2006.

[70] A.N.G. Uerra, I.L.F. Ilpponen, L.U.A.L. Ucia, C.A.R.L.S. Aquing, S.T.B. Aumberger, D.I.S.A. Rgyropoulos, Toward a Better Understanding of the Lignin Isolation Process from Wood, (2006). doi:10.1021/jf060722v.

[71] H. Yang, R. Yan, H. Chen, D.H. Lee, C. Zheng, Characteristics of hemicellulose, cellulose and lignin pyrolysis, Fuel. 86 (2007) 1781–1788. doi:10.1016/j.fuel.2006.12.013.

[72] R.L. Ethington, H.C. Hilbrand, Anisotropy in Wood, in: Fifth Pacific Area National Meeting of the Society, ASTM International, 100 Barr Harbor Drive, PO Box C700, West Conshohocken, PA 19428-2959, 1966: pp. 21-21–18. doi:10.1520/STP45149S.

[73] P. Krizan, The Densification Process of Wood Waste, 1st ed., Sciendo, 2015.

[74] D.W. Green, J.E. Winandy, D.E. Kretschmann, Mechanical Properties of Wood, in: Wood Handbook, 1999.

[75] J.M. Dinwoodie, Wood: Nature's cellular, polymeric fibre-composite, IOM Communications Ltd, 1989.

[76] P. Navi, S.E. Stanzl-Tschegg, Fracture behaviour of wood and its composites . A review COST Action E35 2004 – 2008 : Wood machining – micromechanics and fracture, Symposium A Quarterly Journal In Modern Foreign Literatures. 63 (2009) 139–149. doi:10.1515/HF.2009.012.

[77] M. Hughes, C.A.S. Hill, A. Pfriem, The toughness of hygrothermally modified wood – a review, (2015). doi:10.1515/hf-2014-0184.

[78] V. Repellin, A. Govin, M. Rolland, R. Guyonnet, Energy requirement for fine grinding of torrefied wood, Biomass and Bioenergy. 34 (2010) 923–930. doi:10.1016/j.biombioe.2010.01.039.

[79] Ladan J Naimi, Shahab Sokhansanj, Xiaotao Bi, C.Jim Lim, Staffan Melin, A Study on the Impact of Wood Species on Grinding Performance, 7004 (2012). doi:10.13031/2013.42268.

[80] Z. Miao, T.E. Grift, A.C. Hansen, K.C. Ting, Energy requirement for comminution of biomass in relation to particle physical properties, Industrial Crops and Products. 33 (2011) 504–513. doi:10.1016/j.indcrop.2010.12.016.

[81] M. Temmerman, P.D. Jensen, J. Hébert, Von Rittinger theory adapted to wood chip and pellet milling, in a laboratory scale hammermill, Biomass and Bioenergy. 56 (2013) 70–81. doi:10.1016/j.biombioe.2013.04.020.

[82] C. Nati, R. Spinelli, P. Fabbri, Wood chips size distribution in relation to blade wear and screen use, Biomass and Bioenergy. 34 (2010) 583–587. doi:10.1016/j.biombioe.2010.01.005.

[83] L. Shang, Upgrading Fuel Properties of Biomass by Torrefaction (PhD thesis), Technical University of Denmark, Denmark, (2012).

[84] P.C.A. Bergman, H.J. Veringa, Combined torrefaction and pelletisation, ECN Biomass. (2005) 29.

[85] J.E.G. Van Dam, M.J.A. Van Den Oever, W. Teunissen, E.R.P. Keijsers, A.G. Peralta, Process for production of high density/high performance binderless boards from whole coconut husk. Part 1: Lignin as intrinsic thermosetting binder resin, Industrial Crops and Products. 19 (2004) 207–216. doi:10.1016/j.indcrop.2003.10.003.

[86] J.S. Tumuluru, Effect of process variables on the density and durability of the pellets made from high moisture corn stover, Biosystems Engineering. 119 (2014) 44–57. doi:10.1016/j.biosystemseng.2013.11.012.

[87] A.M. Olsson, L. Salmen, Viscoelasticity of insitu lignin as affected by structure – softwood and hardwood, Acs Symposium Series. 489 (1992) 133–143.

[88] J. Chirife, M. Del, P. Buera, Water Activity , Glass Transition and Microbial

Stability in Concentrated / Semimoist Food Systems, 59 (1994) 921–927.

[89] P. Lehtikangas, Quality properties of pelletised sawdust, logging residues and bark, Biomass and Bioenergy. 20 (2001) 351–360. doi:10.1016/S0961-9534(00)00092-1.

[90] B.J. Ahn, H. sun Chang, S.M. Lee, D.H. Choi, S.T. Cho, G. seong Han, I. Yang, Effect of binders on the durability of wood pellets fabricated from Larix kaemferi C. and Liriodendron tulipifera L. sawdust, Renewable Energy. 62 (2014) 18–23. doi:10.1016/j.renene.2013.06.038.

[91] J. Bradfield, M.P. Levi, Effect of species and wood to bark ratio on pelleting of southern woods, (1984).

[92] J.K. Holm, U.B. Henriksen, J.E. Hustad, L.H. Sørensen, Toward an understanding of controlling parameters in softwood and hardwood pellets production, Energy and Fuels. 20 (2006) 2686–2694. doi:10.1021/ef0503360.

[93] T. Filbakk, G. Skjevrak, O. Høibø, J. Dibdiakova, R. Jirjis, The influence of storage and drying methods for Scots pine raw material on mechanical pellet properties and production parameters, Fuel Processing Technology. 92 (2011) 871–878. doi:10.1016/j.fuproc.2010.12.001.

[94] N.P.K. Nielsen, D. Gardner, T. Poulsen, C. Felby, Importance of temperature, moisture content, and species for the conversion process of wood residues into fuel pellets, Wood and Fiber Science. 41 (2009) 414–425.

[95] J. Bikerman, Causes of poor adhesion - weak boundary layers, Industrial and Engineering Chemistry. 59 (1967) 40–44.

[96] W. Stelte, C. Clemons, J.K. Holm, J. Ahrenfeldt, U.B. Henriksen, A.R. Sanadi, Fuel Pellets from Wheat Straw: The Effect of Lignin Glass Transition and Surface Waxes on Pelletizing Properties, (2011). doi:10.1007/s12155-011-9169-8.

[97] R. Samuelsson, M. Thyrel, M. Sjöström, T.A. Lestander, Effect of biomaterial characteristics on pelletizing properties and biofuel pellet quality, Fuel Processing Technology. 90 (2009) 1129–1134. doi:10.1016/j.fuproc.2009.05.007.

[98] R. Datta, Energy requirements for lignocellulose pretreatment processes, Process Biochemistry. 16 (1981).

[99] S. Mani, L.G. Tabil, S. Sokhansanj, Grinding performance and physical properties of wheat and barley straws, corn stover and switchgrass, Biomass and Bioenergy. 27 (2004) 339–352. doi:10.1016/j.biombioe.2004.03.007.

[100] S. Vasic, S. Stanzl-Tschegg, Experimental and numerical investigation of wood fracture mechanisms at different humidity levels, Holzforschung. 61 (2007) 367–374. doi:10.1515/HF.2007.056.

[101] O. Williams, E. Lester, S. Kingman, D. Giddings, S. Lormor, C. Eastwick, Benefits of dry comminution of biomass pellets in a knife mill, Biosystems Engineering. 160 (2017) 42–54. doi:10.1016/j.biosystemseng.2017.05.011.

[102] F. Pierre, G. Almeida, F. Huber, P. Jacquin, P. Perré, An original impact device for biomass characterisation: Results obtained for spruce and poplar at different moisture contents, Wood Science and Technology. 47 (2013) 537–555. doi:10.1007/s00226-012-0512-9.

[103] G. Kifetew, F. Thuvander, L. Berglund, H. Lindberg, The effect of drying on wood fracture surfaces from specimens loaded in wet condition, Wood Science and Technology. 32 (1998) 83–94. doi:10.1007/BF00702589.

[104] P.J.M. Pelgrom, M.A.I. Schutyser, R.M. Boom, Thermomechanical Morphology of Peas and Its Relation to Fracture Behaviour, Food and Bioprocess Technology. 6 (2013) 3317–3325. doi:10.1007/s11947-012-1031-2.

[105] N. Kaliyan, R. Vance Morey, Factors affecting strength and durability of densified biomass products, Biomass and Bioenergy. 33 (2009) 337–359. doi:10.1016/j.biombioe.2008.08.005.

[106] I. Obernberger, G. Thek, Physical characterisation and chemical composition of densified biomass fuels with regard to their combustion behaviour, Biomass and Bioenergy. 27 (2004) 653–669. doi:10.1016/j.biombioe.2003.07.006.

[107] S. Mani, L.G. Tabil, S. Sokhansanj, Effects of compressive force, particle size and moisture content on mechanical properties of biomass pellets from grasses, Biomass and Bioenergy. 30 (2006) 648–654. doi:10.1016/j.biombioe.2005.01.004.

[108] M. Shaw, Feedstock and Process Variables Influencing Biomass Densification (Master's thesis), University of Saskatchewan, Canada, (2008).

[109] W. Stelte, A.R. Sanadi, L. Shang, J.K. Holm, J. Ahrenfeldt, U.B. Henriksen, Recent developments in biomass pelletization – a review, 7 (2012) 4451–4490.

[110] International Organization for Standardization, ISO 17225-2:2014 - Solid biofuels - Fuel specifications and classes - Part 2: Graded wood pellets, (2014) 7–8.

[111] R. García Fernández, C. Pizarro García, A. Gutiérrez Lavín, J.L. Bueno de las Heras, J.J. Pis, Influence of physical properties of solid biomass fuels on the design and cost of storage installations, Waste Management. 33 (2013) 1151–1157. doi:10.1016/j.wasman.2013.01.033.

[112] K. Kranitz, Effect of natural aging on wood, (2014) 192.

[113] K. Frühmann, A. Reiterer, E.K. Tschegg, S.S. Stanzl-tschegg, Fracture characteristics of wood under mode I, mode II and mode III loading, Philosophical Magazine A. 82 (2002) 3289–3298. doi:10.1080/01418610208240441.

[114] W.T. Simpson, Specific gravity, moisture content, and density relationship for wood, USDA Forest Service. (1993) 13 pp.

[115] Q.N. Nguyen, A. Cloutier, A. Achim, T. Stevanovic, Effect of process parameters and raw material characteristics on physical and mechanical properties of wood pellets made from sugar maple particles, Biomass and Bioenergy. 80 (2015) 338–349. doi:10.1016/j.biombioe.2015.06.010.

[116] L. Baxter, Biomass-coal co-combustion: Opportunity for affordable renewable energy, Fuel. 84 (2005) 1295–1302. doi:10.1016/j.fuel.2004.09.023.

[117] M. Gil, E. Luciano, I. Arauzo, Approach to the breakage behavior of comminuted poplar and corn stover under single impact, Fuel Processing Technology. 131 (2015) 142–149. doi:10.1016/j.fuproc.2014.11.020.

[118] J. Jiang, J. Wang, X. Zhang, M. Wolcott, Characterization of micronized wood and energy-size relationship in wood comminution, Fuel Processing Technology. 161 (2017) 76–84. doi:10.1016/j.fuproc.2017.03.015.

[119] K.A. Rosentrater, Energy Consumption of Corn Stover Size Reduction, (2015).

[120] C. Serrano, E. Monedero, M. Lapuerta, H. Portero, Effect of moisture content, particle size and pine addition on quality parameters of barley straw pellets, Fuel Processing Technology. 92 (2011) 699–706. doi:10.1016/j.fuproc.2010.11.031.

[121] W. Stelte, J.K. Holm, A.R. Sanadi, S. Barsberg, J. Ahrenfeldt, U.B. Henriksen, Fuel pellets from biomass: The importance of the pelletizing pressure and its dependency on the processing conditions, Fuel. 90 (2011) 3285–3290. doi:10.1016/j.fuel.2011.05.011.

[122] N.Y. Harun, M.T. Afzal, Effect of Particle Size on Mechanical Properties of Pellets Made from Biomass Blends, Procedia Engineering. 148 (2016) 93–99. doi:10.1016/j.proeng.2016.06.445.

[123] M.T. Carone, A. Pantaleo, A. Pellerano, Influence of process parameters and biomass characteristics on the durability of pellets from the pruning residues of Olea europaea L, Biomass and Bioenergy. 35 (2011) 402–410. doi:10.1016/j.biombioe.2010.08.052.

[124] D. Bergström, S. Israelsson, M. Öhman, S.A. Dahlqvist, R. Gref, C. Boman, I. Wästerlund, Effects of raw material particle size distribution on the characteristics of Scots pine sawdust fuel pellets, Fuel Processing Technology. 89 (2008) 1324–1329. doi:10.1016/j.fuproc.2008.06.001.

[125] K. Theerarattananoon, F. Xu, J. Wilson, R. Ballard, L. Mckinney, S. Staggenborg, P. Vadlani, Z.J. Pei, D. Wang, Physical properties of pellets made from sorghum stalk, corn stover, wheat straw, and big bluestem, Industrial Crops and Products. 33 (2011) 325–332. doi:10.1016/j.indcrop.2010.11.014.

[126] A. Bharadwaj, L.L. Baxter, A.L. Robinson, Effects of intraparticle heat and mass transfer on biomass devolatilization: Experimental results and model predictions, Energy and Fuels. 18 (2004) 1021–1031. doi:10.1021/ef0340357.

[127] J. Saastamoinen, M. Aho, A. Moilanen, L.H. Sørensen, S. Clausen, M. Berg, Burnout of pulverized biomass particles in large scale boiler - Single particle model approach, Biomass and Bioenergy. 34 (2010) 728–736. doi:10.1016/j.biombioe.2010.01.015.

[128] M.A. Saeed, G.E. Andrews, H.N. Phylaktou, B.M. Gibbs, Global kinetics of the rate of volatile release from biomasses in comparison to coal, Fuel. 181 (2016) 347–357. doi:10.1016/j.fuel.2016.04.123.

[129] S. Clarke, P. Eng, F. Preto, Biomass Densification for Energy Production, Order A Journal On The Theory Of Ordered Sets And Its Applications. 3 (2011) 1–8.

[130] L. Tabil, P. Adapa, M. Kashaninejad, Biomass Feedstock Pre-Processing – Part 2: Densification, (2007).

[131] N. Yancey, C.C. Conner, T. Westover, R. McCulloch, K. Cafferty, M. Plummer, DOE Bioenergy Technologies Office (BETO) Develop and demonstrate preprocessing technologies to, (2015) 1–25.

[132] M. Stasiak, M. Molenda, M. Ba??da, E. Gondek, Mechanical properties of sawdust and woodchips, Fuel. 159 (2015) 900–908. doi:10.1016/j.fuel.2015.07.044.

[133] L. Eltrop, K. Raab, Leitfaden Feste Biobrennstoffe: Planung, Betrieb und Wirtschaftlichkeit von Bioenergieanlagen im mittleren und grossen Leistungsbereich, Fachagentur Nachwachsende Rohstoffe, 2014.

[134] T.M. Runge, C. Zhang, J. Mueller, P. Wipperfurth, Economic and Environmental Impact of Biomass Types for Bioenergy Power Plants, (2013) 44.

[135] T.O. Wilson, Factors affecting wood pellet durability (Master's thesis), The Pennsylvania State University, USA, 2010.

[136] TU Munich, Sketch flat die pellet mill, (2009). https://mediatum.ub.tum.de/node?id=732174.

[137] Sketch ring die pellet, TU Munich. (2009). https://mediatum.ub.tum.de/image/732175 (accessed June 18, 2018).

[138] J.K. Holm, U.B. Henriksen, K. Wand, J.E. Hustad, D. Posselt, Experimental verification of novel pellet model using a single pelleter unit, Energy and Fuels. 21 (2007) 2446–2449. doi:10.1021/ef070156l.

[139] N.P.K. Nielsen, J.K. Holm, C. Felby, Effect of fiber orientation on compression

and frictional properties of sawdust particles in fuel pellet production, Energy and Fuels. 23 (2009) 3211–3216. doi:10.1021/ef800923v.

[140] A.C. Fahrenholz, Evaluating factors affecting pellet durability and energy consumption in a pilot feed mill and comparing methods for evaluating pellet durability (PhD thesis), Kansas University, Manhattan, Kansas, (2012).

[141] A. Zafari, M.H. Kianmehr, Factors affecting mechanical properties of biomass pellet from compost, Environmental Technology (United Kingdom). 35 (2014) 478–486.

[142] A. Zafari, M.H. Kianmehr, R. Abdolahzadeh, Modeling the effect of extrusion parameters on density of biomass pellet using artificial neural network, International Journal Of Recycling of Organic Waste in Agriculture. 2 (2013) 9. doi:10.1186/2251-7715-2-9.

[143] A. Zafari, M.H. Kianmehr, Effect of raw material properties and die geometry on the density of biomass pellets from composted municipal solid waste, BioResources. 7 (2012) 4704–4714. doi:10.15376/biores.7.4.4704-4714.

[144] P. Pradhan, A. Arora, S.M. Mahajani, Pilot scale evaluation of fuel pellets production from garden waste biomass, Energy for Sustainable Development. 43 (2018) 1–14. doi:10.1016/j.esd.2017.11.005.

[145] L.G. Tabil, Binding and pelleting characteristics of alfalfa pellets (PhD thesis), University of Saskatchewan, Canada, 1996.

[146] M. Thomas, D.J. van Zuilichem, a. F.B. van der Poel, Physical quality of pelleted animal feed. 2. contribution of processes and its conditions, Animal Feed Science and Technology. 64 (1997) 173–192. doi:10.1016/S0377-8401(96)01058-9.

[147] W. Stelte, J.K. Holm, A.R. Sanadi, S. Barsberg, J. Ahrenfeldt, U.B. Henriksen, A study of bonding and failure mechanisms in fuel pellets from different biomass resources, Biomass and Bioenergy. 35 (2011) 910–918. doi:10.1016/j.biombioe.2010.11.003.

[148] W. Yanming, C. Zhongjia, Y. Xiangyue, Y. Guosheng, Influence of die temperature and moisture content on the densification of bamboo powder using die heating method, Wood Research. 63 (2018) 655–668.

[149] W. Stelte, Fuel pellets from biomass - Processing, bonding, raw materials (PhD thesis), Technical University of Denmark, Denmark, (2011).

[150] S. Aqa, S.C. Bhattacharya, Densification of preheated sawdust for energy conservation, Energy. 17 (1992) 575–578. doi:10.1016/0360-5442(92)90092-E.

[151] C. Rhén, R. Gref, M. Sjöström, I. Wästerlund, Effects of raw material moisture content, densification pressure and temperature on some properties of Norway spruce pellets, Fuel Processing Technology. 87 (2005) 11–16. doi:10.1016/j.fuproc.2005.03.003.

[152] L. Shang, N.P.K. Nielsen, W. Stelte, J. Dahl, J. Ahrenfeldt, J.K. Holm, M.P. Arnavat, L.S. Bach, U.B. Henriksen, Lab and Bench-Scale Pelletization of Torrefied Wood Chips-Process Optimization and Pellet Quality, Bioenergy Research. 7 (2014) 87–94. doi:10.1007/s12155-013-9354-z.

[153] Y. Huang, M. Finell, S. Larsson, X. Wang, J. Zhang, R. Wei, L. Liu, Biofuel pellets made at low moisture content – Influence of water in the binding mechanism of densified biomass, Biomass and Bioenergy. 98 (2017) 8–14. doi:10.1016/j.biombioe.2017.01.002.

[154] P. Križan, L. Šooš, M. Matúš, I. Onderova, D. Vukelic, Difference Between Compacting of Softwood and Hardwood, in: Scientific Proceedings 2009: Faculty of Mechanical Engineering, STU in Bratislava, Slovakia, 2009: pp. 1–7.

[155] P. Križan, M. Matúš, M. Svátek, J. Beniak, M. Lisý, Determination of Compacting Pressure and Pressing Temperature Impact on Biomass Briquettes Density and Their Mutual Interactions, in: 14th International Multidisciplinary Scientific GeoConference SGEM 2014 on Energy and Clean Technologies, 2014: pp. 133–140. doi:10.5593/SGEM2014/B41/S17.018.

[156] Y. Huang, M. Finell, S. Larsson, X. Wang, J. Zhang, R. Wei, L. Liu, Biofuel pellets made at low moisture content – Influence of water in the binding mechanism of densified biomass, Biomass and Bioenergy. 98 (2017) 8–14. doi:10.1016/j.biombioe.2017.01.002.

[157] S. Döring, Power from Pellets, 2015. doi:10.1017/CBO9781107415324.004.

[158] P.D. Kofman, Preview of European standards for solid biofuels, COFORD

Connect. (2010). http://www.woodenergy.ie/media/coford/content/publications/projectreports/cofordconnects/pp23.pdf (accessed May 16, 2017).

[159] E. Alakangas, International solid biofuels standards published, VTT Technical Research Centre of Finland. 1 (2016) 2–3.

[160] International Organization for Standardization, ISO 17831-1:2015 - Solid biofuels - Determination of mechanical durability of pellets and briquettes, (2015).

[161] F. Huess, J. Astad, J. Nichols, Inherent hazards, poor reporting and limited learning in the solid biomass energy sector: A case study of a wheel loader igniting wood dust, leading to fatal explosion at wood pellet manufacturer, Biomass and Bioenergy. 66 (2014) 450–459. doi:10.1016/j.biombioe.2014.03.039.

[162] P. Daugbjerg Jensen, M. Temmerman, S. Westborg, Internal particle size distribution of biofuel pellets, Fuel. 90 (2011) 980–986. doi:10.1016/j.fuel.2010.11.029.

[163] International Organization for Standardization, ISO 17830:2016 Solid biofuels - Particle size distribution of disintegrated pellets, (2014) 1–8.

[164] J. Riaza, J. Gibbins, H. Chalmers, Ignition and combustion of single particles of coal and biomass, Fuel. 202 (2017) 650–655. doi:10.1016/j.fuel.2017.04.011.

[165] T. Tanaka, Comminution Laws. Several Probabilities, Industrial & Engineering Chemistry Process Design and Development. 5 (1966) 353–358. doi:10.1021/i260020a001.

[166] M. Gil, I. Arauzo, E. Teruel, Influence of input biomass conditions and operational parameters on comminution of short-rotation forestry poplar and corn stover using neural networks, Energy and Fuels. 27 (2013) 2649–2659. doi:10.1021/ef4000787.

[167] M. Gil, I. Arauzo, Hammer mill operating and biomass physical conditions effects on particle size distribution of solid pulverized biofuels, Fuel Processing Technology. 127 (2014) 80–87. doi:10.1016/j.fuproc.2014.06.016.

[168] S. Balasubramanian, R. Sharma, S.V. Kumar, Effect of Moisture Content and Feed Rate on Size Reduction of Pearl Millet, Journal of Food Science and Engineering. 1 (2011) 93–99. http://www.davidpublishing.com/davidpublishing/Upfile/8/22/2011/2011082278652489.pdf.

[169] J. Cai, Y. He, X. Yu, S.W. Banks, Y. Yang, X. Zhang, Y. Yu, R. Liu, A. V. Bridgwater, Review of physicochemical properties and analytical characterization of lignocellulosic biomass, Renewable and Sustainable Energy Reviews. 76 (2017) 309–322. doi:10.1016/j.rser.2017.03.072.

[170] R.K. Raigar, H.N. Mishra, Grinding characteristics, physical, and flow specific properties of roasted maize and soybean flour, Journal of Food Processing and Preservation. 42 (2018) 1–9. doi:10.1111/jfpp.13372.

[171] Y. Liu, J. Wang, M.P. Wolcott, Assessing the specific energy consumption and physical properties of comminuted Douglas-fir chips for bioconversion, Industrial Crops and Products. 94 (2016) 394–400. doi:10.1016/j.indcrop.2016.08.054.

[172] K. Jindal, L.G. Austin, The Kinetics of Hammer Milling of Maize, 14 (1976) 35–39.

[173] J.S. Tumuluru, L.G. Tabil, Y. Song, K.L. Iroba, V. Meda, Grinding energy and physical properties of chopped and hammer-milled barley, wheat, oat, and canola straws, Biomass and Bioenergy. 60 (2014) 58–67. doi:10.1016/j.biombioe.2013.10.011.

[174] V.S.P. Bitra, A.R. Womac, N. Chevanan, P.I. Miu, C. Igathinathane, S. Sokhansanj, D.R. Smith, Direct mechanical energy measures of hammer mill comminution of switchgrass, wheat straw, and corn stover and analysis of their particle size distributions, Powder Technology. 193 (1) (2009) 32–45. doi:10.1016/j.powtec.2009.02.010.

[175] M. Meghwal, T.K. Goswami, Comparative study on ambient and cryogenic grinding of fenugreek and black pepper seeds using rotor , ball , hammer and Pin mill, Powder Technology. 267 (2014) 245–255. doi:10.1016/j.powtec.2014.07.025.

[176] R.J. Gravelsins, O. Trass, Analysis of grinding of pelletized wood waste with the Szego Mill, Powder Technology. 245 (2013) 189–198. doi:10.1016/j.powtec.2013.04.018.

[177] G. Schubert, S. Bernotat, Comminution of non-brittle materials, International Journal of Mineral Processing. 74 (2004) S19–S30. doi:10.1016/j.minpro.2004.08.004.

[178] P.I. Miu, A.R. Womac, C. Igathinathane, S. Sokhansanj, Analysis of Biomass Comminution and Separation Processes in Rotary Equipment – A Review, 2006 ASABE Annual International Meeting. (2006). doi:10.1.1.548.6573.

[179] Q. Zhu, Coal sampling and analysis standards, IEA Clean Coal Centre. (2010) 123. https://www.usea.org/sites/default/files/042014_Coal sampling and analysis standards_ccc235.pdf (accessed April 25, 2017).

[180] O. Williams, C. Eastwick, S. Kingman, D. Giddings, S. Lormor, E. Lester, Investigation into the applicability of Bond Work Index (BWI) and Hardgrove Grindability Index (HGI) tests for several biomasses compared to Colombian La Loma coal, Fuel. 158 (2015) 379–387. doi:10.1016/j.fuel.2015.05.027.

[181] D.T. Van Essendelft, X. Zhou, B.S.J. Kang, Grindability determination of torrefied biomass materials using the Hybrid Work Index, Fuel. 105 (2013) 103–111. doi:10.1016/j.fuel.2012.06.008.

[182] L.M. Hills, Solid Fuel Grindability: Literature Review, Portland Cement Association. (2007) 21.

[183] A.N. Sengupta, An assessment of grindability index of coal, Fuel Processing Technology. 76 (2002) 1–10. doi:10.1016/S0378-3820(01)00236-3.

[184] J. Hari, A. Khalsa, D. Leistner, N. Weller, L.I. Darvell, B. Dooley, Torrefied Biomass Pellets—Comparing Grindability in Different Laboratory Mills, (2016) 1–15. doi:10.3390/en9100794.

[185] L.G. Reddy, Energy requirements in size reduction of solids *, (n.d.).

[186] P. Adapa, L. Tabil, G. Schoenau, Grinding performance and physical properties of non-treated and steam exploded barley, canola, oat and wheat straw, Biomass and Bioenergy. 35 (2011) 549–561.

doi:10.1016/j.biombioe.2010.10.004.

[187] S. Paulrud, J.E. Mattsson, C. Nilsson, Particle and handling characteristics of wood fuel powder: Effects of different mills, Fuel Processing Technology. 76 (2002) 23–39. doi:10.1016/S0378-3820(02)00008-5.

[188] L.J. Naimi, F. Collard, X. Bi, C.J. Lim, S. Sokhansanj, Development of size reduction equations for calculating power input for grinding pine wood chips using hammer mill, Biomass Conversion and Biorefinery. 6 (2016) 397–405. doi:10.1007/s13399-015-0195-1.

[189] M. Manouchehrinejad, I. Van Giesen, S. Mani, Grindability of torrefied wood chips and wood pellets, Fuel Processing Technology. 182 (2018) 45–55. doi:10.1016/j.fuproc.2018.10.015.

[190] Q. Guo, X. Chen, H. Liu, Experimental research on shape and size distribution of biomass particle, Fuel. 94 (2012) 551–555. doi:10.1016/j.fuel.2011.11.041.

[191] H.G. Merkus, Particle size measurement fundamentals, practice, quality, 2009. doi:10.1007/978-1-4020-9016-5.

[192] B.B. Weiner, What is a Continuous Particle Size Distribution?, 2011.

[193] V.S.P. Bitra, A.R. Womac, Y.T. Yang, C. Igathinathane, P.I. Miu, N. Chevanan, S. Sokhansanj, Knife mill operating factors effect on switchgrass particle size distributions, Bioresource Technology. 100 (2009) 5176–5188. doi:10.1016/j.biortech.2009.02.072.

[194] W. Pichler, A. Weidenhiller, J. Denzler, R. Goetzl, M. Pain, M. Weigl, A. Haider, Modelling the particle size distribution of the feedstock for pellets production, 22nd European Biomass Conference and Exhibition, Hamburg, Germany. (2014) 25–26.

[195] T. Allen, Powder Sampling and Particle Size Determination, 1st ed., Elsevier Science, Oxford, UK, 2003.

[196] International Organization for Standardization, ISO 17827-2:2016 Solid biofuels - Determination of particle size distribution for uncompressed fuels - Part 2: Vibrating screen method using sieves with aperture of 3,15 mm and below, (n.d.). https://www.iso.org/standard/60688.html (accessed August 14,

2018).

[197] C.R. Cardoso, T.J.P. Oliveira, J.A.S. Junior, C.H. Ataíde, Physical characterization of sweet sorghum bagasse , tobacco residue , soy hull and fi ber sorghum bagasse particles : Density , particle size and shape distributions, Powder Technology. 245 (2013) 105–114. doi:10.1016/j.powtec.2013.04.029.

[198] A. Trubetskaya, P.A. Jensen, A.D. Jensen, A.D. Garcia Llamas, K. Umeki, P. Glarborg, Effect of fast pyrolysis conditions on biomass solid residues at high temperatures, Fuel Processing Technology. 143 (2016) 118–129. doi:10.1016/j.fuproc.2015.11.002.

[199] A. Trubetskaya, G. Beckmann, J. Wadenbäck, J.K. Holm, S.P. Velaga, R. Weber, One way of representing the size and shape of biomass particles in combustion modeling, Fuel. 206 (2017) 675–683. doi:10.1016/j.fuel.2017.06.052.

[200] C. Yin, M. Momeni, S.K. Kær, P. Due, J. Vej, Physical and combustion characteristics of biomass particles prepared by different milling processes for suspension firing in utility boilers, (2016).

[201] J.M. Johansen, R. Gadsbøll, J. Thomsen, P.A. Jensen, P. Glarborg, P. Ek, N. De Martini, M. Mancini, R. Weber, R.E. Mitchell, Devolatilization kinetics of woody biomass at short residence times and high heating rates and peak temperatures, Applied Energy. 162 (2016) 245–256. doi:10.1016/j.apenergy.2015.09.091.

[202] B. Göktepe, K. Umeki, R. Gebart, Does distance among biomass particles affect soot formation in an entrained flow gasification process?, Fuel Processing Technology. 141 (2016) 99–105. doi:10.1016/j.fuproc.2015.06.038.

[203] M. Gil, E. Teruel, I. Arauzo, Analysis of standard sieving method for milled biomass through image processing. Effects of particle shape and size for poplar and corn stover, Fuel. 116 (2014) 328–340. doi:10.1016/j.fuel.2013.08.011.

[204] A. Haapala, O. Laitinen, P. Karinkanta, H. Liimatainen, J. Niinimäki, Optical characterization of micro-scale cellulose particles and wood powder, Appita Annual Conference. 4 (2013) 70–77.

[205] T. Sato, N. Kobayashi, Y. Itaya, Development of Liquefaction Technique of

Pulverized Ligneous Biomass Powder, in: Aiche Annual Meeting, 2004.

[206] C. Igathinathane, L.O. Pordesimo, E.P. Columbus, W.D. Batchelor, S.R. Methuku, Shape identification and particles size distribution from basic shape parameters using ImageJ, Computers and Electronics in Agriculture. 63 (2008) 168–182. doi:10.1016/j.compag.2008.02.007.

[207] A.R. Womac, C. Igathinathane, P. Bitra, P. Miu, T. Yang, S. Sokhansanj, S. Narayan, Biomass Pre-Processing Size Reduction with Instrumented Mills, American Society of Agricultural and Biological Engineers. 300 (2007) 1–15. doi:10.13031/2013.23306.

[208] G.I. Mantanis, R.A. Young, R.M. Rowell, Swelling of Wood .2. Swelling in Organic Liquids, Holzforschung. 48 (1994) 480–490.

[209] A. Sluiter, B. Hames, R. Ruiz, C. Scarlata, J. Sluiter, D. Templeton, D. Crocker, Determination of structural carbohydrates and lignin in Biomass, 2012. doi:NREL/TP-510-42618.

[210] B. Hames, R. Ruiz, C. Scarlata, A. Sluiter, J. Sluiter, D. Templeton, Preparation of samples for compositional analysis laboratory analytical procedure (LAP), National Renewable Energy Laboratory. (2008) 1–9.

[211] International Organization for Standardization, ISO 18134-1:2015 - Solid biofuels - Determination of moisture content - Oven dry method, (2015).

[212] Z.Y. Lai, H.B. Chua, S.M. Goh, Influence of process parameters on the strength of oil palm kernel shell pellets, Journal of Materials Science. 48 (2013) 1448–1456. doi:10.1007/s10853-012-6897-x.

[213] Disc mill, (n.d.). https://pt.slideshare.net/MNButt/disc-mill/9 (accessed February 5, 2018).

[214] J. Wadenbäck, Nya karaktäriseringsmetoder för fasta bränslen – malbarhet, tändvillighet och sintring, in: Panndagarna, 2011.

[215] Hammer mill, (n.d.). http://www.jasenterprise.com/images/sectional-view-of hammer-mill.jpg (accessed July 14, 2018).

[216] R. Drexel, Single biomass particle combustion. Technical report (DTU Lyngby), 2013.

[217] ISO, ISO 14780:2017 Solid Biofuels - Sample Preparation, (2015).

[218] Horiba scientific, Particle Analyzer CAMSIZER® X2, (2017) 1–16.

[219] Retsch Technology GmbH, Manual Evaluation Software Camsizer® X2, (2017) 1–88.

[220] E.P. Cox, A Method of Assigning Numerical and Percentage Values to the Degree of Roundness of Sand Grains, Journal of Paleontology. 1 (1927) 179–183.

Appendix I

This appendix defines the particle size descriptors and shape factors used to describe the morphology of wood particles in the present thesis (Table A-1). Size and shape descriptors are provided by the Camsizer® X2 software [219].

Table A-1: Size and shape descriptors to characterize the wood particle morphology.

	Definition
Minimum chord length, $d_{c,min}$, is the smallest of all distances of a particle intersection, starting at a randomly chosen point at the perimeter of a projection. It displays the particle width, and it is analogous to sieve analysis.	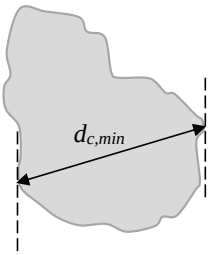
Maximum Feret diameter, $d_{Fe,max}$, is the longest distance between two parallel tangents on opposite sides of a randomly oriented particle (analogous to maximum caliper diameter). The $d_{Fe,max}$ is taken as the true particle length [199].	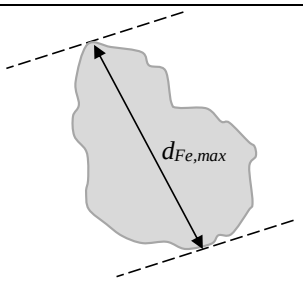
Elongation (or aspect) ratio, ER, displays the width-to-length ratio	$ER = \frac{d_{c,min}}{d_{Fe,max}}$
Circularity[a], C, is determined from the particle area ($A_{particle}$) and the particle perimeter ($P_{particle}$). It indicates how closely the particle projection resembles a circle or square.	$C = 4 \cdot \pi \cdot \frac{A_{particle}}{P^2_{particle}}$

[a]In the Camsizer® X2 software the circularity is actually referred to as sphericity. However, it actually represents the particle circularity defined by Cox [220].

Appendix II

From wood chips to pellets to milled pellets:
the mechanical processing pathway of
Austrian pine and European beech

Marvin Masche, Maria Puig-Arnavat, Peter A. Jensen, Jens K. Holm,
Sønnik Clausen, Jesper Ahrenfeldt, Ulrik B. Henriksen

Powder Technology 350 (2019) 134–145

Contents lists available at ScienceDirect

Powder Technology

journal homepage: www.elsevier.com/locate/powtec

From wood chips to pellets to milled pellets: The mechanical processing pathway of Austrian pine and European beech

Marvin Masche [a,*], Maria Puig-Arnavat [a], Peter A. Jensen [a], Jens Kai Holm [b], Sønnik Clausen [a], Jesper Ahrenfeldt [a], Ulrik B. Henriksen [a]

[a] Department of Chemical and Biochemical Engineering, Technical University of Denmark, 2800 Kgs. Lyngby, Denmark
[b] Bioenergy and Thermal Power, Ørsted, Nesa Allé 1, 2820 Gentofte, Denmark

ARTICLE INFO

Article history:
Received 20 September 2018
Received in revised form 27 February 2019
Accepted 2 March 2019
Available online 07 March 2019

Keywords:
Wood pellet
Wood chip
Hammer mill
Pellet mill
Specific energy
Particle size

ABSTRACT

This study assesses the changes in physical properties (particle size, shape, density) of Austrian pine (softwood) and European beech (hardwood), as they are mechanically processed from wood chips to pellets and then to milled pellets. A series of semi-industrial hammer mills and a semi-industrial pellet mill were used. The specific pelletizing and grinding energy, as well as the pellet mill and hammer mill capacity, were determined. Size, shape, and bulk density of the wood particles obtained at each processing step were studied. The pellet quality was analyzed according to international standards. Results show that the pelletization modifies the internal pellet particle shape and length due to the breakage of particles across their longest dimension, leading to more circular and less elongated particles. However, the particle width was nearly unaffected, indicating a directional fracture behavior for wood particles during pelletization. The particle breaking effect was more dominant for beech particles. Beech contained a lower amount of extractives than pine that led to higher specific pelletizing energy. In addition, beech pellets had a lower quality concerning durability and density. Relationships between specific grinding energies and characteristic product particle sizes were also determined. E.g., the specific energy for grinding pine pellets was about 10 kWh/t oven-dry wood for a characteristic product size of 0.8 mm, while grinding beech pellets required about 7 kWh/t oven-dry wood for a characteristic product size of 0.6 mm. The study concludes that less energy is needed to pelletize pine than beech under the same processing conditions, but more energy is needed to mill pine than beech.

© 2019 Elsevier B.V. All rights reserved.

1. Introduction

Denmark has a long history of encouraging the use of biomass in heat and power production. In 1993, a binding biomass agreement led to the use of biomass in several combined heat and power plants [1]. Today, wood pellets play an important role in the conversion of Danish coal suspension-fired power plants into biomass operation. The use of biomass has the potential to reduce life-cycle greenhouse gas (GHG) emissions from fossil fuel-derived electricity and heat [2]. To reduce the GHG emissions in Denmark, the largest Danish energy company, Ørsted, will stop all use of coal at its power stations by 2023 [3]. Biomass consumption for energy production in Denmark is hence expected to increase from 137 PJ in 2012 to 173 PJ in 2020 [4]. Moreover, Danish imports of wood pellets will increase from 2 million metric tons in 2012 to over 3 million metric tons in 2020 [5].

In the field of biomass pelletization, size reduction of woody feedstock is an important processing step, as it changes the physical properties (e.g., particle size, shape, flowability, bulk density) of biomass. Fig. 1 shows the mechanical processing pathway of pellet feedstock, which includes several size reduction steps. Hammer mills are commonly used for size reduction in a pellet plant. Size reduction increases the total surface-area-to-volume ratio and the inter-particle contact points. Smaller particles improve pellet strength properties [6,7]. They also lead to more durable [8] and denser pellets due to smaller particles rearranging and flowing into void spaces between coarser particles [9]. However, pellet producers will not comminute the raw material more than needed, as grinding biomass to smaller particles requires more energy.

Generally, the energy consumption for biomass grinding depends on particle feed size, moisture content, fiber length, density, biomass type, material feed rate, and milling equipment [10–13]. Temmerman et al. [10] reported higher energy consumptions for grinding wood chips and wood pellets with higher moisture levels. For similar moisture levels, pellets needed less grinding energy than wood chips. Vasic and Stanzl-Tschegg [14] observed that the total fracture energy to split a wood sample into two halves increased with increasing moisture levels, which they attributed to a higher wood ductility. Consequently, wood

* Corresponding author.
E-mail address: marv@kt.dtu.dk (M. Masche).

https://doi.org/10.1016/j.powtec.2019.03.002
0032-5910/© 2019 Elsevier B.V. All rights reserved.

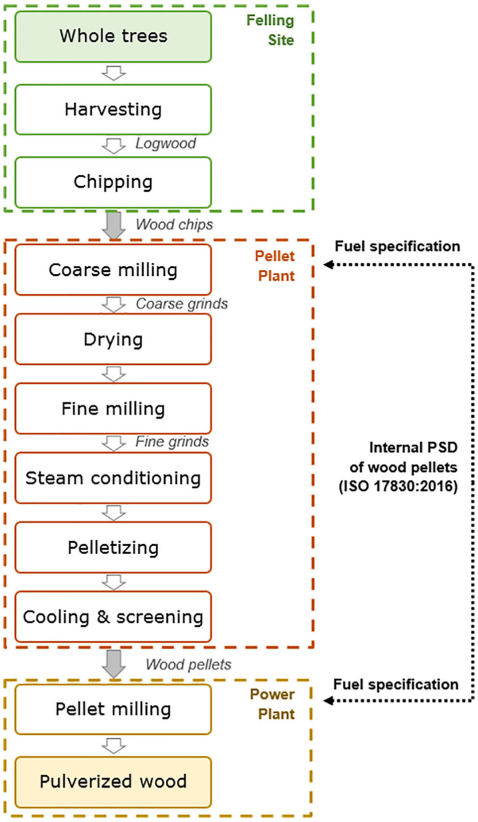

Fig. 1. Major processing steps of converting whole trees to pellets for pulverized wood-fired power plant boilers.

drying results in lower comminution energy [11] and provides smaller particles at similar mill settings [15] due to a more brittle fracture behavior.

It has also been well-documented that the chemical structure of biomass influences its pelletizing performance and pellet quality. Softwoods with greater extractive amounts require less power for pelletizing than hardwoods due to the lubricating effect of extractives that reduces the friction in the pellet die channels [16]. However, there has been some disagreement regarding the role of extractives in the pellet quality. Nielsen et al. [17] found that biomasses with more extractives decreased the pellet durability, while Filbakk et al. [16] established a positive relationship between extractives and pellet durability. In addition, the combining effect of lignin and extractives appears not to be well-understood. Ahn et al. [18] observed that blending bark into the pelletizing process significantly reduced the durability of larch pellets and slightly improved the durability of tulip pellets, while lignin powder steadily increased the durability of larch and tulip pellets. In contrast, Wilson [19] concluded that the lignin content has no noticeable impact on the durability of pellets, which were produced from pure and mixed hardwood and softwood species. During densification at high temperatures, lignin passes from a glassy to a rubbery phase, which improves the binding of adjacent particles [20]. The glass transition temperature of lignin was found to vary between wood species [21] and for different moisture contents [22]. Water acts both as a binder in pellets due to hydrogen bonds between adjacent particles [23] and as a friction-reducing lubricant in the die channel [24].

For large-scale biomass suspension-firing, wood pellets need to be milled before firing in the boiler. It is often believed that wood pellets, after comminution in the existing coal mills, will be broken down to the original particle size distribution (PSD) of the feedstock before pelletizing [25,26]. To obtain information about the pre-densified PSD of material within fuel pellets (i.e., the internal pellet PSD), pellets are disintegrated into their constituents in water according to ISO 17830:2016 [26]. Knowledge about the physical properties of fuel particles is important for achieving an undisturbed flow inside the pneumatic conveying pipe system, and for obtaining a stable flame and high fuel burnout. The internal pellet PSD is hence an important fuel specification for industrial end users with respect to the particle combustion properties.

The literature shows that the size reduction and pelletization of wood is a complicated process affected by the chemical, physical, mechanical, and fracture properties of wood and the equipment used. Most of the studies available only focus on one or two steps of the whole pelletization process. They mainly try to determine the pelletability of different biomass materials, optimize the operation of the pellet mill, or evaluate the resulting pellet quality and milling properties. However, to the best of the authors' knowledge, there are no studies that follow the complete mechanical processing pathway of wood. Considering that the internal PSD of wood pellets plays an essential role in determining the wood pellet quality, it is important to know how the PSD and particle shape is obtained and, furthermore, which steps are crucial in determining the particle size and shape of material within pellets. Thus, it is essential to assess the effect of each processing step on the wood particle size and shape. To achieve this objective, the present study follows the complete mechanical processing pathway of European beech (hardwood) and Austrian pine (softwood). All processing steps are included and carefully examined to provide knowledge of how pelletization and comminution operations alter the physical properties of wood particles. The results of this study will be relevant to pellet producers, who want to produce pellets of desirable quality for use in suspension-fired power plant boilers. Furthermore, studies focusing on pellet comminution usually lack the process history of pellets. Milling studies commonly lack information about the initial feed material characteristics. This study hence includes a thorough characterization of the chemical and physical properties of the wood chips utilized.

2. Materials and methods

2.1. Wood chip preparation

About 50-year-old European beech (*Fagus sylvatica*) trees and ca. 40-year-old Austrian pine (*Pinus nigra*) trees from Central Zealand (Denmark) were used in this work. The composition of the raw lignocellulosic materials was analyzed according to the standard analytical procedures provided by the National Renewable Energy Laboratory [27,28]. The trees were limbed, debarked, and turned into logs of wood (Fig. 2). The bark from the beech stem wood was removed nearly completely, while the pine stem wood showed some bark leftovers that may have resulted in a higher extractives content [29]. The logwood was chipped using a mobile wood chipper (DH 811 L, Doppstadt GmbH, Germany). Chipping represents the first size reduction step that turns the logwood into smaller pieces that can be handled easier by downstream milling operations. The initial moisture content of the logwoods was about 53 wt% for pine and 36 wt% for beech.

2.2. Pellet feedstock processing

The process flow for pelletizing wood at the pellet plant is the same as shown in Fig. 1. First, the fresh wood chips underwent coarse milling in a semi-industrial hammer mill (Optimill 500, Andritz AG, Austria)

Fig. 2. Limbed and debarked beech (left) and pine (right) logwood.

powered by a 110 kW motor and equipped with a 15 mm screen (Fig. 3). The purpose of coarse milling was to produce a more homogenous material that could be dried more evenly. The coarse milling was followed by drying in batch mode on a perforated steel floor, with hot air passing through. The coarse grinds were dried to a moisture content of about 12 wt%. The dried material was then milled in a hammer mill (Multimill 450, Andritz AG, Austria) powered by a 90 kW motor and equipped with a 4 mm screen, which is typically used for the production of 6 mm pellets [30]. The goal of fine milling is to achieve the desired PSD required for pelletizing.

2.3. Pellet production, characterization, and milling

Before pelletizing, the fine grinds were transported to a cascade mixer, where they were conditioned by hot steam to soften the lignin in the wood. The lignin softening enables fine grinds pelletization without adding binders, as the lignin serves as a natural binder to form solid interparticle bridges due to thermoplastic flow [31]. Pellets from the fine grinds were produced using a semi-industrial pellet mill (PM615W, Andritz AG, Austria) powered by a 160 kW motor. The pellet mill comprises a stainless steel, rotating perforated ring die with seven rows of 6 mm die channels (Fig. 4). Fine grinds are distributed over the inner surface of the ring die. Two rotating rollers press the fine grinds through the die channels, where they are compacted due to friction between the wood particles and the die wall. For the pelletization of pine, a die channel length of 50 mm was used, resulting in a die aspect ratio (ratio of channel length to channel diameter) of 8.3. However, to produce beech pellets of acceptable quality, the die aspect ratio had to be changed to 5.8 (die channel length of 35 mm). The need for a lower aspect ratio when pelletizing hardwoods compared to softwoods was also found in the literature [32]. After pelletizing, the hot pellets were cooled by ambient air in an updraft cooler and sieved using a 3.15 mm screen to remove fines.

Pine and beech pellets were then characterized in triplicate according to international standardized methods, and their quality was assessed by ISO 17225-2:2014 [33], which grades wood pellets for industrial use from I1 to I3. Wood pellets of property class I1 are considered as pellets of the highest quality, while I3 pellets are considered as pellets of the lowest quality. The mechanical durability of pellets was measured using a rotating tumbling box according to EN ISO 17831-1:2015 [34], which predicts the amount of fines produced during handling and transportation processes. A sample of 500 g was tumbled at

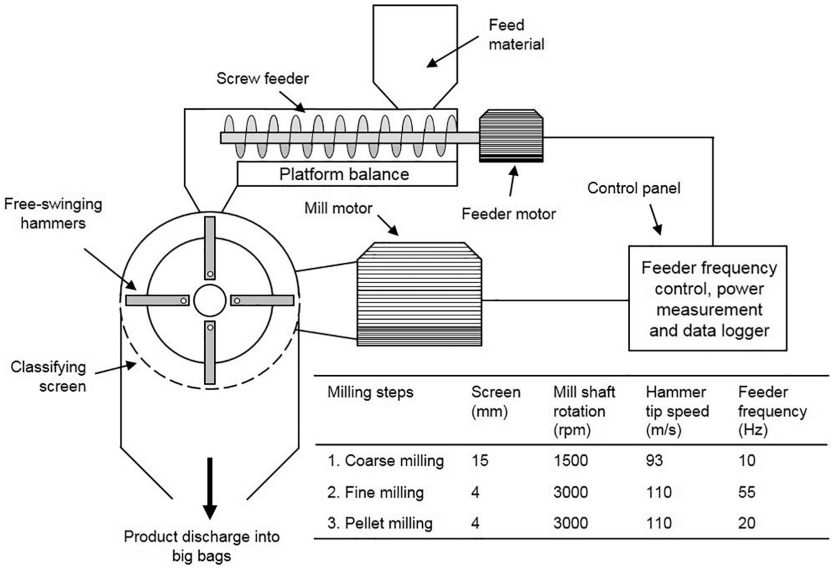

Milling steps	Screen (mm)	Mill shaft rotation (rpm)	Hammer tip speed (m/s)	Feeder frequency (Hz)
1. Coarse milling	15	1500	93	10
2. Fine milling	4	3000	110	55
3. Pellet milling	4	3000	110	20

Fig. 3. Experimental mill setup and the three milling steps performed at the pellet plant.

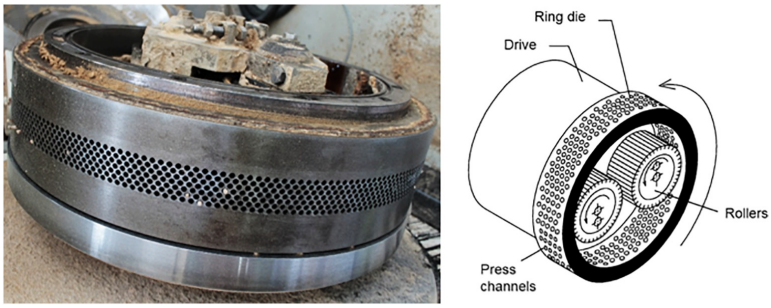

Fig. 4. Perforated ring die (left). Operating principle of the ring die pellet mill (right) adapted from [73].

50 rpm for 500 rotations. The durability is then calculated from the mass of sample remaining after separation of abraded particles.

Finally, pellets were comminuted in the hammer mill using a 4 mm screen that was also used for fine milling. The feeder motor frequency was lowered from 55 Hz to 20 Hz, which had the effect of reducing the feed rate to 64% of the previous value in order to avoid overloading the mill.

2.4. Measurement of specific grinding and pelletizing energy consumption

The milling and pelletizing equipment include a wattmeter to measure the instantaneous power consumption (W). The operating time (h), current (A) and feeding amount (kg) were recorded. A balance under the screw feeder measured the wood feed amount. From these parameters, the capacity in kg/h and total specific energy consumption (SEC) in kWh/t for grinding and pelletizing operations were calculated. The SEC was expressed as follows:

$$\mathrm{SEC} = \int_o^t \frac{P}{m_{feed}} dt \tag{1}$$

Where P represents the total, instantaneous power (W) consumed by the mill or pelletizer. m_{feed} is the amount of wood to be milled (or pelleted). SEC was corrected to a dry wood basis (DW) to allow the comparison among woods with different moisture contents. The idle power consumption of the hammer mill and pellet mill was not measured, as it was considered necessary to operate the milling and pelletizing equipment. Hence, the calculated values for SEC also include the energy required to run the mill empty (no load).

2.5. Wood characterization

2.5.1. Moisture analysis

All moisture contents reported in this study were determined in triplicate by drying the samples up to 16 h in a drying oven at 105 ± 2 °C according to ISO 18134-1:2015 [35]. The moisture content was then calculated based on the mass decrease during drying.

2.5.2. Bulk density measurements

The loose-packed bulk density was determined by pouring the sample into a funnel located at the top of a calibrated vessel of 5 l. A known sample mass was added to the vessel, and the sample volume measured. This procedure was done in triplicate.

2.5.3. Wood size and shape characterization

A vibrating sieve shaker (AS 200 control, Retsch Technology GmbH, Germany) was used to analyze the PSD of the different wood samples. The characteristic sieve size ($d_{sieving}$) is defined based on the square-hole sieves as the minimum aperture size in mm through which each wood particle can pass. For wood chips, the stack comprised nine square-hole sieves with a diameter of 200 mm, and aperture sizes of 1.4, 2.8, 5.6, 7.1, 10, 12.5, 16, 20 and 25 mm, mounted on a collecting pan. For coarse grinds, aperture sizes of 0.5, 1.0, 1.4, 2.0, 2.8, 4.0, 5.6, 7.1, and 10 mm were used. The sieve stack for the analysis of fine grinds, disintegrated wood pellets, and milled wood pellets included sieves of 0.25, 0.5, 1.0, 1.4, 2.0, 2.8, and 3.15 mm. Samples of about 50–150 g were tested. An electronic balance (EW-N, KERN & SOHN GmbH, Germany) weighed the individual sieves and pan before and after sieving. This information was converted into a cumulative (undersize) weight distribution versus $d_{sieving}$. $d_{sieving}$ represents the percentage of sample passing through each sieve. Sieve analysis was run for 10 min with 1 mm amplitude and performed in triplicate.

The wood chips were categorized into eight size classes according to the sieve stack used. Several runs of sieve analysis were performed to get a representative number of particles in each size class. Owing to the various shapes of wood chips, all chip dimensions were reported as means of at least a hundred measurements. Assuming that wood chips can be represented by flat cuboids (Fig. 5), their three dimensions were manually measured using a digital caliper with an accuracy of 0.01 mm. The length represented the longest distance between two parallel tangents restricting the particle along the grain direction. The particle width represented the second longest distance perpendicular to the length (and thus perpendicular to the grain direction). The thickness referred to the third longest distance perpendicular to both length and width. Measurements of the dimensions were performed on air-dried samples, as moisture differences between pine and beech wood chips would reduce the measurement accuracy. The wood chip weight was measured using a precision balance with an accuracy of 0.01 g. The specific chip density can then be calculated as the ratio between weight and volume. With the measurements of all three particle dimensions, the degree of elongation and flatness of a wood chip particle can be classified according to [36]:

$$\mathit{Elongation} = \frac{\mathit{Chip\ width}}{\mathit{Chip\ length}} \tag{2}$$

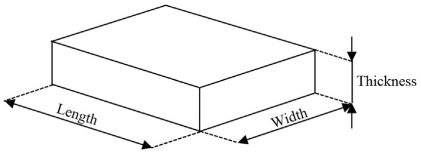

Fig. 5. Illustration of the length, width, and thickness of a typical wood chip.

$$Flatness = \frac{Chip\ thickness}{Chip\ length} \quad (3)$$

To complement the sieve analysis, the size and shape of fine grinds, disintegrated pellets, and milled pellets were also analyzed using a Camsizer® X2 (Retsch Technology GmbH, Germany) operated in X-Jet mode for air pressure dispersion. Measurements were performed in triplicate. The PSD is presented as a cumulative (undersize) volume distribution versus dc,min. dc,min represents the narrowest maximum chord length of a 2D particle projection measured from all measurement directions. Recent studies [37,38] suggest that dc,min gives close results to sieving data. Two shape factors provided by the Camsizer® X2 software were used to characterize the particle shape; elongation ratio (width-to-length ratio) and circularity. The elongation ratio (ER) is equal to one when particles are circles and squares, and it is defined as follows [39]:

$$ER = \frac{d_{c,\,min}}{d_{Fe,\,max}} \quad (4)$$

Where dFe, max refers to the maximum Feret diameter or maximum caliper diameter that is close to the true particle length [40]. The circularity (C) indicates how closely the 2D particle projection resembles a circle. The circularity defined by Cox [41] is described as follows:

$$C = 4{\cdot}\pi{\cdot}\frac{A_{particle}}{P^2_{particle}} \quad (5)$$

Where $A_{Particle}$ and $P_{Particle}$ refer to the particle projection area and the particle perimeter, respectively. An ideal perfect circle has a circularity value of 1.

2.6. Data analysis

The Rosin-Rammler-Bennet-Sperling (RRBS) model is used to describe the PSD of wood. It is a two-parameter distribution function expressed as a cumulative percent (undersize) distribution, which was found to be suitable to describe the PSD of wood pellet feedstock [42]. The RRBS equation is [43]:

$$R(d) = 100 - 100{\cdot}e^{-\left(\frac{d}{d^*}\right)^n} \quad (6)$$

Where R(d) is the cumulative percent (undersize) distribution of material finer than the particle size d, d^* is the characteristic particle size defined as the size at which 63,21% of the PSD lies below, and n is the distribution parameter. The d^* also characterizes the fineness of the wood material. The 10th percentile (D10) and the 90th percentile (D90) of the cumulative undersize distribution were used to determine the distribution span, (D90-D10).

Von Rittinger's comminution law is used to predict the energy consumption for grinding wood. Although Von Rittinger's law was developed for the mineral industry, recent studies [10,37,44] suggest its applicability to determine the energy demand for grinding lignocellulosic biomass. An advantage of this law is the application of the size reduction ratio to normalize the effect of the initial feed particle size. Von Rittinger stated that the energy required for size reduction is directly proportional to the new surface area produced [45], and he defined the relationship as follows [46]:

$$SGEC = K_R\left(\frac{1}{d_p} - \frac{1}{d_f}\right) \quad (7)$$

Where SGEC is the specific grinding energy consumption (in kWh/t), d_p (in mm) is the characteristic particle size of the milled product, and d_f (in mm) is the characteristic particle size of the feed material. In the case of pellet comminution, d_f is the characteristic particle size of the disintegrated pellet material. K_R (in kWh mm t^{-1}) is the material characteristic parameter or Von Rittinger constant, which is a measure of the wood grindability.

3. Results and discussion

3.1. Initial wood characterization

The chemical analysis shows, as it is typical for softwoods [47], that pine has a higher Klason lignin amount than beech (Table 1). On the other hand, beech comprises more carbohydrates, including glucose, a good indicator of the biomass cellulose content, and hemicelluloses, consisting of monomers like xylose, mannose, glucose, galactose, arabinose, rhamnose, and uronic acids. Mannose is the most common monomer in softwoods, while xylose is more prevalent in hardwoods. Pine also has a much higher content of water- and ethanol-soluble extractives than beech. The sum of the chemical composition of beech is lower than 100% unlike pine, probably because beech can contain a fair bit of acetyl groups [48] that are not accounted in the chemical analysis.

The wood chips produced are presented in Fig. 6. On average, sieve analysis showed nearly similar size distributions for pine and beech chips. In Fig. 7, the caliper-measured dimensions of pine and beech chips in the respective sieve size classes are shown. Similar to the sieve analysis, also the caliper-measurements show similar size distributions for pine and beech chips. Comparing Fig. 6. and Fig. 7, the sieve size distribution is mainly determined by the wood chip width, which confirms previous findings [11,49]. The sieve analysis does not represent the real length and thickness of wood chips due to their needle-like shape. The caliper measurements show that all three dimensions of pine and beech chips significantly ($p < .05$) increase in a linear manner with increasing sieve fraction. The chip thickness is significantly smaller than the other two chip dimensions, and wood chips in smaller sieves are more regular regarding their dimensions than those retained on coarser sieves.

The elongation and flatness of wood chips are shown in Supplementary Fig. S1. Smaller chips were a little more elongated than coarser wood chips, which was also observed by Lanning et al. [50] for chips produced from whole trees. The chip flatness ratio shows that, regardless of their length, both wood chips keep nearly the same flat shape. That means a flatness ratio of 0.23 for pine chips and 0.17 for beech chips. These findings are probably linked to the wood fracture mechanism during chipping, which is specific to the individual wood species. The chip length is controlled by the feed rate of the conveyor floor and the mesh size of the screening basket of the mobile chipper. The thickness and width of the wood chips are more a result of how wood fractures due to mechanical stress. As shown in Supplementary Fig. S2, pine chips are thicker than beech chips, but beech chips have a higher specific density than pine. Regardless of the chip length, beech chips are significantly denser (ca. 390 kg/m^3 on average) than pine chips (ca. 230 kg/m^3). The results are in good agreement with Twaddle's [51] result, who observed that the chip thickness is inversely proportional to the specific density, i.e., Douglas fir chips were thicker than denser beech chips.

3.2. Two-stage size reduction

The wood chips went through a two-stage milling process, including coarse and fine milling in a series of hammer mills. Before fine milling, the fresh coarse grinds were dried. The moisture contents and the PSD of milled beech and pine products are shown in Supplementary Fig. S3. As expected, fine milling produced smaller particles and a narrower size distribution span than coarse milling. The two-stage milling process resulted in a higher size reduction and a greater portion of fines for beech than for pine. For instance, the amount of particles below 1 mm increased from 27 to 87% for beech and from 4 to 60% for pine, from

Table 1
Chemical composition of pine and beech wood (% dry matter).

Wood	Carbohydrates					Klason lignin	Acid soluble lignin	Extractives		Ash	Total
	Total	Glucan	Xylan	Mannan	Others[a]			Water-soluble	Ethanol-soluble		
Beech	63.8	39.2	18.0	1.7	4.9	23.4	2.9	0.9	0.9	0.5	92.4
Pine	59.4	38.1	4.3	11.3	5.8	24.8	0.6	4.5	10.6	0.6	100.6

[a] Sum of arabinan, galactan, rhamnan, and uronics.

the first to the second milling stage. Drying the coarse grinds can be expected to favor the production of fines for the fine milling stage [15].

Table 2 presents the results for the milling performance of pine and beech in a series of hammer mills. The first milling stage produced characteristic particle sizes of 2.5 mm for beech compared to 4.0 mm for pine. The second milling stage led to characteristic particle sizes of 0.6 mm for beech and 1.0 mm for pine. Thus, the second milling stage reduced the characteristic particle size by about 75% and provided a product PSD that can be used in a pellet mill. Fine milling caused an additional drying of the material and reduced the initial moisture of coarse grinds (12 wt%) by ca. 30% (Supplementary Fig. S3). The results are in good agreement with previous observations [52,53], where it was observed that decreasing the hammer mill screen size increased the moisture reduction during milling due to both a longer particle retention time in the mill and a larger particle surface area produced [53]. In addition, the friction between particles and between particles and the equipment also causes an energy loss by heat dissipation, which also results in moisture loss.

The specific energy consumption for coarse milling was higher for pine (12.6 kWh/t DW) than for beech chips (8.1 kWh/t DW), as shown in Table 2. The higher moisture content for pine chips probably increased the ductility of wood [14] and thus the grinding energy effort. Pine chips were also thicker than beech, which affects the grinding energy, as more energy is required to fracture a thicker wood sample [54]. The fine milling increased the grinding energy input approximately by a factor of four for pine and a factor of five for beech. On average, fine milling beech required about 12% less energy and led to a 9% higher mill capacity than pine. The higher specific energy consumption for milling pine compared with beech is in line with previous findings [10,12].

3.3. Pellet production and pellet characterization

Table 3 shows the quality parameters of the produced beech and pine pellets, as well as the pelletizing performance. Regarding the determination of the internal PSD of pellets, the ISO procedure 17830:2016 worked well for pine pellets. For beech pellets, the ISO procedure was not able to separate all individual wood particles that constitute a pellet. As a consequence, agglomerated particles were observed after the hot water disintegration procedure. This resulted in an overestimation of larger particles. Higher attractive forces between smaller particles due to van der Waals interactions [55] may explain the greater tendency for beech particles to form agglomerated particles during disintegration in hot water. Attempts to break up the agglomerated particles by using a sieving amplitude of 3 mm, as suggested by Jensen et al. [56], did not lead to a considerably better particle separation (see Supplementary Fig. S4). However, adding, again, hot water to the dried disintegrated beech pellet particles was found to be the best method to achieve a better particle separation. The pellet disintegration results in Table 3 indicate that pine pellets contain 20% fewer particles below 1 mm compared to disintegrated beech pellets.

After pelletizing, beech pellets had a lower moisture content than pine pellets. This could be explained by higher friction in the pellet die during pelletization of beech due to its lower extractive content [17]. Temperature measurements of the steam produced during the pellet production process corroborate the observations made. Pelletizing beech led to a higher temperature (100 °C) than pelletizing pine (70–75 °C). Also, the higher amount of fines in beech sawdust (ca. 50% below 0.5 mm) can increase the friction in the die [57]. Higher friction generates heat that will be quickly transferred to the beech particles causing further drying. This can explain the slightly burnt surfaces on beech pellets that were not observed on pine pellets (Supplementary Fig. S5). The lack of water in beech pellets probably reduces the binding effect of water, which can impact the inter-particle bonding and thus the pellet durability [24].

The bulk density for pine and beech pellets falls within the range of previously reported values (i.e., 498–649 kg/m^3) [58]. However, only pine pellets comply with the international standard for industrial pellets, ISO 17225-2:2014 [33], that requires a bulk density equal to or above 600 kg/m^3. The lower bulk density of beech pellets can be

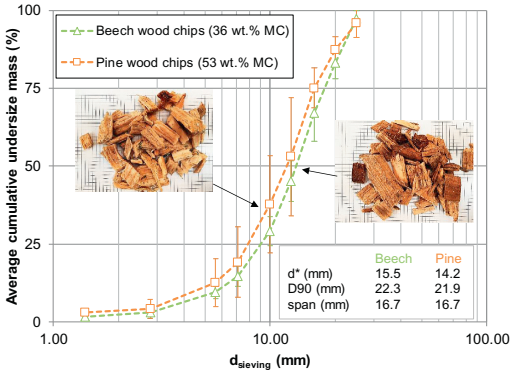

Fig. 6. Average cumulative undersize mass distribution of as-received beech and pine wood chips obtained by sieve analysis. Error bars indicate the first standard deviation from the mean, and they are displayed when greater than the data symbol.

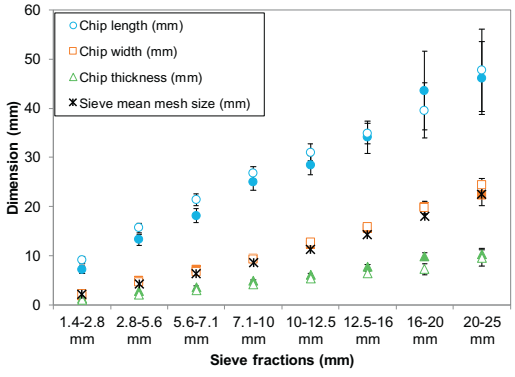

Fig. 7. Average dimensions of beech chips (hollow symbols) and pine chips (solid symbols) in each sieve fraction compared to the mean sieve mesh size. Error bars indicate the 95% confidence internal, and they are displayed when greater than the data symbol.

Table 2
Milling performance of pine and beech in a series of hammer mills. Size parameters are analyzed by sieve analysis and presented as means with three replicates.

Feed material	Screen (mm)	d_f[a](mm)	d_p[b] (mm)	SRR[c]($1/d_p$-$1/d_f$)	Capacity (t DW/h)	K_R[d](kWh mm t^{-1} DW)	Total SGEC[e] (kWh/t DW)
Coarse milling							
Beech chips (36 wt% MC[f])	15.0	15.46	2.45	0.34	0.54	27.0	8.1
Pine chips (53 wt% MC)	15.0	14.18	3.97	0.18	0.36	62.8	12.6
Fine milling							
Coarse beech grinds (12 wt% MC)	4.0	2.45	0.60	1.26	0.98	33.5	43.6
Coarse pine grinds (12 wt% MC)	4.0	3.97	0.97	0.78	0.90	61.8	49.4
Pellet milling							
Beech pellets (4.2 wt% MC)	4.0	0.65[g]	0.57	0.23	2.87	30.5	6.6
Pine pellets (8.5 wt% MC)	4.0	0.95[g]	0.78	0.22	2.75	41.4	9.5

[a] d_f: characteristic particle size of the feed.
[b] d_p: characteristic particle size of the product.
[c] SRR: Von Rittinger's size reduction ratio.
[d] K_R: Von Rittinger's material characteristic parameter.
[e] SGEC: specific grinding energy consumption.
[f] MC: moisture content.
[g] d_f: characteristic particle size of the disintegrated pellet material.

explained by the longer pellets (compared to pine pellets), lower moisture content, and lower specific pellet density.

Pine pellets showed higher specific pellet densities than beech pellets, probably due to the higher die aspect ratio used during their production which caused a higher compaction and pressure build-up in the press channels. Thus, pelletizing increased the specific density compared to beech and pine wood chips by about 190% and 400%, respectively. The specific pellet density as a pellet property is not included in ISO 17225-2:2014 [33], but according to DIN 51731 the specific pellet density should be between 1000 and 1400 kg/m^3 [59]. Judging from the results, the pellet density of beech and pine pellets falls within that range.

Regarding the durability, pine pellets are more durable than beech pellets, indicating a higher ability to resist abrasion during handling and transportation and thus a lower risk of fires and explosions during handling and shipping [60]. According to the ISO 17225-2:2014 standard [33], pine pellets comply with the requirements for class I1, while beech pellets fail to comply with the requirements of the lowest pellet class (i.e., I3) due to their lower bulk density. Differences in durability are a result of the combined effect of die aspect ratio, moisture, extractives, and lignin content. In a previous study [16], it was observed that higher extractives and lignin content resulted in a binding effect, increasing the degree of particle adhesion, and thus better durability. Also, the broader distribution of particle sizes for pine may enhance the pellet quality [57]. It was shown that finer particles fill in the voids formed among larger particles, hence producing denser and more durable pellets [9].

The capacity and energy demand for pelletizing wood are important measures of the pellet production costs. On average, the pellet mill showed higher capacity and significantly lower energy requirement for pelletizing fine pine grinds than for fine beech grinds (Table 3). The results of the chemical composition for pine showed an eightfold

Table 3
Quality parameters of the pellet specimens and performance of 6 mm-sized pine and beech pellets produced in a ring pellet die. Size parameters are presented as means with three replicates.

	Unit	Beech	Pine	Analysis method
Pellet feed properties				
Feed moisture	wt%	8.4	8.8	ISO 18134-1: 2015
Feed d*	mm	0.6	1.0	Sieve analysis
Feed span	mm	1.0	1.4	Sieve analysis
Feed bulk density	kg/m^3	215.1	177.6	ISO 17828: 2015
Pellet quality parameters				
Pellet moisture	wt%, ar	4.2	8.5	ISO 18134-1: 2015
Pellet diameter (D)and length (L)	mm, ar	D, 6.1 L, 11.8	D, 6.1 L, 10.1	ISO 17829: 2015
Number of pellets/100 g sample of pellets		366	350	Counting of pellets screened using a 5.0 mm sieve
Net calorific value	MJ/kg, DW	18.4	19.8	ISO 18125:2017
Bulk density (σ_B)	kg/m^3, ar	580.4	603.3	ISO 17828: 2015
Specific pellet density (σ_P)	kg/m^3, ar	1113.8	1152.6	$\sigma_P = \frac{m}{V_p}$
Interparticle porosity (ε)	–	0.48	0.48	$\varepsilon = 1 - \frac{\sigma_P}{\sigma_B}$
Mechanical durability	wt%, ar	96.7	98.5	ISO 17831-1: 2015
PSD of disintegrated pellets (internal PSD)	wt%, DW	≥100%[a] (<3.15 mm) ≥99.3%[a] (<2 .0mm) ≥84.3%[a] (<1 .0mm)	≥100.0% (<3.15 mm) ≥97.7% (<2 .0mm) ≥62.7% (<1 .0mm)	ISO 17830: 2016 (Sieve analysis)
Pelletizing performance				
Die channel length	mm	35	50	
Capacity	t DW/h	0.68	0.69	
Total SEC	kWh/t DW	90.3	35.0	

[a] Values obtained after the second pellet disintegration in hot water.

Table 4
Physical properties of fine grinds, disintegrated pellets, and milled pellets. Values are presented as means with three replicates, and one standard deviation is indicated in parentheses.

Wood samples	Size and shape parameter analyzed by DIA						Moisture content (wt%)	Loose bulk density (kg/m^3)
	d*[a] (mm)	span[a] (mm)	d*[b] (mm)	span[b] (mm)	ER (−)	C (−)		
Fine beech grinds	0.77	1.25	2.32	3.54	0.38	0.45	8.4	215.1
	(0.05)	(0.04)	(0.10)	(0.07)	(0.01)	(0.02)	(0.1)	(9.2)
Disintegrated[c] beech pellets	0.79	1.41	1.81	2.88	0.51	0.55	6.2	210.5
	(0.12)	(0.14)	(0.13)	(0.19)	(0.04)	(0.03)	(0.1)	(8.7)
Milled beech pellets	0.68	1.08	1.47	2.13	0.52	0.57	3.5	396.1
	(0.03)	(0.04)	(0.05)	(0.05)	(0.01)	(0.01)	(0.1)	(7.3)
Fine pine grinds	1.17	1.61	2.85	3.43	0.41	0.41	8.8	177.6
	(0.02)	(0.02)	(0.03)	(0.06)	(0.01)	(0.03)	(0.1)	(8.2)
Disintegrated pine pellets	1.16	1.65	2.64	3.10	0.48	0.50	6.4	170.8
	(0.09)	(0.03)	(0.07)	(0.08)	(0.03)	(0.03)	(0.1)	(8.5)
Milled pine pellets	0.90	1.18	1.94	2.42	0.49	0.51	7.4	282.8
	(0.04)	(0.04)	(0.03)	(0.05)	(0.02)	(0.01)	(0.1)	(6.2)

[a] Size characteristics calculated based on $d_{c,min}$.
[b] Size characteristics calculated based on $d_{Fe,max}$.
[c] Material obtained after the second pellet disintegration in hot water.

higher amount of extractives (such as wood resin) compared to beech (Table 1). Nielsen et al. [61] reported that biomasses with a lesser amount of these extractives increased the energy required to compress the fine grinds, to force the compressed material into the pellet die channels, and to force the flow of compressed material layer through the die channels. Hence, the higher extractive content in pine probably lubricated the die channels, leading to higher production capacity and lower energy input for pelletization compared to beech.

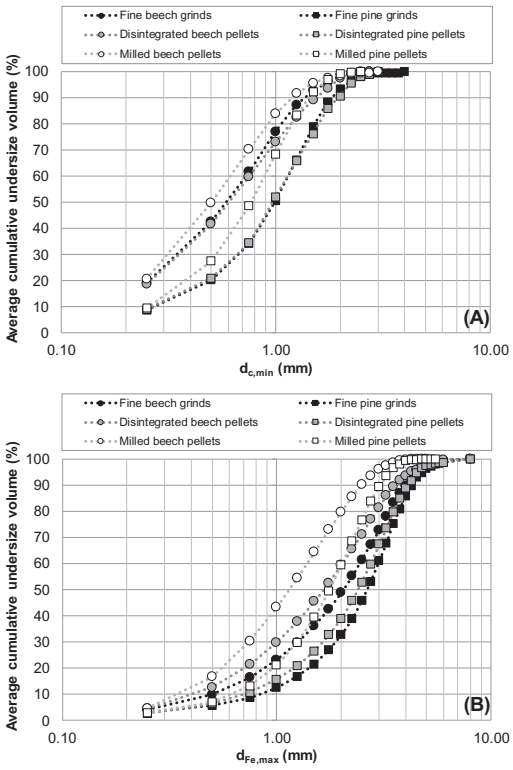

Fig. 8. Average cumulative undersize volume PSD versus $d_{c,min}$ (A) and average cumulative undersize volume PSD versus $d_{Fe,max}$ (B) analyzed by Camsizer® X2.

3.4. Pellet comminution

Table 2 also summarizes the milling performance for beech and pine pellets. Compared to fine milling, pellet comminution shows a significantly lower SGEC, indicating better grindability of the pellets. Hence, during pelletizing, the bond formation between adjacent particles

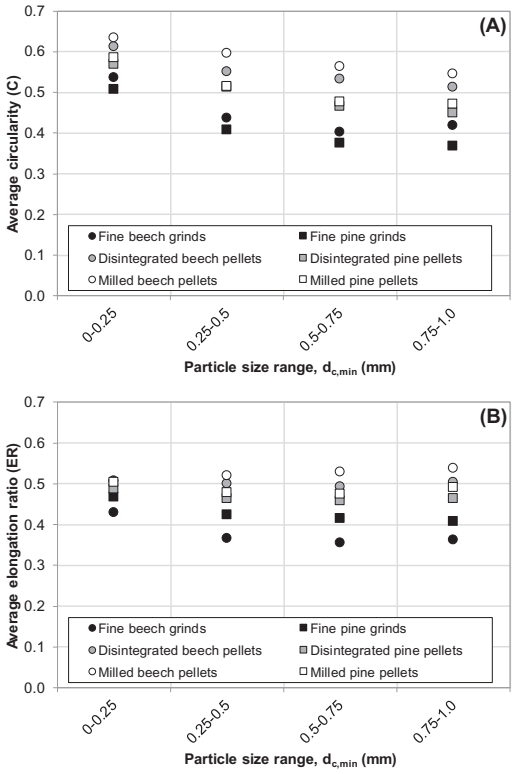

Fig. 9. Average circularity (A) and elongation ratio (B) of fine grinds, disintegrated pellets, and milled pellets for beech and pine analyzed by Camsizer® X2. Values for particles wider than 1 mm were neglected due to the small number of particles analyzed.

creates a densified material that is easier to fracture than the non-densified coarse grinds. However, it has to be noted that the higher throughput (capacity) for pellet comminution probably favors lower specific energy compared to fine milling. It is difficult to compare the specific energy data with other pellet milling studies, which used lab-scale hammer mills [10,62].

Similar to fine milling, a lower K_R value for milling beech pellets was found, indicating a lower milling energy consumption compared to pine pellets. This can be explained by the less durable beech pellets or the finer internal beech pellet particles or. Beech particles may have a shorter residence time in the milling chamber, as they have a higher probability to pass through the 4 mm hammer mill screen. On the other hand, coarser pine particles probably have a longer residence time that increases the possibility of more breaking actions induced by the hammers, entailing a higher grinding energy consumption. In addition, the higher moisture level in pine pellets probably resulted in a higher ductility [14] and hence the specific energy. The higher extractives content in pine may also affect the specific energy. It was reported that extractives could interfere with the mechanical processing of wood [11]. For example, resins can build up on cutting tools, which will become dull [63].

The different qualities of beech and pine pellets seemed not to affect the hammer mill capacity, as a grinding capacity of ca. 3 t DW/h was obtained in both cases. Interestingly, the comminution of the pellets led to a similar size reduction ratio of about 0.2, regardless of the differences in the feed material. During hammer milling of the pellets, a drying effect was observed (cf. Table 3 and Table 4). The drying effect was slightly higher for milling beech pellets than for milling pine pellets probably because of the greater surface area of beech particles, which facilitates better moisture evaporation inside the hammer mill chamber.

3.5. Physical properties of fine grinds, disintegrated pellets, and milled pellets

The PSDs of milled pellets, disintegrated pellets, and fine grinds versus the particle width ($d_{c,min}$) and the particle length ($d_{Fe,max}$) determined by digital image analysis are shown in Fig. 8A and Fig. 8B, respectively. Table 4 summarizes the physical properties of the different wood particles. The comminution of beech and pine pellets in a hammer mill shifted the PSD to the left in both Fig. 8A and Fig. 8B, indicating a reduced width and length compared to internal pellet particles. This final milling step resulted in characteristic particle widths and lengths of 0.68 mm and 1.47 mm for milled beech pellets and 0.90 mm and 1.94 mm for milled pine pellets, respectively. Thus, the final milling step did not only disintegrate pellets into constituent internal particles but achieved some size reduction of the particles. This study hence provides further evidence for both structural pellet breakdown and size reduction of the internal pellet particles during pellet comminution, which Temmerman et al. [10] assumed merely based on energy consumption data. Fig. 8A shows that the size reduction in width was larger for pine pellet particles than for beech pellet particles. However, beech particles always show a finer PSD than pine particles, probably due to the different breakage mechanism of softwoods and hardwoods. The latter ones are characterized by the presence of vessel elements (pores), while softwoods have none. These vessel elements affect the wood crack path, i.e., the crack may enter the vessel element [64] and crack propagation becomes easier [65], thus producing smaller particles. Comminuting pellets produced a narrower (uniform) particle size range compared to fine grinds and disintegrated pellets. Williams et al. [66] also reported an enhanced uniformity for comminuted pellet particle sizes compared to the pre-densified material. It is hence concluded that pellet comminution is accompanied by a reduction of the coarse particles to smaller sizes, which leads to a steeper and narrower size distribution curve. Regarding the particles length ($d_{Fe,max}$) in Fig. 8B, on average, all beech samples have more particles with a length below 1 mm than pine samples, indicating that beech particles are shorter than those from pine. Differences can be linked to the wood cell wall structure. The shorter length for beech fibers is typical for hardwoods compared to softwoods [67].

The 2D derived shape factors are presented in Fig. 9. The changes in particle shape from fine grinds to disintegrated pellets to milled pellets reflect changes occurring during fine grinds densification in the pellet mill and pellet comminution in the hammer mill, respectively. The overall trend is that pine and beech particles become rounder and less elongated with the number of processing steps, including pelletization, and pellet comminution. However, the change in shape from disintegrated pellet particles to milled pellet particles is smaller than from fine grinds to disintegrated pellet particles. Fig. 9 shows that the circularity increases with decreasing particle size, indicating that the finer particles are more circular than coarser particles. This finding concurs well with Tannous et al.'s study [68], who observed a similar trend for milled Douglas fir particles. Due to the anisotropic cell wall structure of wood, beech and pine particles show a needle-like shape, indicated by low elongation ratios. On average, fine beech grinds have lower elongation ratios (ER = 0.38) than fine pine grinds (ER = 0.42). As mentioned previously, lower elongation ratios were also found for beech chips compared to pine chips. For coarser particles, the elongation ratios between the two wood species differ largely. For smaller particles, the degree of elongation is more similar, as the structure difference between biomasses seems to reduce with decreasing particle size [69].

Regarding the effect of the pellet mill on the particles, it was observed that it does not alter the particle width, as differences between the characteristic particle size of fine grinds and disintegrated pellets

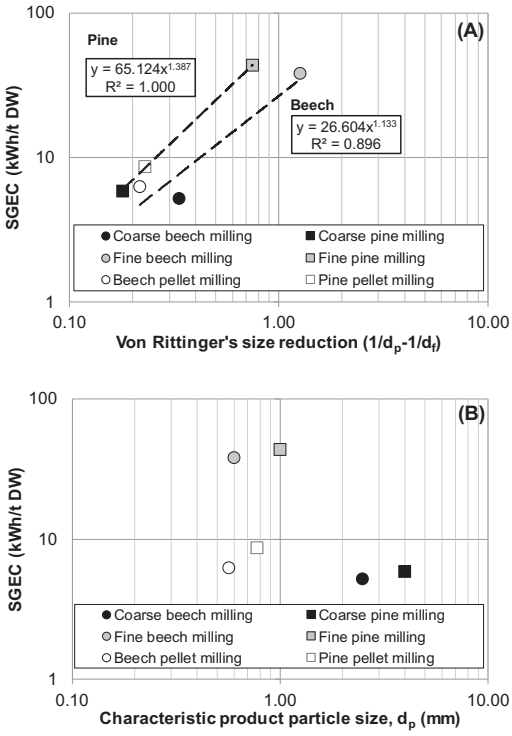

Fig. 10. Specific grinding energy consumption vs. Von Rittinger's size reduction ratio (A) and specific grinding energy consumption vs. characteristic product particle size (B).

Table 5
Estimation of the process energies for milling and pelletizing prior to the combustion of wood pellets based on the net calorific value of the oven dry matter (NCV_d).

Wood	NCV_d (MJ/kg, DW)	Pellet plant			Power plant $SEC_{pellet\ milling}/NCV_d$ (%)	Total (%)
		$SEC_{coarse\ milling}/NCV_d$ (%)	$SEC_{fine\ milling}/NCV_d$ (%)	$SEC_{pelletizing}/NCV_d$ (%)		
Beech	18.4	0.16	0.85	1.77	0.13	2.91
Pine	19.8	0.23	0.90	0.64	0.17	1.94

are negligible (Fig. 8A). This result concurs well with Trubetskaya et al.'s [70] findings. However, it reduces the particle length for both samples, e.g., the amount of particles shorter than 1 mm is 23% for fine beech grinds and 30% for disintegrated beech pellet particles (Fig. 8B). For pine, the amount of particles shorter than 1 mm increases from 12% for fine grinds to 16% for disintegrated pellet particles. The small increase in shorter particles after the pellet mill suggests that particles break across their largest dimension in the process of pellet formation, indicating a directional particle breakage behavior. During pelletizing, wood particles are forced into the die channels by the two rollers that move due to the friction and movement of the rotating ring die. Hence, the particle breakage may be explained by shearing of wood particles occurring between the rollers and the rotating die. The smaller increase in shorter particles was larger for beech during pelletizing. Due to their lower extractives content, beech particles will show greater friction in the roller-pellet die contact area, which probably favors a more brittle fracture behavior of beech particles. Vasic and Stanzl-Tschegg [14] showed that pine has a more ductile fracture response than beech so that the rigid beech is more likely to break during stress. The change in particle length inevitably affects the internal pellet particle shape (Fig. 9). In particular, the average circularity for pine increases from 0.41 (fine grinds) to 0.50 (disintegrated pellets) and from 0.45 (fine grinds) to 0.55 (disintegrated pellets) for beech. In the same way, the elongation ratio increases from 0.41 (fine grinds) to 0.48 (disintegrated pellets) for pine, and from 0.38 (fine grinds) to 0.51 (disintegrated pellets) for beech. The final pellet milling step had only a negligible effect on the wood particle shape. Thus, changes in circularity and elongation ratio between fine grinds and internal pellet particles are directly related with the length reduction observed on disintegrated pellet particles compared to fine grinds. Hence, the pelletizing process modified the elongated wood particle shape of fine grinds more than the subsequent pellet milling step in the hammer mill.

Table 4 presents loose bulk density values for the various wood types. On average, all beech samples show higher bulk densities than pine due to a higher particle density and smaller particles. Smaller beech particles can be embedded in the voids between larger particles, thus favoring a better packing structure. Milling wood pellets leads to a further reduction of the inter-particle gaps due to the production of finer particles that allow better packing ability [71]. Thus, final bulk densities of milled pellet product of ca. 400 kg/m^3 for beech and 280 kg/m^3 for pine were obtained. Differences in bulk density may also be linked to the different particle shape. Fine grinds comprise more elongated and less circular particles than milled pellets, which can cause mechanical interlocking between particles and an increase in porosity of the bulk solid [72]. This leads to less compaction and lower bulk density. Rezaei et al. [62] observed a similar trend for needle-like milled chip particles compared to more spherical milled pellet particles.

3.6. Implications for wood pellet producers and power plant operators

For pellet producers and power plant operators, the energy for mechanical processes (i.e., size reduction and pelletization) has to be minimized to achieve optimal process efficiencies. Fig. 10A and Fig. 10B plot the SGEC versus the size reduction (comminution) ratio of Von Rittinger's comminution law and the SGEC versus the characteristic product particle size, respectively. A strong power law relationship ($R^2 = 1.00$ for pine and $R^2 = 0.90$ for beech) was found between SGEC and the size reduction ratio. Fine milling represents the most energy-consuming milling process in both cases. Milling beech requires less energy, leads to a higher size reduction ratio, and produces finer particles than pine. However, higher energy is required to pelletize beech than pine.

To assess how much energy of the actual energy value of the wood is used for milling and pelletizing operations, the ratio of the specific energy consumption for milling (or pelletizing) to the net calorific value of the oven dry matter (NCV_d) was determined (Table 5). It should be stated that the energy required for milling and pelletizing is electrical energy, which is inherently more valuable than thermal energy (heat). Generally, milling and pelletizing represent only a little proportion (between 1.9 and 2.9%) of the NCV_d. For beech, pelletizing energy represents the highest proportion of NCV_d, which is almost three times as much as for pine. The lack of extractives can probably explain why beech is more difficult to pelletize than pine. Thus, to facilitate the pelletizing process and enhance the pellet quality, pellet producers should pelletize beech mixed with pine or use binders such as brewers spent grains [32]. Due to the better grindability (i.e.,the lower grinding energy) of beech pellets, switching to beech pellets will slightly improve the overall power plant efficiency and also provide finer fuel particles for suspension-firing.

4. Conclusions

This study investigated the physical changes occurring during the mechanical processing of beech and pine trees into chips, pellets, and milled pellets. The experimental data provide valuable new knowledge of how pelletizing and hammer-milling operations modify the physical properties (size, shape, density) of beech and pine. The following conclusions can be drawn from the experimental study:

- The pelletizing process alters the shape and length of the wood particles. There is a reduction in the particle length during pelletizing, which results in higher particle circularity and elongation (width-to-length) ratio values. The average elongation ratio for beech particles increased from 0.38 (fine grinds) to 0.51 (disintegrated pellets) to 0.52 (milled pellets). In comparison, pine particles increased in elongation from 0.42 (fine grinds) to 0.48 (disintegrated pellets) to 0.49 (milled pellets).
- Milling beech produced more fines than pine in all milling steps. For practical milling operations, beech wood requires less energy for milling than pine.
- The relationship between specific grinding energy for grinding wood and the size reduction ratio of Von Rittinger's comminution law followed a power law. Von Rittinger's law can thus be applied to predict the energy required to grind wood chips, coarse grinds, and wood pellets.
- Sieve analysis represents well the width of wood particles, but not the particle length. Digital image analysis allows direct size and shape measurements and provides more detailed data than traditional sieve analysis.
- Rosin-Rammler-Bennet-Sperling characteristic particle sizes of the milled wood chips, milled coarse grinds, and milled wood pellets are smaller than the hammer mill screen opening.
- Pelletizing beech requires more energy than pine. This behavior is attributed to a lower extractives content in beech.
- Beech pellets are more difficult to disintegrate in water following the standard procedure ISO 17830:2016. In that case, it is recommended to perform the disintegration procedure twice.

- The wood bulk densities are sensitive to the particle size, shape, and moisture content. Bulk densities for milled beech pellets featuring finer, more circular, and less elongated particles were higher than those of coarser, less circular, and more elongated milled pine pellets.

Nomenclature

$A_{Particle}$	Particle projection area (mm^2)
m_{Pellet}	Amount of wood pellets (t)
$P_{Particle}$	Particle perimeter (mm)
ar	As received
C	Circularity (dimensionless)
d	Particle size (mm)
D	Pellet diameter (mm)
d^*	RRBS Characteristic particle size (mm)
D90	Particle size at 90th percentile of the cumulative undersize distribution (mm)
$d_{c,min}$	Shortest maximum chord (mm)
d_f	RRBS Characteristic particle size (mm) of the feed
$d_{Fe,max}$	Maximum Feret diameter (mm)
d_p	RRBS Characteristic particle size (mm) of the product
DW	Dry wood basis
ER	Particle elongation ratio (dimensionless)
K_R	Von Rittinger's material characteristic parameter ($kWh\ mm\ t^{-1}$)
L	Pellet length (mm)
n	RRBS Uniformity constant (dimensionless)
P	Absorbed mill power (kW)
PSD	Particle size distribution
R(d)	Cumulative undersize distribution (%)
RRBS	Rosin-Rammler-Bennet-Sperling
SEC	Specific energy consumption (kWh/t)
wt%	Weight percent

Acknowledgements

The authors thank Energiteknologiske Udviklings- og Demonstrationsprogram (EUDP) for the financial support received as part of the ForskEL project "AUWP – Advanced Utilization of Wood Pellets" (Project number: 12325). The authors are also grateful both to Bregentved Estate for providing the wood species and Danish Technological Institute (DTI) for performing the pelletizing and milling tests.

Appendix A. Supplementary data

Supplementary data to this article can be found online at https://doi.org/10.1016/j.powtec.2019.03.002.

References

[1] J.S. Gregg, S. Bolwig, O. Solér, L. Vejlgaard, S.H. Gundersen, P.E. Grohnheit, I.T. Herrmann, K.B. Karlsson, Experiences with Biomass in Denmark Systems, 2014.
[2] M.D. Staples, R. Malina, S.R.H. Barrett, The limits of bioenergy for mitigating global life-cycle greenhouse gas emissions from fossil fuels, Nat. Energy 2 (2017)https://doi.org/10.1038/nenergy.2016.202.
[3] The Ørsted Way Let's Create a World that Runs Entirely on Green Energy, Ørsted, https://orsted.com/-/media/Aarsrapport2017/Orsted_report_Summary_2017_Final_EN 2017, Accessed date: 1 June 2018.
[4] From Sustainable Biomass to Competititve Bioenergy, State of Green, https://stateofgreen.com/en/uploads/2015/11/From-Sustainable-Biomass-to-Competitive-Bioenergy.pdf 2015, Accessed date: 24 May 2018.
[5] Usda Staff, The Market for Wood Pellets in Denmark, 2013 3–5http://gain.fas.usda.gov/Recent GAIN Publications/The Market for Wood Pellets in Denmark_The Hague_Denmark_11-5-2013.pdf.
[6] D. Bergström, S. Israelsson, M. Öhman, S.A. Dahlqvist, R. Gref, C. Boman, I. Wästerlund, Effects of raw material particle size distribution on the characteristics of Scots pine sawdust fuel pellets, Fuel Process. Technol. 89 (2008) 1324–1329, https://doi.org/10.1016/j.fuproc.2008.06.001.
[7] P. Lehtikangas, Quality properties of pelletised sawdust, logging residues and bark, Biomass Bioenergy 20 (2001) 351–360, https://doi.org/10.1016/S0961-9534(00)00092-1.
[8] M.T. Carone, A. Pantaleo, A. Pellerano, Influence of process parameters and biomass characteristics on the durability of pellets from the pruning residues of Olea europaea L, Biomass Bioenergy 35 (2011) 402–410, https://doi.org/10.1016/j.biombioe.2010.08.052.
[9] L.G. Tabil, Binding and Pelleting Characteristics of Alfalfa Pellets, PhD thesis University of Saskatchewan, Canada, 1996.
[10] M. Temmerman, P.D. Jensen, J. Hébert, Von Rittinger theory adapted to wood chip and pellet milling, in a laboratory scale hammermill, Biomass Bioenergy 56 (2013) 70–81, https://doi.org/10.1016/j.biombioe.2013.04.020.
[11] R.J. Gravelsins, Studies of Grinding of Wood and Bark-Wood Mixtures with the Szego Mill, PhD thesis University of Toronto, Canada, 1998.
[12] L.J. Naimi, A Study of Cellulosic Biomass Size Reduction, PhD thesis The University of British Columbia, Canada, 2016.
[13] K. Frühmann, A. Reiterer, E.K. Tschegg, S.S. Stanzl-tschegg, Fracture characteristics of wood under mode I, mode II and mode III loading, Philos. Mag. A. 82 (2002) 3289–3298, https://doi.org/10.1080/01418610208240441.
[14] S. Vasic, S. Stanzl-Tschegg, Experimental and numerical investigation of wood fracture mechanisms at different humidity levels, Holzforschung 61 (2007) 367–374, https://doi.org/10.1515/HF.2007.056.
[15] P.J.M. Pelgrom, M.A.I. Schutyser, R.M. Boom, Thermomechanical morphology of peas and its relation to fracture behaviour, Food Bioprocess Technol. 6 (2013) 3317–3325, https://doi.org/10.1007/s11947-012-1031-2.
[16] T. Filbakk, G. Skjevrak, O. Høibø, J. Dibdiakova, R. Jirjis, The influence of storage and drying methods for Scots pine raw material on mechanical pellet properties and production parameters, Fuel Process. Technol. 92 (2011) 871–878, https://doi.org/10.1016/j.fuproc.2010.12.001.
[17] N.P.K. Nielsen, D. Gardner, T. Poulsen, C. Felby, Importance of temperature, moisture content, and species for the conversion process of wood residues into fuel pellets, Wood Fiber Sci. 41 (2009) 414–425.
[18] B.J. Ahn, H. sun Chang, S.M. Lee, D.H. Choi, S.T. Cho, G. seong Han, I. Yang, Effect of binders on the durability of wood pellets fabricated from Larix kaemferi C. and Liriodendron tulipifera L. sawdust, Renew. Energy 62 (2014) 18–23, https://doi.org/10.1016/j.renene.2013.06.038.
[19] T.O. Wilson, Factors Affecting Wood Pellet Durability, Master's thesis The Pennsylvania State University, USA, , 2010.
[20] W. Stelte, J.K. Holm, A.R. Sanadi, S. Barsberg, J. Ahrenfeldt, U.B. Henriksen, A study of bonding and failure mechanisms in fuel pellets from different biomass resources, Biomass Bioenergy 35 (2011) 910–918, https://doi.org/10.1016/j.biombioe.2010.11.003.
[21] A.M. Olsson, L. Salmen, Viscoelasticity of insitu lignin as affected by structure – softwood and hardwood, ACS Symp. Ser. 489 (1992) 133–143.
[22] J. Chirife, M. Del, P. Buera, Water activity, glass transition and microbial stability in concentrated/semimoist food systems, 5, 1994, 921–927.
[23] R. Samuelsson, M. Thyrel, M. Sjöström, T.A. Lestander, Effect of biomaterial characteristics on pelletizing properties and biofuel pellet quality, Fuel Process. Technol. 90 (2009) 1129–1134, https://doi.org/10.1016/j.fuproc.2009.05.007.
[24] N. Kaliyan, R. Vance Morey, Factors affecting strength and durability of densified biomass products, Biomass Bioenergy 33 (2009) 337–359, https://doi.org/10.1016/j.biombioe.2008.08.005.
[25] S. Döring, Power from pellets, 2015, https://doi.org/10.1017/CBO9781107415324.004.
[26] International Organization for Standardization, ISO 17830:2016, Solid biofuels - Particle size distribution of disintegrated pellets, 2014 1–8.
[27] A. Sluiter, B. Hames, R. Ruiz, C. Scarlata, J. Sluiter, D. Templeton, D. Crocker, Determination of Structural Carbohydrates and Lignin in Biomass, 2012 (doi:NREL/TP-510-42618).
[28] B. Hames, R. Ruiz, C. Scarlata, A. Sluiter, J. Sluiter, D. Templeton, Preparation of Samples for Compositional Analysis Laboratory Analytical Procedure (LAP), 2008.
[29] E. Alakangas, Properties of wood fuels used in Finland – BIOSOUTH -project, Bulk Solids Handling, 2005.
[30] I. Obernberger, G. Thek, Effects of Pelletizing Pressure and the Addition of Woody Bulking Agents on the Physical and Mechanical, Earthscan Ltd, 2010 241–272http://bios-bioenergy.at/uploads/media/The-Pellet-Handbook-Flyer.pdf, Accessed date: 8 August 2017.
[31] J.S. Tumuluru, C.T. Wright, K.L. Kenny, J.R. Hess, A Review on Biomass Densification Technologies for Energy Application, Idaho National Laboratory, 2010.
[32] J.K. Holm, U.B. Henriksen, J.E. Hustad, L.H. Sørensen, Toward an understanding of controlling parameters in softwood and hardwood pellets production, Energy Fuel 20 (2006) 2686–2694, https://doi.org/10.1021/ef0503360.
[33] International Organization for Standardization, ISO 17225-2:2014, Solid biofuels - Fuel specifications and classes - Part 2: Graded Wood Pellets, 2014 7–8.
[34] International Organization for Standardization, ISO 17831-1:2015, Solid biofuels - Determination of Mechanical Durability of Pellets and Briquettessh Standards, 2015.
[35] International Organization for Standardization, ISO 18134-1:2015, Solid Biofuels - Determination of Moisture Content - Oven Dry Method, 2015.
[36] S.J. Blott, K. Pye, Particle shape: a review and new methods of characterization and classification, Sedimentology 55 (2008) 31–63, https://doi.org/10.1111/j.1365-3091.2007.00892.x.
[37] O. Williams, G. Newbolt, C. Eastwick, S. Kingman, D. Giddings, S. Lormor, E. Lester, Influence of mill type on densified biomass comminution, Appl. Energy 182 (2016) 219–231, https://doi.org/10.1016/j.apenergy.2016.08.111.
[38] M. Masche, M. Puig-Arnavat, J. Wadenbäck, S. Clausen, P.A. Jensen, J. Ahrenfeldt, U.B. Henriksen, Wood pellet milling tests in a suspension-fired power plant, Fuel Process. Technol. 173 (2018) 89–102, https://doi.org/10.1016/j.fuproc.2018.01.009.
[39] Retsch Technology GmbH, Manual Evaluation Software Camsizer® *X2* (2017) 1–88.

[40] A. Trubetskaya, G. Beckmann, J. Wadenbäck, J.K. Holm, S.P. Velaga, R. Weber, One way of representing the size and shape of biomass particles in combustion modeling, Fuel. 206 (2017) 675–683, https://doi.org/10.1016/j.fuel.2017.06.052.
[41] E.P. Cox, A method of assigning numerical and percentage values to the degree of roundness of sand grains, J. Paleontol. 1 (1927) 179–183.
[42] W. Pichler, A. Weidenhiller, J. Denzler, R. Goetzl, M. Pain, M. Weigl, A. Haider, Modelling the Particle Size Distribution of the Feedstock for Pellets Production, 22nd European Biomass Conference and Exhibition, Hamburg, Germany 2014 25–26.
[43] T. Allen, Powder Sampling and Particle Size Determination, 1st ed. Elsevier Science, Oxford, UK, 2003.
[44] L.J. Naimi, S. Sokhansanj, X. Bi, C.J. Lim, A.R. Womac, A.K. Lau, S. Melin, Development of size reduction equations for calculating energy input for grinding Lignocellulosic particles, Appl. Eng. Agric. 29 (2013) 93–100, https://doi.org/10.13031/2013.42523.
[45] L.G. Austin, A commentary on the kick, bond and Rittinger laws of grinding, Powder Technol. 7 (1973) 315–317, https://doi.org/10.1016/0032-5910(73)80042-7.
[46] T. Tanaka, Comminution Laws. Several probabilities, Indus. Eng. Chem. Process Des. Dev. 5 (1966) 353–358, https://doi.org/10.1021/i260020a001.
[47] R.H. White, Effect of lignin content and extractives on the higher heating value of wood, Wood Fiber Sci. 19 (1987) 446–452http://swst.metapress.com/index/1NJ2H77X84TJ8057.pdf.
[48] Acetyl-Methoxyl Content of Softwoods & Hardwoods, The University of Tennessee, http://biorefinery.utk.edu/technical_reviews/methoxyl acetyl content wood.pdf 2018, Accessed date: 5 July 2018.
[49] H. Hartmann, T. Böhm, P. Daugbjerg Jensen, M. Temmerman, F. Rabier, M. Golser, Methods for size classification of wood chips, Biomass Bioenergy 30 (2006) 944–953, https://doi.org/10.1016/j.biombioe.2006.06.010.
[50] D.N. Lanning, J.H. Dooley, C.J. Lanning, Shear Processing of Wood Chips into Feedstock Particles, 2012 ASABE Annual International Meeting, vol. 1, 2012 703–714.
[51] A. Twaddle, The influence of species, chip length, and ring orientation on chip thickness, TAPPI J. 80 (1997) 121–131.
[52] L.S. Esteban, J.E. Carrasco, Evaluation of different strategies for pulverization of forest biomasses, vol. 166, 2006 139–151, https://doi.org/10.1016/j.powtec.2006.05.018.
[53] O. Oyedeji, O. Fasina, S. Adhikari, T. McDonald, S. Taylor, The effect of storage time and moisture content on grindability of loblolly pine (Pinus taeda L.), Eur. J. Wood Wood Prod. 74 (2016) 857–866, https://doi.org/10.1007/s00107-016-1070-x.
[54] R. Marton, N. Tsujimoto, E. Eskelinen, Energy consumption in thermomechanical pulping, TAPPI J. 64 (1981) 71–74.
[55] Z. Lu, X. Hu, Y. Lu, Particle morphology analysis of biomass material based on improved image processing method, Int. J. Anal. Chem. 2017 (2017) 1–9, https://doi.org/10.1155/2017/5840690.
[56] P. Daugbjerg Jensen, M. Temmerman, S. Westborg, Internal particle size distribution of biofuel pellets, Fuel 90 (2011) 980–986, https://doi.org/10.1016/j.fuel.2010.11.029.
[57] W. Stelte, A.R. Sanadi, L. Shang, J.K. Holm, J. Ahrenfeldt, U.B. Henriksen, Recent Developments in Biomass Pelletization – A Review, vol. 7, 2012 4451–4490.
[58] M.R. Wu, D.L. Schott, G. Lodewijks, Physical properties of solid biomass, Biomass Bioenergy 35 (2011) 2093–2105, https://doi.org/10.1016/j.biombioe.2011.02.020.
[59] C. Kirsten, V. Lenz, H. Schröder, J. Repke, Hay pellets — the influence of particle size reduction on their physical – mechanical quality and energy demand during production, Fuel Process. Technol. 148 (2016) 163–174, https://doi.org/10.1016/j.fuproc.2016.02.013.
[60] P. Lehtikangas, Storage effects on pelletised sawdust, logging residues and bark, Biomass Bioenergy 19 (2000) 287–293, https://doi.org/10.1016/S0961-9534(00)00046-5.
[61] N.P.K. Nielsen, D.J. Gardner, C. Felby, Effect of extractives and storage on the pelletizing process of sawdust, Fuel. 89 (2010) 94–98, https://doi.org/10.1016/j.fuel.2009.06.025.
[62] H. Rezaei, C.J. Lim, A. Lau, S. Sokhansanj, Size, shape and flow characterization of ground wood chip and ground wood pellet particles, Powder Technol. 301 (2016) 737–746, https://doi.org/10.1016/j.powtec.2016.07.016.
[63] M. Grabner, U. Müller, N. Gierlinger, R. Wimmer, Effects of heartwood extractives on mechanical properties of larch, IAWA J. 26 (2005) 211–220.
[64] M.P.C. Conrad, G.D. Smith, G. Fernlund, Fracture of solid wood: a review of structure and properties at different length scales, Wood Fiber Sci. 35 (2003) 570–584.
[65] E.N. Landis, P. Navi, Modeling crack propagation in wood and wood composites. A review. Cost action E35 2004-2008: wood machining - micromechanics and fracture, Holzforschung 63 (2009) 150–156, https://doi.org/10.1515/HF.2009.010.
[66] O. Williams, E. Lester, S. Kingman, D. Giddings, S. Lormor, C. Eastwick, Benefits of dry comminution of biomass pellets in a knife mill, Biosyst. Eng. 160 (2017) 42–54, https://doi.org/10.1016/j.biosystemseng.2017.05.011.
[67] M. Akgul, A. Tozluoglu, Some chemical and morphological properties of juvenile woods from beech (Fagus orientalis L.) and pine (Pinus nigra A.) plantations, Trends Appl. Sci. Res. 4 (2009) 116–125, https://doi.org/10.3923/tasr.2009.116.125.
[68] K. Tannous, P.S. Lam, S. Sokhansanj, J.R. Grace, Physical properties for flow characterization of ground biomass from Douglas fir wood, Part. Sci. Technol. 31 (2013) 291–300, https://doi.org/10.1080/02726351.2012.732676.
[69] Q. Guo, X. Chen, H. Liu, Experimental research on shape and size distribution of biomass particle, Fuel. 94 (2012) 551–555, https://doi.org/10.1016/j.fuel.2011.11.041.
[70] A. Trubetskaya, Y. Poyraz, R. Weber, J. Wadenbäck, Secondary comminution of wood pellets in power plant and laboratory-scale mills, Fuel Process. Technol. 160 (2017) 216–227, https://doi.org/10.1016/j.fuproc.2017.02.023.
[71] N. Chevanan, A.R. Womac, V.S. Bitra, S. Sokhansanj, Effect of particle size distribution on loose-filled and tapped densities of selected biomass after knife mill size reduction, Appl. Eng. Agric. 27 (2011) 631–644, https://doi.org/10.13031/2013.38194.
[72] A. Bodhmage, Correlation between Physical Properties and Flowability Indicators for Fine Powders, Master's thesis University of Saskatchewan, Canada, 2006http://www.collectionscanada.gc.ca/obj/s4/f2/dsk3/SSU/TC-SSU-07032006115722.pdf.
[73] Sketch ring die pellet, TU Munich2009https://mediatum.ub.tum.de/image/732175, Accessed date: 18 June 2018.

Supplementary data

Fig. S6: Average shape factors of beech and pine wood chips as a function of the chip length. Error bars indicate the 95% confidence internal, and they are displayed when greater than the data symbol.

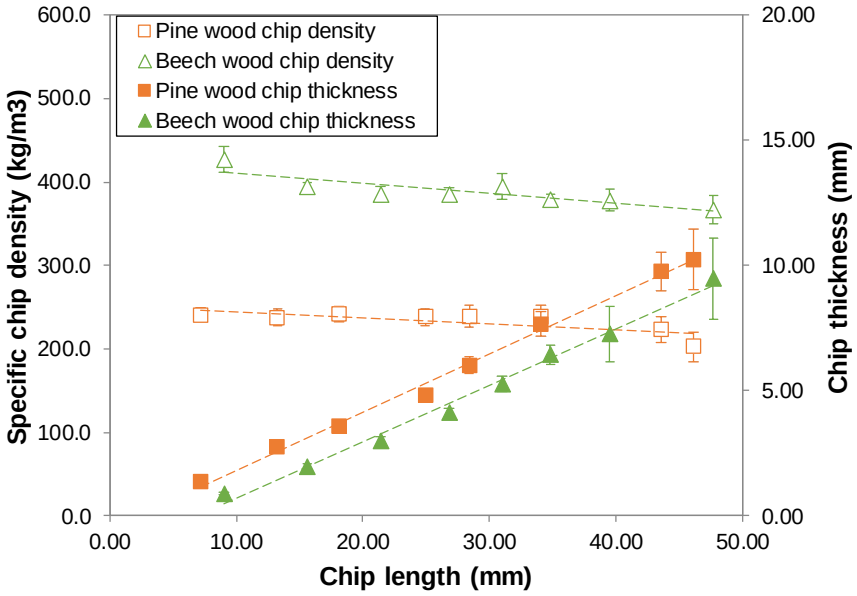

Fig. S7: Average specific density and thickness of beech and pine wood chips as a function of the chip length. Error bars indicate the 95% confidence internal, and they are displayed when greater than the data symbol.

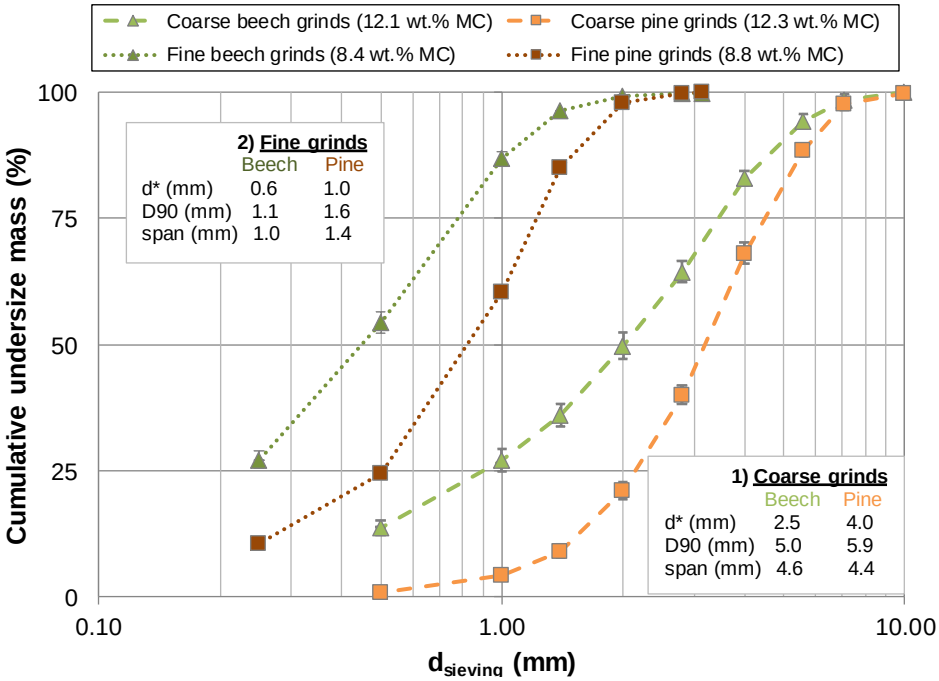

Fig. S8: Average cumulative undersize mass distribution of coarse and fine grinds of beech and pine obtained by sieve analysis. Error bars indicate the first standard deviation from the mean, and they are displayed when greater than the data symbol.

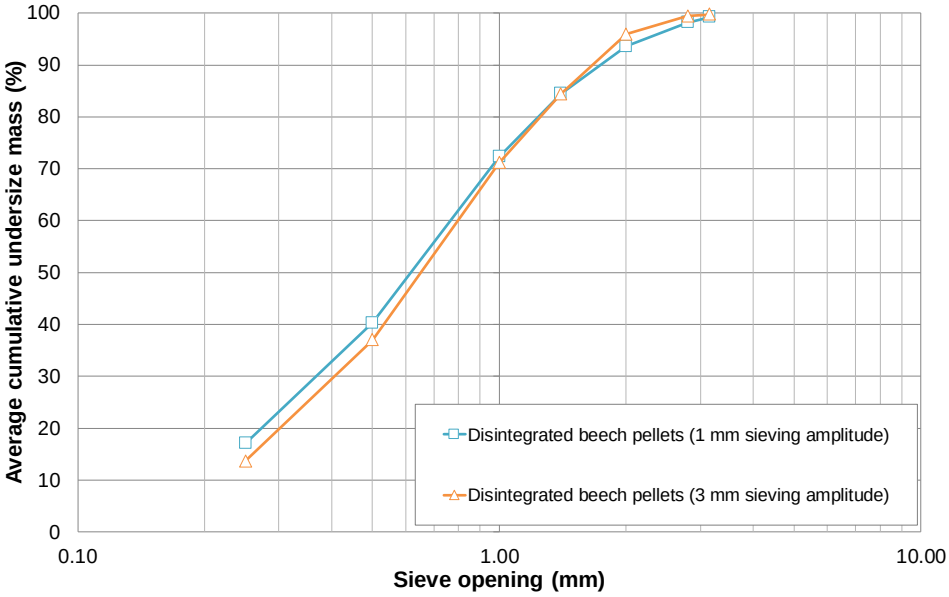

Fig. S9: Influence of sieving amplitude on the particle size distribution of disintegrated beech pellets. Average sieving data are presented.

Fig. S10: Appearance of beech pellets (left) and pine pellets (right).

Appendix III

Wood pellet milling tests in a suspension-fired power plant

Marvin Masche, Maria Puig-Arnavat, Johan Wadenbäck, Sønnik Clausen, Peter A. Jensen, Jesper Ahrenfeldt, Ulrik B. Henriksen

Fuel Processing Technology 173 (2018) 89–102

Contents lists available at ScienceDirect

Fuel Processing Technology

journal homepage: www.elsevier.com/locate/fuproc

Research article

Wood pellet milling tests in a suspension-fired power plant

Marvin Masche[a,*], Maria Puig-Arnavat[a], Johan Wadenbäck[b], Sønnik Clausen[a], Peter A. Jensen[a], Jesper Ahrenfeldt[a], Ulrik B. Henriksen[a]

[a] Department of Chemical and Biochemical Engineering, Technical University of Denmark, 2800 Kgs. Lyngby, Denmark
[b] Amagerværket, HOFOR A/S, Kraftværksvej 37, 2300 Copenhagen S, Denmark

ARTICLE INFO

Keywords:
Wood pellets
Roller mills
Specific grinding energy consumption
Particle size
Particle shape

ABSTRACT

This paper investigates the milling behavior of two industrial wood pellet qualities (designated I1 and I2 as per ISO 17225-2:2014) in large-scale coal roller mills, each equipped with a dynamic classifier. The purpose of the study was to test if pellet comminution and subsequent particle classification (i.e., the classifier cut size) are affected by the internal pellet particle size distribution obtained after pellet disintegration in hot water. Furthermore, optimal conditions for comminuting pellets were identified. The milling behavior was assessed by determining the specific grinding energy consumption and the differential mill pressure. The size and shape of comminuted pellets sampled from burner pipes were analyzed by dynamic image analysis and sieve analysis, respectively. The results showed that the internal pellet particle size distribution affected both the milling behavior and the classifier cut size. I2 pellets with coarser internal particles than I1 pellets required more energy for milling, led to a higher mill pressure drop and showed a larger classifier cut size. Comminuted pellet particles sampled from burner pipes were notably finer than internal pellet (feed) particles. At similar mill-classifier conditions, characteristic particle sizes of 0.50 mm for comminuted I1 pellets (compared to 0.83 mm for material within I1 pellets) and of 0.56 mm for comminuted I2 pellets (compared to 1.09 mm for material within I2 pellets), respectively, were obtained. Pellet comminution at lower mill loads and lower primary airflow rates reduced the mill power consumption, the mill pressure drop, and the classifier cut size. However, this was at the expense of a higher specific grinding energy consumption. Derived 2D shape parameters for comminuted and internal pellet particles were similar. Mill operating changes had a negligible effect on the original elongated wood particle shape. To achieve the desired comminuted product fineness (i.e., the classifier cut size) with lower specific grinding energy consumption, power plant operators need to choose pellets with a finer internal particle size distribution.

1. Introduction

Wood pellets as a renewable energy commodity for heat and power generation have experienced tremendous growth over the past decade in Europe [1,2]. European energy policies have driven this development to mitigate greenhouse gas emissions by 20% by 2020 [3]. In particular, USA, Canada, and Russia have responded to the increasing demand for wood pellets by enhancing pellet production, with many large-scale pellet plants being constructed for the European market [4]. When tons of solid biomass need to be transported overseas, pelletized biomass is more cost-efficient than wood chips because of higher energy and bulk density [5]. Furthermore, pelletization improves storage and handling characteristics with fewer dust emissions [6] that may increase the risk of explosions during transshipment [7]. To mitigate industrial greenhouse gas emissions, retrofitting power plants from coal to wood pellets by utilizing the existing milling equipment and auxiliary infrastructure offers a cost-efficient and practical option at low capital investment [8]. Furthermore, the converted plants preserve grid reliability compared to intermittent renewable energies like wind and solar [9]. Countries, like Denmark and United Kingdom, have already converted, or are currently converting their existing suspension-fired power plants from coal to operate 100% on biomass, mostly wood pellets [8].

The size reduction of solid particles is a significant process in suspension-fired power plants and is commonly performed in hammer mills or roller mills [8,10] to achieve a homogenous fuel distribution that is pneumatically transported to the burners. Previous studies [11–13] showed that roller mills were not capable of producing a product as fine as hammer mills. Regarding the particle shape, Trubetskaya et al. [12] found no difference between roller-milled and hammer-milled particles. However, roller mills required less power for

* Corresponding author.
E-mail address: marv@kt.dtu.dk (M. Masche).

https://doi.org/10.1016/j.fuproc.2018.01.009
Received 25 September 2017; Received in revised form 9 January 2018; Accepted 9 January 2018
0378-3820/ © 2018 Elsevier B.V. All rights reserved.

grinding than hammer mills [12,13]. The energy needed for milling biomass depends on the feed moisture, particle size reduction ratio, feedstock characteristics [14], feed rate and mill operating parameters [15]. Comminuting fibrous and orthotropic elastic wood that is capable of absorbing energy before size reduction [16] requires more energy than coal regardless of mill type [17].

The comminuted particle size and shape are essential properties for suspension-firing, as they influence the particle dynamics, particle heat and mass transfer [18]. For proper combustion control, the finer and more uniform the fuel is, the higher the chance to achieve complete combustion in the available boiler residence time [19]. To provide control over the fineness (i.e., the cut size) of the comminuted product conveyed to the burners, coal roller mills apply static or dynamic classifiers [8,20], which classify particles based on their shape, size, and density [21]. The cut size is based on Stokes' law [22] that is only valid for the drag force of a spherical particle [23]. Williams et al. [17] found that the classification system of a ring-roller mill for the comminution of densified biomasses followed the Stokes' law, indicated by an increasing sphericity with decreasing particle size. In large-scale mill classifiers, there are particle size limits for coal suspension-firing. In particular, 75% of pulverized coal needs to pass a 200 mesh sieve (75 μm) [24]. Equivalent limits for woody biomass particles have not been established. However, a size reduction to the same level as coal may not be required due to the higher volatile content of biomasses in combustion systems [19]. Esteban and Carrasco [10] recommend 95% of wood particles (dry weight basis) to be below 1 mm for optimal combustion. Adams et al. [25] found that 25% of biomass (dry weight basis) below 100 μm was ideal for excellent flame stability.

The study aims to assess the large-scale milling behavior of industrial wood pellet qualities in vertical roller mills (VRMs) at the suspension-fired combined heat and power (CHP) plant Amagerværket unit 1 (AMV1), located in Copenhagen (Denmark). AMV1 has a capacity of 80 MW electricity and 250 MW heat. Originally designed for coal, AMV1 was converted in 2010 to operate 100% on biomass, mainly wood pellets. The purpose of the study is to test if large-scale pellet comminution in VRMs and subsequent particle separation in dynamic classifiers are affected by the particle size distribution (PSD) of material within pellets, also known as the internal pellet PSD. To the best knowledge of the authors, this is the first study that compares the large-scale milling behavior of industrial wood pellet qualities. The results provided can be valuable to optimize the overall milling and combustion process for plant operators facing the problems of changing from coal to biomass pellets. Thus, the main objectives of the study are:

- To evaluate the sampling method for comminuted pellets conveyed to the burners.
- To compare the morphology (size and shape) of material within pellets with that from pellets comminuted at different mill loads.
- To analyze the influence of different pellet qualities on the milling process.
- To identify optimal conditions for comminuting wood pellets.

2. Materials and methods

2.1. Materials

Two industrial wood pellet qualities characterized in triplicate according to standardized methods were used (Table 1). The first quality fully conformed to the requirements of industrial pellets of class I1 according to ISO 17225-2:2014 [26] and was hence designated as I1. They were mainly softwood pellets made from Norway spruce (*Picea abies*) and Scots pine (*Pinus sylvestris*). They were produced in the Baltic countries. The second pellet quality met the specifications set out for industrial pellets of class I2 [26] and was hence designated as I2. They originated from the Southeastern United States and were made of ca. 93% softwood, mainly Southern yellow pine wood species, such as loblolly pine (*Pinus taeda)*, and 7% mixed hardwood species. The major difference between both pellet qualities was the internal PSD, which was obtained after pellets have been disintegrated in hot deionized water and dried in an oven [27]. Sieve analysis was then performed to determine the internal PSD of the dried material. The internal PSD of I1 pellets featured a 20% higher mass fraction of particles below 1 mm compared to I2 pellets.

2.2. Vertical roller mills and dynamic classifiers

Pellets were comminuted in three coal VRMs (type LM 19.2 D, Loesche GmbH, Germany), each equipped with a dynamic (or rotary) classifier (type LSKS 27 ZD-4 So, Loesche GmbH, Germany). The mills were denoted as M10 (mill 10), M20 (mill 20) and M30 (mill 30). The mills, i.e., the milling table, were driven by an electric motor via a vertical gearbox. A schematic representation of the design features of a Loesche coal VRM is shown in Fig. 1. The technical specifications for the mills are summarized in Table 2. The throughput rate for wood pellets is reduced due to their lower energy density compared to coal [8].

The pellet milling process comprises comminution, drying, particle classification and product discharge to the burners. As shown in Fig. 1, pellets fall from the side into the center of the rotating milling table, which is equipped with a dam ring for the adjustment of the milling bed thickness. Centrifugal forces move the pellets under two tapered, locally fixed, grinding rollers that are mounted in rocker arms. Compression force originating from the hydraulic-pneumatic, spring-loaded roller system comminutes the pellets. The rollers also achieve a sliding movement that results in additional shearing forces to comminute the pellets. To produce higher shearing forces, the existing roller mills at AMV1 were retrofitted. Holes were drilled into the roller track, and a surface material with higher hardness was applied to the roller surface. The rollers are driven by the grinding material and are moving vertically during the comminution process. As the rollers roll over the milling bed, the rocker arms, which are coupled to the pistons of the two linked hydraulic cylinders, start to move. Centrifugal forces again expel the comminuted pellet material over the rim of the milling table into the vicinity of the surrounding louvre ring. The louvre ring directs a hot primary airflow, which is tempered by a cooler to around 130 °C to avoid pellet pre-ignition and mill fires, upwards into the spinning rotor of the dynamic classifier. By this means, the comminuted pellet material is dried and lifted to the classifier [28]. The internal flow path of material from the milling table to the classifier is shown in Fig. 1.

In the classifier, drag or centripetal forces (generated by the airflow to the rotor), and mass or centrifugal forces (generated by the rotor rotation) act upon the particles [20]. If the mass force is greater than the drag force, coarse particles are rejected by the classifier and fall back to the milling table via the grit cone for further size reduction. Else, if the drag force is greater than the mass force, the primary airflow lifts the fine particles upwards in the classifier housing [29]. The balance between both forces governs the particle separation [24]. If both forces are in equilibrium for a specific particle mass, the rotor classifies the particle with 50% efficiency, which is referred to as the classifier cut size. Plant operators can control the cut size, and thus the degree of product fineness by adjusting the classifier rotor speed, dam ring height, milling table speed, airflow rate ($\dot{m}_{Air}$), hydraulic grinding pressure (HGP) of the roller, and pellet feed rate ($\dot{m}_{Pellet}$) [20,30,31]. The fines eventually leave the mill at a mill outlet temperature of 60 °C via four outlet pipes to four burners. In total, AMV1 has 12 front-wall-fired burners, each fed by a separate burner pipe distributed in three different levels, one for each mill (Fig. 2).

2.3. Sampling equipment

Wood pellets were sampled from the end of a continuously moving conveyor belt before entering the mill using a falling stream sampler.

Table 1
Specifications of the two industrial wood pellet qualities graded according to ISO 17225-2:2014 [26].

Parameters	Unit	I1 Pellets	I2 Pellets	Method
Proximate analysis				
Moisture content	wt%, ar, w.b.	6.6	5.7	EN ISO 18134–1: 2015
Ash content	wt%, d.b.	0.6	0.6	EN ISO 18122: 2015
Volatile matter	wt%, d.b.	84.5	83.9	EN ISO 18123: 2015
Fixed carbon	wt%, d.b.	14.9	15.5	By difference
Ultimate analysis				
Carbon	wt%, d.b.	50.7	51.1	EN ISO 16948: 2015
Nitrogen	wt%, d.b.	0.2	0.1	EN ISO 16948: 2015
Hydrogen	wt%, d.b.	6.1	6.1	EN ISO 16948: 2015
Oxygen	wt%, d.b.	42.4	42.0	EN 14588:2010 (by difference)
Net calorific value	MJ/kg, ar	17.5	18.0	EN 14918: 2009
Pellet diameter (D) and length (L)	mm, ar	D, 6.2 and 8.3; L, 12.3	D, 6.7; L, 12.9	EN ISO 17829: 2015
Bulk density	kg/m^3, as received	653.1	669.2	EN ISO 17828: 2015
Mechanical durability (fines)	wt%, ar	98.5	99.1	EN ISO 17831-1: 2015
PSD of disintegrated pellets (internal PSD)	wt%, d.b.	≥99.5% (< 3.15 mm) ≥98.7% (< 2.0 mm) ≥79.2% (< 1.0 mm)	≥98.0% (< 3.15 mm) ≥93.9% (< 2.0 mm) ≥59.4% (< 1.0 mm)	EN ISO 17830: 2016

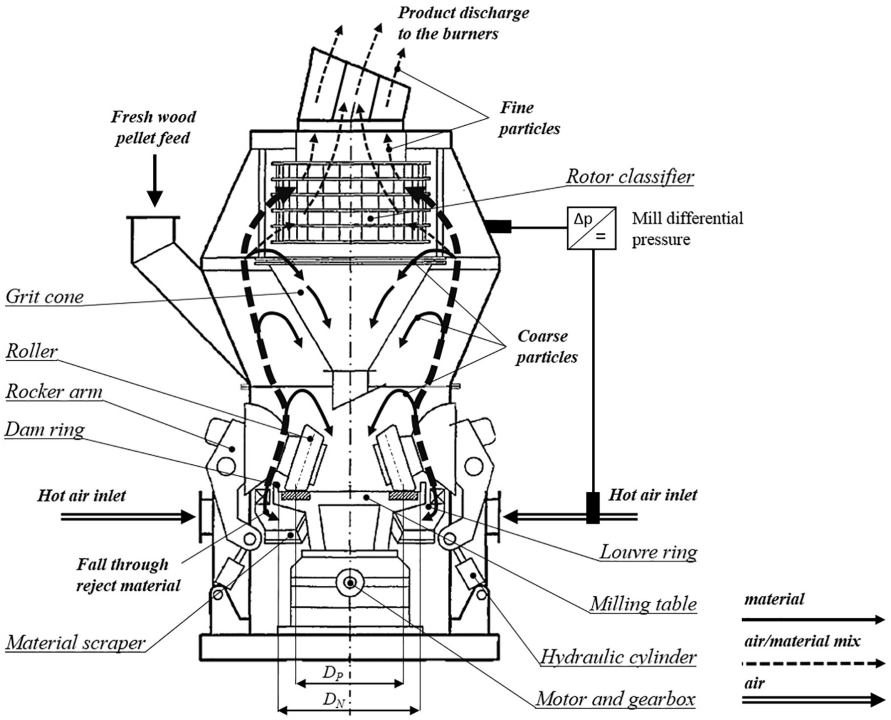

Fig. 1. Schematic representation of a large-scale coal VRM and the internal material flow within the mill.
Adapted from [57].

According to ISO 14488:2007 [32], isoaxial and isokinetic sampling with cyclone was used as a sampling probe to extract the fine comminuted pellet product via a vacuum with a mean air velocity of 30 m/s from inside the burner pipes. The air velocity was measured by an airflow meter in the wood dust-laden environment. The samples were extracted from the burner pipe center, as it shows a more stable particle flow than along the pipe wall [33]. Dustless connectors were installed at the sampling ports to eliminate any wood dust leakage while inserting and removing the sampling device. The sampling ports for wood dust leaving M10 were placed in horizontal sections of the pipes, while those ports exiting M20 and M30 are located in vertical sections of the pipe (Fig. 2). The mill-burner configuration shows that the outlet pipes exiting M20 were configured nearly symmetrically. The pipe length was approximately equal from mill outlet to burners B22 and B23 and from mill outlet to burners B21 and B24, respectively. However, this was not the case for pipes exiting M10 and M30. For

Table 2
Technical specifications of the three Loesche coal VRMs.

Description	Specification
Throughput rate (t/h)	Up to 36 (for coal) Up to 28.8 (for biomass)
Number of rollers	2
Roller inclination	15°
Nominal milling table diameter (m), D_N	1.9
Diameter milling path (m), D_P	1.5
Milling table speed (rpm)	42
Motor drive power (kW)	315
Separator	Dynamic classifier

subsequent particle shape and size analysis, collected wood dust samples were split into representative subsamples by a rotating sample divider (type PT100, Retsch Technology GmbH, Germany).

2.4. Milling tests

Table 3 shows the conditions for different roller milling scenarios during steady-state operation. Average values for the operating conditions were recorded in the central control room at AMV1. The measured range of mill operating parameters and the sensor types used are summarized in Table 4. In total, the following 12 milling scenarios were chosen:

- Scenario 1: test the precision of sampling comminuted pellets conveyed to the burners,
- Scenario 2: compare the comminuted pellet PSD obtained by sieving and Camsizer X2,
- Scenarios 2–4: compare sampling from vertical and horizontal mill outlet pipes,
- Scenarios 5–6: compare the size and shape of disintegrated I1 and I2 pellets versus I1 and I2 pellets comminuted at similar steady-state milling conditions,
- Scenarios 6–7: test the influence of airflow rate and classifier rotor speed changes,
- Scenarios 7–12: test the influence of mill load changes when milling I1 and I2 pellets.

Table 3
Operating conditions of the mill-classifier system for various test scenarios[a].

#	Mill	Pellets	$\dot{m}_{Pellet}$ (t/h)	$\dot{m}_{Air}$ (t/h)	Mill air/fuel ratio[b]	Rotor speed[c] (%)	HGP (MPa)
1	M30	I1	28.8	56.8	2.0	13.1	7.0
2	M10	I1	20.5	46.8	2.3	17.2	6.6
3	M20	I1	20.4	46.5	2.3	17.7	6.5
4	M30	I1	20.3	46.4	2.3	17.4	6.5
5	M20	I1	20.6	46.8	2.3	17.4	6.6
6	M20	I2	20.6	46.7	2.3	17.5	6.7
7	M20	I2	20.6	52.2	2.5	13.0	6.7
8	M20	I2	16.6	43.7	2.6	13.0	6.3
9	M20	I2	14.3	41.2	2.9	13.0	6.1
10	M20	I1	20.5	46.5	2.3	17.6	6.7
11	M20	I1	17.4	43.0	2.5	16.6	6.4
12	M20	I1	14.4	39.6	2.7	15.7	6.1

[a] Dam ring height and milling table speed are constant.
[b] Mill air/fuel ratio is the ratio of primary airflow rate to pellet feed rate into the VRM.
[c] Rotor speed is given as the percentage of the maximum speed.

2.5. Pellet milling behavior

The specific grinding energy consumption (SGEC) was used as a measure of the total energy consumed during the grinding process, and expressed by the following equation:

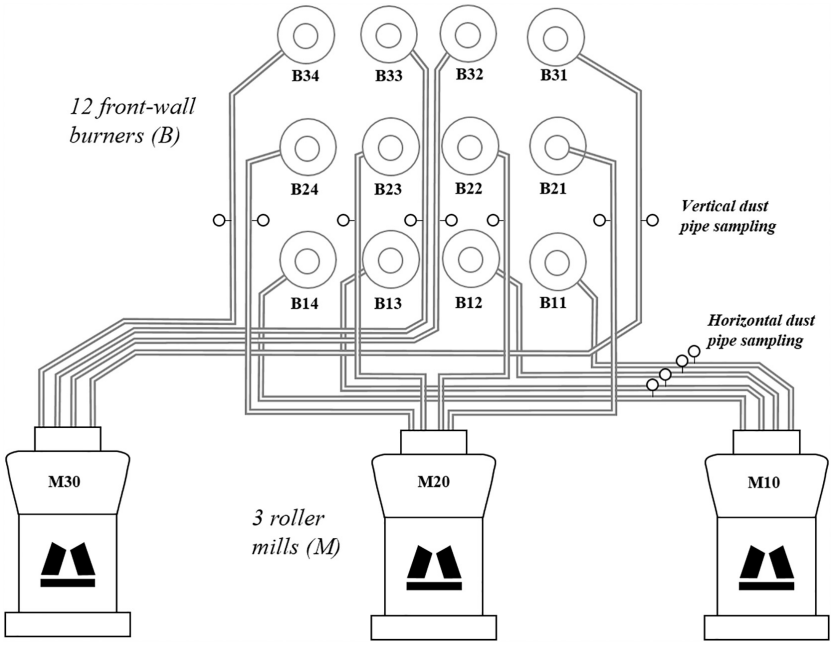

Fig. 2. Mill-burner configuration at AMV1.

Table 4
Measured range of mill operational parameters and the sensors used.

Parameter	Range	Sensor type
$\dot{m}_{Pellet}$ (t/h)	14.3–28.8	Load cell
$\dot{m}_{Air}$ (t/h)	39.6–56.8	Pitot tube + pressure transducer
Classifier rotator speed (%)[a]	13.0–17.7	Proximity switch
Δp (kPa)	2.0–3.8	Pressure transducer
Mill inlet temperature set point (°C)	130	PT 100 + transducer
Mill exit temperature set point (°C)	60	PT 100 + transducer
HGP (MPa)	6.1–7.0	Force transducer
Motor power (kW)	178.5–287.3	Torque transducer

[a] Rotor speed is given as the percentage of the maximum speed.

$$SGEC = \int_0^t \frac{P}{m_{Pellets}} dt \quad (1)$$

where $m_{Pellets}$ was the amount of wood pellets (t) measured by continuous weighing the conveyor belt to the mill. P was the total, instantaneous power (kW) consumed while comminuting at time t (h), which was obtained from a data logger. P was assumed to go directly into the grinding process as the mill table is rotated. *SGEC* was hence a result of the pellet feed rate and the grindability of the pellets under given operating conditions. However, *SGEC* is only an estimate of the actual motor energy required for grinding, as the idle power without pellets has to be deducted from the total power consumption, and as some amount is dissipated as thermal energy. Thus, the energy transferred to comminute pellets specifically is not provided. The differential pressure (Δp) across the mill was used as a measure of the instantaneous mill load due to the level of material being ground and material circulating within the mill. It represented the static differential pressure measured at the mill inlet and outlet (Fig. 1). A low drop in pressure is desirable, but factors such as $\dot{m}_{Pellets}$, $\dot{m}_{Air}$, and mill geometry lead to an increased Δp [34].

2.6. Fine comminuted pellet size and shape characterization

2.6.1. Sieve analysis

A vibratory sieve shaker (type AS 200 control, Retsch Technology GmbH, Germany) determined the comminuted pellet PSD. The stack comprised seven square-hole sieves each with a diameter of 200 mm, and aperture sizes of 0.09, 0.25, 0.50, 1.00, 1.40, 2.00 and 2.80 mm, mounted on a collecting pan. About 50 g of comminuted pellets were tested. An electronic balance (type EW-N, KERN & SOHN GmbH, Germany) weighed the individual sieves and pan before and after sieving. This information was converted into a cumulative (undersize) weight distribution, representing the percentage of sample passing through each sieve. Sieve analysis was run for 10 min with 1 mm amplitude and performed in duplicate.

2.6.2. Dynamic image analysis

A dynamic image analyzer (type Camsizer® X2, Retsch Technology GmbH, Germany) recorded the size and shape of comminuted pellets using two linked cameras (basic and zoom camera) with a resolution of 4.2 megapixels per image, covering a measuring range from 30 µm to 8 mm. The particles are individually detected as projected areas, digitalized and the images processed. The X-Jet mode of the Camsizer® X2 was used to disperse the agglomerated wood dust falling from a vibrating feeder by a compressed air-driven venturi nozzle. Preliminary tests were run to estimate the optimal compressed air pressure (30 kPa) and sample size (15–20 g). The measurements were done in triplicate.

Compared to sieve analysis, the PSD from Camsizer® X2 is presented as a cumulative (undersize) volume distribution versus $x_{c,min}$. $x_{c,min}$ stands for the shortest maximum chord of a 2D particle projection measured from all measurement directions, and thus represents the width of a particle projection. Preliminary tests and a previous study [17] show that this parameter gives the closest results to those obtained by sieve analysis. Camsizer® X2 software also provides the aspect ratio (width-to-length ratio) and circularity values among other 2D shape factors. The Camsizer® definition of the circularity is the ISO 9276-6:2008 standard definition squared [35]. Both shape factors are commonly used for describing comminuted wood particle shapes [12,17]. The aspect ratio (AR) ranging between zero and one is defined as follows:

$$AR = \frac{x_{c,min}}{Fe_{max}} \quad (2)$$

where Fe_{max} is the maximum Feret diameter (longest distance between two parallel tangents of the particle at any arbitrary angle) or maximum caliper diameter. Trubetskaya et al. [36] showed that Fe_{max} is suitable to represent the length of particles. The circularity (C), which is also a measure of the particle roundness [37], indicates how closely the particle resembles a circle:

$$C = \frac{4 \bullet \pi \bullet A_{particle}}{P_{particle}^2} \quad (3)$$

where $A_{Particle}$ and $P_{Particle}$ refer to the particle projection area and the particle perimeter, respectively. A value of one corresponds to a perfect circle.

2.6.3. Data analysis

The Rosin-Rammler-Bennet-Sperling (RRBS) model describes the comminuted product PSD. It is a two-parameter distribution function expressed as a cumulative percent (undersize) distribution. Previous studies [38–40] showed good correlation between RRBS fit parameters and measured milled particle sizes. The RRBS equation is [41]:

$$R(d) = 100 - 100 \bullet e^{-\left(\frac{d}{d^*}\right)^n} \quad (4)$$

where R(d) is the cumulative percent (undersize) distribution of material finer than the particle size d, d^* is the characteristic particle size defined as the size at which 63,21% of the PSD lies below, and n is the distribution parameter. A plot of ln[ln[100 / (100 − R(d))]] against ln (d) on the double logarithmic scale gives a straight line of slope n. The smaller the n-value, the wider the product PSD, whereas higher n-values imply a more uniform product distribution [42].

The 90th percentile (D90) of the cumulative undersize distribution was used to show the effect of operating conditions of the mill-classifier system on the comminuted product fineness. Yu et al. [43] found a very strong positive correlation between classifier cut size and product fineness (*D90*), as well as between cut size and fine product yield. A smaller cut size led to a finer dust collected and a smaller fine product yield.

Von Rittinger's comminution law was used to analyze the relationship between *SGEC* and particle size reduction obtained by the mill-classifier system [44]:

$$SGEC = K_R \left(\frac{1}{d_p} - \frac{1}{d_f} \right) \quad (5)$$

where d_p is the 90th percentile passing size of the comminuted product and d_f is the 90th percentile passing size of the material within the pellet feed. The material characteristic parameter K_R (kWh mm t^{-1}) allows to characterize the pellet grindability by a single value. Recent studies [14,17,45] suggest the applicability of Von Rittinger's law to predict the energy consumption during milling of biomass pellets.

2.7. Statistical analysis

Statistical analyses were performed using R Studio (version 1.0.143, R Studio Inc., Boston, USA). Pearson's correlation coefficients (r) were

Table 5
Dust flow characteristics in the burner pipes exiting M30 (Scenario 1, Table 3). Average values from five samples and their 95% confidence interval indicated in parentheses. Particle size analysis was performed by mechanical sieving.

# pipe	Wood dust sample flow $\dot{m}_{Dust}$(g/s)[1]	n	d* (mm)	D90 (mm)
1	1.31 (0.08)[a]	0.93 (0.05)[a]	0.38 (0.02)[a]	0.94 (0.01)[a]
2	3.31 (0.24)[b]	1.18 (0.06)[b]	0.59 (0.03)[b]	1.18 (0.04)[b]
3	2.77 (0.21)[c]	1.18 (0.05)[b]	0.53 (0.03)[c]	1.02 (0.04)[c]
4	5.11 (0.16)[d]	1.26 (0.02)[c]	0.67 (0.01)[c]	1.27 (0.02)[d]

Note: different letters on average values in the same column indicate statistical significance at 5%.
[1] The amount of wood dust sampled divided by the sampling time.

calculated to study the strength of the linear relationship between two parameters. Multiple comparisons using one-way analysis of variance (ANOVA) followed by a Tukey's HSD test for post-hoc analysis were conducted to determine if there were significant differences between the means of independent groups. All results were considered statistically significant at the 95% confidence level ($p < 0.05$).

3. Results and discussion

3.1. Precision testing of isokinetic sampling equipment

Table 5 shows the flow characteristics of comminuted wood particles inside the vertical pipes exiting M30. It is clear that the distribution of comminuted wood particles and their characteristics are different among all four pneumatic pipes. Mill outlet pipes 2 and 3 nearly provide similar RRBS fit parameters and sample mass flows. The statistical analysis shows there is no statistically significant difference between pipe 2 and 3 regarding the uniformity constant (*n*-value). Pipe 1 yields the finest and lowest wood dust sample flow, while pipe 4 provides the coarsest and largest wood dust sample flow. Thus, the larger fraction of coarse particles in pipe 4 makes up the bulk of the weight of the sampled wood dust, whereas the higher fraction of finer particles in pipe 1 may be the reason for the lower mass flow.

Differences among burner pipes can be attributed to an inappropriate distribution of mass of wood dust from the classifier to each of the pipes, to different air velocities in the pipe, and to the pipe geometry. The mill-burner configuration in Fig. 2 shows that M30 outlet pipes have no equal distances from the classifier to the burners. A longer pipe will result in a pressure drop due to static and dynamic effects in the pipe, causing a reduction of the flow of suspended wood dust particles. As pipe 1 is much longer than pipe 4, the pressure drop is more significant indicated by a four times lower sample mass flow. The reduced mass flow also leads to a lower velocity in the pipe, which will affect dust sampling [46]. Considering a similar sampling velocity for all pipes, the reduced pipe velocity in pipe 1 will cause a finer dust sample compared to pipe 4 indicated by lower *d** and *D90* values. Differences in flow characteristics were also observed for M10 outlet pipes. Sampling from M20 outlet pipes showed similar flow characteristics that were attributed to their symmetric configuration. As a result, the focus of the present study was on M20. Relatively low confidence intervals in Table 5 indicate that isokinetic sampling and sieve analysis are precise and reliable methods.

Characterizing the flow properties of comminuted biomass particles inside a pneumatic pipe is more complex than for coal, due to their wider range of particle sizes and non-spherical particle shape [33,47]. Compared to coal, the flowability and flow stability of biomass particles are worse, increasing the risk of arching and blockage during the pneumatic conveying process [48]. The fine comminuted product was extracted isokinetically so that the suction velocity at the probe tip was equal to the mean conveying airflow velocity in the pipe. Qian and Yan [47], however, found that pneumatically conveyed biomass and flour, which was used to simulate pulverized coal, traveled slower in horizontal pipes than the conveying air due to their different size and shape. The slip velocity between the particles and the conveying air was lower for flour particles. Assuming a similar behavior for comminuted wood in the upward vertical pipes, as it was not possible to measure their mass flow and velocity, undersampling may have occurred. Due to the higher sampling velocity, the inertia of coarser particles will keep them from following the streamlines that converge into the sampling probe, and a finer sample will be obtained [46]. Under these conditions, there is a risk of underestimating the actual wood particle sizes. The slip velocity between the wood particles and the conveying air will require further quantitative investigation.

3.2. Wood particle size determination by sieve analysis and Camsizer® X2

Fig. 3 shows the PSD of comminuted I1 pellets analyzed by mechanical sieving and Camsizer® X2 operated in the X-Jet mode. It shows very good agreement for particles larger or equal 0.5 mm. That supports the observation of Gil et al. [40] that sieving data mainly describe the width of particles, especially for the large size fractions. However, sieving seems to underestimate the fraction retained on the 0.25 mm and 0.09 mm sieves. That could be explained by an increased dust cohesiveness when decreasing the particle size [49]. Particles below 0.5 mm become more sticky and cohesive and hence increase the tendency to block the sieve openings by forming agglomerates. These

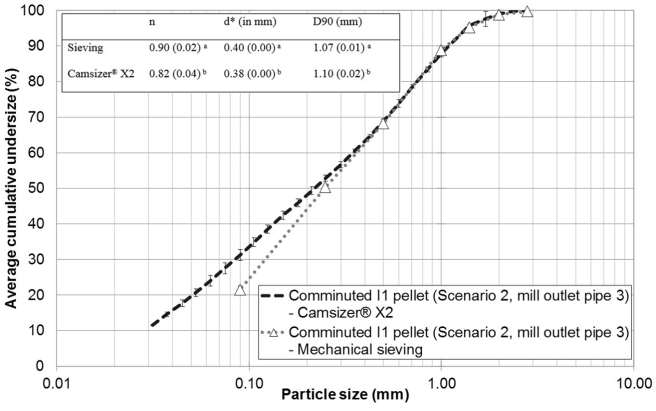

Fig. 3. Comminuted pellet sampled from M20 burner pipes PSDs and RRBS fit parameters n and d*, and D90 analyzed by sieving and Camsizer® X2 (Scenario 2, Table 3). Error bars indicate the 95% confidence interval of three repeated measurements.

agglomerates remain on the sieve and thus diminish the mass of comminuted wood pellets in the finer fraction. The attractive forces (or agglomeration strength) between small particles mainly stem from van der Waals interactions [50]. Jensen et al. [51] showed that the accuracy of particle size analysis by sieving was reduced with decreasing particle size. The authors assumed that this was due to the increased tendency of particles clogging the openings of sieves with small mesh sizes. Rezaei et al. [52] ascribed the underestimation of the width of milled wood pellet particles by sieve analysis by its fractionation mechanism and particle interactions.

Derived 2D shape factors analyzed by Camsizer® X2 indicated that the average circularity for comminuted particles increased for smaller particles. Thus, fines (i.e., particles below 0.5 mm) with $C = 0.54$ were more circular (i.e., rounder) than the coarse fraction (i.e., particles above 1.0 mm) with $C = 0.50$. Compared to coal particles that are nearly spherical [11], comminuted wood particles are very elongated due to the anisotropic wood structure [53], indicated by average particle aspect ratios of about $AR = 0.53$. The study of the impact of the circular and elongated particle shape on inter-particle interactions would be a valuable contribution to the understanding of possible particle agglomerations on sieves with small apertures.

The RRBS model fits well the size distribution of comminuted pellets analyzed by both sieving ($R^2 > 0.998$) and Camsizer® X2 ($R^2 > 0.988$), with sieving achieving a slightly better fit. Small error bars in PSD data in Fig. 3 indicate that we expect to get similar results from repeated measurements with high precision (i.e., reliability). Sieving does not provide information about the particle shape and is less accurate to describe the product fineness. Thus, the Camsizer® X2 was used for the other milling scenarios to assess the size and shape of comminuted wood dust particles simultaneously.

3.3. Comparison between horizontal and vertical pipe sampling

The PSD of wood dust sampled from burner pipes exiting all three mills at AMV1 is shown in Fig. 4. The mill-burner configuration is shown in Fig. 2. Sampling distributions from M10 show an excess of fine particles, whereas PSDs from M20 and M30 are shifted towards coarser particle sizes. Differences can be attributed to the pipe orientation where the sampling point is mounted. Dust sampling from horizontal pipes may lead to particle segregation, where coarser particles move at the bottom level and fine particles are in suspension. Other studies [33,54] also confirmed the effect of particle segregation in horizontal pipe sections. Samples from horizontal pipes are thus less representative. In contrast, the vertical M20 pipe network is more representative due to its symmetry. It is more likely to achieve a uniform particle concentration in these pipes. The lowest error bars for the average PSD from M20 pipes compared to the PSDs from M10 and M30 pipes support this statement.

3.4. Milling behavior of I1 and I2 pellets

The PSDs of disintegrated I1 and I2 pellets compared with comminuted I1 and I2 pellets sampled from M20 burner pipes are shown in Fig. 5. Although the internal PSD of I2 pellets showed about 20% coarser particles below 1 mm compared to I1 pellets, the mill classifier nearly discharges a similar comminuted product to the burners. The statistical analysis showed no statistically significant difference in n and d^* between comminuted I1 and I2 pellets. Table 6 shows that compared to the pellet feed material (i.e., disintegrated pellets), the d^* and $D90$ values significantly decrease by 40% and 19% for I1 pellets, respectively, and by 49% and 24% for I2 pellets, respectively. It shows that the mill classifier limits coarser wood particles sent to the burners. However, isokinetic dust sampling may under-represent the amount of coarse particles, as mentioned in Section 3.1.

The mill classifier, however, did not achieve the same comminuted product fineness (i.e., classifier cut size) indicated by statistically different ($p < 0.05$) $D90$ values of comminuted I1 and I2 pellets (Table 6). Differences in the product fineness may be explained by wood pellet characteristics, such as internal pellet PSD and wood properties. In particular, the different anatomical structure of softwood and hardwood species may cause a different grinding behavior in the mill. The isokinetic sampling method could also explain these differences. Archary et al. [55] found that sampling coal at the center of vertically oriented burner pipes resulted in a higher concentration of coarse comminuted particles, while the fine particle fraction moved near the pipe wall. Hence, a coarser PSD of the comminuted I2 pellets may lead to an even higher concentration of coarser particles at the inner part of the pipe that is collected by the isokinetic sampling device. Error bars in Fig. 5 are larger for comminuted I2 pellets than for I1 pellets, indicating a greater level of variation of the wood dust PSD in the burner pipes. The coarser comminuted I2 pellets, hence, seem to produce more unstable particle flow characteristics compared to the finer comminuted I1 pellets. This result is in accordance with recent work [33]. Thus, it might be more difficult to maintain a stable combustion when using I2 pellets. Fig. 5 shows that about 76% of comminuted I2 pellets are below 1 mm compared to 84% of comminuted I1

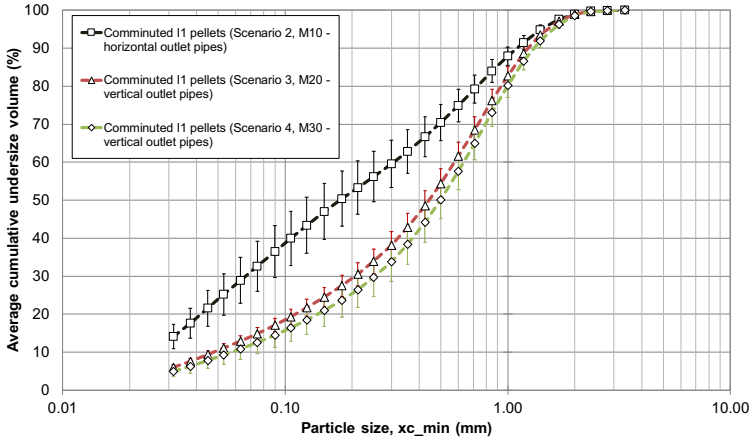

Fig. 4. Vertical versus horizontal pipe sampling of comminuted I1 pellets (Scenarios 2–4, Table 3). Each line represents the average PSD of four burner pipes of that mill. Error bars show one standard deviation within the different fuel pipes of the same mill.

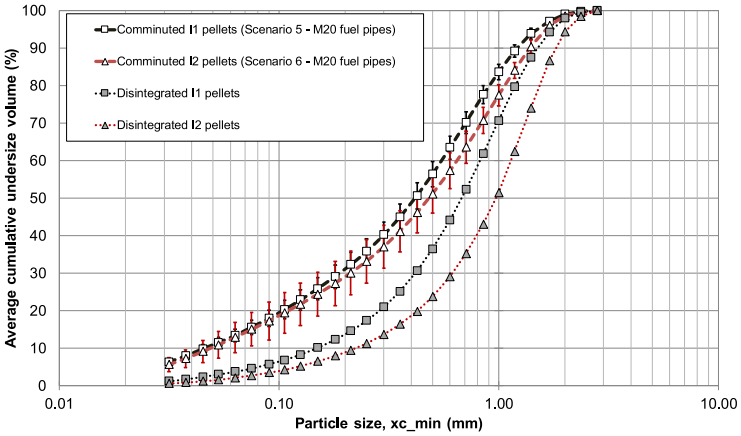

Fig. 5. PSD comparison between disintegrated and comminuted pellets (Scenarios 5 and 6, Table 3). Error bars represent one standard deviation within the different fuel pipes of the mill, and they are displayed when greater than the data symbol.

Table 6
Milling performance and PSD characteristics of comminuted I1 and I2 pellets sampled from M20 burner pipes compared to disintegrated I1 and I2 pellets. Average values are presented and one standard deviation between fuel pipes is indicated in parentheses.

	n	d* (mm)	D90 (mm)	K_R (kWh mm/t)	P (kW)	SGEC[1] (kWh/t)	Δp (kPa)
Comminuted I1 pellets (Scenario 5)	0.97[a] (0.03)	0.50[a] (0.10)	1.22[a] (0.07)	60.9[a]	197.5[a] (3.1)	9.6[a]	3.4[a] (0.2)
Disintegrated I1 pellets	1.37[b] (0.06)	0.83[b] (0.01)	1.51[b] (0.01)				
Comminuted I2 pellets (Scenario 6)	0.97[a] (0.08)	0.56[a] (0.13)	1.39[c] (0.07)	81.8[b]	287.3[b] (3.3)	13.9[a]	4.4[b] (0.1)
Disintegrated I2 pellets	1.40[b] (0.01)	1.09[c] (0.04)	1.82[d] (0.02)				

Note: different letters on average values in the same column indicate statistical significance at 5%.
[1] Dynamic classifier and fan power not included in SGEC.

pellets. Hence, it will be more likely to achieve complete combustion of comminuted I1 pellets [10].

I2 pellets required a 45% higher power consumption for milling, a 45% higher *SGEC* and led to a 29% higher Δ*p* compared to I1 pellets (Table 6). The higher Δ*p* may result from a higher accumulation of pellet material on the milling bed due to a larger quantity of coarse particles rejected by the classifier. Parameters such as moisture content, feed size, and mill operating conditions [14,15] are known to influence the energy required for milling. The small difference in the durability of I1 and I2 pellets (Table 1) does probably not explain the different *SGEC*, as noted by Temmerman et al. [14]. They further stated that the higher the moisture content in wood pellets, the more energy was required during hammer milling. In the present study, however, comminuting moister I1 pellets showed a lower energy consumption. The hot airflow entering the mill may facilitate fast drying of the material to be milled. As shown by Williams et al. [45], dry comminution led to more consistent grinding energies across biomasses. Thus, the higher energy consumption required for comminuting I2 pellets compared to I1 pellets may be mainly due to the larger difference in PSD between the material within the pellet feed and the fine comminuted pellet product. This is in agreement with the Von Rittinger's comminution law [14]. The effect of pellets made from different wood species on the mill power consumption and the comminuted product fineness remains unclear and requires further investigation.

Fig. 6 shows derived 2D shape factors (aspect ratio and circularity) of comminuted and disintegrated pellets. The values for coarsest particles were neglected due to the small number of particles analyzed, leading to bad statistics. Overall, average circularity and aspect ratio distributions of disintegrated and comminuted pellets show similar trends regardless the differences in internal pellet PSD. That indicates that the effect of roller mills on the particle shape is negligible. The observed particle shape may be therefore related to the raw material size reduction step before pelletization that is commonly performed in hammer mills. Pichler et al. [38] obtained similar aspect ratios for dry spruce sawdust particles comminuted in a hammer mill. Our experimental results corroborate previous findings from Trubetskaya et al. [12] and Williams et al. [17] who found that comminuting pellets in lab-scale and large-scale roller mills only had little effect on the particle shape.

Regarding circularity, the average values increase from 0.45 for the coarsest particles to about 0.57 for the finest particles (Fig. 6b). A clear tendency can be seen that smaller disintegrated and comminuted I1 and I2 pellet particles are more circular (i.e., rounder) than coarser particles. Disintegrated and comminuted wood pellets have low aspect ratios, which increase with particle size. There is a notable difference in the average aspect ratio between I1 and I2 pellet particles (Fig. 6a), which decreases with smaller particle sizes. I2 pellet particles appear to be more elongated than I1 pellet particles indicated by lower aspect ratios. Differences may be related to the different wood properties, such as microstructure and strength. For example, the comminuted wood shape may depend on the shearing resistance in different wood directions [53]. To illustrate, a particle aspect ratio of about 0.5 indicates a 2D particle area about twice as long as wide. The particles hence appear to be rather a flake or cuboid-like than spherical, which was also observed by Momeni [11] and Trubetskaya et al. [36]. With 2D image analysis lacking the third dimension, Trubetskaya et al. [36] analyzed the thickness of wood pellets comminuted in a roller mill at Avedøre power plant. For particles with a width below 0.85 mm, the thickness was found to be about 0.6 times the particle width. Larger particles (0.85–1.14 mm) had a thickness of about 0.4 times the particle width. Thus, an average wood particle comminuted in a power plant roller mill with a width ($x_{c,min}$) of 1 mm has a typical length (Fe_{max}) of 2 mm and a

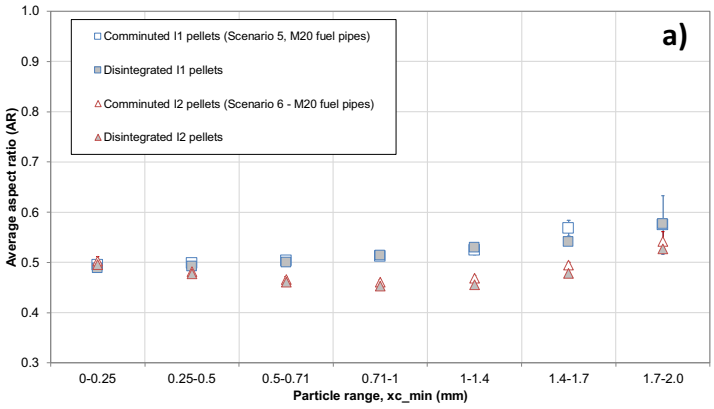

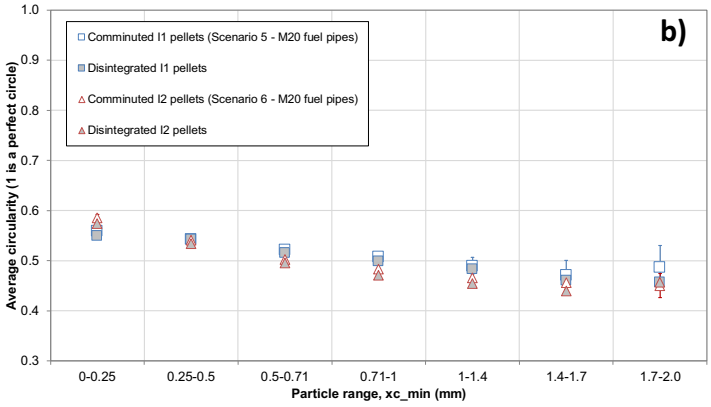

Fig. 6. Average aspect ratio (a) and circularity (b) of disintegrated and comminuted I1 and I2 pellets (Scenarios 5 and 6, Table 3). Error bars indicate one standard deviation within different fuel pipes of the mill, and they are displayed when greater than the data symbol.

thickness of about 0.4 mm. An adequate geometric representation of a comminuted wood particle, e.g., for combustion modeling purposes, may be a flat cuboid (plate).

3.5. Influence of airflow rate and classifier rotor speed

The airflow rate was reduced, and the rotor speed was increased for comminuting I2 pellets, while dam ring height, milling table speed, *HGP*, and $\dot{m}_{Pellet}$ remained constant (Scenarios 6 and 7, Table 3). Overall, a finer comminuted product conveyed to the burners is expected by adjusting the rotor speed and $\dot{m}_{Air}$ [20]. The results are in good agreement with what was expected. Fig. 7 shows that the average dust PSD from the burner pipes shifts to the left at Scenario 6 compared to Scenario 7. The d^* and *D90* values decrease by 27% and 14%, respectively, indicating a smaller classifier cut size when comminuting I2 pellets at Scenario 6. However, this is at the expense of a 26% higher *P*, a 25% higher *SGEC* and a 16% higher Δp, indicating a lower grinding efficiency. The *SGEC* seems to vary with the comminuted product fineness (i.e., classifier cut size). Both the higher *P* and higher Δp may be attributed to a higher material layer on the milling bed. Decreasing $\dot{m}_{Air}$ reduces the drag force to the rotor. Thus, less coarse wood particles may be carried through the classifier, and instead, fall onto the milling table. The thicker milling bed corresponds to a longer particle residence time (higher circulation load) on the milling table. Thus, particles will experience more grinding actions under the roller, leading to a finer and wider PSD (lower RRBS *n*-value). Along with the increased rotor speed, only fine particles will be lifted into the rotor classifier by the airflow. On the other hand, a stronger airflow and reduced rotor speed lead to a faster emptying of the mill, and a shorter particle residence time on the milling table. The comminuted product PSD then becomes coarser and narrower (higher RRBS *n*-value). Derived shape factors were similar to those shown in Section 3.4. To attribute the individual contribution to the product fineness and absorbed mill power, the adjustments of airflow rate and the rotor speed need to be tested independently.

3.6. Influence of mill load and airflow rate

The general concept in modern CHP plants is to adjust the mill load (i.e., mill productivity) according to the needs of the boiler. A measure of the mill load is the pellet feed rate to the mill. More pellets entering the mill will increase the mill load, and hence the production rate. A higher $\dot{m}_{Pellet}$ means more material on the milling table, thus increasing the milling bed thickness that will lead to a higher Δp (Table 7). This expectation is supported by a very strong positive, but not statistically significant trend between $\dot{m}_{Pellet}$ and Δp ($r = 0.80$, $p = 0.058$), as shown in Table 8. To compensate for a thicker milling bed that requires a higher grinding effort, $\dot{m}_{Pellet}$ was regulated along with *HGP*. Thus, the *HGP* provided by the spring-loaded roller system increases with a higher $\dot{m}_{Pellet}$ (i.e., thicker milling bed) and vice versa (Table 3). The

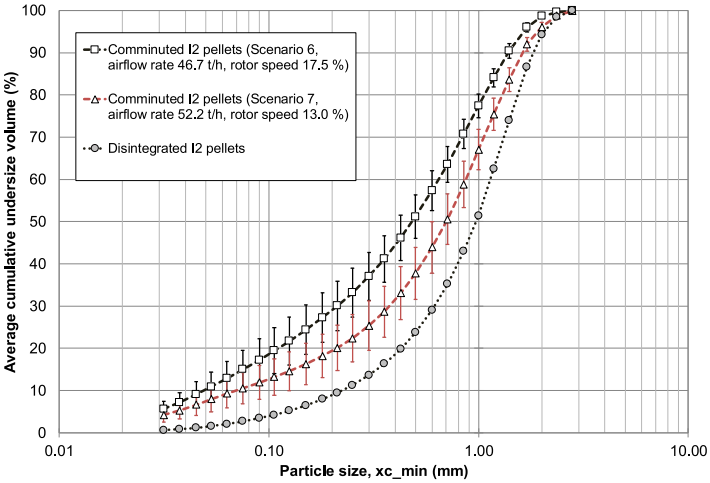

Fig. 7. Average cumulative PSD of I2 pellets comminuted at different airflow rates and rotor speeds (Scenarios 6 and 7, Table 3). Error bars represent one standard deviation within the different fuel pipes of the mill.

Pearson's correlation coefficient of r = 1.00 ($p < 0.001$) confirms that there is a perfect linear relationship between $\dot{m}_{Pellet}$ and *HGP* (Table 8). *HGP* was also increased with the pellet feed rate to reduce the risk of mill choking (i.e., a situation that occurs when Δp exceeds a threshold). Besides increasing *HGP*, $\dot{m}_{Air}$ was also regulated in a strong linear manner with $\dot{m}_{Pellet}$ (r = 0.90, $p < 0.05$). The greater amount of comminuted material in the mill requires a greater airflow volume for its transport through the classifier separation zone.

Table 7 shows the influence of various mill loads on the milling performance of I1 and I2 pellets. The general trend shows that a lower power consumption was achieved for a lower $\dot{m}_{Pellet}$. The power required for comminuting I1 and I2 pellets decreased from 213.6 kW at 20.4 t/h to 190.7 kW at 14.4 t/h for I1 pellets and from 228.9 kW at 20.6 t/h to 178.5 kW at 14.3 t/h for I2 pellets, respectively. This is because the resistance of the roller moving through the milling bed decreases, as the milling bed thickness reduces. The correlation matrix in Table 8 confirms that there is a statistically significant positive relationship between *P* and $\dot{m}_{Pellet}$ (r = 0.88, $p < 0.05$). Being the most power-consuming unit of the CHP plant, the *SGEC* is a suitable indicator of the grinding efficiency. When operating at higher loads, the roller mills achieve a lower *SGEC* (Table 7), hence indicating a higher grinding efficiency. A statistically significant negative correlation (r = −0.94, $p < 0.01$) was found between *SGEC* and $\dot{m}_{Pellet}$ (Table 8). On the other hand, Von Rittinger's K_R increased with $\dot{m}_{Pellet}$ (r = 0.92, $p < 0.01$). Consequently, the larger the difference between the feed PSD and the product PSD, the higher the grinding energy, which is in agreement with Von Rittinger's comminution theory.

At high *HGP*, particles theoretically experience more destructive breakage with the development of a finer product that is lifted through the classifier out to the burner pipes [29]. However, this could not be observed in this study. Instead, the increase in the $\dot{m}_{Air}$ may be a more dominant factor to affect the classifier cut size, thus resulting in a coarser final comminuted pellet product originating from a decreased classifier separation (Fig. 8). Higher d^* and *D90* values in Table 7 indicate a reduced residence time (lower circulation load) of the pellet material in the mill. Wood particles experience fewer roller-grinding actions, which lead to a coarser comminuted product. This is due to the increased airflow that provides a higher airspeed to sweep away coarser particles to the classifier. Hence, the classifier cut size increases with increasing mill airflow rate. Consequently, at lower airflow rates, the classifier cut size decreases, and the comminuted product becomes finer. There exists a critical particle size below which it is impossible to comminute the particle further by compressive forces [56]. However, values are unknown for wood material, and they will vary between wood species due to their complex compression failure modes and different chemical composition [17].

Generally, at all airflow rates, a wider wood dust PSD (lower RRBS *n*-value) was observed compared to disintegrated pellets. The dust PSD became wider (lower RRBS *n*-value) with a decreasing mill airflow rate. The lower the RRBS *n*-value, the finer the comminuted product. The results of the particle shape characterization for disintegrated I1 and I2 pellets compared to I1 and I2 pellets comminuted at various mill loads are shown in Supplementary Figs. S1 and S2. Overall, mill load changes had a negligible effect on the original elongated wood particle shape. Thus, VRMs regardless of their load do not seem to alter the wood particle shape.

Table 7
Effect of pellet feed rate on the milling performance. Average values are presented, and one standard deviation between pipes is indicated in parentheses.

	$\dot{m}_{Pellet}$ (t/h)	$\dot{m}_{air}$ (t/h)	n	d* (mm)	D90 (mm)	K_R (kWh mm/t)	P (kW)	SGEC[a] (kWh/t)	Δp (kPa)
Disintegrated I1 pellets			1.37 (0.06)	0.83 (0.01)	1.51 (0.01)				
Comminuted I1 pellets (Scenario 10)	20.5	46.5	0.96 (0.04)	0.57 (0.07)	1.34 (0.04)	125.0	213.6 (1.9)	10.5	2.9
Comminuted I1 pellets (Scenario 11)	17.4	43.0	0.93 (0.01)	0.53 (0.03)	1.29 (0.08)	103.6	204.2 (1.5)	11.7	2.4
Comminuted I1 pellets (Scenario 12)	14.4	39.6	0.87 (0.04)	0.41 (0.03)	1.14 (0.11)	61.9	190.7 (3.1)	13.3	2.0
Disintegrated I2 pellets			1.40 (0.01)	1.09 (0.04)	1.82 (0.02)				
Comminuted I2 pellets (Scenario 7)	20.6	52.2	1.00 (0.11)	0.77 (0.07)	1.62 (0.07)	163.9	228.9 (1.1)	11.1	3.8
Comminuted I2 pellets (Scenario 8)	16.6	43.7	0.95 (0.06)	0.68 (0.08)	1.53 (0.07)	111.4	192.4 (1.1)	11.6	2.8
Comminuted I2 pellets (Scenario 9)	14.3	41.2	0.88 (0.07)	0.46 (0.08)	1.20 (0.09)	44.0	178.5 (1.2)	12.5	2.6

[a] Dynamic classifier and fan power not included in SGEC.

Table 8
Pearson's correlation coefficient (r) matrix for comminuting I1 and I2 pellets.

	$\dot{m}_{Pellet}$	$\dot{m}_{Air}$	HGP	n	d*	D90	K_R	P	SGEC	Δp
$\dot{m}_{Pellet}$	1.00									
$\dot{m}_{Air}$	0.90[a]	1.00								
HGP	1.00[c]	0.89[a]	1.00							
n	0.79	0.59	0.81[a]	1.00						
d*	0.78	0.44	0.79	0.81	1.00					
D90	0.74	0.40	0.76	0.80	1.00[c]	1.00				
K_R	0.92[b]	0.72	0.93[b]	0.73	0.89[a]	0.87[a]	1.00			
P	0.88[a]	0.76	0.89[a]	0.62	0.71	0.66	0.93[b]	1.00		
SGEC	−0.94[b]	−0.87[a]	−0.93 [b]	−0.65	−0.70	−0.67	−0.81 [a]	−0.73	1.00	
Δp	0.80	0.49	0.81	0.85[a]	0.89[a]	0.87[a]	0.81[a]	0.74	−0.71	1.00

[a] $p < 0.05$.
[b] $p < 0.01$.
[c] $p < 0.001$.

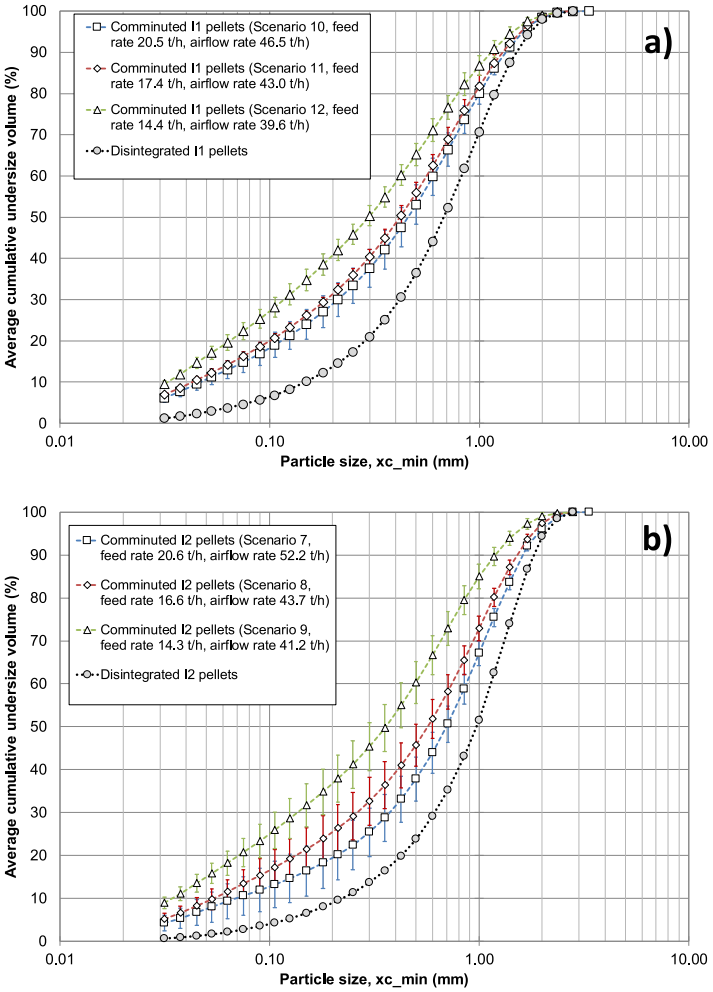

Fig. 8. Average cumulative PSD of disintegrated I1 pellets (a) and I2 pellets (b) in comparison to I1 pellets comminuted at different airflow rates (Scenarios 7–12, Table 3). Error bars indicate one standard deviation within the different fuel pipes of the mill, and they are displayed when greater than the data symbol.

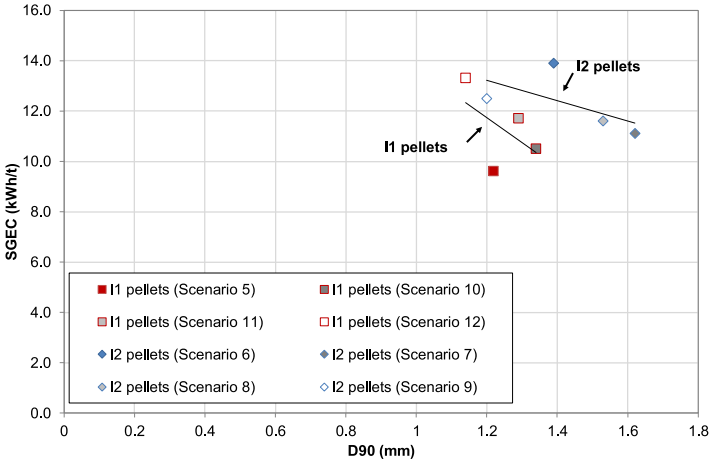

Fig. 9. Specific energy consumption for comminuting I1 and I2 pellets at different steady state conditions as a function of the classifier cut size indicated by the *D90* value.

3.7. Implications for power plant operators and wood pellet producers

This paper provides an understanding of the roller mill operation and knowledge about the large-scale comminuted wood pellet characteristics (product fineness, shape, PSD). The obtained results may be a valuable basis for plant operators who wish to convert their existing coal plants to burn wood pellets. The accurate characterization of the comminuted product in power plants is crucial to optimize the milling and classifier performance, hence achieving an efficient and homogeneous wood combustion in a suspension-fired boiler. Sieve analysis, which is limited to the measurement of only one single dimension (i.e., particle width) may be rudimentary and should be replaced by an image analysis system suitable to characterize the comminuted product fineness and shape.

To achieve the desired comminuted product fineness (i.e., classifier cut size), plant operators should be aware that the internal PSD of pellets is a decisive pellet specification. Fig. 9 shows the average *SGEC* for the tested milling scenarios from M20 versus the classifier cut size indicated by the *D90* value. It is clear that, on average, the comminution of I1 pellets leads to a finer comminuted product inside the burner pipes at a lower *SGEC* compared to I2 pellets. The milling scenario 5 gave the best grinding efficiency for I1 pellets indicated by the lowest *SGEC* and smallest *D90*. This indicates that the mill/air ratio of 2.3 seems to be ideal for comminuting pellets with a finer internal PSD. For comminuting I2 pellets, the milling scenario 9 may be the optimal choice to achieve the desired product fineness, however, accepting a higher *SGEC*. The geometric representation of the comminuted wood particles can be also valuable for combustion modeling, assuming a flat cuboid geometry.

The study also found that roller mills have a negligible effect on the particle shape. This suggests that the pellet production process and/or the size reduction of the raw material before pelletization may define the shape of comminuted particles for suspension-firing. The particle shape may be furthermore affected by the microstructure of wood material, which is used for pelletization. The proper choice of wood species for pelletization may yield the desired shape of comminuted particles.

4. Conclusions

The large-scale milling behavior of two industrial wood pellet qualities in coal roller mills, equipped with dynamic classifiers, at a suspension-fired power plant was investigated. The following conclusions can be drawn from the experimental study:

- The size distribution of comminuted wood pellets by sieve analysis and Camsizer® X2 (X-Jet mode) can be well fit with the Rosin-Rammler-Bennet-Sperling model.
- Isokinetic wood dust sampling from vertical and symmetric mill outlet pipes is the preferred sampling method. Sampling from horizontal pipes increases the risk of particle segregation. Sampling from asymmetric pipes shows a more uneven wood dust distribution regarding fineness and mass flow of the comminuted particles.
- The internal particle size distribution of wood pellets affects the large-scale pellet milling behavior and the subsequent particle size classification (i.e., classifier cut size). Pellets with finer internal particles lead to a finer comminuted product (smaller cut size) with lower specific grinding energy consumption.
- Roller mills do not affect the original elongated wood particle shape, regardless of the mill operating conditions. Differences in the aspect ratios of comminuted and internal particles from different pellet qualities are probably explained by the wood microstructure in the pellet.
- The operation of the roller mill at higher loads and higher primary airflow rates has unfavorable effects on the mill power consumption, the differential mill pressure, and the classifier cut size. Only the specific energy consumption can be reduced, when the mill operates at higher loads.
- The specific energy consumption for pellet comminution varies with the classifier cut size. At a constant mill load, an increased rotor speed and a reduced airflow rate lead to a smaller classifier cut size. However, this is at the expense of a higher energy consumption and a higher differential mill pressure.

Nomenclature

$\dot{m}_{Air}$	airflow rate to the mill (t/h)
$\dot{m}_{Dust}$	wood dust sample flow (g/s)
$\dot{m}_{Pellet}$	fresh wood pellet feed rate (t/h)
$A_{Particle}$	particle projection area (mm^2)
m_{Pellet}	amount of wood pellets (t)
$P_{Particle}$	particle perimeter (mm)
Δp	differential mill pressure (kPa)
AMV	Amagerværket (Amager power station)

AR	particle aspect ratio (dimensionless)
ar	as received
C	circularity (dimensionless)
CHP	combined heat and power
d	particle size (mm)
D	pellet diameter (mm)
d^*	RRBS characteristic particle size (mm)
d.b.	dry basis
D90	particle size at 90th percentile of the cumulative undersize distribution (mm)
d_f	90th percentile feed passing size (mm)
D_N	nominal milling table diameter (m)
D_P	diameter milling path (m)
d_p	90th percentile product passing size (mm)
Fe_{max}	maximum Feret diameter (mm)
HGP	hydraulic grinding pressure (MPa)
K_R	Von Rittinger's material characteristic parameter (kWh mm t^{-1})
L	pellet length (mm)
M10	mill 10
M20	mill 20
M30	mill 30
n	RRBS uniformity constant (dimensionless)
P	absorbed mill power (kW)
PSD	particle size distribution
R(d)	cumulative undersize distribution (%)
RRBS	Rosin-Rammler-Bennet-Sperling
SGEC	specific grinding energy consumption (kWh/t)
VRM	vertical roller mill
w.b.	wet basis
wt%	weight percent
$xc_{,min}$	shortest maximum chord (mm)

Acknowledgements

The authors thank Energinet.dk for the financial support received as part of the ForskEL project "AUWP – Advanced Utilization of Wood Pellets" (Project number: 12325). The authors wish also to thank and acknowledge all those involved for their considerable support and contribution to the study.

Appendix A. Supplementary data

Supplementary data to this article can be found online at https://doi.org/10.1016/j.fuproc.2018.01.009.

References

[1] M. Cocchi, L. Nikolaisen, M. Junginger, C.S. Goh, R. Hess, J. Jacobson, L.P. Ovard, D. Thrän, C. Hennig, M. Deutmeyer, P.P. Schouwenberg, Global wood pellet industry market and trade study, IEA Bioenergy Task 40: "Sustainable Bioenergy Trade.", 2011, pp. 6–10 https://www.nachhaltigwirtschaften.at/resources/iea_pdf/reports/iea_task40_wood_pellet_industry_market.pdf , Accessed date: 8 August 2017.

[2] S. Döring, Power from Pellets: Technology and Applications, 1st ed., Springer-Verlag, Berlin Heidelberg, 2013, http://dx.doi.org/10.1007/978-3-642-19962-2.

[3] G. Eskeland, N. Rive, T. Mideksa, The 2020 European climate goals and the electricity sector, 11th Annual Conference on Global Economic Analysis, Helsinki, Finland, 2008, pp. 1–2, , http://dx.doi.org/10.1016/j.enpol.2011.10.038.

[4] M. Grbovic, Export Potential of U.S. - Produced Switchgrass and Wood Pellets for the EU Market (Master's Thesis), University of Tennessee, USA, 2010.

[5] S. Caillat, E. Vakkilainen, Biomass Combustion Science, Technology and Engineering, 1st ed., Woodhead Publishing Limited, 2013, http://dx.doi.org/10.1533/9780857097439.3.189.

[6] P. Gilbert, C. Ryu, V. Sharifi, J. Swithenbank, Effect of process parameters on pelletisation of herbaceous crops, Fuel 88 (2009) 1491–1497, http://dx.doi.org/10.1016/j.fuel.2009.03.015.

[7] P. Lehtikangas, Storage effects on pelletised sawdust, logging residues and bark, Biomass Bioenergy 19 (2000) 287–293, http://dx.doi.org/10.1016/S0961-9534(00)00046-5.

[8] W.R. Livingston, The status of large scale biomass firing: the milling and combustion of biomass materials in large pulverised coal boilers, IEA Bioenergy Task 32: Biomass Combustion and Co-firing, 2016, pp. 21–23.

[9] M. Odenberger, The role of combustion in the future energy system, Keynote Presentation at the Nordic Flame Days, in: Stockholm, Sweden, 2017.

[10] L.S. Esteban, J.E. Carrasco, Evaluation of Different Strategies for Pulverization of Forest Biomasses, 166 (2006), pp. 139–151, http://dx.doi.org/10.1016/j.powtec.2006.05.018.

[11] M. Momeni, Fundamental Study of Single Biomass Particle Combustion (PhD Thesis), Department of Energy Technology, Aalborg University, Denmark, 2012.

[12] A. Trubetskaya, Y. Poyraz, R. Weber, J. Wadenbäck, Secondary comminution of wood pellets in power plant and laboratory-scale mills, Fuel Process. Technol. 160 (2017) 216–227, http://dx.doi.org/10.1016/j.fuproc.2017.02.023.

[13] S.A. Martin, Comparison of Hammermill and Roller Mill Grinding and the Effect of Grain Particle Size on Mixing and Pelleting (Master's Thesis), Kansas State University, USA, 1985.

[14] M. Temmerman, P.D. Jensen, J. Hébert, Von Rittinger theory adapted to wood chip and pellet milling, in a laboratory scale hammermill, Biomass Bioenergy 56 (2013) 70–81, http://dx.doi.org/10.1016/j.biombioe.2013.04.020.

[15] S. Mani, L.G. Tabil, S. Sokhansanj, Grinding performance and physical properties of wheat and barley straws, corn stover and switchgrass, Biomass Bioenergy 27 (2004) 339–352, http://dx.doi.org/10.1016/j.biombioe.2004.03.007.

[16] A. Malmgren, Talking about the revolution, World Coal. (2015) 1–4 http://www.bioc-ltd.com/images/Talking_about_the_revolution-World_Coal-Nov_2015.pdf , Accessed date: 8 June 2017.

[17] O. Williams, G. Newbolt, C. Eastwick, S. Kingman, D. Giddings, S. Lormor, E. Lester, Influence of mill type on densified biomass comminution, Appl. Energy 182 (2016) 219–231, http://dx.doi.org/10.1016/j.apenergy.2016.08.111.

[18] C. Yin, Biomass co-firing, Biomass Combustion Science, Technology and Engineering, Elsevier Science & Technology, Cambridge, UK, 2013, pp. 84–105, , http://dx.doi.org/10.1533/9780857097439.3.189.

[19] M.A. Saeed, G.E. Andrews, H.N. Phylaktou, B.M. Gibbs, Global kinetics of the rate of volatile release from biomasses in comparison to coal, Fuel 181 (2016) 347–357, http://dx.doi.org/10.1016/j.fuel.2016.04.123.

[20] G.G. Mejeoumov, Improved Cement Quality and Grinding Efficiency by Means of Closed Mill Circuit Modeling (PhD Thesis), Texas A&M University, USA, 2007.

[21] O. Altun, H. Benzer, Selection and mathematical modelling of high efficiency air classifiers, Powder Technol. 264 (2014) 1–8, http://dx.doi.org/10.1016/j.powtec.2014.05.013.

[22] E. Ortega-Rivas, Unit Operations of Particulate Solids: Theory and Practice, CRC Press, 2011.

[23] N. Paul, S. Biggs, J. Shiels, R.B. Hammond, M. Edmondson, L. Maxwell, D. Harbottle, T.N. Hunter, Influence of shape and surface charge on the sedimentation of spheroidal, cubic and rectangular cuboid particles, Powder Technol. 322 (2017) 75–83, http://dx.doi.org/10.1016/j.powtec.2017.09.002.

[24] J.L. Afolabi, The Performance of a Static Coal Classifier and Its Controlling Parameters, PhD thesis University of Leicester, UK, 2012.

[25] T.N. Adams, D.R. Raymond, C. Schmid, Optimization of a Swirl Burner for Pulverized-wood Fuels, 71–5 Tappi, 1988, pp. 91–96.

[26] International Organization for Standardization, ISO 17225–2:2014 Solid Biofuels - Fuel Specifications and Classes - Part 2: Graded Wood Pellets, (2014), pp. 7–8.

[27] International Organization for Standardization, ISO 17830:2016 Solid Biofuels - Particle Size Distribution of Disintegrated Pellets, (2014), pp. 1–8.

[28] M. Schmidt, Two products from a single grinding mill, Miner. Process. 54 (2013) 3–14.

[29] S. Palaniandy, N.A. Kadir, M. Jaafar, Value adding limestone to filler grade through an ultra-fine grinding process in jet mill for use in plastic industries, Miner. Eng. 22 (2009) 695–703, http://dx.doi.org/10.1016/j.mineng.2009.02.010.

[30] T. Fahrland, K.H. Zysk, Cements ground in the vertical roller mill fulfil the quality requirements of the market, Cem. Int. 11 (2013) 64–69.

[31] D. Altun, H. Benzer, N. Aydogan, C. Gerold, Operational parameters affecting the vertical roller mill performance, Miner. Eng. 103–104 (2017) 67–71, http://dx.doi.org/10.1016/j.mineng.2016.08.015.

[32] International Organization for Standardization, ISO 14488:2007 Particulate Materials - Sampling and Sample Splitting for the Determination of Particulate Properties, (2007), p. 11.

[33] J.R. Coombes, Y. Yan, Experimental investigations into the flow characteristics of pneumatically conveyed biomass particles using an electrostatic sensor array, Fuel 151 (2015) 11–20, http://dx.doi.org/10.1016/j.fuel.2014.11.048.

[34] D. Lindsley, Power Plant Control and Instrumentation: The Control of Boilers and HRSG Systems, The Institution of Engineering and Technology, 2000 doi:10.1049/PBCE058E.

[35] Retsch Technology GmbH, CAMSIZER® Characteristics, (2009), p. 8 http://www.horiba.com/fileadmin/uploads/Scientific/Documents/PSA/Manuals/CAMSIZER_Characteristics_Nov2009.pdf (accessed December 15, 2017).

[36] A. Trubetskaya, G. Beckmann, J. Wadenbäck, J.K. Holm, S.P. Velaga, R. Weber, One way of representing the size and shape of biomass particles in combustion modeling, Fuel 206 (2017) 675–683, http://dx.doi.org/10.1016/j.fuel.2017.06.052.

[37] D.A. Robinson, S.P. Friedman, Observations of the effects of particle shape and particle size distribution on avalanching of granular media, Physica A 311 (2002) 97–110, http://dx.doi.org/10.1016/S0378-4371(02)00815-4.

[38] W. Pichler, A. Weidenhiller, J. Denzler, R. Goetzl, M. Pain, M. Weigl, A. Haider, Approaches to describe the particle properties of wood pellet feedstock, World Bioenergy 2014, Jönköping, Sweden, 2014, pp. 2–3, , http://dx.doi.org/10.13140/2.1.3203.3286.

[39] W. Pichler, A. Weidenhiller, J. Denzler, R. Goetzl, M. Pain, M. Weigl, A. Haider, Modelling the particle size distribution of the feedstock for pellets production, 22nd

European Biomass Conference and Exhibition, Hamburg, Germany, 2014.
[40] M. Gil, I. Arauzo, Hammer mill operating and biomass physical conditions effects on particle size distribution of solid pulverized biofuels, Fuel Process. Technol. 127 (2014) 80–87, http://dx.doi.org/10.1016/j.fuproc.2014.06.016.
[41] T. Allen, Powder Sampling and Particle Size Determination, 1st ed., Elsevier Science, Oxford, UK, 2003.
[42] G.V. Barbose-Cànovas, E. Ortega-Rivas, P. Juliano, H. Yan, Food Powders, Springer US, Boston, USA, 2005, http://dx.doi.org/10.1007/0-387-27613-0.
[43] Y. Yu, R.R. Liu, J. Liu, Correspondence analysis and establishment of evaluation model of classification performance indices for a turbo air classifier, Mater. Werkst. 45 (2014) 900–911, http://dx.doi.org/10.1002/mawe.201400249.
[44] T. Tanaka, Comminution laws. Several probabilities, Ind. Eng. Chem. Process. Des. Dev. 5 (1966) 353–358, http://dx.doi.org/10.1021/i260020a001.
[45] O. Williams, E. Lester, S. Kingman, D. Giddings, S. Lormor, C. Eastwick, Benefits of dry comminution of biomass pellets in a knife mill, Biosyst. Eng. 160 (2017) 42–54, http://dx.doi.org/10.1016/j.biosystemseng.2017.05.011.
[46] J.D. Wilcox, Isokinetic flow and sampling, J. Air Pollut. Control Assoc. 5 (1956) 226–245, http://dx.doi.org/10.1080/00966665.1956.10467715.
[47] X. Qian, Y. Yan, Flow measurement of biomass and blended biomass fuels in pneumatic conveying pipelines using electrostatic sensor-arrays, IEEE Trans. Instrum. Meas. 61 (2012) 1343–1352, http://dx.doi.org/10.1109/TIM.2011.2175034.
[48] L. Cai, C. Jiaying, X. Guiling, X. Pan, C. Xiaoping, Z. Changsui, Experimental investigation and stability analysis on dense-phase pneumatic conveying of coal and biomass at high pressure, Korean J. Chem. Eng. 30 (2013) 295–305, http://dx.doi.org/10.1007/s11814-012-0165-2.
[49] J. Tomas, S. Kleinschmidt, Improvement of flowability of fine cohesive powders by flow additives, Chem. Eng. Technol. 32 (10) (2009) 1470–1483, http://dx.doi.org/10.1002/ceat.200900173.
[50] S. Kwon, G.L. Messing, The effect of particle solubility on the strength of nanocrystalline agglomerates: boehmite, Nanostruct. Mater. 8 (1997) 399–418, http://dx.doi.org/10.1016/S0965-9773(97)00180-3.
[51] P. Daugbjerg Jensen, M. Temmerman, S. Westborg, Internal particle size distribution of biofuel pellets, Fuel 90 (2011) 980–986, http://dx.doi.org/10.1016/j.fuel.2010.11.029.
[52] H. Rezaei, C.J. Lim, A. Lau, S. Sokhansanj, Size, shape and flow characterization of ground wood chip and ground wood pellet particles, Powder Technol. 301 (2016) 737–746, http://dx.doi.org/10.1016/j.powtec.2016.07.016.
[53] Q. Guo, X. Chen, H. Liu, Experimental research on shape and size distribution of biomass particle, Fuel 94 (2012) 551–555, http://dx.doi.org/10.1016/j.fuel.2011.11.041.
[54] C. Wagner, K.H. Esbensen, Representative sampling of suspended particulate materials in horizontal ducted flow: evaluating the prototype “EF-sampler,”, J. Chem. Eng. Proc. Technol. 3 (2012), http://dx.doi.org/10.4172/2157-7048.1000139.
[55] H. Archary, W. Schmitz, L. Jestin, Mass flow and particle size monitoring of pulverised fuel vertical spindle mills, Chemical and Process Engineering - Inzynieria Chemiczna I Procesowa, 37 2016, pp. 175–197, , http://dx.doi.org/10.1515/cpe-2016-0016.
[56] K. Kendall, The impossibility of comminuting small particles by compression, Nature 272 (1978) 710–711, http://dx.doi.org/10.1038/272710a0.
[57] Cement seminar: process technology (roller mills), Holderbank Management & Consulting, 1993, pp. 1–14 http://222.255.19.250/picture/PRJ-MEC/VAN/Holcim/Raw Grinding Systems.pdf accessed July 18, 2017.

Supplementary data

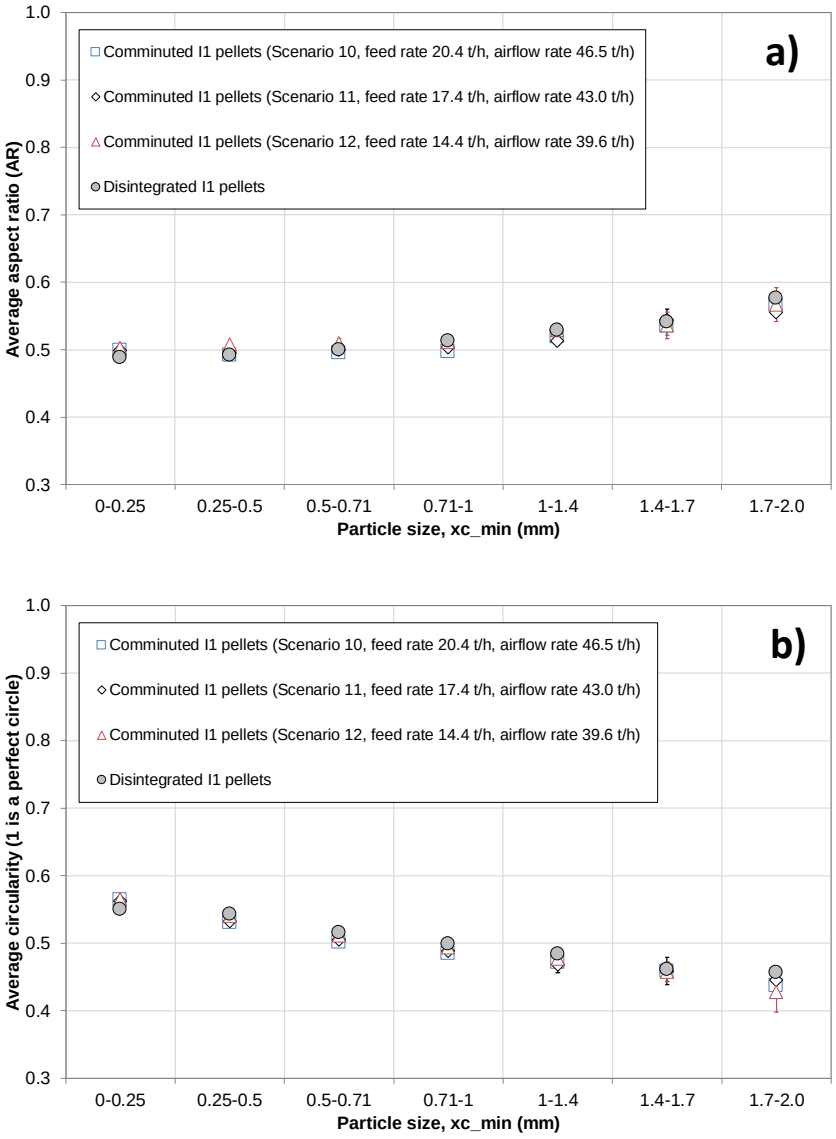

Figure S11: Average aspect ratio (a) and circularity (b) of disintegrated I1 pellets compared to I1 pellets comminuted at different mill loads. Error bars indicate one standard deviation within different fuel pipes, and they are displayed when greater than the data symbol.

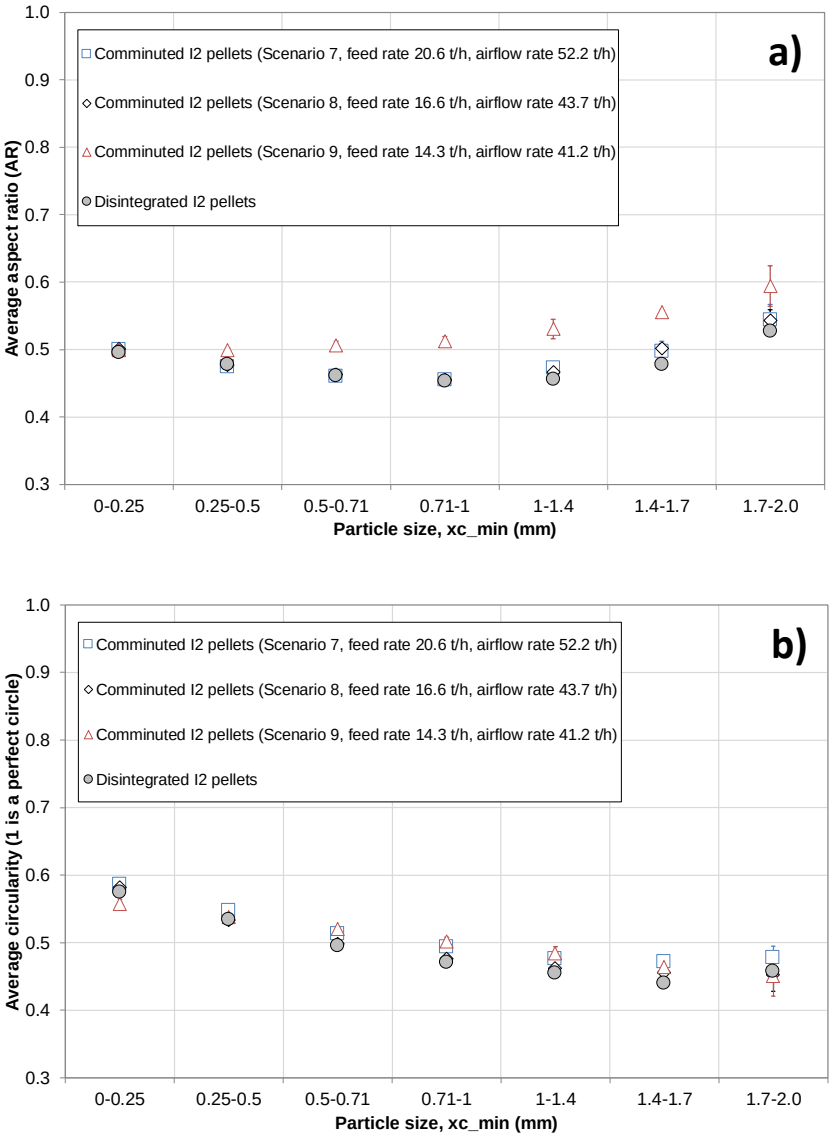

Figure S12: Average aspect ratio (a) and circularity (b) of disintegrated I2 pellets compared to I2 pellets comminuted at different mill loads. Error bars indicate one standard deviation within different fuel pipes, and they are displayed when greater than the data symbol.

Appendix IV

Grinding performance of wood pellets in laboratory-scale mills

Marvin Masche, Maria Puig-Arnavat, Peter A. Jensen, Jens K. Holm, Sønnik Clausen, Jesper Ahrenfeldt, Ulrik B. Henriksen

Grinding performance of wood pellets in laboratory-scale mills

Marvin Masche[a], Maria Puig-Arnavat[a], Peter A. Jensen[a], Jens Kai Holm[b], Sønnik Clausen[a], Jesper Ahrenfeldt[a], Ulrik B. Henriksen[a]*

[a]Department of Chemical and Biochemical Engineering, Technical University of Denmark, 2800 Kgs. Lyngby, Denmark

[b]Bioenergy and Thermal Power, Ørsted, Nesa Allé 1, 2820 Gentofte, Denmark

*Corresponding author. E-mail address: marv@kt.dtu.dk (M. Masche)

Abstract

This study investigates the influence of wood pellet properties on the pellet grindability in two lab-scale open-circuit compression mills (i.e., disc mill and roller mill). Pellet properties include wood type, moisture content, internal pellet particle size distribution, and three mechanical properties (density, durability, diametral compressive strength). Grinding is performed on as-received and oven-dried pellets. Two industrial pellet qualities and two semi-industrial pellets are used. The grinding performance is assessed by measuring the grinding energy and analyzing the changes in particle morphology (size and shape) with respect to the internal pellet particle morphology. The study shows that drying improves the pellet grindability in both mills indicated by lower grinding energy and greater size reduction of the internal pellet particles (i.e., higher product fineness). The disc mill produces finer particles than the roller mill, but this is at the expense of higher grinding energy. The roller mill is not able to disintegrate all pellets into their constituent particle sizes. Hence, it is suggested to operate the roller mill in closed-circuit with classification equipment for achieving higher size reduction degrees. The size reduction degree can be linked to the pellet properties (e.g., plant origin, internal particle size distribution) and the milling principle. The maximum diametral compressive strength of pellets can be strongly related to their internal particle size distribution, which may predict the grinding energy effort in compression mills. Finally, a simple grindability test is suggested to determine the relative grindability of pellets, i.e., whether they are easy or difficult to grind.

Keywords

Wood pellet; grindability; mill; specific grinding energy; particle size; particle shape;

1. Introduction

European countries, e.g., UK and Denmark, are rapidly switching their existing coal-fired power plants to biomass. In particular, wood pellets are the preferred biomass source for large-scale combined heat and power (CHP) stations [1]. For example, the largest Danish energy company, Ørsted, will stop all use of coal for heat and power generation by 2023 [2]. Compared to other reliable low-carbon generation technologies (e.g., nuclear, hydro, tidal, and carbon and capture storage), biomass has a higher potential to offer flexibility to the grid [3]. The increasing demand for wood pellets in European countries has led to a rapid expansion of wood pellets exports from the Southern US. By 2020, wood pellet imports into the EU are expected to be about 15-30 million tons [1].

Before burning in the boiler, wood pellets need to be milled. In existing pulverized coal-fired power plants, tube-ball mills and roller mills are one of the most common mill types [4]. In the Danish Herning CHP plant, disc mills are used. However, they reportedly lead to high maintenance costs and no further size reduction of biomass pellets [5]. The conversion of dedicated roller mills from coal to process wood pellets has already been successfully demonstrated in existing coal-fired power stations in Europe [6,7] and roller mills are the preferred option because of their low operating and maintenance costs and improved availability [3].

The particle size distribution (PSD) of the milled pellets affects the combustion efficiency, the unburned carbon levels in the ash, and the combustion stability. The degree of particle size reduction achieved will be affected by pellet properties, including chemical structure and mechanical properties (e.g., strength, durability, compressibility). One way to assess the pellet suitability for size reduction is to determine its grindability. It is a measure of the pellet resistance to grinding, and as such reflects some physical pellet properties, such as strength, tenacity, and fracture. The grindability is measured in terms of quantity of milled product below a certain particle size. Generally, it increases with decreasing milled product fineness [8]. The grindability also influences mill operating properties, such as power consumption and capacity [9]. Hence, a grindability test allows comparing the relative grindability of different pellets before their utilization in power plant mills. The experimental data may also be used to model the comminution process in different mills. However, the

reliability of the test is influenced by various variables, including test sample preparation, mill design, process parameters, and the measurement technique to determine the grinding power.

Traditionally, existing mills are designed based on the grinding properties of coal. Several standard grindability tests have hence been developed for coal over the years: the Hardgrove Grindability Index (*HGI*) for ball, ring, and roller mills [10], the Bond Work Index (*BWI*) for tube and ball mills [11], and the Hybrid Working Index (*HWI*) for planetary ball mills [12]. All these tests may be used to estimate the grinding behavior of coal in industrial-scale mills. Alternative grindability measures of coal include counting the number of mill rotations to reach a specified fineness [13] and methods based on its proximate analysis [14]. Currently, there is a lack of reliable standard grindability tests for lignocellulosic biomass. Recent studies [11,15] reported that the classical *HGI* method is insufficient for determining the grindability of non-thermally treated biomass. The wood pellet industry and large-scale CHP plant operators are thus in need of a standardized grindability test to provide quantitative data on the grinding behavior of wood pellets in an industrial-scale mill.

The purpose of the study is to investigate the grindability characteristics of wood pellets of different properties in two laboratory-scale mills. The objective is to address the lack of knowledge regarding wood pellet size reduction and to quantify and compare the influence of different working principles on the grindability properties of wood pellets. The knowledge gained from the study is fundamental for the design and operation of the grinding and conveying operations of a pulverized wood-firing system [16,17]. Studies of the physical properties of the milled product allow conclusions on the course of the size reduction process and enable comparisons with other size reduction processes. The grindability is assessed by determining the specific grinding energy and by evaluating the change in particle size and shape compared to the internal pellet particle size and shape. Usually, such comparison is scarce in the literature and lacks elaborateness. Furthermore, the influence of wood pellet properties, including chemical composition (softwood or hardwood), moisture content, internal pellet PSD, and three mechanical properties (density, durability, diametral compressive strength) on grinding energy and size distribution of the milled product is investigated. As a result of the evaluation, a simple laboratory mill setup is suggested to test the relative grindability of wood pellets.

2. Materials and methods

2.1 Materials

Four different wood pellet types, i.e., I1, I2, beech, and pine pellets (Fig. 1) are used in this study. The two industrial pellet types are designated as I1 and I2 according to ISO 17225-2:2014 [18]. These pellets were characterized and tested in the biomass-converted CHP plant Amagerværket (*AMV*) unit 1 in Copenhagen, Denmark [19]. Beech and pine pellets were produced using a semi-industrial pellet mill, as described elsewhere [20]. The chemical composition of all wood pellets is listed in Table 2.

Table 2: Chemical composition of wood pellets (% dry matter).

Wood pellets	Carbohydrates					Klason lignin	Acid soluble lignin	Extractives		Ash	Total
	Total	Glucan	Xylan	Mannan	Others[a]			Water-soluble	Ethanol-soluble		
Beech	63.8	39.2	18.0	1.7	4.9	23.4	2.9	0.9	0.9	0.5	92.4
Pine	59.4	38.1	4.3	11.3	5.8	24.8	0.6	4.5	10.6	0.6	100.6
I1	60.8	40.0	12.7	4.0	4.1	22.4	1.8	4.6	5.7	0.9	96.2
I2	60.5	39.5	6.7	9.3	5.0	27.2	0.9	3.6	6.4	0.9	99.5

[a] Sum of arabinan, galactan, rhamnan, and uronics.

The analysis of the chemical composition of lignocellulosic biomass was performed according to the standard analytical procedures provided by the National Renewable Energy Laboratory [21,22]. The xylan to mannan ratio in hemicellulose (and the syringyl to (syringyl + guaiacyl) ratio in lignin) can be used as an indicator of the plant origin and to distinguish between hardwood and softwood [23]. Hemicellulose in hardwood is mainly xylan, whereas softwood is rich in mannans. Beech and pine pellets are 100 % hardwood pellets and 100 % softwood pellets, respectively. The exact composition of I1 and I2 pellets is not known, but based on the xylan to mannan ratio, I1 pellets probably have a higher proportion of hardwood, while I2 pellets rather have a higher softwood content. Table 3 also lists the specifications of the four wood pellet types. Pellets were characterized in duplicate according to standardized methods.

Table 3: Specifications of wood pellets. Average values are presented.

Parameters	Unit	I1 pellets	I2 pellets	Beech pellets	Pine pellets	Method
Proximate analysis						
Moisture content	wt.%, ar	8.0	7.3	5.4	9.6	EN ISO 18134-1: 2015
Ash content	wt.%, DW	0.6	0.6	0.4	0.4	EN ISO 18122: 2015
Volatile matter	wt.%, DW	84.5	83.9	85.3	85.5	EN ISO 18123: 2015
Fixed carbon	wt.%, DW	14.9	15.5	14.3	14.1	By difference
Physical properties						
Pellet diameter (D) and length (L)	mm, ar	D, 6.2; L, 12.3	D, 6.7; L, 11.9	D, 6.1; L, 11.8	D, 6.1; L, 10.1	EN ISO 17829: 2015
Bulk density (σ_B)	kg/m3, ar	653.1	669.2	580.4	603.3	EN ISO 17828: 2015
Particle density (σ_P)	kg/m3, ar	1212.7	1183.5	1113.8	1152.6	$\sigma_P = \frac{m}{V_p}$
Mechanical durability	wt.%, ar	98.6	98.7	97.2	98.2	EN ISO 17831-1: 2015
Number of pellets/ 100g sample of pellets	-	245	278	366	350	Counting of pellets screened using a 5.0 mm sieve
PSD of disintegrated pellets (internal PSD)	wt.%, DW	≥ 99.5 % (< 3.15 mm) ≥ 98.7 % (< 2.0 mm) ≥ 79.2 % (< 1.0 mm)	≥ 98.0 % (< 3.15 mm) ≥ 93.9 % (< 2.0 mm) ≥ 59.4 % (< 1.0 mm)	≥100.0%[a] (< 3.15 mm) ≥ 99.3%[a] (< 2.0 mm) ≥ 84.3%[a] (< 1.0 mm)	≥100.0% (< 3.15 mm) ≥ 97.7% (< 2.0 mm) ≥ 62.7% (< 1.0 mm)	EN ISO 17830: 2016 Sieve analysis

[a]Values obtained after the second pellet disintegration in hot water.

2.2 Moisture content of pellets

The pellet moisture content is determined twice by drying a 300 g sample up to 16 h in a drying oven at 105±2°C according to ISO 18134-1:2015 [24]. The moisture content is calculated based on the mass decrease during drying. To test the influence of the moisture content on the grinding properties (e.g., grinding energy and milled pellet characteristics), grinding tests were run with oven-dried pellets and as-received (wet) pellets. The oven-dried pellet samples were stored and sealed in airtight zip lock bags to prevent moisture uptake.

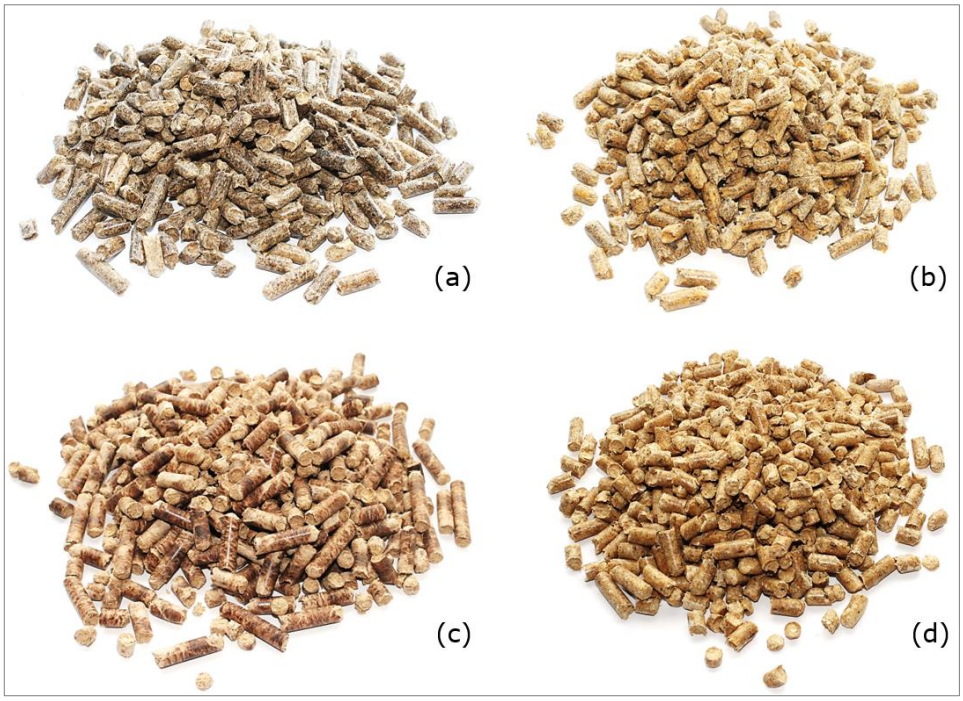

Fig. 1: Wood pellets used in the milling experiments: I1 pellets (a), I2 pellets (b), beech pellets (c), and pine pellets (d).

2.3 Internal particle size distribution of pellets

Pellets are disintegrated in hot deionised water and subsequently dried in an oven according to ISO 17830:2016 [25] to determine their internal PSD. As shown previously [20,26], this method represents approximately the PSD of the milled raw material before pelletization.

2.4 Mechanical (strength) properties of pellets

The mechanical (strength) properties of pellets can affect the grinding process, including grinding energy and final milled product characteristics. The strength of the inter-particle bonds formed during pelletizing is estimated by testing the specific density, diametral compressive resistance, and mechanical durability of pellets. For more accurate comparison, tests were performed on oven-dried pellets to compensate for moisture differences between as-received pellet samples, which will affect the grinding properties.

2.4.1 Specific density

The specific density of a pellet is simply calculated based on its known mass and volume.

The pellet ends are flattened with sandpaper to make them exact cylinders. Twenty pellets per wood pellet type are selected.

2.4.2 Mechanical durability

The mechanical durability (or abrasive resistance) of pellets is measured using a tumbling device according to EN ISO 17831-1:2015 [27], which predicts the fine production during storage, handling, and shipping. Tumbling tests are performed in duplicate. Generally, pellets with low durability, i.e., a high amount of fines increase the risk of fires and explosions during storage and handling processes.

2.4.3 Diametral compressive strength

The diametral compression test, also referred to as Brazilian-test [28], is another way to assess the mechanical strength of wood pellets. The test may be appropriate to resemble how pellets will break in compression mills, such as roller or disc mills. Pellets were tested diametrically, as this is probably the way they will align between the milling table and rollers in a large-scale vertical roller mill, and between the two burr discs in a disc mill. Unlike the durability test, where pellets tumble at constant rotation and bounce against each other and the tumbling device wall, compression tests apply a continuous force until the material breaks.

The compressive strength is measured using a computer controlled universal testing machine (type Z030, Zwick Roell GmbH & Co, Germany) with an Xforce K load cell of maximum 30 kN. A single pellet is radially compressed at a constant rate of 10 mm/min between two flat metal platens. The upper one is attached to the testing machine, while the bottom one is fixed. Initially, the machine applied a small load (< 10 N) to the pellet to keep it in position.

Commonly, compression tests are applied for brittle materials to measure the maximum compressive load that a material can bear before cracking. However, for wood pellets, an ideal point of failure cannot be expected due to their plastic and ductile fracture behavior. Thus, the compressive strength is defined as the maximum force (F_{max}) in N required to deform (strain) a pellet by 4 mm. As the maximum force is expected to depend on the pellet dimensions, it is reasonable to normalize the force by division with

the pellet dimensions. The diametral compressive strength (σ_c), determined in MPa, is then calculated using the following equation [29]:

$$\sigma_c = \frac{F_{max}}{\pi LB} \quad (1)$$

Where L is the pellet length (mm) and B is 50 % contact width of the pellet diameter (mm). Pellets are sanded to produce smooth ends for length measurements. The force-deformation data for each specimen is recorded using testXpert II testing software V3.61. Tests are carried out on 10 replicates per pellet sample.

Table 4: Laboratory mill setups and operating conditions for pellet grindability tests. Roller mill adapted from [30].

Mill	Disc mill	Roller mill
Setup		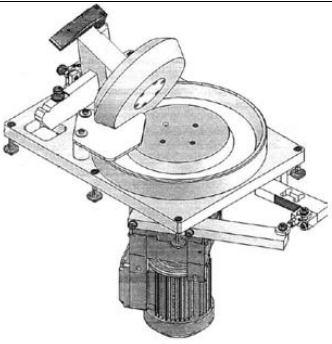
Working principle	Compression and shearing	Compression and shearing
Motor	0.60 kW	0.12 kW
Feeder	Vibrating feeder	Dosing feeder
Wattmeter	Available	Available
Feed rate	500 ccm/min	500 ccm/min
#Repetitions	3	3

2.5 Laboratory grinding equipment

Two laboratory mills with different particle size reduction principles are used for the pellet grindability tests (Table 4); a disc mill (*DM*) and a roller mill (*RM*), which are examples of open-circuit grinding. The *DM* and *RM* are equipped with a wattmeter to measure the instantaneous power consumption (W). After deducting the mill idle power

(P_0), the net specific grinding energy consumption (*SGEC*) is calculated using the following equation:

$$SGEC = \int_0^t \frac{P - P_0}{m_{Pellets}} dt \quad (2)$$

Where $m_{Pellets}$ is the amount of pellets (g) to be milled. *P* is the total instantaneous power (kW) consumed while comminuting at time *t* (h), and it is obtained from a data logger (type NI USB-6009, National Instruments, USA).

2.5.1 Disc mill

The disc mill is a commercial coffee grinder (type Kenia, Mahlkönig, Germany) that comminutes the wood pellets in the gap between two grinding burr discs, one stationary and one rotating. By changing the gap size, the desired product fineness is adjusted. For the grinding experiments, the minimum distance between the discs is used to achieve the finest comminuted product. The disc mill applies similar grinding forces as an impact mill [15].

2.5.2 Roller mill

The laboratory roller mill located at *AMW* consists of one roller attached to a lever arm. Additional weights are added to the lever arm to increase the roller grinding pressure, which is transferred from the lever arm to the roller. The milling table is shaped as a circular trough, and is driven by an electric motor, while the roller moves due to the movement of the table. A control panel allows adjusting the table speed and feed rate, and it displays the actual (net) energy that is needed to grind the pellets. The feeder system of the roller mill consists of a feed hopper mounted to a rotating dosing feeder, which has rounded holes along its shaft. The holes are 20 mm in diameter and 8 mm deep. As a result, the pellets undergo some crushing before they are fed onto the milling table. The pellet material then passes one time under the roller. The roller-milled product instantly leaves the table by suction from a cyclone vacuum cleaner into a plastic beaker. Originally, the roller mill was designed to mill coal and analyze its grinding energy consumption, which is not possible for the HGI test. For grinding wood pellets, the mill was modified by adding rounded holes into the milling table to increase friction and facilitate the trapping of particles between milling table and roller. Some of the key design parameters of the mill are summarized in Table 5.

Table 5: Roller mill specifications.

Parameter	Dimension
Roller width	57 mm
Roller inclination	15°
Roller diameter	216 mm
Roller grinding pressure	0.3 MPa[a]
Nominal milling table diameter	332 mm
Milling table speed	2.4 rpm

[a]Roller weight (3.6 kg) plus additional weight (16.3 kg)

2.6 Laboratory mill conditions

To compare the results from different mills, uniform grinding conditions are applied by maintaining a constant pellet flow rate controlled by a vibrating feeder (type DR15/40, Retsch, Germany). The bulk density of pellets will affect their flow rate. Hence, the optimal frequency of the feeder is determined in pretests to realize the same flow rate for different pellet samples. Josh [31] found that coals of varying density varied largely in volume, but had similar grinding energies. This favors denser fuels with a smaller volume. To correct this, the feeder flow rate is expressed in volume per minute instead of mass per minute, making grindability comparisons feasible. The application of a conveying feeder allows predicting a continuous milling process. The grinding conditions for the two mills are summarized in Table 4. Prior to milling, pellets are screened using a 3.15 mm sieve to remove fines.

2.7 Wood particle size and shape characterization

The size and shape of disintegrated and milled wood pellets are determined by a dynamic image analyzer (Camsizer® X2, Retsch Technology GmbH, Germany) operated in X-Jet mode for air pressure dispersion. More information about the experimental method can be found elsewhere [19]. Measurements are done in duplicate. The measured PSD is presented as a cumulative (undersize) volume distribution versus $d_{c,min}$, which represents the shortest maximum chord length of a 2D particle projection measured from all measurement directions. $d_{c,min}$ refers to the width of a particle projection, which is the dimension measured by sieve analysis [32]. The particle shape is characterized by using the elongation ratio (width-to-length ratio) and circularity

provided by Camsizer® software. The elongation ratio (*ER*) is equal to one when particles are circles and squares, and it is defined as follows:

$$ER = \frac{d_{c,min}}{d_{Fe,max}} \quad (3)$$

Where $d_{Fe,max}$ is the maximum Feret diameter (i.e., longest distance between two parallel tangents restricting the particle at any arbitrary angle), representing the length of particles as shown by Trubetskaya et al. [33]. The circularity (*C)* indicates how closely the 2D particle projection resembles a circle, and it can be expressed as follows [34]:

$$C = 4 \cdot \pi \cdot \frac{A_{particle}}{P^2_{particle}} \quad (4)$$

Where $A_{Particle}$ and $P_{Particle}$ refer to the particle projection area and the particle perimeter, respectively. An ideal perfect circle has a circularity value of 1.

2.8 Data analysis

The Rosin-Rammler-Bennet-Sperling (RRBS) model is used to describe the PSD of wood. It is a two-parameter distribution function expressed as a cumulative percent (undersize) distribution. The RRBS equation is [35]:

$$R(d) = 100 - 100 \cdot e^{-\left(\frac{d}{d^*}\right)^n} \quad (5)$$

where *R(d)* is the cumulative percent (undersize) distribution of material finer than the particle size *d*, d^* is the characteristic particle size defined as the size at which 63,21 % of the PSD lies below, and *n* is the distribution parameter. A plot of ln[ln[100/(100-R(d)]] against ln(d) on the double logarithmic scale will give a straight line of slope *n*, if the PSD fits the RRBS equation. The d^* also characterizes the fineness of a wood sample.

Von Rittinger's comminution law is used to predict the energy consumption for grinding wood [36]. Although Von Rittinger's law is developed for the mineral industry, recent studies [37–39] suggest its applicability to determine the energy demand for grinding lignocellulosic biomass. An advantage of this law is the application of the size reduction ratio to normalize the effect of the initial feed particle size. Von Rittinger stated that the energy required for size reduction is directly proportional to the new surface area produced [40], and he defined the relationship as follows [41]:

$$SGEC = K_R \left(\frac{1}{d_p} - \frac{1}{d_f}\right) \quad (6)$$

Where d_p is the characteristic particle size of the milled product and d_f is the characteristic particle size of the feed material. In case of pellet comminution, d_f is the characteristic

particle size of the disintegrated pellet material. The material characteristic parameter, Von Rittinger's constant K_R (kWh mm t^{-1}) is a measure for the wood grindability.

3. Results and discussion

3.1 Initial wood pellet characterization

3.1.1 Internal pellet particle size and shape

The internal PSD of pellets after disintegration in hot water and subsequent drying is shown in Fig. 2a. Interestingly, beech pellets and I1 pellets have about the same internal PSD curve, while pine pellets and I2 pellets have a similar internal PSD. The fraction of particles below 1 mm is about 50% for pine pellets and I2 pellets, whereas beech pellets and I1 pellets show a 20% higher particle fraction below 1 mm. The measured PSDs are also fitted to the RRSB model for the disintegrated wood pellet samples (Fig. 2b). The experimental data shows a very good fit (R^2 between 0.988 and 0.994) to the RRSB model. The model can thus be applied to describe the sample fineness (d^*). Internal pine pellet particles have the largest d^* (1.16 mm), followed by I2 pellets (1.09 mm), beech pellets (0.99 mm), and I1 pellets (0.83 mm). The different internal PSDs are related to the different pellet process history.

The shape of the internal pellet particles is characterized regarding their circularity and elongation ratio (Fig. 3). Similar to the internal pellet PSD, also the shape seems to be related to the wood type and microstructure as indicated by similar trends for disintegrated hardwood pellets and disintegrated softwood pellets, respectively. Disintegrated I1 and beech pellet particles appear more circular and less elongated than disintegrated I2 and pine pellet particles. Furthermore, the particle circularity increased with decreasing particle size, which corroborates previous results [20,42]. The elongation ratio of disintegrated hardwood pellet particles seems reasonably constant across different particle size ranges, while disintegrated softwood pellet particles become less elongated with decreasing particle sizes. For the smallest particle fraction, the length of wood particles is twice the width.

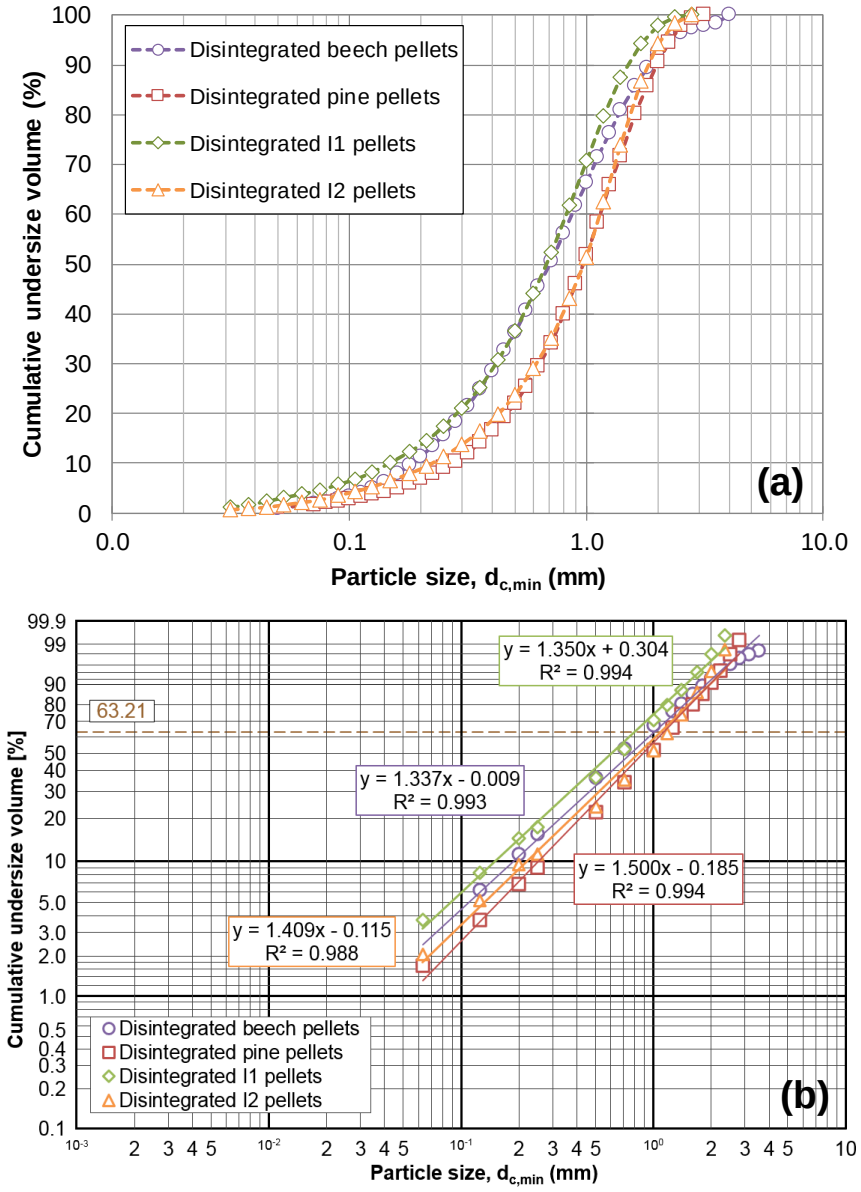

Fig. 2: Average cumulative undersize PSD (a) and the corresponding RRSB model (b) of disintegrated wood pellets.

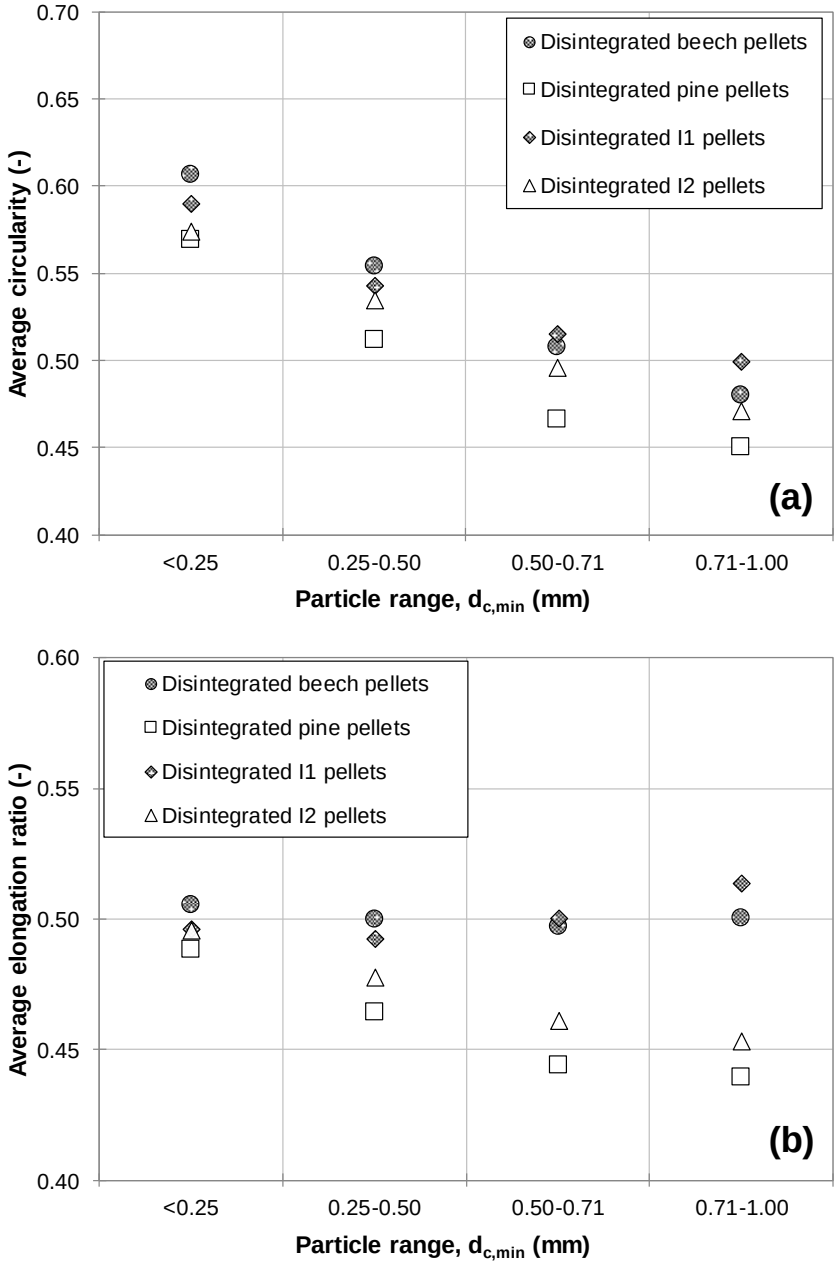

Fig. 3: Average circularity (a) and elongation ratio (b) of disintegrated pellets. Values for particles larger than 1.00 mm are neglected due to the small number of particles analyzed.

3.1.2 Mechanical durability of pellets

In Fig. 4, the influence of the moisture content on the mechanical durability of wood pellets is shown. The general trend is that all as-received pellet samples have higher mechanical durability than their corresponding dried samples. Lehtikangas [43] reported that pellet drying results in larger cavities filled with air, while the water in as-received pellets will fill these cavities, thus acting as a binder. This helps to produce stronger bonds between particles, resulting in a higher degree of adhesion (i.e., fewer fines). However, more durable pellets may only be obtained up to a moisture content of 12 % (w.b.) [44].

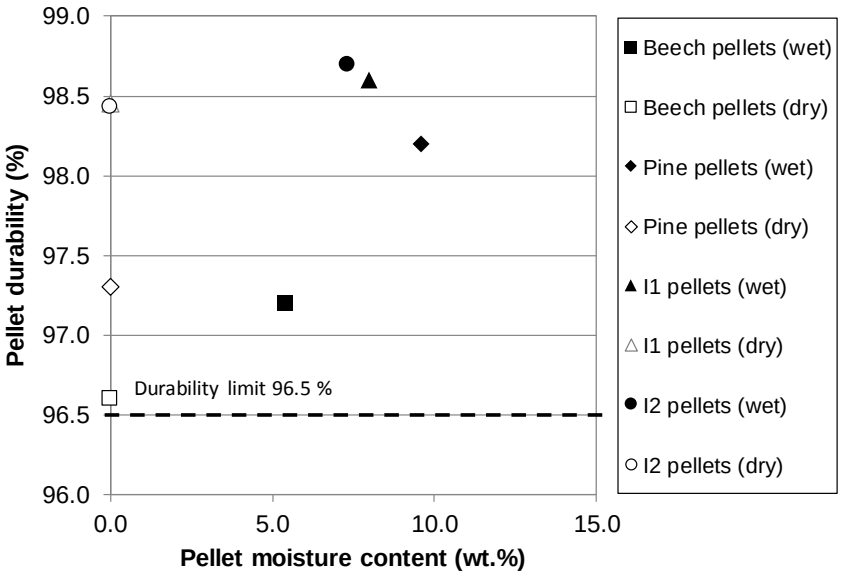

Fig. 4: Average values for the mechanical durability of as-received (wet) and dried pellet samples. Error bars indicate the first standard deviation from the mean, and they are displayed when greater than the data symbol.

Furthermore, Fig. 4 shows that the durability of industrially produced pellets is less affected by moisture variations compared to semi-industrial pellets. This highlights differences in inter-particle bonding in semi-industrial and industrial pellets, which may be due to their different processing conditions. According to ISO 17225-2:2014 [18], a mechanical durability greater or equal to 96.5 % is required for the lowest industrial pellet quality. This limit is set to minimize the production of fines during pellet handling

and the risk associated with them, e.g., fires and dust explosions [45]. Fig. 4 shows that all pellet samples even after drying conform to the ISO requirement. The general trend is that I2 pellets have the highest durability followed by I1 pellets, pine pellets, and beech pellets. Table 6 summarizes the mechanical properties of oven-dried wood pellet samples.

Table 6: Summary of the mechanical properties of oven-dried pellet samples.

Pellet sample		Specific pellet density (kg/m3)	Mechanical durability (%)	Maximum diametral compressive strength (MPa)
Beech pellets	AVG	1219.2	96.6	30.0
	SD	11.2	0.1	5.9
	CV (%)	0.9	0.1	19.6
Pine pellets	AVG	1140.1	97.3	46.9
	SD	12.5	0.0	2.3
	CV (%)	1.1	0.0	5.0
I1 pellets	AVG	1173.5	98.5	13.3
	SD	31.5	0.0	2.7
	CV (%)	2.7	0.0	20.7
I2 pellets	AVG	1111.1	98.4	32.6
	SD	21.0	0.1	4.8
	CV (%)	1.9	0.1	14.6

The present study also shows that the number of pellets present in a 100 g sample (Table 3) has a very strong statistically significant effect ($r=-0.96$, $p<0.05$) on the pellet durability. Lehtikangas [43] noted that most of the fines originate from the end parts of pellets. Consequently, a higher number of pellets in a given sample will lead to a higher amount of fines, i.e., lower durability. On the other hand, the internal pellet PSD does not seem to affect the pellet durability ($r=-0.32$, $p>0.05$), while another study [46] reported a negative correlation between pellet durability and particle size.

3.1.3 Specific density of pellets

The specific pellet density of oven-dried pellets varied from ca. 1110 to 1220 kg/m3 (Table 6). As hardwood particles are generally denser than softwood particles [47], the

two hardwood pellet types (beech pellets and I1 pellets) also showed higher specific densities than the two softwood pellet types (pine pellets and I2 pellets). The specific pellet density has no strong effect ($r=-0.63$, $p>0.05$) on the pellet durability, which is consistent with previous findings [43,48]. In addition, no strong correlation is found between the internal pellet PSD and specific pellet density ($r=-0.53$, $p>0.05$), which corroborates previous findings [49–51].

3.1.4 Diametral compressive strength of pellets

The diametral compression test is another way to assess the mechanical strength of wood pellets, where a continuous force is applied until the material fails [52]. Fig. 5 shows the typical force-deformation curve for each pellet type at a compression rate of 10 mm/min. All four force-deformation curves showed a non-linear relationship and can be well represented by a third-degree polynomial (R^2=0.986-0.997). As expected, all wood pellets exhibited a ductile stress-strain behavior during diametral compression, which is also observed by other authors [53,54]. No pellet fractured suddenly. Instead, pellets are slowly distorted, as shown for a beech pellet in Fig. 6, indicating no clear point of failure due to a ductile compression failure mode. Williams et al. [53] described this failure mode as delamination of particles, indicating the weak inter-particle bonds that form the pellet.

The characteristic ductile trend of the force-deformation curve shows how, at first, the compressive force increases at a nearly constant slope up to a point, where the slope of the curve decreases. This point can be probably associated with the breakage of the pellet into several pellet fragments (see Fig. 6). Beyond this point, deformation happens at a constant force, as these fragments realign between the two platens before they are continuously compressed up to deformation of 4 mm. It is clear that the compressive strength will increase substantially with increasing deformation due to densification of the specific pellet fragments. Gibson and Ashby [55] showed a similar trend. When wood was compressed, they reported that it produced a stress-strain curve with three distinct regions: a linear elastic part, a long plateau, and a region of final densification. In the present study, I1 pellets show the smallest elastic deformation region (i.e., least stiffness) indicated by the smallest slope, when compared to the other three pellet types. Interestingly, these three pellet types follow the same trend up to deformation of 2 mm, noting that the force required to break the inter-particle bonds formed during pelletizing

is probably similar for these pellets. Afterwards, the compression force increased differently for the different pellets.

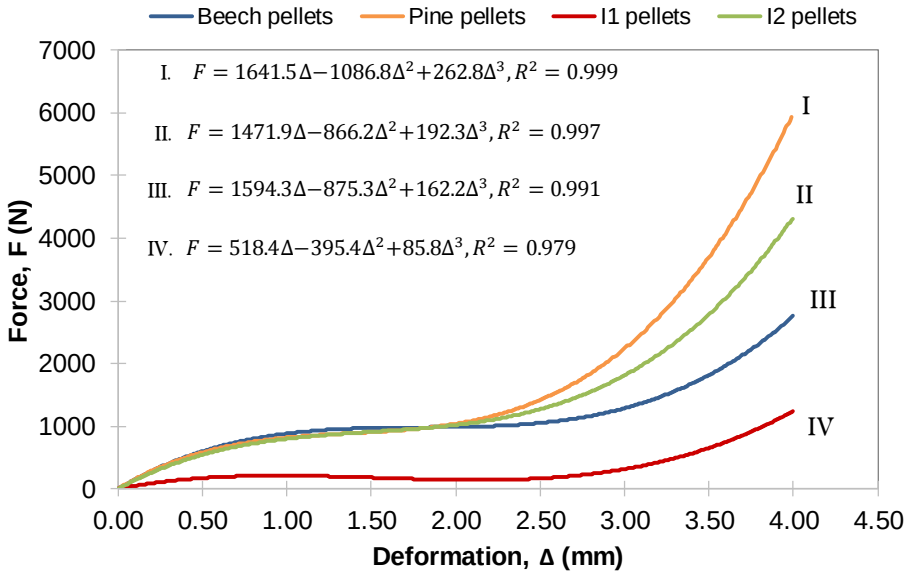

Fig. 5: Typical force-deformation curve for each pellet type in diametral compression at a compression rate of 10 mm/min.

By analyzing the repeatability of the diametral compression strength test, relatively large coefficients of variation (CVs) are obtained compared to relatively low CV from the pellet durability tests (Table 6). The CV may serve as a convenient measure of the level of data heterogeneity. Thus, the low CV from the durability test indicates very repeatable results, as stated previously [56]. However, the high CV from the compression test means bad repeatability of the results from the same pellet quality, which is also observed by other researchers [48,53]. This is mainly due to the wood pellet properties, including sample size and heterogeneity in wood [57]. In the present study, the compression strength results followed a normal distribution. Thus, the method to analyze the compressive strength of pellets seems reliable in describing the pellet mechanical properties.

Fig. 6: Beech pellet before (left) and after (right) diametral compression strength test.

Values for the maximum compression strength required to deform the pellet by 4 mm are given in Table 6. Both Fig. 5 and Table 6 show that hardwood pellets (beech and I1 pellets) have lower maximum compressive strengths than softwood pellets (pine and I2 pellets). In hardwoods, ray cells form a greater portion of the volume than in softwoods, which may contribute to the different mechanical behavior of wood. The presence of ray cells can cause fiber misalignment (e.g., distortion of longitudinal fibers around ray cells) identified to reduce the compressive strength [57]. While other studies showed a strong relationship between specific pellet density and compression strength [53,54], the present study did not confirm this. A possible explanation for that may be the different processing pathway of the pellets. Instead, the maximum compressive strength seems to depend strongly on the characteristic particle size of the material within the pellets ($r=0.97$, $p<0.05$). In other words, the coarser the internal pellet particle size, the higher the maximum compressive strength. The inter-particle bonds formed during pelletizing coarser particles appear to be stronger than pellets made of finer particles. However, the extractive content and compaction pressure in the pellet press can affect the compressive strength [54,58]. The present study showed no correlation between pellet durability and compressive strength ($r=-0.19$), which is in line with Williams et al.'s study [53].

3.2 Pellet grinding behavior in lab-scale mills

3.2.1 Effect of moisture content on SGEC

The effect of pellet moisture content on the specific grinding energy in the disc mill and roller mill is shown in Fig. 7a and Fig. 7b. The general trend in both mills is that milling dried wood pellets reduced the *SGEC* compared to milling as-received samples. The average *SGEC* from all pellets decreased from 7.95 to 4.30 kWh/t in the disc mill and from 0.72 to 0.63 kWh/t in the roller mill. Moisture acts as a plasticizer, which makes the pellets softer [59] and leads to a more ductile behavior of wood, resulting in a higher amount of energy absorbed before fracture [60]. On the other hand, drying induces irreversible cell wall damage [61], which leads to a more brittle pellet fracture surface that is easier to break down into smaller particles. The results in the present study are in good agreement with previous findings in the literature [38,39,59]. Strong positive correlations were found between the characteristic internal pellet particle size (d^*) and the specific energies for grinding dried pellets in the disc mill ($r=0.88$, $p>0.05$) and roller mill ($r=1.00$, $p<0.05$). Thus, the present study provides new support that pellets with coarser internal pellet particles require a higher grinding energy effort, as reported recently [19].

The disc mill cannot handle moist pellets as easily as the roller mill. The largest impact of the pellet moisture was found to be for the disc mill, especially for softwood pellets where the *SGEC* increased from 4.6 kWh/t for dry pellets to 15.3 kWh/t for as received pellets. For pine, a temperature increase of the milled material of up to 58 °C was measured by a thermocouple, which is due to the higher energy absorption of the wet particles. The wet wood particles have probably a higher tendency to blind the gap between the two discs of the disc mill compared to dried particles, thus reducing the rate at which the milled material can be discharged from the mill. As a result, the *SGEC* for the disc mill increases due to the accumulation of particles, which is referred to as mill choking in the literature [11]. Dry grinding also results in similar *SGEC* among pellets. Hence, a reduction in the fuel moisture content before comminution is attractive, as it will result in energy savings. Also, a drier fuel will improve the boiler performance and reduce stack emissions [62]. Furthermore, the roller mill appears to be not sensitive to the pellet material, as *SGEC* values are similar regardless of the pellet

type used. However, the disc mill *SGEC* values vary considerably for the different pellets.

3.2.2 Effect of moisture content on particle size reduction

Fig. 7a shows that both mills produce finer particles at lower grinding energy consumption when grinding dried pellets compared with grinding as-received pellets. This suggests that grinding of dry samples produces a more brittle fracture behavior of the internal pellet particles. This matches previous grinding results [39,59]. It also highlights the importance of a lower material moisture content, which offers energy saving potential and higher product fineness. For milling dried pellets in the disc mill, the trend for the characteristic product particle size is as followsa: beech pellets (0.51 mm) < I2 pellets (0.61 mm) < I1 pellets (0.64 mm) < pine pellets (0.76 mm). Similarly, the trend for the grindability in the roller mill is: pine pellets (0.93 mm) < I2 pellets (0.96 mm) < I1 pellets (1.18 mm) < beech pellets (1.34 mm). The disc mill clearly produces finer particles than the roller mill, which is at the expense of a higher grinding energy. It also shows that pellet grinding characteristics vary with the type of mill. For example, milling beech pellets in the disc mill shows very favorable grinding characteristics, while beech pellets in the roller mill in open-circuit is not favorable.

The actual size reduction effect of the mill on the pellets with respect to the internal pellet PSD is shown in Fig. 7b. A size reduction ratio larger than zero indicates that the mill could achieve an actual size reduction of the internal pellet particles, while values below zero indicate that the mill could not reduce the size of internal pellet particles further. It is clear that the size reduction effect depends on both the applied grinding system and pellet characteristics (e.g., moisture content). Hence, it is clear that the disc mill achieved a much higher size reduction for all pellet samples compared to the roller mill. In the roller mill, the negative size reduction ratio for I1 pellets and beech pellets implies that the roller mill failed to reduce the size of the actual internal pellet particles. Hence, the roller action is not sufficient to break the inter-particle bonds between adjacent wood particles that form I1 pellets and beech pellets.

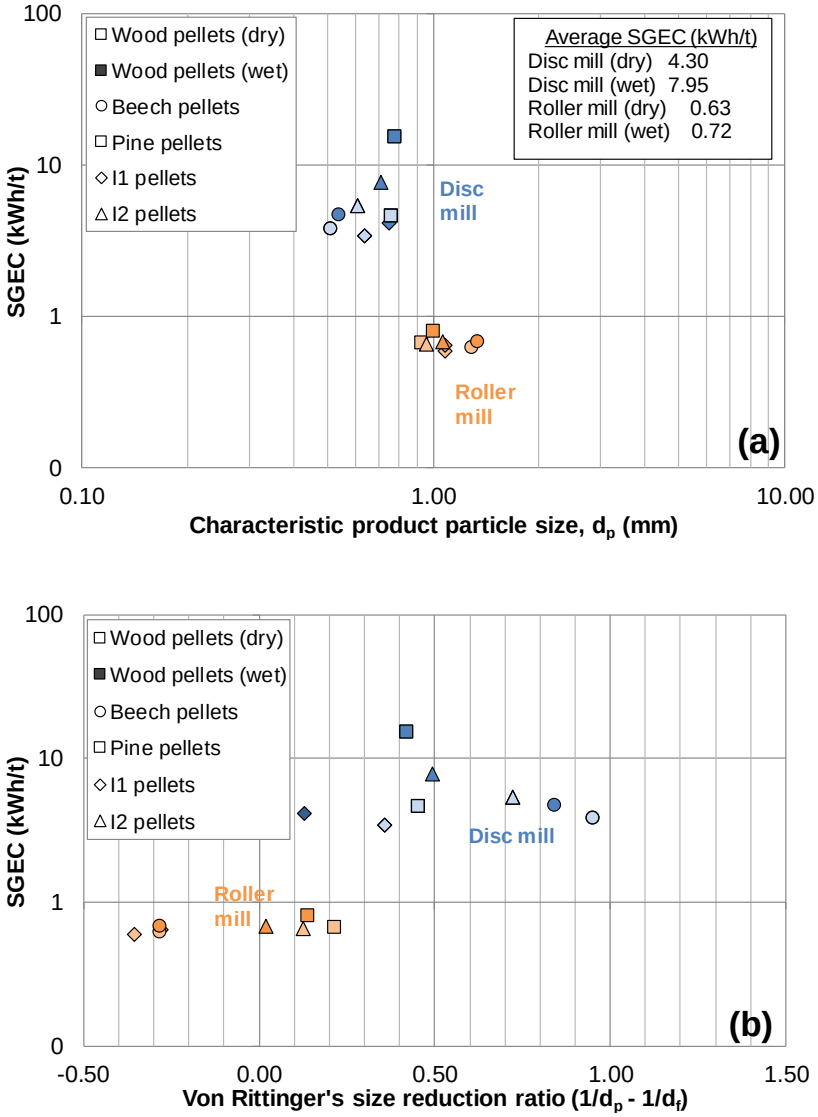

Fig. 7: Specific grinding energy consumption vs. characteristic product particle size (a) and specific grinding energy consumption vs. Von Rittinger's size reduction ratio (b).

3.2.3 Effect of grinding equipment on physical milled pellet properties

The size and shape of wood particles affect their heat and mass transfer, thus leading to different thermal conversion efficiencies. For energy conversion purposes, the size and

shape characteristics of milled wood pellets are the main criterion for selecting a specific mill type. Fig. 8a to Fig. 8d demonstrate the influence of the size reduction equipment on the PSD of the milled pellet product. The *DM* produced the lowest fraction of larger particles compared to the roller mill indicated by the lowest *D90* values. The product PSD after disc milling is shifted to the left compared to the original disintegrated pellet PSD, suggesting a clear size reduction effect, as mentioned earlier. The finest settings of the *DM* also favor the size reduction of internal pellet particles due to a higher shearing impact. While the *DM* produced similarly shaped PSD curves for all pellet types, the *RM* yielded a unique distribution curve, indicating the pellets are fractionated differently. It is also clear that the *RM* achieved a further size reduction of the internal pine pellet and I2 pellet particles, as the milled product PSD is shifted to the left compared to the disintegrated PSD.

However, Fig. 8a and Fig. 8c show that the *RM* is only able to break the beech pellets and I1 pellets down rather than achieving a size reduction of the internal pellet particles (cf. Fig. 7b). For example, even after three passages under the roller, the *RM* could not achieve a further size reduction of the internal I1 pellet particles (Supplementary Fig. S1). Overall, each mill design produces a comminuted product with different size and shape characteristics. Particles of different sizes and shapes affect the heat and mass transfer differently, which has to be considered for industrial-scale applications. Quantifying the effect of the particle size and shape on the heat and mass transfer is however not the scope of this work.

Based on the available data on *SGEC* and particle size reduction ratio during milling, the Von Rittinger's constant (K_R) was calculated for continuous grinding in the open-circuit milling systems (i.e., disc mill and roller mill). It is clear that milling as-received pellets led to a higher *SGEC* and lower Von Rittinger's size reduction ratios, and thus higher values for K_R compared to milling dried pellets. This indicates an inefficient mill operation and lower fuel grindability when milling as-received pellets. On the other hand, milling of dried pellets enhances the mill operation and fuel grindability. Consequently, a low K_R indicates a higher fuel grindability. In particular, for the disc mill, average K_R values of 22.4 for as-received pellets were calculated compared to K_R = 7.8 for dried pellets. For dry milling in the disc mill, the trend of K_R for the different pellets is as follows: pine pellets had the highest value (K_R = 10.1) followed by I1 pellets (K_R = 9.5), I2 pellets (K_R = 7.5), and beech pellets (K_R = 4.0). Thus, switching from pine

pellets to beech pellets, in the Danish Herning CHP plant that also employs disc mills can increase the fuel grindability.

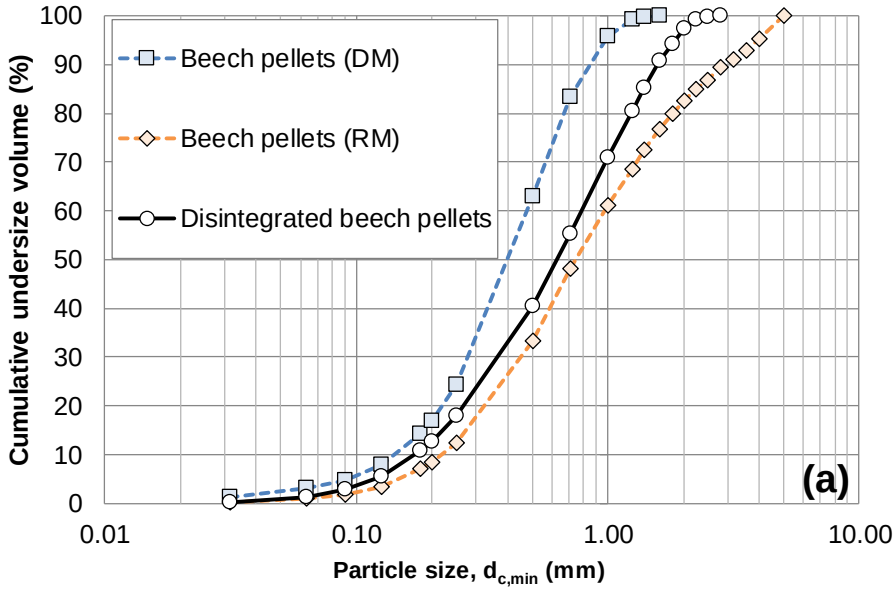

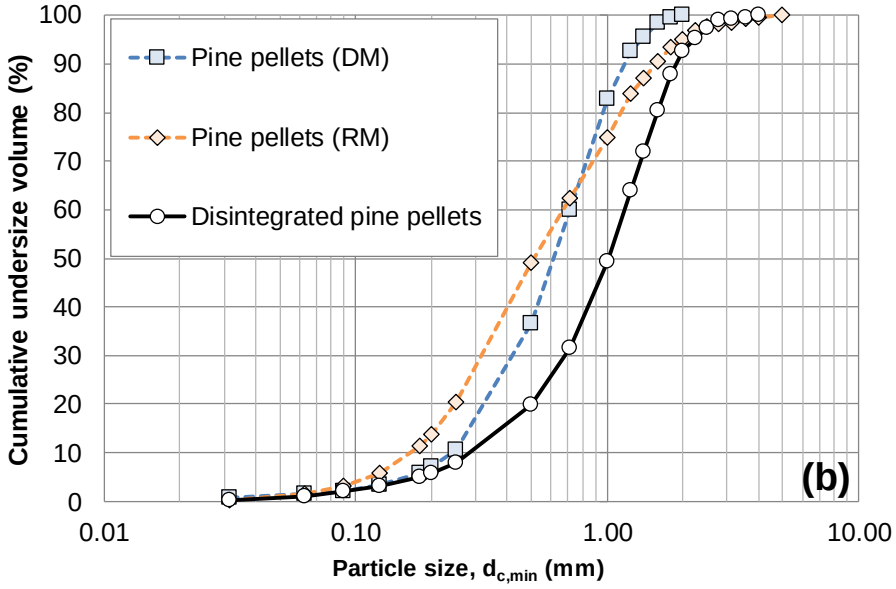

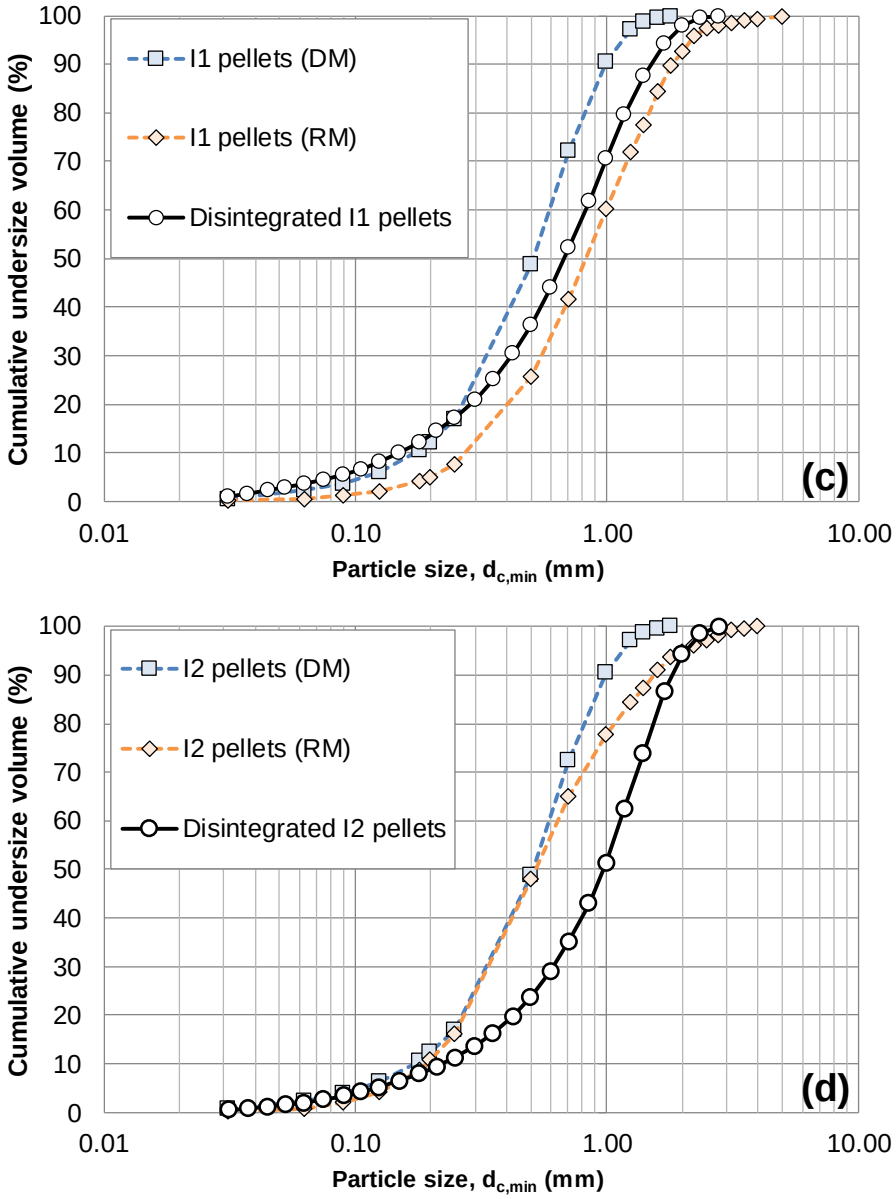

Fig. 8: Average PSD of oven-dried beech pellets (a), pine pellets (b), I1 pellets (c), and I2 pellets (d) milled in the disc mill (*DM*) and roller mill (*RM*) compared to the disintegrated pellet PSD.

Accordingly, for the roller mill, an average K_R = 4.4 for as-received pellets and K_R = 0.8 for dried pellets. For dry milling in the roller mill, I2 pellets had the highest value (K_R = 5.2) followed by pine pellets (K_R = 3.1), I1 pellets (K_R = -1.7), and beech pellets (K_R = -2.4). Negative values for K_R indicate that the roller mill could not achieve a significant size reduction of the internal I1 and beech pellet particles, as mentioned earlier. Hence, the open-circuit operation of the roller mill is not recommended for wood pellets due to the small size reduction ratios achieved. Instead, there is a need for a closed-circuit mill operation with classification equipment and return of coarse particles back to the milling table for re-grinding. Overall, it is clear that the value for K_R is dependent on the mill design and pellet material.

The impact of the mill on the shape of the milled pellet particles is shown in Fig. 9a and Fig. 9b. Only the results for beech and pine pellets are presented, which were produced from well-defined wood species and under similar processing conditions. Thus, they allow comparison and drawing conclusions. It was observed that the particle shape is closely related to the original wood properties. On average, all milled beech pellet particles show a higher circularity and higher elongation ratio than milled pine pellet particles. This trend is similar to that of disintegrated wood pellet particles. Rose [63] suggested that the mill type has a larger impact on the particle shape than the material characteristics, while Bond [64] stated that the material properties have a more dominant influence on the particle shape than the size reduction method applied. Furthermore, the produced particle shape depends on the type of mill operation. The average circularity for particles below 1 mm is higher for beech pellets milled in the *RM* (0.58) than in the *DM* (0.55). The same circularity trend is shown for pine pellets. Regarding the elongation ratio for milled beech pellet particles, the *DM* produced particles with a higher ratio (0.54), on average, than the *RM* (0.51). For pine pellets, the milled particle elongation ratio is also highest in the *DM* (0.49) than in the *RM* (0.47).

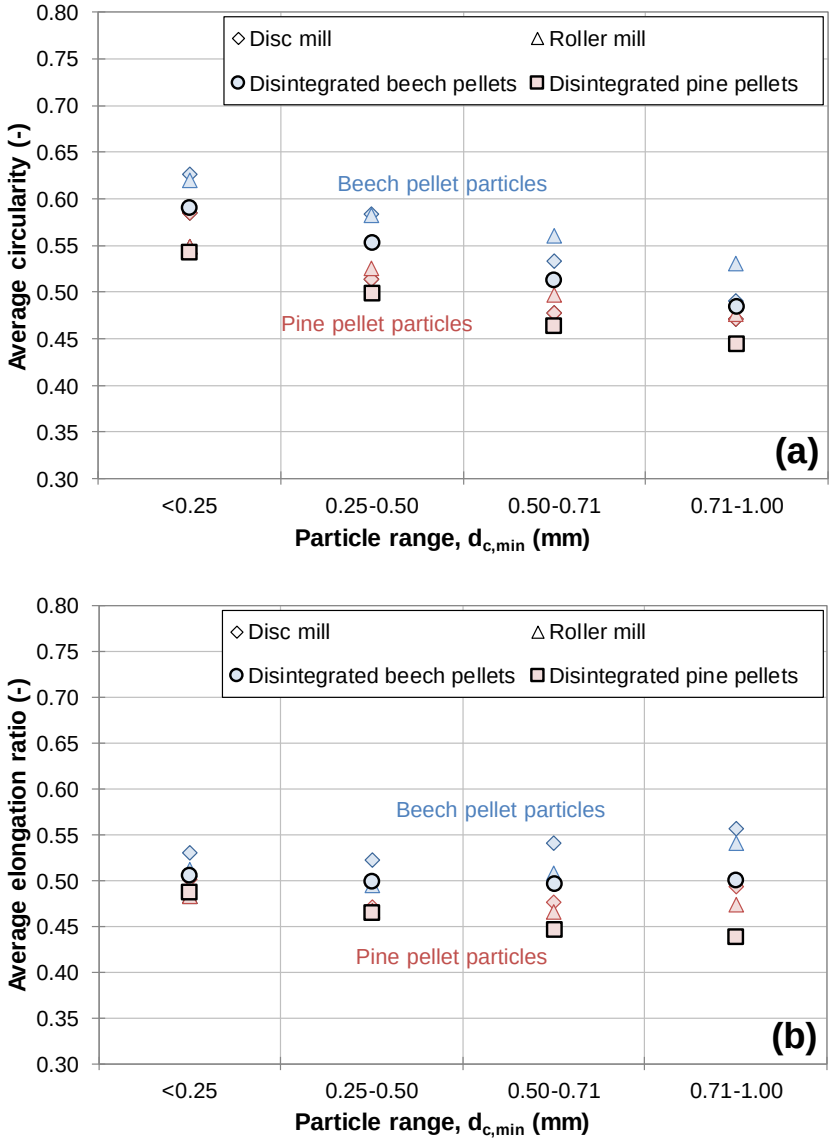

Fig. 9: Average circularity (a) and elongation ratio (b) of beech and pine pellets milled in the four different laboratory mills. Values for particles larger than 1.00 mm are neglected due to the small number of particles analyzed.

3.2.4 Implications for wood pellet industry and power plant managers

The grinding energy is one of the main concerns of power plant managers, who consider fuels with a reduced grinding effort a more economical choice. In an attempt to correlate

the mechanical properties of pellets with the specific energy for pellet grinding, the specific pellet density and mechanical durability probably have a minor role in the determination of the grinding energy for wood pellets. However, strong correlations were observed between the maximum diametral compressive strength of the dried pellets and grinding energies for disc mill ($r=0.87$, $p>0.05$) and roller mill ($r=0.96$, $p<0.05$). As stated previously, the diametral compressive strength also correlated with the characteristic internal pellet particle size. The study hence suggests that the internal pellet PSD and diametral compressive strength results may be used to provide information about the specific energy requirements for grinding wood pellets in compression mills. However, further research is needed to improve the repeatability of the compression strength test.

The study has also shown the benefits that wood pellet drying will provide, i.e., an increased pellet grindability indicated by lower *SGEC*, higher size reduction of internal pellet particles, and higher milled product fineness. The reduced grinding energy is due to a decreased mill load, which has advantages regarding maintenance costs and mill availability [65]. In biomass-converted suspension-fired power plants, the existing coal roller mills feature an integrated drying step typically. However, in new power plants that feature mill types with no integrated drying step, e.g., hammer mills, new drying concepts may be installed to benefit of dry grinding.

To date, there are no standard grindability tests for non-thermally treated wood pellets that can predict their *SGEC* and milled pellet fineness. Based on the present research, there is no absolute value to characterize pellet grindability. Instead, to assess the ease of grinding of different wood pellets, their relative grindability can be determined. In doing so, a test apparatus needs to meet a number of requirements: among them are simple operation, low-cost apparatus, and high repeatability and reproducibility. Based on the two mill designs, the disc mill (i.e., coffee grinder) is a very suitable lab-scale apparatus to determine the relative grindability of different wood pellets. The disc mill is simple and fast to operate, relatively affordable, and requires very little space. The possibility to determine the pellet grindability through simple testing can reduce the demand for laborious and potentially expensive experiments. To produce suitable reliability and repeatability of the relative grindabilities, the following test routine is recommended:

1. *Sample preparation:* As-received pellets should be oven-dried to reduce mill wear, mill choking, and compensate for moisture differences in the pellets. A 3.15 mm sieve with round openings should be used to remove fragments of broken pellets.
2. *Process parameters*: The test should be performed for a fixed volumetric pellet flow rate, e.g., using a vibrating feeder, which allows predicting continuous milling. The desired product fineness should be adjusted via the rotary knop of the disc mill. The gap between the two discs is constant for all milling tests.
3. *Measurement of grinding energy:* The apparatus should be equipped with a wattmeter to measure the net specific grinding energy.
4. *Repeatability:* The milling test shall be repeated three times and average values for the *SGEC* and characteristic milled pellet particle size are calculated.
5. *Relative grindability:* The value for the relative grindability is calculated based on Von Rittinger's comminution law, i.e., the energy required for size reduction is proportional to the new surface area produced. Relative grindabilities for different pellet samples are then reported.

4. Conclusions

This paper investigates the grinding behavior of four wood pellet types in different lab-scale mills based on the characteristics of the milled product and the specific grinding energy. The experimental data is related to the initial pellet properties. The following observations were made:

- The moisture content of wood pellets affects their durability and grindability characteristics in mills. Drying increases the pellets brittleness, which improves their grindability, resulting in energy savings and higher milled product fineness.
- Wood pellets exhibit a ductile fracture behavior during the diametral compressive strength test, which can provide a basic understanding of how pellets will fracture in a compression mill. The maximum compressive strength depends strongly on the internal particle size distribution of pellets, which hence seems to be decisive for the grinding energy effort in compression mills.
- The shape of milled pellet particles depends mainly on the shape of the internal pellet particles, as grinding does not change the inherent wood particle shape significantly.

- The roller mill is less sensitive to the pellet moisture content and wood type. The size reduction degree during milling seems to be governed by the pellet properties (i.e., plant origin and internal particle size distribution). The disc mill produced a higher proportion of fine particles but required higher grinding energy than the roller mill.
- A simple continuous open-circuit lab-scale disc mill is suggested to determine the relative grindability of wood pellets in terms of grinding effort and milled product characteristics.
- Further research has to be undertaken to investigate the performance of wood pellets in a closed-circuit mill equipped with a classification system to simulate an industrial mill classifier operation.

Nomenclature

$A_{Particle}$	particle projection area (mm^2)
m_{Pellet}	amount of wood pellets (t)
$P_{Particle}$	particle perimeter (mm)
ER	particle elongation ratio (dimensionless)
ar	as received
C	circularity (dimensionless)
d	particle size (mm)
D	pellet diameter (mm)
d^*	RRBS characteristic particle size (mm)
DW	dry wood basis
D90	particle size at 90th percentile of the cumulative undersize distribution (mm)
$d_{c,min}$	shortest maximum chord (mm)
d_f	RRBS characteristic particle size (mm) of the feed
$d_{Fe,max}$	maximum Feret diameter (mm)
d_p	RRBS characteristic particle size (mm) of the product
K_R	Von Rittinger's material characteristic parameter (kWh mm t^{-1})
L	pellet length (mm)
n	RRBS uniformity constant (dimensionless)
P	absorbed mill power (kW)

PSD	particle size distribution
R(d)	cumulative undersize distribution (%)
RRBS	Rosin-Rammler-Bennet-Sperling
SEC	specific energy consumption (kWh/t)
w.b.	wet basis
wt.%	weight percent

Acknowledgements

The authors thank Energiteknologiske Udviklings- og Demonstrationsprogram (EUDP) for the financial support received as part of the ForskEL project "AUWP – Advanced Utilization of Wood Pellets" (Project number: 12325).

References

[1] European Commission, State of play on the sustainability of solid and gaseous biomass used for electricity, heating and cooling in the EU, (2014). https://ec.europa.eu/energy/sites/ener/files/2014_biomass_state_of_play_.pdf (accessed April 26, 2018).

[2] The Ørsted Way Let's create a world that runs entirely on green energy, Ørsted. (2017). https://orsted.com/-/media/Aarsrapport2017/Orsted_report_Summary_2017_Final_EN (accessed June 1, 2018).

[3] H. Lechner, The Future of Biomass in the Renewables Portfolio, (2017). https://www.drax.com/wp-content/uploads/2017/12/Future-biomass-renewables-portfolio-Poyry-Drax.pdf (accessed April 2, 2018).

[4] M. Colechin, A. Malmgren, Best Practice Brochure: Co-Firing of Biomass, (2005). http://webarchive.nationalarchives.gov.uk/tna/+/http:/www.dti.gov.uk/files/file20737.pdf (accessed February 15, 2017).

[5] C.B. Petersen, Conversion of a traditional coal fired boiler to a multi fuel biomass unit, Burmeister & Wain Energy A/S – BWE. (2011) 1–18. http://www.bwe.dk/download/articles_pdf/art-pge2011.pdf (accessed May 1, 2018).

[6] W.R. Livingston, The status of large scale biomass firing: The milling and

combustion of biomass materials in large pulverised coal boilers, IEA Bioenergy Task 32: Biomass Combustion and Co-Firing. (2016) 21–23. http://www.ieabcc.nl/publications/IEA_Bioenergy_T32_cofiring_2016.pdf (accessed August 13, 2017).

[7] A. Malmgren, Talking about the revolution, World Coal. (2015) 1–4. http://www.bioc-ltd.com/images/Talking_about_the_revolution-World_Coal-Nov_2015.pdf (accessed June 8, 2017).

[8] B. Beke, Grindability of Materials, in: The Process of Fine Grinding, Springer Netherlands, Dordrecht, 1981: pp. 35–45. doi:10.1007/978-94-009-8258-1_6.

[9] C. Spero, Developments in laboratory testing and evaluation of coal grindability, Queensland Coal Symposium 29-30. (1991) 73–82.

[10] Q. Zhu, Coal sampling and analysis standards, IEA Clean Coal Centre. (2010) 123. https://www.usea.org/sites/default/files/042014_Coal sampling and analysis standards_ccc235.pdf (accessed April 25, 2017).

[11] O. Williams, C. Eastwick, S. Kingman, D. Giddings, S. Lormor, E. Lester, Investigation into the applicability of Bond Work Index (BWI) and Hardgrove Grindability Index (HGI) tests for several biomasses compared to Colombian La Loma coal, Fuel. 158 (2015) 379–387. doi:10.1016/j.fuel.2015.05.027.

[12] D.T. Van Essendelft, X. Zhou, B.S.J. Kang, Grindability determination of torrefied biomass materials using the Hybrid Work Index, Fuel. 105 (2013) 103–111. doi:10.1016/j.fuel.2012.06.008.

[13] L.M. Hills, Solid Fuel Grindability: Literature Review, Portland Cement Association. (2007) 21.

[14] A.N. Sengupta, An assessment of grindability index of coal, Fuel Processing Technology. 76 (2002) 1–10. doi:10.1016/S0378-3820(01)00236-3.

[15] J. Hari, A. Khalsa, D. Leistner, N. Weller, L.I. Darvell, B. Dooley, Torrefied Biomass Pellets—Comparing Grindability in Different Laboratory Mills, (2016) 1–15. doi:10.3390/en9100794.

[16] J. Dai, J.R. Grace, Blockage of constrictions by particles in fluid-solid transport, International Journal of Multiphase Flow. 36 (2010) 78–87. doi:10.1016/j.ijmultiphaseflow.2009.08.001.

[17] J.S. Tumuluru, L.G. Tabil, Y. Song, K.L. Iroba, V. Meda, Grinding energy and physical properties of chopped and hammer-milled barley, wheat, oat, and

canola straws, Biomass and Bioenergy. 60 (2014) 58–67. doi:10.1016/j.biombioe.2013.10.011.

[18] International Organization for Standardization, ISO 17225-2:2014 - Solid biofuels - Fuel specifications and classes - Part 2: Graded wood pellets, (2014) 7–8.

[19] M. Masche, M. Puig-Arnavat, J. Wadenbäck, S. Clausen, P.A. Jensen, J. Ahrenfeldt, U.B. Henriksen, Wood pellet milling tests in a suspension-fired power plant, Fuel Processing Technology. 173 (2018) 89–102. doi:10.1016/j.fuproc.2018.01.009.

[20] M. Masche, M. Puig-Arnavat, P.A. Jensen, J.K. Holm, S. Clausen, J. Ahrenfeldt, U.B. Henriksen, From wood chips to pellets to milled pellets: the mechanical processing pathway of Austrian pine and European beech. Manuscript submitted for publication, (n.d.).

[21] A. Sluiter, B. Hames, R. Ruiz, C. Scarlata, J. Sluiter, D. Templeton, D. Crocker, Determination of structural carbohydrates and lignin in Biomass, 2012. doi:NREL/TP-510-42618.

[22] B. Hames, R. Ruiz, C. Scarlata, A. Sluiter, J. Sluiter, D. Templeton, Preparation of samples for compositional analysis laboratory analytical procedure (LAP), National Renewable Energy Laboratory. (2008) 1–9.

[23] Y. Huang, L. Wang, Y. Chao, D.S. Nawawi, T. Akiyama, T. Yokoyama, Y. Matsumoto, Relationships between Hemicellulose Composition and Lignin Structure in Woods, Journal of Wood Chemistry and Technology. 36 (2016) 9–15. doi:10.1080/02773813.2015.1039543.

[24] International Organization for Standardization, ISO 18134-1:2015 - Solid biofuels - Determination of moisture content - Oven dry method, (2015).

[25] International Organization for Standardization, ISO 17830:2016 Solid biofuels - Particle size distribution of disintegrated pellets, (2014) 1–8.

[26] A. Trubetskaya, Y. Poyraz, R. Weber, J. Wadenbäck, Secondary comminution of wood pellets in power plant and laboratory-scale mills, Fuel Processing Technology. 160 (2017) 216–227. doi:10.1016/j.fuproc.2017.02.023.

[27] International Organization for Standardization, ISO 17831-1:2015 - Solid biofuels - Determination of mechanical durability of pellets and briquettes, (2015).

[28] G.V. Barbose-Cànovas, E. Ortega-Rivas, P. Juliano, H. Yan, Food powders: physical properties, processing, and functionality, Springer, 2005. doi:10.1007/s13398-014-0173-7.2.

[29] Z.Y. Lai, H.B. Chua, S.M. Goh, Influence of process parameters on the strength of oil palm kernel shell pellets, Journal of Materials Science. 48 (2013) 1448–1456. doi:10.1007/s10853-012-6897-x.

[30] J. Wadenbäck, Nya karaktäriseringsmetoder för fasta bränslen – malbarhet, tändvillighet och sintring, in: Panndagarna, 2011.

[31] N.R. Joshi, Relative grindability of bituminous coals on volume basis, Fuel. 58 (1979) 477–478. doi:10.1016/0016-2361(79)90091-7.

[32] M. Gil, E. Teruel, I. Arauzo, Analysis of standard sieving method for milled biomass through image processing. Effects of particle shape and size for poplar and corn stover, Fuel. 116 (2014) 328–340. doi:10.1016/j.fuel.2013.08.011.

[33] A. Trubetskaya, G. Beckmann, J. Wadenbäck, J.K. Holm, S.P. Velaga, R. Weber, One way of representing the size and shape of biomass particles in combustion modeling, Fuel. 206 (2017) 675–683. doi:10.1016/j.fuel.2017.06.052.

[34] E.P. Cox, A Method of Assigning Numerical and Percentage Values to the Degree of Roundness of Sand Grains, Journal of Paleontology. 1 (1927) 179–183.

[35] T. Allen, Powder Sampling and Particle Size Determination, 1st ed., Elsevier Science, Oxford, UK, 2003.

[36] L.J. Naimi, S. Sokhansanj, X. Bi, C. J. Lim, A. R. Womac, A. K. Lau, S. Melin, Development of Size Reduction Equations for Calculating Energy Input for Grinding Lignocellulosic Particles, Applied Engineering in Agriculture. 29 (2013) 93–100. doi:10.13031/2013.42523.

[37] O. Williams, G. Newbolt, C. Eastwick, S. Kingman, D. Giddings, S. Lormor, E. Lester, Influence of mill type on densified biomass comminution, Applied Energy. 182 (2016) 219–231. doi:10.1016/j.apenergy.2016.08.111.

[38] M. Temmerman, P.D. Jensen, J. Hébert, Von Rittinger theory adapted to wood chip and pellet milling, in a laboratory scale hammermill, Biomass and Bioenergy. 56 (2013) 70–81. doi:10.1016/j.biombioe.2013.04.020.

[39] O. Williams, E. Lester, S. Kingman, D. Giddings, S. Lormor, C. Eastwick,

Benefits of dry comminution of biomass pellets in a knife mill, Biosystems Engineering. 160 (2017) 42–54. doi:10.1016/j.biosystemseng.2017.05.011.

[40] L.G. Austin, A commentary on the Kick, Bond and Rittinger laws of grinding, Powder Technology. 7 (1973) 315–317. doi:10.1016/0032-5910(73)80042-7.

[41] T. Tanaka, Comminution Laws. Several Probabilities, Industrial & Engineering Chemistry Process Design and Development. 5 (1966) 353–358. doi:10.1021/i260020a001.

[42] K. Tannous, P.S. Lam, S. Sokhansanj, J.R. Grace, Physical properties for flow characterization of ground biomass from douglas fir wood, Particulate Science and Technology. 31 (2013) 291–300. doi:10.1080/02726351.2012.732676.

[43] P. Lehtikangas, Quality properties of pelletised sawdust, logging residues and bark, Biomass and Bioenergy. 20 (2001) 351–360. doi:10.1016/S0961-9534(00)00092-1.

[44] I. Obernberger, G. Thek, Physical characterisation and chemical composition of densified biomass fuels with regard to their combustion behaviour, Biomass and Bioenergy. 27 (2004) 653–669. doi:10.1016/j.biombioe.2003.07.006.

[45] A. Bergström, Prevention of fires and dust explosions when handling biomass, in: 8th Co-Firing with Biomass Workshop, Copenhagen, 2018.

[46] N. Kaliyan, R. Vance Morey, Factors affecting strength and durability of densified biomass products, Biomass and Bioenergy. 33 (2009) 337–359. doi:10.1016/j.biombioe.2008.08.005.

[47] O. Mohammed, Comparison study between hardwood and softwood, Journal of Babylon University. 3 (2016) 563–568.

[48] S.H. Larsson, R. Samuelsson, Prediction of ISO 17831-1:2015 mechanical biofuel pellet durability from single pellet characterization, Fuel Processing Technology. 163 (2017) 8–15. doi:10.1016/j.fuproc.2017.04.004.

[49] S. Mani, L.G. Tabil, S. Sokhansanj, Effects of compressive force, particle size and moisture content on mechanical properties of biomass pellets from grasses, Biomass and Bioenergy. 30 (2006) 648–654. doi:10.1016/j.biombioe.2005.01.004.

[50] M.T. Carone, A. Pantaleo, A. Pellerano, Influence of process parameters and biomass characteristics on the durability of pellets from the pruning residues of Olea europaea L, Biomass and Bioenergy. 35 (2011) 402–410.

doi:10.1016/j.biombioe.2010.08.052.

[51] P. Adapa, L. Tabil, G. Schoenau, A. Opoku, Pelleting characteristics of selected biomass with and without steam explosion pretreatment, International Journal of Agricultural and Biological Engineering. 3 (2010) 62–79. doi:10.3965/j.issn.1934-6344.2010.03.062-079.

[52] S.L. Graham, Degradation of biomass fuels during long term storage in indoor and outdoor environments (PhD thesis), University of Nottingham, United Kingdom, The University of Nottingham, United Kingdom, 2015.

[53] O. Williams, S. Taylor, E. Lester, S. Kingman, D. Giddings, C. Eastwick, Applicability of Mechanical Tests for Biomass Pellet Characterisation for Bioenergy Applications, Materials. 11 (2018) 1329. doi:10.3390/ma11081329.

[54] C. Salas-bringas, T. Filbakk, G. Skjevrak, O. Lekang, O. Høibø, R.B. Schüller, Compression rheology and physical quality of wood pellets pre-handled with four different conditions, Annual Transactions of the Nordic Rheology Society. 18 (2010).

[55] L.J. Gibson, M.F. Ashby, Cellular Solids: Structure And Properties, Pergamon, 1988. doi:10.1017/CBO9781139878326.

[56] M. Temmerman, F. Rabier, P.D. Jensen, H. Hartmann, T. Böhm, Comparative study of durability test methods for pellets and briquettes, Biomass and Bioenergy. 30 (2006) 964–972. doi:10.1016/j.biombioe.2006.06.008.

[57] L. Benabou, Kink band formation in wood species under compressive loading, Experimental Mechanics. 48 (2008) 647–656. doi:10.1007/s11340-007-9098-9.

[58] S.J. Mitchual, K. Frimpong-Mensah, N.A. Darkwa, Effect of species, particle size and compacting pressure on relaxed density and compressive strength of fuel briquettes, International Journal of Energy and Environmental Engineering. 4 (2013) 1–6. doi:10.1186/2251-6832-4-30.

[59] Y.J. Lee, M.G. Lee, W.B. Yoon, Effect of seed moisture content on the grinding kinetics, yield and quality of soybean oil, Journal of Food Engineering. 119 (2013) 758–764. doi:10.1016/j.jfoodeng.2013.06.034.

[60] P. Navi, S.E. Stanzl-Tschegg, Fracture behaviour of wood and its composites . A review COST Action E35 2004 – 2008 : Wood machining – micromechanics and fracture, Symposium A Quarterly Journal In Modern Foreign Literatures. 63 (2009) 139–149. doi:10.1515/HF.2009.012.

[61] G. Kifetew, F. Thuvander, L. Berglund, H. Lindberg, The effect of drying on wood fracture surfaces from specimens loaded in wet condition, Wood Science and Technology. 32 (1998) 83–94. doi:10.1007/BF00702589.

[62] C. Bullinger, M. Ness, Coal drying improves performance and reduces emissions, Fuel and Energy Abstracts. 44 (2003) 134. doi:10.1016/S0140-6701(03)81585-0.

[63] H.E. Rose, Particle shape and surface area, Powders in Industry. (1961) 130–149.

[64] F.C. Bond, Control particle shape and size, Chemical Engineering. 61 (1954) 195–198.

[65] M.T. Akkoyunlu, H.H. Erdem, S. Pusat, Determination of economic upper limit of drying processes in coal-fired power plants, Drying Technology. 34 (2016) 420–427. doi:10.1080/07373937.2015.1060489.

Supplementary data

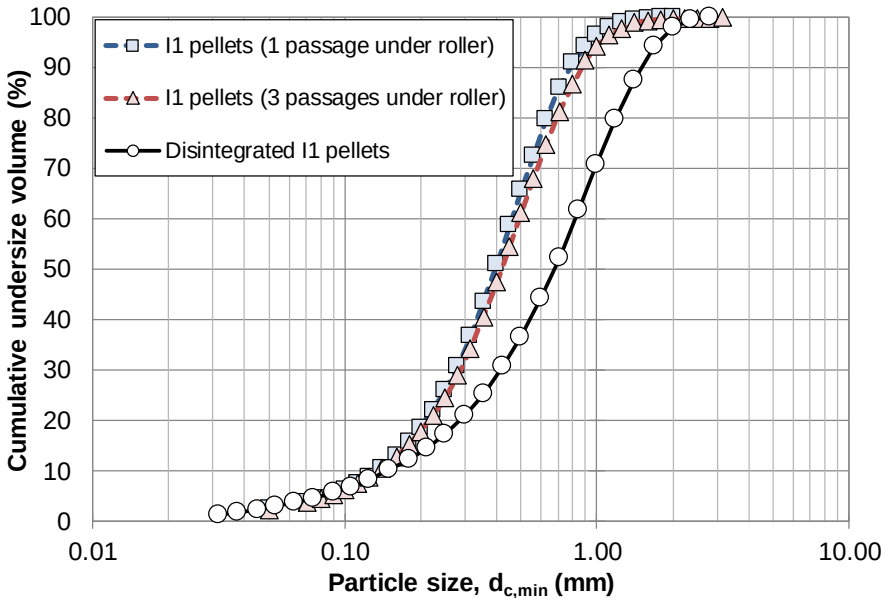

Fig. S1: Influence of the number of passages under the roller on the average particle size distribution of roller-milled I1 pellets compared to the disintegrated pellet particle size distribution.

Appendix V

An investigation of the grindability of wood pellets in a lab-scale roller mill with classifier

Marvin Masche, Maria Puig-Arnavat, Peter A. Jensen, Jens K. Holm, Sønnik Clausen, Jesper Ahrenfeldt, Ulrik B. Henriksen

An investigation of the grindability of wood pellets in a lab-scale roller mill with classifier

Marvin Masche[a], Maria Puig-Arnavat[a], Peter A. Jensen[a], Jens Kai Holm[b], Sønnik Clausen[a], Jesper Ahrenfeldt[a], Ulrik B. Henriksen[a]*

[a]Department of Chemical and Biochemical Engineering, Technical University of Denmark, 2800 Kgs. Lyngby, Denmark

[b]Bioenergy and Thermal Power, Ørsted, Nesa Allé 1, 2820 Gentofte, Denmark

*Corresponding author. E-mail address: marv@kt.dtu.dk (M. Masche)

Abstract

The purpose of this study is to investigate the grinding behavior of wood pellets in a lab-scale roller mill in closed-circuit with zigzag classifier to simulate a continuous grinding operation similar to an industrial vertical roller mill. Two industrial pellet qualities and two semi-industrial pellets (beech and pine) were used. The grinding behavior was assessed by determining the specific grinding energy and characterizing the size and shape of milled and internal pellet particles using a dynamic image analyzer. The pellet grinding behavior is compared to an industrial-scale mill-classifier system and a lab-scale open-circuit system. The study showed that the proposed lab-scale mill with classifier is useful to assess the grinding properties (milled product fineness and grinding energy) of the different pellets. Beech pellets required the lowest grinding energy to achieve a specific size reduction ratio compared to the other three pellet samples, which showed similar grinding energies. Thus, utilizing beech pellets in the industrial roller mills has the potential to improve the grinding performance. The comparison with the industrial grinding properties of industrial pellets showed that the lab-scale method requires less energy to obtain similar size reduction ratios than the industrial mill. However, similar trends with regard to the pellet type and size reduction ratio on grinding energy were observed. Therefore, the proposed lab-scale mill with classifier has a great potential to be applied as a standard method to predict the pellet grindability at industrial scale.

Keywords: Wood pellets; Grindability; Grinding energy; Particle size; Classifier

1. Introduction

As Denmark seeks to achieve its ambitious goal of a fossil fuel-free energy system by 2050, energy from biomass and wind will play an increasing role in the future. With an increase in intermittent wind energy production, the future energy system will also require a high degree of flexibility and reliability on the demand side. A substantial role in providing a flexible supply of electricity and district heating to Danish homes and businesses have combined heat and power (CHP) plants. The conversion of pulverized coal-fired CHP plants to biomass sources is hence a key step in the green transition of the Danish energy sector. By utilizing the existing efficient CHP plants and infrastructure, the conversion of CHP plants to biomass represents a low-cost option, which extends the lifetime of current CHP plants. All electricity and heat consumption in Denmark is expected to be based on renewables by 2035 [1].

Energy from biomass in Denmark is primarily wood pellets, as they are suitable for long-distance ocean transportation. Denmark depends on imports, as its production of pellets from local forests is not able to fulfill the rising demand for wood pellets for commercial heat and power generation. Wood pellets have a substantial potential to save greenhouse gas emissions, especially when substituting coal for power production (ca. 1940 kg CO_2eq/ton pellets) [2]. For the effective utilization of wood pellets for CHP generation, knowledge about their milling behavior in the existing power plant coal mills is crucial.

The milling process in power plants comprises fuel drying using hot air, comminution in the coal mill, particle classification (and circulation), and product discharge to the burners.

For the optimal conversion of fuel particles, mill classifiers need to control the milled product fineness. For coal, about 75% of pulverized particles need to pass a 75 µm sieve screen [3]. Equivalent limits for biomass have not been established. Generally, particle sizes as fine as coal are not needed due to the higher volatile content and reactivity of biomass in combustion systems. Hence, a reduction to the same size as coal is unnecessary and wasteful of mill power [4]. Esteban and Carrasco [5] recommended that ca. 95 % of particles (dry matter) shall pass a 1 mm screen to achieve optimal combustion of woody biomass, which implies adjustments of the current coal mill classifier settings. Generally, the classification system classifies particles based on Stokes' law [6], which is based on the assumption that particles resemble a sphere [7].

The design of air classifiers is constantly changing in an effort to develop more efficient and cleaner power plants. Traditionally, vertical roller mills in coal-fired power plants were equipped with static classifiers, which have no moving parts in the separation chamber. Nowadays, they are often upgraded with modern dynamic classifiers, which employ a rotor cage to exert a radial forced centrifugal field [8]. The cut size is then controlled by adjusting the rotor speed. Dynamic classifiers result in a much sharper classification operation [9], indicating a higher efficiency in rejecting overly coarse fuel particles, which will reach the boiler bottom before complete burnout. To optimize the particle burnout during combustion, power plant operators need information about the milled product particle size distribution (PSD).

There is a need to test the grindability (i.e., the resistance to grinding) of wood pellets and the subsequent classification process of milled pellet particles prior to industrial-scale operation. However, to date, there is no standard method available to relate the milling behavior of wood pellets to large-scale applications. Recent studies [10,11] have shown that the standard Hardgrove grindability test developed for coal has drawbacks for assessing the grindability performance of non-thermally treated biomass due to its fibrous structure and low density. Furthermore, this test lacks information about the grinding energy and the milling behavior in vertical roller mills with subsequent particle classification. Information about the fuel grindability is important, as it affects the power consumption and capacity of the mill [12]. The physical properties of milled pellets allow conclusions on the course of the classification process of milled pellets and their suitability for suspension-firing.

The results of the grindability tests can be applied to support the introduction of new fuel pellets for heat and power production. Avoiding fuel pellets with undesired properties has great economic and practical motivation for power plants. Examples include higher combustion efficiencies, reduced boiler downtime, lower levels of unburned carbon in the ash, and lower NOx emissions. Recent results from recent field experiments carried out in vertical roller mills with integrated dynamic classifier suggest that the internal PSD of wood pellets affects the classifier cut size and specific grinding energy [13]. This large-scale mill classifier system can be considered as a black-box, where only the input (i.e., wood pellets) and output characteristics (i.e., classifier product) of the milling circuit are known. The classifier feed and classifier

reject cannot be known without appropriate sampling inside the mill, which makes it difficult to describe and model the milling and classification process accurately.

Hence, this study aims to focus on the grinding behavior of wood pellets in a lab-scale roller mill in closed-circuit with zigzag classifier. This mill system simulates a continuous milling operation similar to an industrial mill classifier system. It allows collecting samples around the classifier. The study aims to test if results from laboratory and field experiments can be sufficiently correlated. Accurate correlation of the grinding results has the potential to reduce the need for costly pilot-or industrial-scale experiments. This knowledge is hence extremely important for power plant operators. To the best of the authors' knowledge, this is the first study of this kind. Moreover, the characteristics (i.e., grinding energy requirement and product PSD) of the closed-circuit lab-scale system will be examined and compared to the characteristics obtained with recent data from an open-circuit roller mill system. The results provided can be valuable to optimize the mill and classifier operating conditions and reduce the energy requirements for milling, which will improve the total plant efficiencies.

2. Materials and methods

2.1 Materials

Two industrial pellet qualities, designated in the following as I1 and I2 pellets, and beech and pine pellets produced in a semi-industrial pellet mill are used in this study. I1 and I2 pellets were used in the biomass-converted suspension-fired power plant Amagerværket unit 1 (Denmark) [13]. The chemical and physical properties of the four pellet types were determined elsewhere [14]. I1 pellets probably contain more hardwood, as they have a substantially higher ratio of xylan to mannan in hemicellulose than I2 pellets, which probably contain more softwood. As reported in [14], the characteristic particle size (d^*) of material within pine pellets is the largest with 1.16 mm, followed by I2 pellets (1.09 mm), beech pellets (0.99 mm), and I1 pellets (0.83 mm). To compensate for moisture differences between pellets in their as-received state, they were dried at 105±2°C in a drying oven according to ISO 18134-1:2015 [15]. Milling tests were then run with oven-dried pellet samples.

2.2 Experimental procedure

The equipment in this study comprises a lab-scale roller mill-classifier system, whose experimental data is compared to data from a lab-scale roller mill without classifier [14] and an industrial-scale mill-classifier system [13]. Table 7 summarizes the technical specifications of the three systems and their steady state milling operating conditions. All milling experiments are carried out as continuous processes.

2.2.1 Lab-scale roller mill

The roller mill operates as a continuous open-circuit mill (i.e., without classification equipment). It is described in more detail elsewhere [14]. It has to be stated that due to the design of the feeder system, all feed material undergoes some crushing before it falls onto the table. The entire comminuted pellet product is then removed from the table for subsequent particle size and shape analysis.

2.2.2 Lab-scale mill-classifier system

To resemble the particle classification process in industrial milling applications, the milling system described above is additionally equipped with a vertical zigzag air classifier for particle classification (and circulation). This system, which is also called the CMT-mill (Germany) [16], is an example of a continuous closed-circuit grinding system. The CMT-mill is the third generation of lab-scale mills that was originally developed for coal by professor Zelkowski [17]. Fig. 10a illustrates the design features of the CMT mill. The mill represents the mill start-up to reach steady-state operation. Its operation is shown in Fig. 11. The system consists of two steps; milling and separation. First, screened pellets ($m_{pellets}$) are poured into the feeder system, then milling is initiated. The pellets fall from the feeder onto the milling table, where the roller runs over them once. The milled product ($m_{product}$) is then sucked from the milling table through a cyclone into a collecting beaker.

Separation is then initiated. The $m_{product}$ is poured into the feeder system and directed into the zigzag air classifier, which consists of multiple rectangular sections joined together at an angle of 90° to create a zigzag shape. The $m_{product}$ is separated in an upward air stream based on the particle falling behavior (i.e., particle drag force) in the zigzag classifier (Fig. 10b). At the joints between two sections, turbulent vortices are formed, where the particles pass through. The separation occurs where the drag force

is larger than the gravitational force. The fine particle fraction (m_{ff}) is entrained upwards. Hence, this fraction represents the amount of suspended particles. On the other hand, the coarse particle fraction (m_{cf}) falls to the bottom due to gravity. This coarse fraction is referred to as the recirculating fraction.

The particle separation is controlled by the settings of the volumetric airflow (i.e., the separator air velocity), which are adjusted by a valve at the bottom of the zigzag classifier. The fine and coarse fraction are collected and weighed. The m_{ff} is removed from the mill circuit, while the m_{cf} is recirculated (Fig. 11). For the following milling cycle, the mill is fed with the recirculated material (i.e., the m_{cf}) mixed with an amount of new pellets (m_{new}) with the same weight as the m_{ff} that was removed from the circuit. This procedure is repeated until the total net specific grinding energy (SGE_{net}) and the fine fraction produced are constant, thus reaching steady-state mill operation. On average, about 5-7 cycles are needed to achieve steady state mill conditions. The m_{ff} and the grinding energies are calculated by an average of the last two milling cycles. The physical properties (i.e., the particle size and shape) of the last fine fraction (i.e., the wood dust for suspension-firing) are then determined.

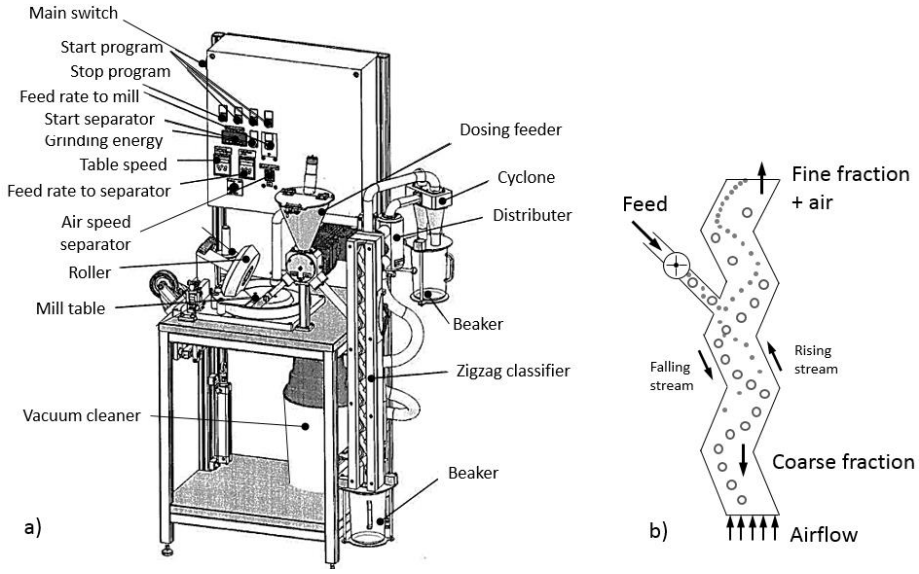

Fig. 10: Schematic view of the CMT mill (a). Adapted from [16]. Separation principle of the zigzag classifier (b).

For a steady-state separation process in the classifier, the mass balance is as follows:

$$m_{product} = m_{ff} + m_{cf} \quad (1)$$

Furthermore, the process recovery for separating the fine (R_f) and coarse (R_c) fractions can be calculated as follows:

$$R_f = \frac{m_{ff}}{m_{product}} \cdot 100\% \quad \text{and} \quad R_c = \frac{m_{cf}}{m_{product}} \cdot 100\% \quad (2)$$

Whereby the total mass balance of R_f and R_c shall add up to 1.

To evaluate the recirculation of the coarse particles in the milling circuit, the mill recirculation factor (C_f) is calculated. The recirculation factor, i.e., the amount of fine fraction that is replaced with fresh material, can be expressed as follows:

$$C_f = \frac{m_{product}}{m_{ff}} = \frac{1}{R_f} \cdot 100\% \quad (3)$$

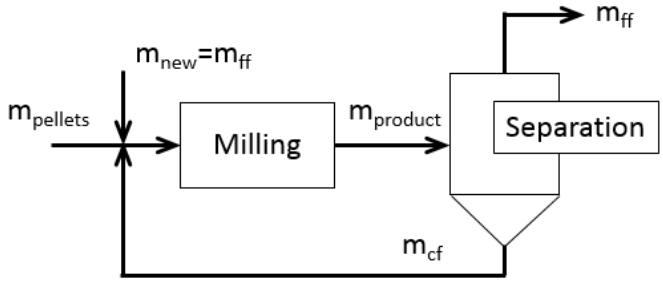

Fig. 11: Principle of the continuous lab-scale closed-circuit milling operation.

To characterize the separation behavior of the milled particles in the zigzag classifier, a so-called separation efficiency function (or Tromp curve) is introduced. It allows to determine the sharpness of separation [18] and thus indicates what percentage of the classifier feed is selected as fines or rejected as coarse particles. For example, the efficiency function for describing the percentage of the separator reject (T_c) defined as follows [19]:

$$T_c(x) = R_c \frac{q_c(x)}{q_{product}(x)} \quad (4)$$

Where $q_c(x)$ is the frequency distribution of the coarse fraction, $q_{product}(x)$ the frequency distribution of the milled product (i.e., the classifier feed), and x the particle size. The

performance of the zigzag classifier can then be assessed in terms of two parameters, namely, the cut size, χ_{50} (in mm) and the sharpness index (β). χ_{50} corresponds to the 50% value on the Tromp curve. Particles of this size have an equal chance to end up either in the coarse fraction or fine fraction. The sharpness index is measured as follows:

$$\beta = \frac{\chi_{75}}{\chi_{25}} \leq 1 \quad (5)$$

Where χ_{75} (in mm) is the particle size corresponding to the 75% value of the separation curve and χ_{25} (in mm) to the 25% value. Hence, ideal separation is when β=1, and the smaller the β, the poorer the separation.

The net energy (in J) that is used for grinding is displayed on a control panel. The mill allows to analyze the specific grinding energy with respect to the total pellet sample (SGE_{net} in kWh/t) and with respect to the amount of fine fraction (SGE_{ff} in kWh/t FF). The latter one predicts the specific grinding energy for the fine wood dust that is produced by the power plant mills for combustion in a suspension-fired boiler. The specific grinding energy with respect to the fine fraction produced (SGE_{ff}) can be expressed as follows:

$$SGE_{ff} = SGE_{net} \cdot R_f \quad (6)$$

2.2.3 Industrial-scale mill classifier system

Comparative grinding data comes from large-scale experiments carried out with I1 and I2 wood pellets in coal vertical roller mills (type LM 19.2 D, Loesche GmbH, Germany), each equipped with a dynamic classifier (type LSKS 27 ZD-4 So, Loesche GmbH, Germany) at Amagerværket unit 1 (Denmark) [13]. The operation of the industrial-scale mill can be considered as a continuous closed-circuit system. Thus, all pellet material entering the mill ($m_{pellets}$) measured by weighing the conveyor belt leaves as comminuted and classified product (m_{ff}) through fuel pipes to the burners. The average PSD of the comminuted product collected from all four burner pipes will give information about the mill classifier performance (i.e., the classifier product fineness). Specific grinding energies were presented as gross values (SGE_{gross}), thus including the idle mill motor power.

Table 7: Overview of the technical specifications and average steady-state operating conditions of mills considered in the present study.

	CMT roller mill	Roller mill	Vertical roller mill
Specifications/ notes			
Application	Laboratory	Laboratory	Industry
Mill operation	Closed-circuit	Open-circuit	Closed-circuit
Classifier type	Zigzag classifier	No	Dynamic classifier
Feeder system	Dosing feeder	Dosing feeder	Conveyor belt
Number of rollers	1	1	2
Passes under roller	1	1	unknown
Roller inclination	15°	15°	15°
Mill table diameter (m)	0.33	0.33	1.9
Motor drive power (kW)	0.12	0.12	315
Energy consumption data	SGE_{net}	SGE_{net}	SGE_{gross}
Mill operating conditions			
Roller grinding pressure (MPa)	0.3	0.3	6.1-6.7
Milling table speed (rpm)	2.4	2.4	42
Feed rate to mill table (kg/h)	15	15	14,000-21,000
Feed rate to classifier (kg/h)	n/a	6.4	n/a
Pellet conditions			
Moisture content (wt.%)	ca. 0[a]	ca. 0[a]	6-7
Fines (broken pellets) removed using a 3.15 mm sieve	without fines	without fines	with fines

[a]dried pellet samples.

2.3 Data analysis

The Rosin-Rammler-Bennet-Sperling (RRBS) model was used to describe the comminuted pellet PSD. It was shown that there is a good correlation between RRBS fit parameters and measured particle sizes [20]. The RRBS equation is expressed as follows [21]:

$$R(d) = 100 - 100 \cdot e^{-\left(\frac{d}{d^*}\right)^n} \quad (7)$$

Where *R(d)* is the cumulative percent (undersize) distribution of material finer than the particle size *d*, d^* is the characteristic particle size defined as the size at which 63,21 % of the PSD lies below, and *n* is the distribution parameter. A plot of ln[ln[100/(100-

R(d)]] against ln(d) on the double logarithmic scale will give a straight line of slope *n*, if the PSD fits the RRBS equation. The d^* characterizes the wood sample fineness. The 10th percentile (*D10*) and the 90th percentile (*D90*) of the cumulative undersize distribution were used to determine the distribution span, (*D90-D10*).

Von Rittinger's comminution law was used to analyze the relationship between *SGE* and particle size reduction obtained by the mill-classifier system [22]:

$$SGE = K_R \left(\frac{1}{d_p} - \frac{1}{d_f}\right) \quad (8)$$

Where K_R (kWh mm t^{-1}) is the Von Rittinger's constant, which is a measure of the wood grindability. d_p is the characteristic particle size of the milled product and d_f is the characteristic particle size of the disintegrated pellet material, which can be considered as the feed material. The general applicability of Von Rittinger's law to predict the energy consumption during milling of biomass pellets has been shown recently [23–25].

2.4 Wood size and shape characterization

The collected wood samples (i.e., classifier fine fraction, classifier coarse fraction, and classifier feed) from the LS mill classifier system were subjected to size and shape characterization. This was done using a dynamic image analyzer (Camsizer® X2, Retsch Technology GmbH, Germany), operated in X-Jet mode for air pressure dispersion. Information about the analyzer can be found elsewhere [13]. Each sample is analyzed twice. The measured PSD is presented as a cumulative (undersize) volume distribution versus $d_{c,min}$, which represents the shortest maximum chord length of a 2D particle projection measured from all measurement directions. It refers to the width of a particle projection, which is the dimension measured by sieve analysis [26]. The Camsizer® X2 software provides several shape factors. For the shape characterization, the elongation ratio (width-to-length ratio) and circularity are derived. The elongation ratio (*ER*) is equal to one when particles are spheres and squares, and it is defined as follows:

$$ER = \frac{d_{c,min}}{d_{Fe,max}} \quad (9)$$

Where $d_{Fe,max}$ is the maximum Feret diameter (i.e., longest distance between two parallel tangents restricting the particle at any arbitrary angle), representing the particle

length [27]. The circularity (*C)* indicates how closely the 2D particle projection resembles a circle. It is also a measure of the roundness. Hence, with an increase in roundness, the circularity also increases. The circularity is defined as follows [28]:

$$C = 4 \cdot \pi \cdot \frac{A_{particle}}{P^2_{particle}} \quad (10)$$

Where $A_{Particle}$ and $P_{Particle}$ refer to the particle projection area and the particle perimeter, respectively. An ideal perfect circle has a circularity value of 1.

3. Results and discussion

3.1 Comparison between lab-scale open-and closed-circuit grinding

The mill power requirement for the open-and closed-circuit system is examined in the following. Fig. 12. shows the SGE_{net} and fine fractions obtained for each cycle until reaching steady-state conditions for the closed-circuit operation in the lab-scale mill. Results are shown for I1 pellets and for a zigzag classifier velocity of 3.0 m/s. The SGE_{net} for the 0th cycle (i.e., 0.59 kWh/t) represents the energy required to grind new pellets, which is equivalent to the SGE_{net} obtained for an open-circuit system without classification. The SGE_{net} for the following mill cycles shows the energy demand for grinding the recirculated (or coarse) milled pellet fraction mixed with new pellets. After reaching steady-state conditions, the closed-circuit system clearly reduces the grinding energy compared to the open-circuit system. In particular, the SGE_{net} can be decreased by about 40%. The fine fraction also decreases at steady-state conditions compared to the start-up of the mill, which will increase the specific grinding energy with respect to the fine fraction (SGE_{ff}) accordingly. The grinding energy results for the other pellet samples are summarized in Table 8. The general trend is that the closed-circuit operation reduces the grinding energy effort by about 40 % compared to the open-circuit system.

The average fine fractions (R_f) produced at steady-state conditions are listed in Table 8. For the different pellet samples, the fine fraction is in the following order: I1 pellets (17.0%) > beech pellets (13.6%) > pine pellets (10.6%) > I2 pellets (9.8%). Accordingly, the recirculation factor (i.e., the inverse of the fine fraction), for the different samples is in the following order: I2 pellets (10) > pine pellets (9) > beech pellets (7) > I1 pellets (6), indicating that milling I2 pellets leads to the highest material recirculation factor, while milling I1 pellets results in the lowest recirculation factor.

In general, the circulation load should be as low as possible to avoid reducing the capacity of the mill. Thus, a larger number of passes between the roller and milling table is required for I2 pellets to fulfill the size requirement of the zigzag classifier. Consequently, lower recirculation factors for beech and I1 pellets indicate that a larger fine fraction leaves the zigzag classifier compared to pine and I2 pellets, which has grinding energy-saving potential. I1 pellets require the lowest energy to produce a fine fraction of a certain size (2.6 kWh/t FF), followed by beech pellets (2.7 kWh/t FF), pine pellets (3.7 kWh/t FF), and I2 pellets (3.8 kWh/t FF). The closed-circuit operation shows a strong correlation between the characteristic internal pellet particle size (d^*) and the SGE_{ff} (r=0.89, p>0.05). Thus, similar to the open-circuit roller mill operation, as reported in [14], the internal pellet PSD also appears to have some an effect on the grinding energy in a closed-circuit grinding system.

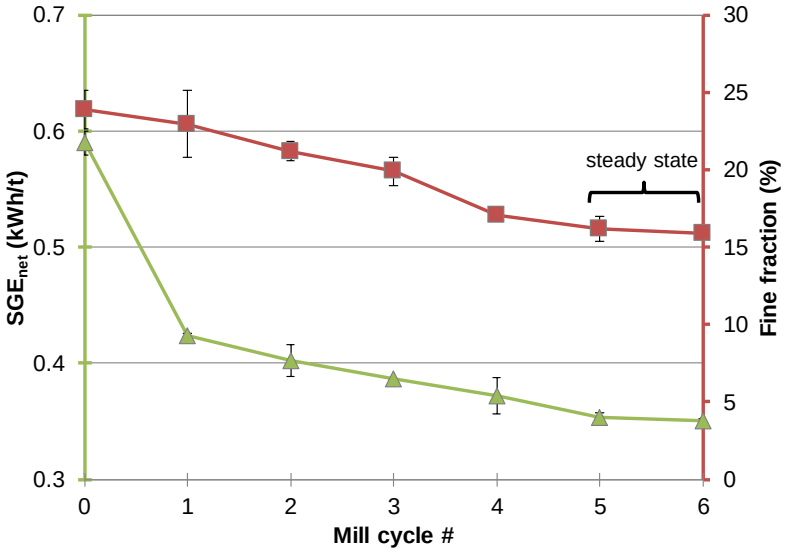

Fig. 12: Net specific grinding energies with respect to the total sample and fine fractions obtained for each milling cycle in the closed-circuit lab-scale mill running on I1 wood pellets. Each data point represents the average of two repetitions, and error bars correspond to one standard deviation.

Other characteristics of the milling circuit are the milled material characteristics (i.e., PSD, shape). Fig. 13a plots the measured cumulative PSD curves of the closed-circuit product (i.e., the classifier fine fraction from the last milling cycle) compared to the closed-circuit reject (i.e., classifier coarse fraction) and the open-circuit product. For

comparison, the disintegrated wood pellet PSD is also included. The closed-circuit grinding system uses a classifier air velocity of 3.0 m/s. Additionally, the measured PSD fitted to the RRBS model for the different wood samples are plotted versus the particle size ($d_{c,min}$) on a double logarithmic scale (Fig. 13b). The experimental data shows a very good fit (R^2 between 0.940 and 0.996) to the RRBS model described in equation (7), with the closed-circuit product showing the best fit and the closed-circuit reject showing the lowest correlation coefficient. The correlation coefficient hence increases with finer PSDs. The high correlation coefficient indicates that the RRBS model is very suitable to describe the fineness (d^*) of different wood samples.

Table 8: Specific energy comparison between lab-scale open-circuit and closed-circuit for grinding oven-dried pellets. Data of the closed-circuit system are shown after reaching steady-state conditions (cf. Table 7). Average values are presented.

	Lab-scale open-circuit (no classifier)	Lab-scale closed-circuit (with classifier[a])			
	SGE_{net} (kWh/t)	SGE_{net} (kWh/t)	R_f (%)	SGE_{ff} (kWh/t FF)	C_f (-)
Beech pellets	0.62	0.37	13.6	2.72	7.4
Pine pellets	0.67	0.39	10.6	3.68	9.4
I1 pellets	0.59	0.40	16.0	2.56	6.3
I2 pellets	0.65	0.38	9.8	3.78	10.2

[a]operated with a separator air velocity of 3.0 m/s (or airflow of 9.3 kg/h).

Typical particle size characteristics (d^*, *D10*, *D90*, and span) of these different samples are presented in Table 9. The fineness for each PSD can be read off from the constant line at a value of 63.21% (Fig. 13b). It is clear that the closed-circuit grinding system is more efficient in achieving a finer and narrower product PSD than the open-circuit system. Characteristic product particle sizes of 0.63 mm and 1.18 mm are found for the closed-circuit and the open-circuit respectively. In comparison, the disintegrated I1 pellets show a characteristic particle size of 0.83 mm. This indicates that the mill operated in open-circuit is not able to completely reduce the particle size back to the internal (original) pellet PSD, as mentioned already in [14]. Instead, the mill produces agglomerated pellet particles rather than individual particles. Green [29] stated that

mills that apply compression forces have some problems with non-brittle or ductile materials. These mills tend to flatten these materials, leading to particle agglomerations. In the present study, this explanation may be considered, as the open-circuit product leaves the milling table with a coarser PSD than the disintegrated pellet material.

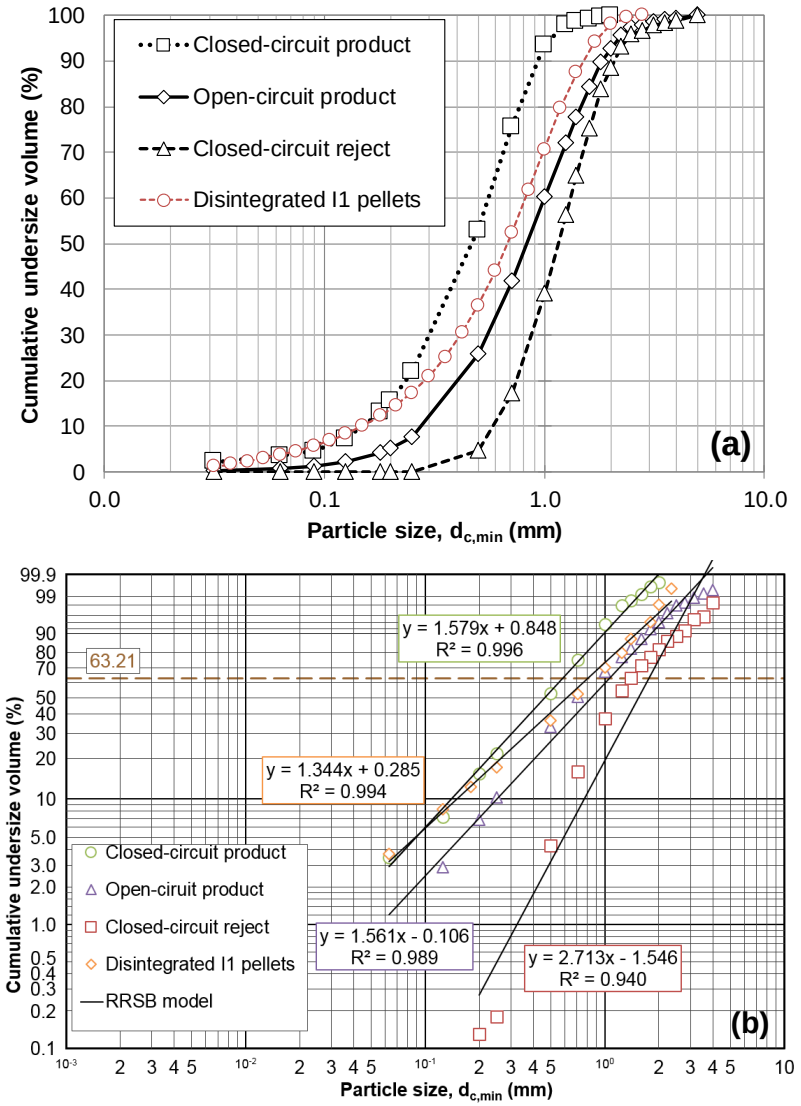

Fig. 13: Comparison of the cumulative undersize PSD (a) and the corresponding RRBS model (b) between open-and closed-circuit milling systems for I1 wood pellets. Presented distribution curves are the average of three measurements.

In the closed-circuit system, the roller-milled product is fed into the zigzag classifier. Moving in the classifier that has a high degree of turbulence in its channel, wood particles repeatedly collide with the walls and each other, and their agglomerates can break up. Then only those particles whose downward force caused by gravity is less than that caused by the air drag force will end up in the classifier fine fraction. In addition, the recirculation of the coarse material back to the mill for further size reduction improves the product fineness by more than 50% compared to the open-circuit. As expected, the classifier reject has the largest and widest PSD of all samples. The coarse fraction of the classifier reject clearly comprises agglomerated pellet particles (or pellet fragments) that cannot be separated by the airflow in the zigzag classifier. Thus, only the closed-circuit product (i.e., the suspended wood dust) with more than 95% of particles below 1 mm will comply with the specifications set by Esteban and Carrasco [5] to achieve optimal burnout.

Table 9: Comparison of particle size characteristics for I1 pellets milled in open-circuit and closed-circuit and compared to disintegrated I1 pellets. Average values are presented.

	D10 (mm)	d^* (mm)	D90 (mm)	span (mm)
Disintegrated pellets	0.15	0.83	1.51	1.36
Open-circuit product	0.30	1.18	1.81	1.52
Closed-circuit system[a]				
Product (fine fraction)	0.17	0.63	1.02	0.84
Reject (coarse fraction)	0.59	1.71	2.08	1.59

[a]classifier operated with an air velocity of ca. 3.0 m/s (or airflow of 9.3 kg/h).

The average particle elongation ratio and circularity values for the wood sample products from the open-and closed-circuit are illustrated in Fig. 14a and b. The agglomerated pellet particles from the open-circuit product and the closed-circuit reject have a fairly constant and similar circularity for the particle size ranges presented (Fig. 14a). Wood particles in the finest size fraction (< 0.25 mm) show the highest circularity. The particles from the closed-circuit product show an increasing circularity with decreasing particle size. The measurement of the circularity is a proxy measure to

estimate the particle sphericity [30]. Hence, the inverse correlation between size and shape of the particles from the closed-circuit product probably indicates that the zigzag classifier follows the Stokes' law to select the product particle sizes. Compared to the original shape of the disintegrated pellet particles, the mill system seems not to modify the particle circularity.

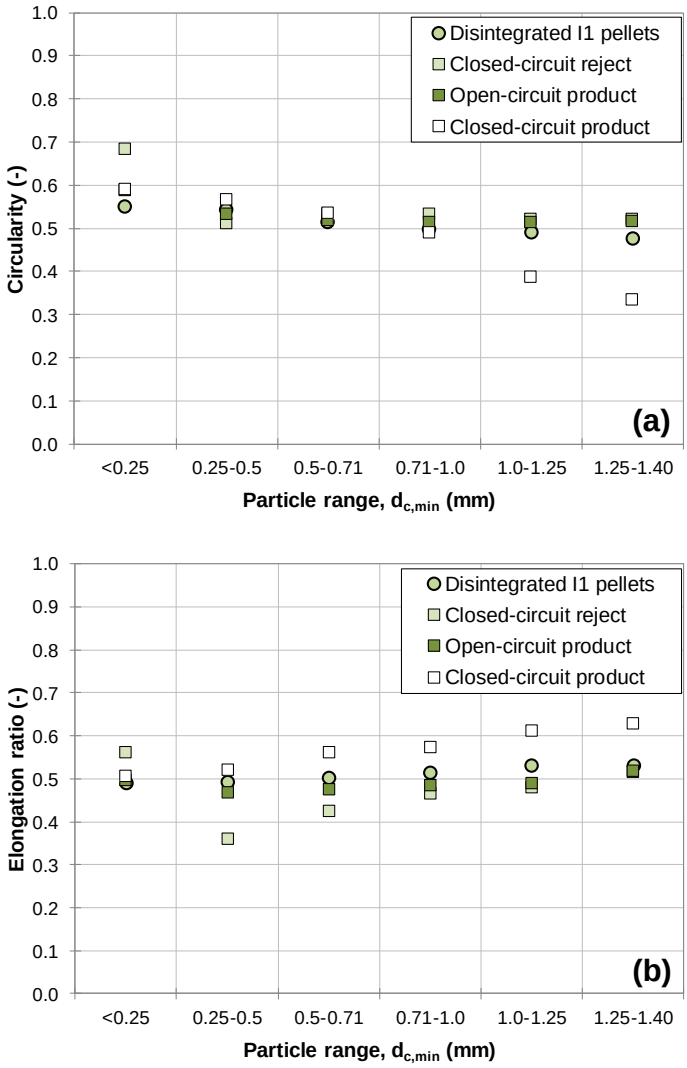

Fig. 14: Comparison of the average circularity (a) and elongation ratio (b) between open-and closed-circuit milling systems. Presented values are the average of three measurements.

Fig. 14b shows that the particles in the closed-circuit reject are more needle-like than the particles found in the closed-circuit product. On the other hand, the open-circuit product particles have a nearly constant elongation across the wide particle size range measured. On average, the closed-circuit product has less elongated particles than the disintegrated pellet particles. Thus, the classification of the roller-milled product is based on both size and shape. Both properties affect the drag force on the particle and hence the separation process in the zigzag classifier.

Table 10: Characteristic product particle sizes (d_p) for the different pellet samples in open-circuit grinding and closed-circuit grinding. Values are shown in comparison to the characteristic feed particle size (d_f). Average values are presented.

	Beech pellets	Pine pellets	I1 pellets	I2 pellets
Disintegrated pellet d_f (mm)	0.99	1.16	0.83	1.09
Open-circuit product d_p (mm)	1.34	0.93	1.18	0.96
Closed-circuit[a] product d_p (mm)	0.51	0.66	0.63	0.57

[a]classifier operated with an air velocity of 3.0 m/s (or airflow of 9.3 kg/h).

The general trend is that switching from open-circuit to closed-circuit produces a higher milled product fineness across the different pellet samples (Table 10). Thus, the additional classifier operation and recirculation of coarser particles in closed-circuit causes a larger size reduction ratio compared to the characteristic disintegrated pellet particle size. According to the milled product fineness achieved in closed-circuit after steady-state conditions, beech pellets show the finest particles (0.51 mm), followed by I2 pellets (0.57 mm), I1 pellets (0.63 mm), and pine pellets (0.66 mm).

3.2 Performance of the zigzag classifier

To evaluate the actual performance of the zigzag air classifier, the particle separation efficiency curve (or Tromp curve) from a steady state process at a separator air velocity of 3.0 m/s is plotted, as an example, for the roller-milled I1 pellets. From the real separation process, the process recovery (R_i) for separating the fine fraction is about 16 wt.% after reaching steady state conditions. The remaining 84 wt.% of the milled I1 pellets end up in the bottom of the classifier. The latter part represents the coarse fraction or recirculating load that is fed back to the mill for re-grinding. To plot the separation efficiency curve, the frequency distribution of the fine and coarse fraction

need to be weighted with the respective process recovery proportions. Fig. 15a plots the weighted frequency distributions for the fine and coarse fraction in comparison to the frequency distribution of the total classifier feed (or milled I1 pellet product).

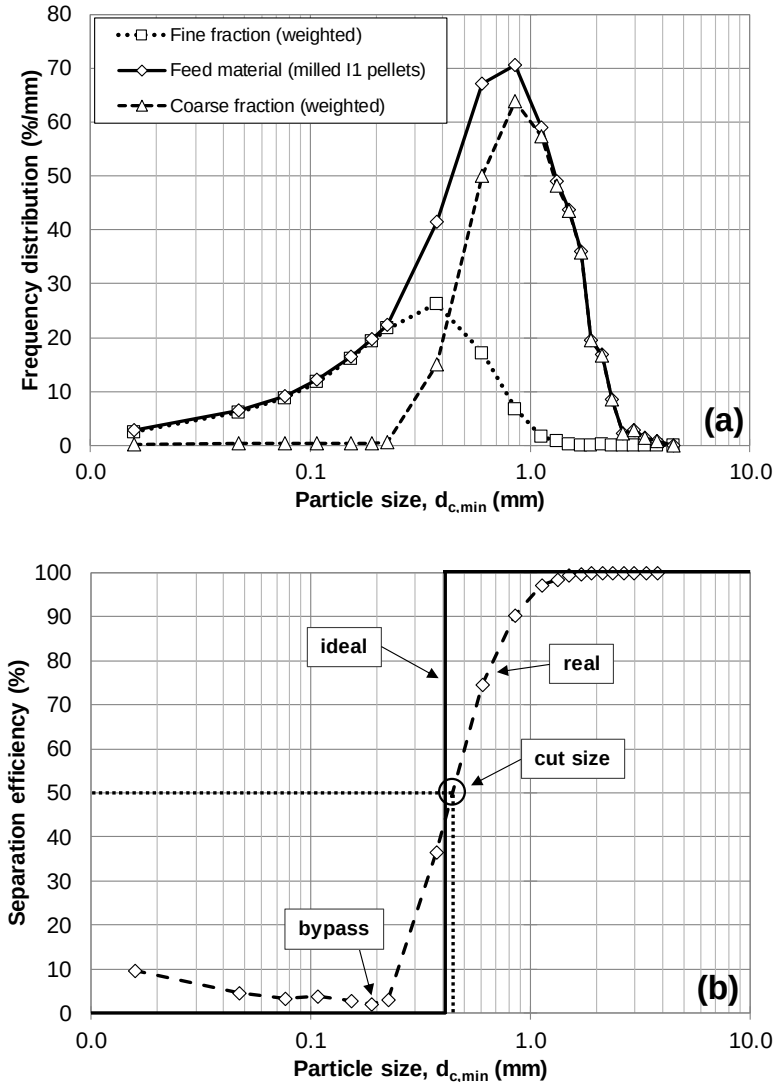

Fig. 15: Weighted frequency distributions of the wood sample streams around the zigzag classifier (a) and separation efficiency curve or Tromp curve (b).

The separation efficiency curve (Fig. 15b) is then plotted according to equation (4). From the plot, it can be seen what fraction of the classifier feed is subjected to the

underflow or overflow streams at a given size fraction. The x-axis displays the particle size, and the y-axis denotes the probability for being separated as a fine fraction and a coarse fraction. The ideal separation curve would be a straight line at the cut size (i.e., a unit step function), where all particles below the cut size would leave the classifier and particles larger than are recirculated back to the mill. As shown in Fig. 15b, an ideal classification is not achieved in the real process, as the curve does not reach 0%. The separation process in the zigzag classifier is hence not 100% efficient. The curve minimum shows the so-called bypass fraction (ca. 2 %), which represents the portion of fine material (good product) that will be returned to the mill along with the coarse stream for further size reduction. Generally, separation processes shall result in a bypass below 10 % [31]. The low bypass fraction indicates a very effective separation process in the zigzag classifier, as only a small amount of fine (good) particles will be classified into the coarse fraction of the classifier.

3.3 Effect of air velocity in zigzag classifier in the lab-scale closed-circuit

Fig. 16 shows the effect of varying the air velocity entering the zigzag classifier on the steady-state classifier product (i.e., fine fraction) PSD compared to the PSD of the disintegrated pellets. The results are shown for I1 pellets. Decreasing the air velocity from 3.0-1.1 m/s shifts the classifier product PSD towards finer particles. The characteristic product particle size decreases from 0.63 to 0.45 mm, and the distribution span becomes narrower when decreasing the air velocity in the classifier (Table 11). All classifier product PSDs are finer than the disintegrated pellet PSD. This indicates an actual size reduction (grinding) effect of the closed-circuit grinding system, as product particles are finer than the internal pellet pellets.

In addition, the classifier fine fraction (R_f) decreases with decreasing air velocity, indicating that fewer particles end up in the classifier product, as the drag force applied on the wood particles decreases. As shown in Table 11, the steady-state fine fraction increases from 16.0 to 10.4 % with decreasing air velocity. Consequently, the circulation factor increases, as a higher coarse fraction recirculates back to the mill (i.e., the classifier cut size decreases and the separation sharpness increases). As a result, the specific grinding energy increases with decreasing air velocity from 2.6-3.9 kWh/t FF.

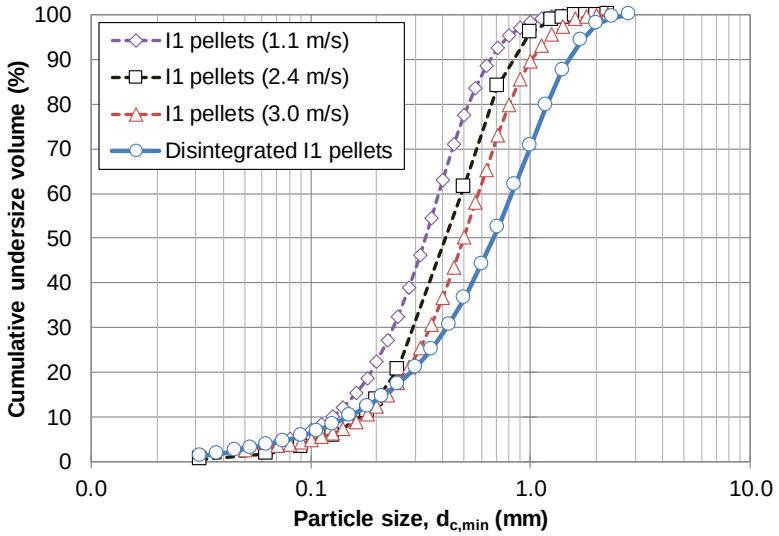

Fig. 16: Effect of air velocity on the classifier product PSD in comparison to the disintegrated I1 pellet PSD.

Table 11: Effect of air velocity on the specific grinding energy and classifier product characteristics for I1 pellets. Average values are presented.

Zigzag classifier air velocity (m/s)	R_f (%)	C_f (-)	SGE_{ff} (kWh/t FF)	d_p (mm)	span (mm)
1.1	10.4	9.6	3.91	0.45	0.53
2.4	13.7	7.3	3.03	0.57	0.66
3.0	16.0	6.3	2.56	0.63	0.84

3.4 Comparison between lab-scale and industrial-scale closed-circuit grinding

Fig. 17a and Fig. 17b plot the specific energy for grinding pellets versus the characteristic product particle size and the specific grinding energy versus the Von Rittinger's size reduction ratio, respectively. The lab-scale closed-circuit data are shown for the four pellet samples tested at different air velocities in the zigzag classifier (cf. Table 12). All plots show an interesting trend. The experimental data of the lab-scale closed-circuit show a strong power-law relationship (R^2=0.961-0.999) between the SGE and the size reduction ratio and between the SGE and the characteristic product particle size.

For a fixed value of d_p=0.5 mm, the SGE ranking for the different pellet samples is BP-LS < I1-LS < I2-LS < PP-LS (Fig. 17a). This indicates that grinding beech pellets requires the lowest energy to be reduced to a characteristic particle size of 0.5 mm, while pine pellets need the highest energy. Beech and pine have distinct structural differences, which may explain the different fracture behavior. Moreover, pine pellets have a larger internal pellet PSD than pine pellets. Studies [32,33] have shown that larger feed sizes require more energy for milling than finer feed sizes. The present study has some similarities with [13], which shows that milling hardwood (beech) pellets in a hammer mill requires less energy compared to pine pellets. In this study, the energy-size relationship for milling I2 pellets and pine pellets is very similar, indicating a similar breakage behavior of pine and I2 pellets. This finding may be explained by their similar internal pellet PSD and chemical composition.

To achieve a Von Rittinger's size reduction ratio of about 1 (1/mm), the SGE ranking for the different pellet samples in the lab-scale closed-circuit is also BP-LS < I1-LS < I2-LS < PP-LS (Fig. 17b). Taking into account the initial PSD of the material within pellets, the well-defined (hardwood) beech pellets show a clearly different energy-size reduction relationship than the other three pellets, which either are pure softwoods or blended with softwoods. More specifically, beech pellets achieve the same size reduction ratio at a lower energy requirement than the other three pellets. Considering that I1 pellets have the lowest internal pellet PSD (cf. Table 10), the wood origin also appears to have a larger influence on the specific grinding energy requirements.

Table 12: Information related to Fig. 17. More mill conditions are given in Table 7.

Denotation	Pellet	Application	SEC net/gross	Mill operating conditions
BP-LS	Beech	Laboratory	net	air velocity[a] ca. 1.0, 2.4, and 2.9 m/s
PP-LS	Pine	Laboratory	net	air velocity[a] ca. 1.1 and 2.9 m/s
I1-LS	I1	Laboratory	net	air velocity[a] ca. 1.1, 2.2, and 3.0 m/s
I2-LS	I2	Laboratory	net	air velocity[a] ca. 1.1, 2.3, and 2.7 m/s
I1-IS	I1	Industry	gross	test scenarios 10-12
I2-IS	I2	Industry	gross	test scenarios 7-9

[a]Average measured velocity in the zigzag classifier during operation (i.e., not empty classifier velocity).

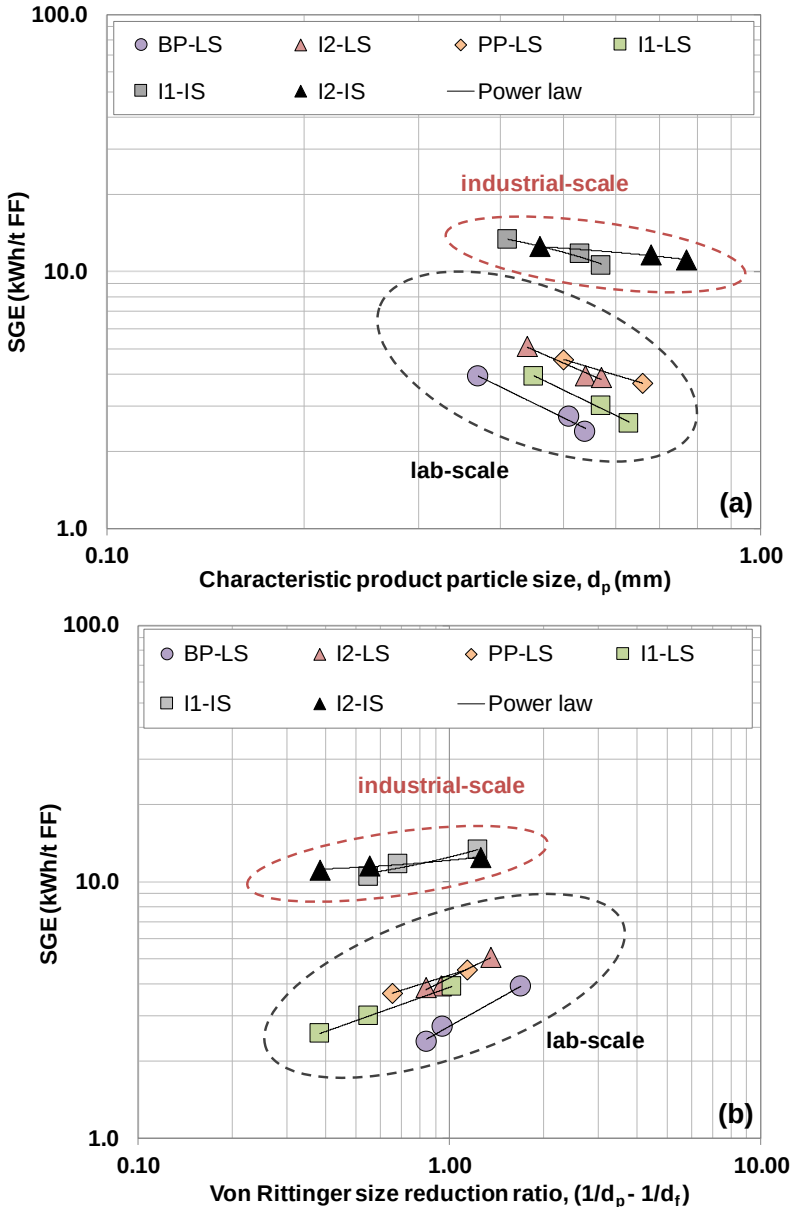

Fig. 17: Specific grinding energy consumption vs. Von Rittinger's size reduction ratio (a) and specific grinding energy consumption vs. characteristic product particle size (b). Denotations and milling conditions are listed in Table 12.

Depending on the air velocity in the zigzag classifier, the lab-scale closed-circuit grinding system can produce a similar characteristic product particle size and size reduction ratio compared to the wood dust produced from the industrial-scale mills (Fig. 17a-b). However, the specific energy requirement of the industrial mill is higher than for the lab-scale mills. It has to be stated that the specific energy consumption of the industrial mills has been presented as a gross value, while for the lab-scale grinding system the net value has been determined. Hence, the no-load power of the industrial mill is not deducted, which may contribute to a higher overall energy requirement. Moreover, the industrial mill features two rollers, while the lab-scale mill has one roller. This has to be considered when evaluating the mill power consumption. Shi et al. [34] assessed the performance of coal vertical roller mills using models, including the prediction of the mill power. They formulated an equation to predict the mill power consumption, where the number of rollers was one of the variables affecting the mill power. It is further clear that a higher number of passes under the roller in the lab-scale roller mill will increase the mill power consumption and hence increases the total SGE. In the industrial mill, the energy-size and energy-size reduction relationships between I1 and I2 pellets are relatively similar. In the lab-scale system (Fig. 17b), the similar energy-size reduction relationship can be confirmed for I1 and I2 pellets. Only Fig. 17a presents some differences in the energy requirement for grinding I1 and I2 pellets to the same product particle size. The general trend is that I1 pellets require less energy than I2 pellets to be reduced to the same product fineness.

Fig. 18 shows the cumulative PSD of the lab-scale classifier product for I1 pellets in comparison with the milled I1 wood pellet product sampled from the burner pipes at the power plant. As mentioned previously, the characteristic product particle sizes (at which 63.21 % of the PSD lies below) are very similar from both the lab-scale and industrial-scale roller mill. However, a major difference of the PSD curves lies in the inclination. The PSD curves obtained from the industrial mill are shallower and have a lower inclination than the PSD obtained from the lab-scale mill, indicating a broader wood dust PSD of the industrial mill product compared to the lab-scale product. Therefore, the particle classification process in the lab-scale zigzag classifier is more selective compared to the classification process in the industrial-scale dynamic classifier, resulting in a more effective product split and a narrower PSD. The high fine fraction (below 0.4 mm) for the industrial mill product can additionally be attributed to

the fact that the fines (e.g., pellet dust) are present in the industrial milling circuit. In comparison, the pellet fines have been removed by sieving before milling in the lab-scale closed-circuit.

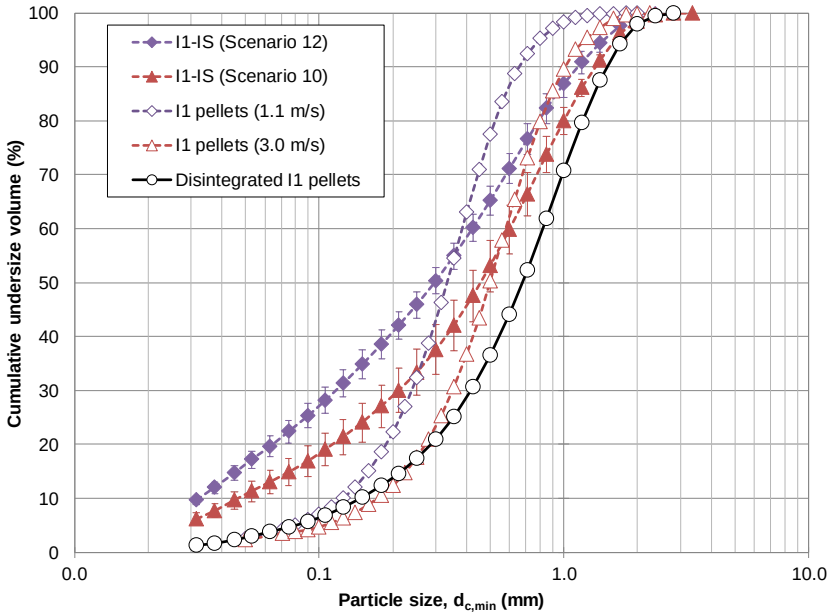

Fig. 18: Comparison between lab-scale and industrial-scale wood dust PSD.

4. Conclusions

This study investigated the grinding performance of wood pellets in a lab-scale roller mill in closed-circuit with a zigzag classifier. Grinding data are compared with the lab-scale open-circuit grinding system and the industrial-scale closed-circuit grinding system. The following conclusions can be drawn from the experimental study:

- The proposed lab-scale mill was able to evaluate the different grinding properties of the four wood pellets (beech, pine, and two mixed industrial pellet qualities).
- The relationships between the grinding energy and the characteristic product particle size and between the grinding energy and the Von Rittinger's size reduction ratio were well described by a power-law relationship.
- To achieve a characteristic product particle size, beech pellets required the lowest grinding energy compared to the other three pellet samples, which have

shown approximately similar grinding energies. Thus, utilizing beech pellets in the industrial roller mills has the potential to improve the grinding performance.

- The comparison of the grinding behavior of the two industrial pellet qualities in the lab-and industrial-scale mill showed that the lab-scale method requires lower grinding energies for obtaining similar size reduction ratios. However, the tendencies with respect to the effect of pellet type and size reduction ratio on grinding energy was reasonably similar. Hence, the application of the lab-scale mill can have great economic and practical motivation for power plant operators, as there is no need for costly pilot-or industrial-scale experiments.
- The comparison between open- and closed-circuit roller-milling showed that the closed-circuit operation achieves an actual size reduction effect on the internal pellet particles (i.e., higher and narrower product fineness) and lower grinding energy than the open-circuit operation.

Nomenclature

$A_{Particle}$	particle projection area (mm^2)
$P_{Particle}$	particle perimeter (mm)
ER	particle elongation ratio (dimensionless)
ar	as received
C	circularity (dimensionless)
d^*	RRBS characteristic particle size (mm)
d.b.	dry basis
D90	particle size at 90th percentile of the cumulative undersize distribution (mm)
$d_{c,min}$	shortest maximum chord (mm)
d_f	RRBS characteristic particle size (mm) of the feed
$d_{Fe,max}$	maximum Feret diameter (mm)
d_p	RRBS characteristic particle size (mm) of the product
K_R	Von Rittinger's material characteristic parameter (kWh mm t^{-1})
n	RRBS uniformity constant (dimensionless)
PSD	particle size distribution
R(d)	cumulative undersize distribution (%)
RRBS	Rosin-Rammler-Bennet-Sperling
SEC	specific energy consumption (kWh/t)

Acknowledgements

The authors thank Energiteknologiske Udviklings- og Demonstrationsprogram (EUDP) for the financial support received as part of the ForskEL project "AUWP – Advanced Utilization of Wood Pellets" (Project number: 12325).

References

[1] Biomass for energy: Why coal and gas should be replaced by wood pellets and wood chips, Danish Energy Association. (2018). https://www.danskenergi.dk/sites/danskenergi.dk/files/media/dokumenter/2017-09/BiomassForEnergy.pdf (accessed October 18, 2018).

[2] R. Sikkema, M. Junginger, W. Pichler, S. Hayes, A.P.C. Faaij, The international logistics of wood pellets for heating and power production in Europe: Costs, energy-input and greenhouse gas balances of pellet consumption in Italy, Sweden and the Netherlands, Biofuels, Bioproducts and Biorefining. 4 (2010) 132–153. doi:10.1002/bbb.208.

[3] J.L. Afolabi, The performance of a static coal classifier and its controlling parameters (PhD thesis), University of Leicester, UK, 2012.

[4] M.A. Saeed, G.E. Andrews, H.N. Phylaktou, B.M. Gibbs, Global kinetics of the rate of volatile release from biomasses in comparison to coal, Fuel. 181 (2016) 347–357. doi:10.1016/j.fuel.2016.04.123.

[5] L.S. Esteban, J.E. Carrasco, Evaluation of different strategies for pulverization of forest biomasses, 166 (2006) 139–151. doi:10.1016/j.powtec.2006.05.018.

[6] E. Ortega-Rivas, Unit operations of particulate solids: theory and practice, 1st ed., CRC Press, 2011.

[7] N. Paul, S. Biggs, J. Shiels, R.B. Hammond, M. Edmondson, L. Maxwell, D. Harbottle, T.N. Hunter, Influence of shape and surface charge on the sedimentation of spheroidal, cubic and rectangular cuboid particles, Powder Technology. 322 (2017) 75–83. doi:10.1016/j.powtec.2017.09.002.

[8] N.M. Isa, Performance enhancement of a coal classifier (PhD thesis), University of Leicester, UK, (2012).

[9] A. Malmgren, Talking about the revolution, World Coal. (2015) 1–4. http://www.bioc-ltd.com/images/Talking_about_the_revolution-World_Coal-Nov_2015.pdf (accessed June 8, 2017).

[10] O. Williams, C. Eastwick, S. Kingman, D. Giddings, S. Lormor, E. Lester, Investigation into the applicability of Bond Work Index (BWI) and Hardgrove Grindability Index (HGI) tests for several biomasses compared to Colombian La Loma coal, Fuel. 158 (2015) 379–387. doi:10.1016/j.fuel.2015.05.027.

[11] J. Hari, A. Khalsa, D. Leistner, N. Weller, L.I. Darvell, B. Dooley, Torrefied Biomass Pellets—Comparing Grindability in Different Laboratory Mills, (2016) 1–15. doi:10.3390/en9100794.

[12] C. Spero, Developments in laboratory testing and evaluation of coal grindability, Queensland Coal Symposium 29-30. (1991) 73–82.

[13] M. Masche, M. Puig-Arnavat, J. Wadenbäck, S. Clausen, P.A. Jensen, J. Ahrenfeldt, U.B. Henriksen, Wood pellet milling tests in a suspension-fired power plant, Fuel Processing Technology. 173 (2018) 89–102. doi:10.1016/j.fuproc.2018.01.009.

[14] M. Masche, M. Puig-Arnavat, P.A. Jensen, J.K. Holm, S. Clausen, J. Ahrenfeldt, U.B. Henriksen, Open-circuit grinding of wood pellets in laboratory-scale mills. Manuscript submitted for publication, (2018).

[15] International Organization for Standardization, ISO 18134-1:2015 - Solid biofuels - Determination of moisture content - Oven dry method, (2015).

[16] J. Wadenbäck, Nya karaktäriseringsmetoder för fasta bränslen – malbarhet, tändvillighet och sintring, in: Panndagarna, 2011.

[17] V. Werner, J. Zelkowski, K. Schönert, Lab-scale roller table mill for investigating the grinding behaviour of coal, Powder Technology. 105 (1999) 30–38. doi:10.1016/S0032-5910(99)00115-1.

[18] H.G. Merkus, Particle size measurement fundamentals, practice, quality, 2009. doi:10.1007/978-1-4020-9016-5.

[19] M. Stieß, Mechanische Verfahrenstechnik, (1997) 146–178. doi:10.1007/978-3-662-08599-8.

[20] W. Pichler, A. Weidenhiller, J. Denzler, R. Goetzl, M. Pain, M. Weigl, A. Haider, Approaches to describe the particle properties of wood pellet feedstock, World Bioenergy 2014, Jönköping, Sweden. (2014) 2–3. doi:10.13140/2.1.3203.3286.

[21] T. Allen, Powder Sampling and Particle Size Determination, 1st ed., Elsevier Science, Oxford, UK, 2003.

[22] T. Tanaka, Comminution Laws. Several Probabilities, Industrial & Engineering Chemistry Process Design and Development. 5 (1966) 353–358. doi:10.1021/i260020a001.

[23] O. Williams, G. Newbolt, C. Eastwick, S. Kingman, D. Giddings, S. Lormor, E. Lester, Influence of mill type on densified biomass comminution, Applied Energy. 182 (2016) 219–231. doi:10.1016/j.apenergy.2016.08.111.

[24] M. Temmerman, P.D. Jensen, J. Hébert, Von Rittinger theory adapted to wood chip and pellet milling, in a laboratory scale hammermill, Biomass and Bioenergy. 56 (2013) 70–81. doi:10.1016/j.biombioe.2013.04.020.

[25] M. Masche, M. Puig-Arnavat, P.A. Jensen, J.K. Holm, S. Clausen, J. Ahrenfeldt, U.B. Henriksen, From wood chips to pellets to milled pellets: the mechanical processing pathway of Austrian pine and European beech. Manuscript submitted for publication, (n.d.).

[26] M. Gil, E. Teruel, I. Arauzo, Analysis of standard sieving method for milled biomass through image processing. Effects of particle shape and size for poplar and corn stover, Fuel. 116 (2014) 328–340. doi:10.1016/j.fuel.2013.08.011.

[27] A. Trubetskaya, G. Beckmann, J. Wadenbäck, J.K. Holm, S.P. Velaga, R. Weber, One way of representing the size and shape of biomass particles in combustion modeling, Fuel. 206 (2017) 675–683. doi:10.1016/j.fuel.2017.06.052.

[28] E.P. Cox, A Method of Assigning Numerical and Percentage Values to the Degree of Roundness of Sand Grains, Journal of Paleontology. 1 (1927) 179–183.

[29] D.W. Green, R.H. Perry, Perry's Chemical Engineers' Handbook, 8th ed., McGraw-Hill Education, 2007.

[30] S.J. Blott, K. Pye, Particle shape: a review and new methods of characterization and classification, Sedimentology. 55 (2007). http://doi.wiley.com/10.1111/j.1365-3091.2007.00892.x.

[31] Sixto Humberto Aguero, Process Analysis and Energy Efficiency Improvement on Portland Limestone Cement Grinding Circuit (Master's thesis), University of British Columbia, Canada, (2015).

[32] J. Jiang, J. Wang, X. Zhang, M. Wolcott, Characterization of micronized wood and energy-size relationship in wood comminution, Fuel Processing Technology. 161 (2017) 76–84. doi:10.1016/j.fuproc.2017.03.015.

[33] M. Shaw, Feedstock and Process Variables Influencing Biomass Densification (Master's thesis), University of Saskatchewan, Canada, (2008).

[34] F. Shi, T. Kojovic, M. Brennan, Modelling of vertical spindle mills. Part 1: Sub-models for comminution and classification, Fuel. 143 (2015) 595–601. doi:10.1016/j.fuel.2014.10.085.

Appendix VI

Combustion behavior of single particles of raw and pelletized wood

Marvin Masche, Benjamin E. Clausen, Zhimin Lu, Maria Puig-Arnavat,
Peter A. Jensen, Jens K. Holm, Sønnik Clausen,
Jesper Ahrenfeldt, Ulrik B. Henriksen

Combustion behavior of single particles of raw and pelletized wood

Marvin Masche[a], Benjamin E. Clausen[a], Zhimin Lu[b], Maria Puig-Arnavat[a], Peter A. Jensen[a], Jens K. Holm[c], Sønnik Clausen[a], Jesper Ahrenfeldt[a], Ulrik B. Henriksen[a]*

[a]Department of Chemical and Biochemical Engineering, Technical University of Denmark, 2800 Kgs. Lyngby, Denmark

[b]School of Electric Power, Guangdong Province Key Laboratory of Efficient and Clean Energy Utilization, South China University of Technology, No. 381, Wushan Road,

Tianhe District, Guangzhou 510640, China

[c]Bioenergy and Thermal Power, Ørsted, Nesa Allé 1, 2820 Gentofte, Denmark

*Corresponding author. E-mail address: marv@kt.dtu.dk (M. Masche)

Abstract

The present paper investigates the thermal conversion behavior of 3 mm single cube particles made of raw and pelletized beech and pine. Pellets were produced at pressures of 100 and 200 MPa and die temperatures of 75 and 125°C using a cubic-shaped die equipped with a heating cast. Combustion experiments were performed in a single particle combustion reactor at suspension-firing conditions (ca. 1260°C and 5 vol.% oxygen). Times for devolatilization and char combustion were determined. The results show that pelletizing produced a more compact structure with apparent densities between 810 and 1020 kg/m3 for beech pellets and between 980 and 1060 kg/m3 for pine pellets compared to raw beech (770 kg/m3) and raw pine (420 kg/m3). Increasing the pelletizing pressure has a larger effect on the apparent pellet density than increasing the die temperature. The devolatilization time increased linearly with the apparent wood density. Different char conversion rates may be a combining effect of pellet fragmentation, different char yields, and different material properties. During the devolatilization process, pine pellets showed better dimensional stability than beech pellets. Weaker inter-particle bonds in beech pellets resulted in a longitudinal expansion by up to 80% during devolatilization, while pine pellets expanded by up to 40% in longitudinal (press) direction. In addition, raw pine cubes shrank more than beech due to their different chemical structure, and the shrinking was larger in tangential direction

than in longitudinal direction. The results of the study suggest that the apparent wood density has a significant influence on the particle devolatilization behavior at suspension-fired conditions.

Keywords
Biomass; combustion; single pellet; swelling; shrinking

1. Introduction

In recent years, the use of pelletized woody biomass for energy generation has become more prevalent in Europe due to the '20-20-20' EU climate and energy targets [1]. The increasing production of heat and power from biomass in Europe has led to a high demand for industrial wood pellets imported mainly from the Baltic countries, Canada, and the US [2]. Usually, wood pellets are fired in suspension-fired power plants that were originally designed for firing coal. However, the combustion properties of coal differ from those of wood. Generally, wood pellets have lower heating value, lower ash content, higher volatile matter, and after size reduction, milled pellet particles are coarser and more irregular particles than coal [3]. These differences can affect the particle combustion behavior with respect to ignition, devolatilization, and char combustion, and thereby flame stability and particle burnout. Hence, understanding the fundamentals of wood particle combustion is crucial in the optimization of boiler performances.

Particles entering pulverized fuel-fired boilers are rapidly heated at high heating rates (> 10,000 K/s) and peak temperatures of up to 1600°C [4]. Comprehensive studies on biomass combustion characteristics are typically performed in single particle combustion setups or drop tube reactors at high temperatures [3,5–16]. These studies provide data on the conversion process of single biomass particles, including ignition, devolatilization, and char combustion. Generally, the char combustion is the most time-consuming step of the total conversion process. For that reason, fuel particles with rapid char combustion are desired for pulverized-fuel firing.

Single particle combustion experiments have been useful in understanding the key parameters that influence the particle conversion process. It is a question of how large wood particles can be for suspension firing, as large particles may cause problems concerning flame stability and unburned carbon in the ash. Studies have shown that large particles increase the char yield [5], and particles with a higher length-to-diameter

ratio heat more rapidly due to their larger surface area, resulting in faster conversion rates [3]. Momeni [3] also demonstrated that wood pellets comminuted in a roller mill and hammer mill showed similar conversion behaviors although roller-milled particles were much larger, which was attributed to the different specific particle surface areas. Furthermore, an increased oxygen concentration and increased temperature speed up the particle conversion process, thus shortening the devolatilization and burnout times. It is well known from coal and biomass combustion studies that the particle devolatilization time is strongly influenced by heat transfers (external and internal) and intrinsic pyrolysis kinetics [17–19]. The char conversion step may be controlled both by the diffusion (external and internal) of gas-phase species that react with the char (char-O_2, char-CO_2, char-H_2O, and char-H_2) and by the intrinsic heterogeneous kinetics [20–22]. While wood pellets are directly combusted in the as-received state in stoker boilers, pellets are milled and dried before combustion in suspension-fired boilers.

Several studies on single biomass particle combustion at suspension-fired conditions have been conducted using raw and torrefied particles (3-5 mm), which were exposed to an oxidizing atmosphere at high temperatures [5,8,16]. Linear relationships between devolatilization time and particle mass were reported by Lu et al. [5] for raw and torrefied wood particles of various sizes, and by Luo et al. [16] for wood species with different apparent densities. Lighter particles have a lower thermal capacity, and thus heat up and devolatilize faster [5]. Lu et al. [5] also showed that the char burnout time of raw and torrefied wood particles was strongly influenced by the char particle mass, and thereby by the char yield.

Only a few studies have investigated the influence of the pelletization process on the combustion behavior. The pelletization process increases the apparent (specific) wood density that may influence the combustion behavior. Some studies have investigated the combustion behavior of single wood pellets at furnace temperatures of 700 - 1000˚C [6,7,23]. In Biswas et al.'s study [6], only a very weak effect of the pellet density on char combustion time was observed. This may be because the combustion was controlled by the oxygen supply to the reactor, and not by local diffusion to the pellet, or that the intrinsic kinetics have controlled the conversion time. In the work of Rhén et al. [7], it is concluded that the pellet density, the pellet feedstock composition, and the char yield influence the char conversion time. The pellet feedstock particle size distribution (PSD) shows only a minor effect on the char combustion [23]. Hence,

different combustion behaviors may be achieved depending on the pelletization process and feedstock type. To the best of the authors' knowledge, no studies are evaluating the effect of pelletization pressure on the combustion characteristics of single wood pellets and their comparison with raw wood particles of similar sizes. Thus, this study investigates the combustion characteristics (devolatilization time, char conversion time, and swelling/shrinking) of raw and pelletized particles of beech and pine in a single particle combustion (SPC) reactor. The aim is to examine the influence of apparent density and pelletizing conditions on the combustion characteristics of wood.

2. Materials and methods

2.1 Materials

Raw materials were stem wood of European beech (*fagus sylvatica*) and Austrian pine (*pinus nigra*). Their chemical composition was determined elsewhere [24]. The net calorific value, elemental composition, and alkali content were analyzed in accordance with ISO standards. The proximate analysis was performed in a simultaneous thermal analyzer (type STA 409 PC, Netzsch GmbH, Germany). A wood sample (ca. 10 mg) was heated up to 110ºC in a nitrogen atmosphere at a heating rate of 10ºC/min. The temperature was maintained at 110ºC for 10 min to determine the moisture content. The temperature was then increased to 800°C and hold for 20 min to determine the volatile content. Afterwards, the sample was cooled down to 110°C. The ash content was then determined by heating the sample to 850°C in air.

2.2 Single particle preparation

Thin slices of wood were cut from the stem using a horizontal band saw. A hollow cubic-shaped die with a square cross-section of ca. 3.2x3.2 mm^2 was used to punch out wood cube samples. Different samples were taken in the radial direction (Fig. 19A), as the wood density was found to vary along the stem radius [25]. In total, 30 samples were prepared for each wood type. A 0.3 mm through-hole was drilled in the longitudinal direction of the cube to insert a tungsten-rhenium thermocouple wire, which also holds the particle in suspension during combustion in the SPC reactor. The moisture content of the single wood cubes was about 12 wt.% for beech and 17 wt.% for pine. Each wood particle was weighed on a microbalance (±0.01 mg). The average length of the raw pine and beech cubes was about 3.1±0.2 mm, while the cross-section

was about (3.2±0.2 x 3.2±0.2) mm^2. The particle density was then calculated from the particle mass and the particle dimensions measured by a caliper.

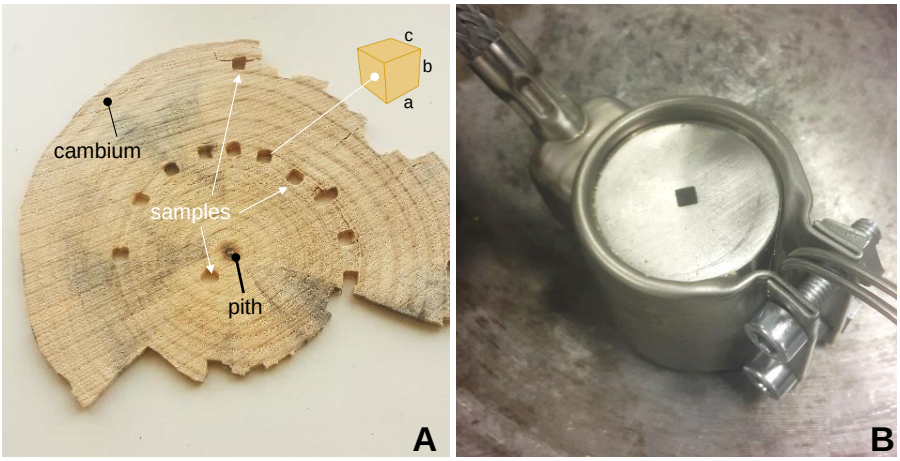

Fig. 19: Wood cubes punched out at different locations of a wood slice and definition of raw cube dimensions; a) tangential direction, b) longitudinal direction, and c) radial direction (A). Cubic die equipped with a heating cast (B).

2.3 Single pellet preparation

For the combustion in the SPC reactor, pellets were produced with dimensions of about 3x3x3 mm to compare their combustion behavior with the raw wood particles. To produce wood pellets of similar dimensions, a cubic metal die equipped with a heating cast was manufactured in-house (Fig. 19B). The finely hammer-milled wood sample was screened through sieves with a mesh opening of 0.25 and 0.50 mm. All over-sized wood particles (>0.50 mm) were removed, as they would cause problems feeding the die. Thus, only a narrow PSD (0.25-0.50 mm) was used for pelletizing. Generally, the pellet feedstock PSD has been found to have only a minor impact on the pellet conversion times [23]. Before pelletizing, the wood particles were kept for several days to be air-dried at ambient atmosphere. The moisture content of the particles before pelletizing was about 9 wt. %.

The cubic die consists of the following parts: a die with a square-hole cross-section (i.e., pressing area) of about 3.2x3.2 mm^2, a removable bottom part that functions as a

backstop, and a removable top part to compress the pellet. The compression of the raw material in the die is achieved by pressing, with a hydraulic press, the top metal part against the backstop. The compression force is measured using a 50 kN load cell. The die temperature is controlled using two thermocouples connected to a controller. A wood sample of about 0.030g ± 0.001g was fed into the die. As reported by Holm et al. [26], it is a valid assumption that the needle-like particles orient themselves perpendicular to the press channel in the die. Pellets were produced at die temperatures of 75 and 125°C and at compaction pressures of 100 and 200 MPa, which was held for 5 seconds. The pellet was then pressed out of the die by removing the backstop and using a long metal part. The pellet density right after the ejection was calculated from the measured dimensions and particle mass.

It was observed that pellets expanded in length after ejection from the die (i.e., after three days), which resulted in a reduction of their apparent densities. In the literature, this effect is called elastic spring-back [27,28]. It can be explained by the rheological behavior of the elastic wood fiber polymers (i.e., cellulose, hemicellulose, and lignin). These polymers tend to spring back to their original structure before compression if the bonds between adjacent particles within the pellet are too weak [27]. To avoid incorrect density values, only the relaxed pellet density measured right before the combustion tests was considered. A 0.3 mm through-hole was also drilled in the longitudinal press direction of the pellet to insert a tungsten-rhenium thermocouple wire for the combustion tests. Depending on the pellet expansion, the length of pine pellets was about 3.1±0.2 mm, while the length of beech pellets was about 3.2±0.3 mm. The cross-section of the pine and beech pellets was not affected by the rheological behavior of the wood polymers. A constant cross-section of about 3.2x3.2 mm^2 was measured for all pellets produced under the given conditions. The moisture content of the pellets produced was between 6 and 8 wt. %.

2.4 Experimental procedure

A laboratory scale SPC reactor consisting of a hydrogen-fired burner and a gas supply system are used in the combustion experiments. The same reactor has been used previously to investigate the combustion behavior of raw and torrefied wood particles [5,8,16] and the effect of operating conditions and size and shape of biomass particles on their combustion characteristics [3]. Descriptions of the experimental setup can be

found elsewhere [3,5]. The gas temperature, gas velocity, and oxygen concentration are adjustable, thus enabling conditions similar to industrial pulverized-fuel fired boilers. The reactor conditions were selected by regulating the flow rate of the inlet gases (i.e., H_2, O_2, N_2) to the metal burner. Mass flow controllers calibrated by a bubble flow meter are used to adjust the flow rates. The selected flow rates were as follows: 8.4 Nl/min for H_2, 5.4 Nl/min for O_2, and 22.3 Nl/min for N_2.

A suction pyrometer consisting of a Pt/Pt-Rh thermocouple is installed to measure the temperature at the center of the reactor, where the samples are combusted. The flue gas is sucked into the pyrometer with a flow of 3 l/min at about 4°C by a vacuum pump, which is attached to a condensate separator. The dried and air-cooled flue gases were then sent to a gas analyzer (type Rosemount™ NGA 2000, Emerson, USA), which measured the oxygen (O_2) concentration (d.b.). The gas analyzer is calibrated by performing two measurements on a known gas (i.e., CO). At the center of the reactor (i.e., where the sample is burnt), the temperature and O_2 concentration were recorded to be 1262°C (± 26°C) and around 5.0 vol.% (± 0.08%), respectively. The measured temperature is reasonably close to the temperature in large-scale pulverized-fuel boilers [29]. The O_2 concentration depends on the fuel/air mixture and flame position [13]. Thus, the measured O_2 may not be unusual [3].

Knowing the measured gas temperature and gas flow rates, the average gas flow velocity is calculated to be 1.52 m/s. The calculation is based on the ideal gas law. Assuming a fully developed, laminar flow profile in the reactor tube, the average velocity is half of the maximum velocity, which occurs at the centerline of the tube, i.e., where the sample is burnt. Thus, the maximum velocity around the sample was around 3 m/s. Based on stoichiometric calculations, the average O_2 concentration (d.b.) in the flue gas was 5.1 vol.%, which is close to the measured value (5.0 vol.%, d.b.). The theoretical atmosphere in which the wood samples are exposed to at the center of the reactor can then be determined to be 3.8 vol.% O_2 (w.b.) and 26.3 vol.% H_2O (w.b.).

After achieving steady-state reactor operating conditions, the combustion experiments could be initiated. First, a non-porous ceramic tube is introduced into the reactor to shield the sample from the hot gas flame, thus preventing particle ignition before reaching the reactor center position. Then, the wood sample held by a thin thermocouple wire is attached to a ceramic guide, which was then inserted from the opposite side of

the reactor through the protection tube to the reactor center. The protection tube is then rapidly withdrawn from the reactor, thus exposing the sample to the hot gas environment. The heat transfer from the tube to the sample can be neglected, as reported previously [3].

The entire particle conversion process was recorded by a high-quality camera (Stingray F-033B/F-033C, Allied Vision Technology GmbH, Germany). The camera was run at 84 frames per second. The camera was positioned perpendicular to the sample insertion port. Image post-processing allowed the determination of the characteristic particle conversion times, which were defined as described in [23]:

- *Devolatilization time:* the time a visible flame around the sample is seen, i.e., combustion of volatilized pyrolysis gases.
- *Char combustion time:* the time from the moment when the flame around the sample ceases (simultaneously, the sample begins glowing) until the sample stops glowing (and shrinking).
- *Total conversion time:* the sum of devolatilization and char combustion time.

2.5 Moisture content analysis

The moisture content of the wood samples was determined in a drying oven (at 105±2°C for 16 h) according to ISO 18134-1:2015. Based on the mass decrease during drying, the moisture content was calculated.

2.6 SEM analysis

Morphology analysis of the initial wood sample structure and the corresponding char samples was performed by SEM (type TM3000, Hitachi High Technologies America, USA). Chars were collected during the combustion experiments when the devolatilization was completed. Char particles were quickly ejected from the SPC reactor, water-cooled, and quenched by nitrogen.

3. Results and discussion

3.1 Beech and pine wood characterization

The results from the chemical and thermal analysis are summarized in Table 2. Both biomass fuels have comparable amounts of volatiles and fixed carbon and low ash contents. Pine has - as it is typical for softwoods - higher extractives and lignin content

than the hardwood beech. This may affect the pellet quality, as lignin acts as a natural binder [30] and extractives act as friction-reducing lubricants in the press channel [31]. The slightly higher carbon content in pine can explain its higher net calorific value. The higher potassium content in beech (860 mg/kg) may speed up the particle conversion rate compared to pine with lower potassium (630 mg/kg), as potassium was found to have a catalytic effect on the thermal decomposition of biomass [15]. The chemical composition of the remaining ash (inorganic) elements in the two biomasses are reasonably similar.

Table 13: Chemical composition of beech and pine.

Parameters	Unit	European beech	Austrian pine	Method/reference
Structural analysis				
Glucan	wt.%, d.b.	39.2	38.1	[24]
Hemicellulose	wt.%, d.b.	24.6	21.4	[24]
Klason lignin	wt.%, d.b.	23.4	24.8	[24]
Exhaustive extractives	wt.%, d.b.	1.7	11.9	[24]
Proximate analysis				
Moisture content	wt.%, ar	8.3	6.9	STA
Ash content	wt.%, d.b.	0.5	0.5	STA
Volatile matter	wt.%, d.b.	84.0	83.7	STA
Fixed carbon	wt.%, d.b.	15.5	15.8	By difference
Ultimate analysis				
Carbon	wt.%, d.b.	50.7	51.1	EN ISO 16948: 2015
Nitrogen	wt.%, d.b.	0.2	0.1	EN ISO 16948: 2015
Hydrogen	wt.%, d.b.	6.1	6.1	EN ISO 16948: 2015
Oxygen	wt.%, d.b.	42.4	42.0	EN 14588:2010
Net calorific value	MJ/kg, ar	17.5	18.0	EN 14918: 2009
Ash composition				
Aluminum	mg/kg	35	52	EN ISO 16967:2015 (ICP-OES)
Calcium	mg/kg	880	810	EN ISO 16967:2015 (ICP-OES)
Iron	mg/kg	200	66	EN ISO 16967:2015 (ICP-OES)
Potassium	mg/kg	860	630	EN ISO 16967:2015 (ICP-OES)
Magnesium	mg/kg	360	220	EN ISO 16967:2015 (ICP-OES)
Sodium	mg/kg	31	25	EN ISO 16967:2015 (ICP-OES)
Phosphorus	mg/kg	84	130	EN ISO 16967:2015 (ICP-OES)
Silicon	mg/kg	380	370	EN ISO 16967:2015 (ICP-OES)
Titanium	mg/kg	3	6	EN ISO 16967:2015 (ICP-OES)

3.2 Apparent density of raw and pelletized wood cubes

Fig. 12 shows the apparent densities of wood particles and pellets used in the combustion experiments. The single raw pine cube samples have significantly lower, but more homogenous apparent densities along the stem radius than the beech cubes. In particular, average densities of 770 (±55) kg/m3 for raw beech cubes and 420 (±23) kg/m3 for raw pine cubes were determined. The more complex structure of hardwood can probably explain the larger variation in density, while softwoods have a fairly regular cellular structure [32].

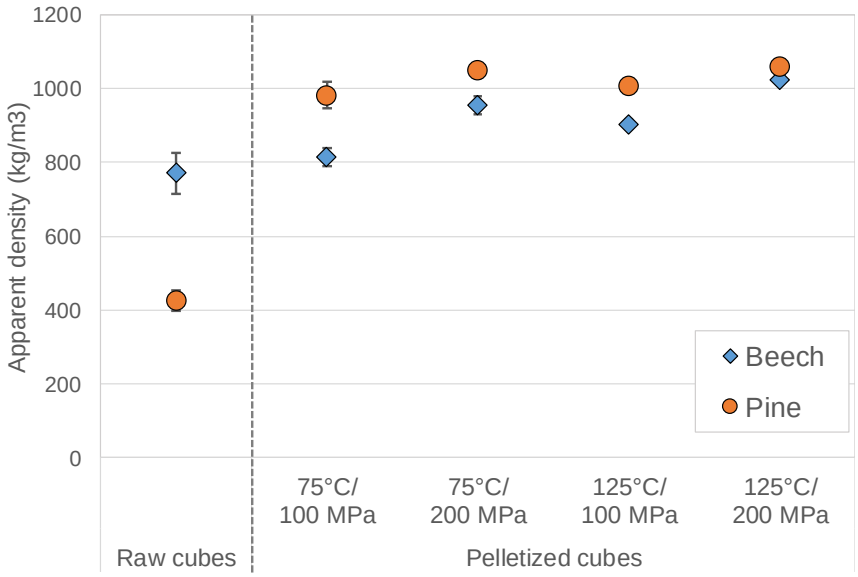

Fig. 20: Apparent densities of raw wood cubes and wood cubes produced under different pelletizing conditions.

The biomass type plays an important role during the pelletizing process. Pelletizing beech particles at 75°C and 100 MPa only slightly increased the density (by ca. 50 kg/m3) compared to raw beech cubes, but pelletizing pine particles increased the density (by ca. 560 kg/m3) compared to raw pine cubes (Fig. 12). The general trend is that pelletizing pine produces denser cubes than pelletizing beech under all pelletizing conditions tested. Similar findings were reported by Križan et al. [33], who investigated the density of briquettes produced from softwoods (pine and spruce) and hardwoods (beech and oak). They attributed the higher briquette density of softwoods to their

higher percentage of lignin and cellulose. However, the present study did not find significant differences in these components. Instead, the amount of extractives largely differs between both wood materials, i.e., pine has a sevenfold higher extractives amount than beech.

The higher extractives amount in pine probably enhances the binding of durable adjacent wood particles in the pellet, and thus the pellet density. The high die temperature and compaction pressure cause the softening of natural binders in wood, including organic extractives (e.g. fats) and lignin [34] and their migration to the pellet surface [35]. Their flow produces solid bridges between adjacent particles in the pellet [34], resulting in larger adhesive strengths [36]. Stronger adhesion between particles reduces the risk of pellet expansion (i.e., spring-back). Probably because of a larger spring-back, beech pellets are slightly larger than pine pellets, as mentioned previously. When the compaction pressure is released and the pellet is ejected from the hot die, stronger solid bridges are formed between pine particles during cooling compared to pellets produced from beech particles. The SEM micrographs of the pellet structure in radial direction show smaller gaps between pine pellet particles compared to beech pellet particles at similar pelletizing conditions (Fig. 15c-f). The smaller gaps confirm better adhesion and stronger solid bridges between pine particles, which is important in obtaining high unit densities and reducing pellet expansion.

The effect of the die temperature and compaction pressure on the apparent density is presented in Fig. 12. Overall, pellets produced from pine had individual densities varying from 980 to 1060 kg/m3, while beech pellets had densities varying from 815 to 1020 kg/m3. The results show that beech and pine pellets produced at the highest temperature and pressure (125°C and 200 MPa) result in the highest apparent densities. An increase in compaction pressure from 100 to 200 MPa leads to a larger increment of density (120-140 kg/m3 for beech and 55-65 kg/m3 for pine) than an increase in the die temperature from 75 to 125°C (70-80 kg/m3 for beech and 10-25 kg/m3 for pine). This indicates that the compaction pressure has a greater influence on the pellet density than the die temperature. The changes in the pelletizing conditions have a greater impact on pine compared to beech. The positive effect of increasing the compaction pressure and the die temperature on the apparent density of compacted woody biomass corroborates previous findings [31,33,37]. It has to be stated that a lower die aspect

ratio (i.e., the ratio of die channel length to diameter) for pelletizing beech compared to pine is considered to improve the quality of beech pellets [26].

3.3 Combustion characteristics

3.3.1 Video analysis

The total conversion process of a single raw beech cube (811 kg/m3) and a pelletized beech cube (821 kg/m3) in the SPC reactor is illustrated in sequence in Table 14. Based on the video sequences from the particle combustion experiments, the devolatilization and char combustion (glowing and shrinking) are identified. After removing the protection tube, the cubes are exposed to the hot gas environment, which induces rapid heating and drying. Gaseous volatile components are then released. The ignition of the volatiles produces a visible flame around the cube. The bright glowing of the cube bottom during devolatilization may indicate the depletion of gaseous volatile components and the beginning of char combustion on the cube bottom. After the extinction of the volatile flame, the char combusts long-lastingly and heterogeneously, glowing and shrinking. The end of shrinking defines the end of char combustion. After char combustion some of the ash residue remains. The ignition time was not quantified in the present study due to the large uncertainty in interpreting the ignition times. It was shown that single wood particles ignite very quickly (<0.6 s) under similar reactor conditions, but with a large scatter in the data [8]. It is not clear if particles are ignited by homogeneous or heterogeneous ignition [38].

Generally, the particle surface area-to-volume ratio influences the external heat transfer and diffusion of oxygen, and thus influence the particle conversion times [3]. Due to the nature of sample preparation, small variations in the dimensions of raw and pelletized wood cubes were inevitable. Momeni [3] showed that particles with a higher surface area-to-volume ratio (but similar mass) will convert faster. However, this effect can be neglected in the present study, as raw and pelletized wood cubes show nearly identical surface area-to-volume ratios prior to combustion.

The combustion behavior of pelletized wood cubes was very different from that of raw wood cubes. During devolatilization, the pelletized wood cubes swelled considerably, while the raw wood cubes shrank compared to the initial cube dimensions (Table 14). While the shrinking of raw wood particles during devolatilization was repeatedly reported by several authors [39–42], only one study observed the swelling of pellets

produced in a single die pelletizer by means of SEM analysis [6]. In the present study, the cubic shape allows to quantify the shrinking/swelling behavior in longitudinal and tangential direction. Based on the video footage, the initial cube dimensions were compared to the cube dimensions after devolatilization. Shrinking/swelling in radial direction could not be measured. During char combustion, the wood pellets fragmented into their constituent particles, while no fragmentation took place of the raw wood cubes (Table 14). The fragmentation of pellets may affect the char combustion times.

Table 14: Total conversion process of a raw and pelletized beech cube in the SPC reactor (1262°C, 5.0 vol.% O_2, 1.5 m/s gas velocity), including their residence times.

	Heating and drying (<1s)	Devolatilization	Devolatilization end	Char combustion (glowing)	Char combustion (shrinking)	Ash residue
Single raw beech cube (811 kg/m3)	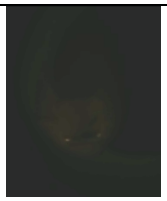		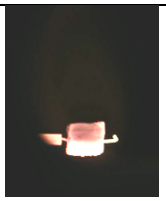		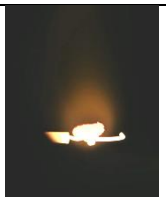	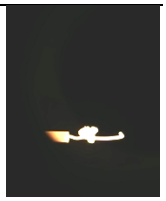
	0.00 s	4.59 s	6.73 s	12.33 s	23.24 s	27.83 s
Single pelletized beech cube (821 kg/m3)	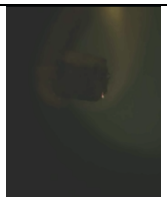	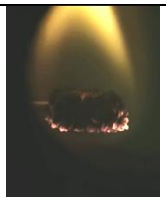	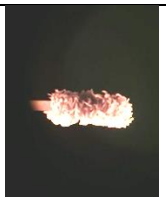	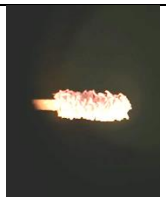	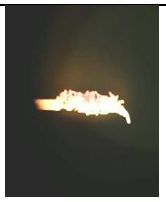	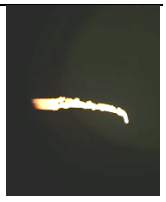
	0.00 s	4.21 s	7.07 s	9.98 s	15.58 s	20.63 s

3.3.2 Shrinking behavior of raw wood during devolatilization

The shrinking of raw cubes cannot be attributed to the evaporation of moisture, as the tested cubes have a considerably low moisture content before the combustion experiments. For raw wood cubes, the reduction in longitudinal (or fiber) direction was smaller than in tangential direction (Fig. 14). This phenomenon during wood pyrolysis was also observed by other authors [39,43]. While raw pine cubes shrank in longitudinal direction in the range of 12-14%, the shrinking in tangential direction was between 22 and 26%. On the other hand, the shrinking of raw beech cubes in longitudinal direction

was in the range of 6-10 % and between 16 and 19 % in tangential direction. Byrne and Nagle [41] showed that shrinking depends on the direction due to the wood anisotropy, which corroborates the findings in this study. Generally, the raw cubes will lose weight rapidly in the SPC reactor due moisture evaporation and devolatilization. The wood microstructure is composed of cellulose microfibrils embedded in a hemicellulose-lignin matrix [43]. The shrinking in longitudinal direction may then be explained by the decomposition of cellulose microfibrils, which are highly aligned parallel to the longitudinal cell axis [41]. The tangential shrinking is probably due to the decomposition of the hemicellulose and lignin components [39].

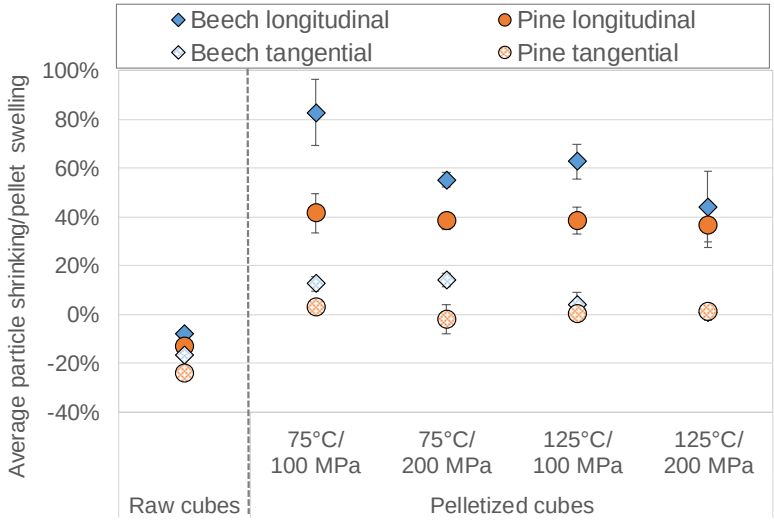

Fig. 21: Average swelling of pine and beech pellets during devolatilization in the SPC reactor. Error bars indicate the first standard deviation from the mean, and they are displayed when greater than the data symbol.

The larger shrinking in both directions of raw pine cubes compared to beech can be explained by differences in the hemicellulose content between pine and beech. It was reported that hemicellulose promotes a rigid char structure in the pyrolyzed solid [43]. Shen et al. [43] observed that birch (hardwood) samples, due to their higher hemicellulose content than pine (softwood) samples, were more difficult to change the structure. Hence, in the present study, the larger content of hemicellulose in beech (cf. Table 2) probably leads to a more rigid char structure and hence a better dimensional stability compared to pine indicated by a smaller beech shrinking.

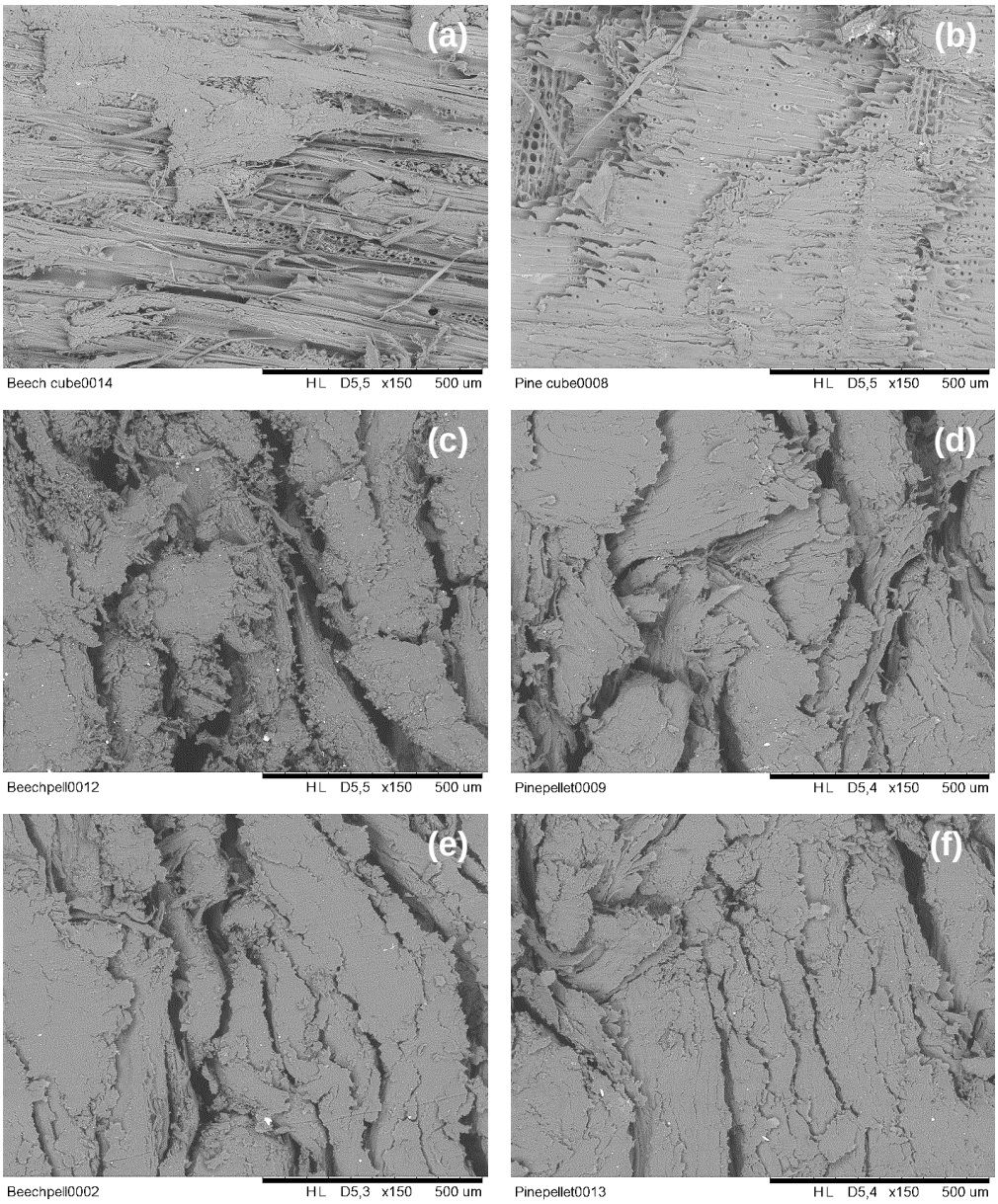

Fig. 22: Scanning electron micrographs of the original structure of (a) raw beech cube, (b) raw pine cube, (c) pelletized beech cube (75°C and 100 MPa), (d) pelletized pine cube (75°C and 100 MPa), (e) pelletized beech cube (125°C and 200 MPa), and (f) pelletized pine cube (125°C and 200 MPa). Raw cubes are shown in tangential section and pellets in radial section.

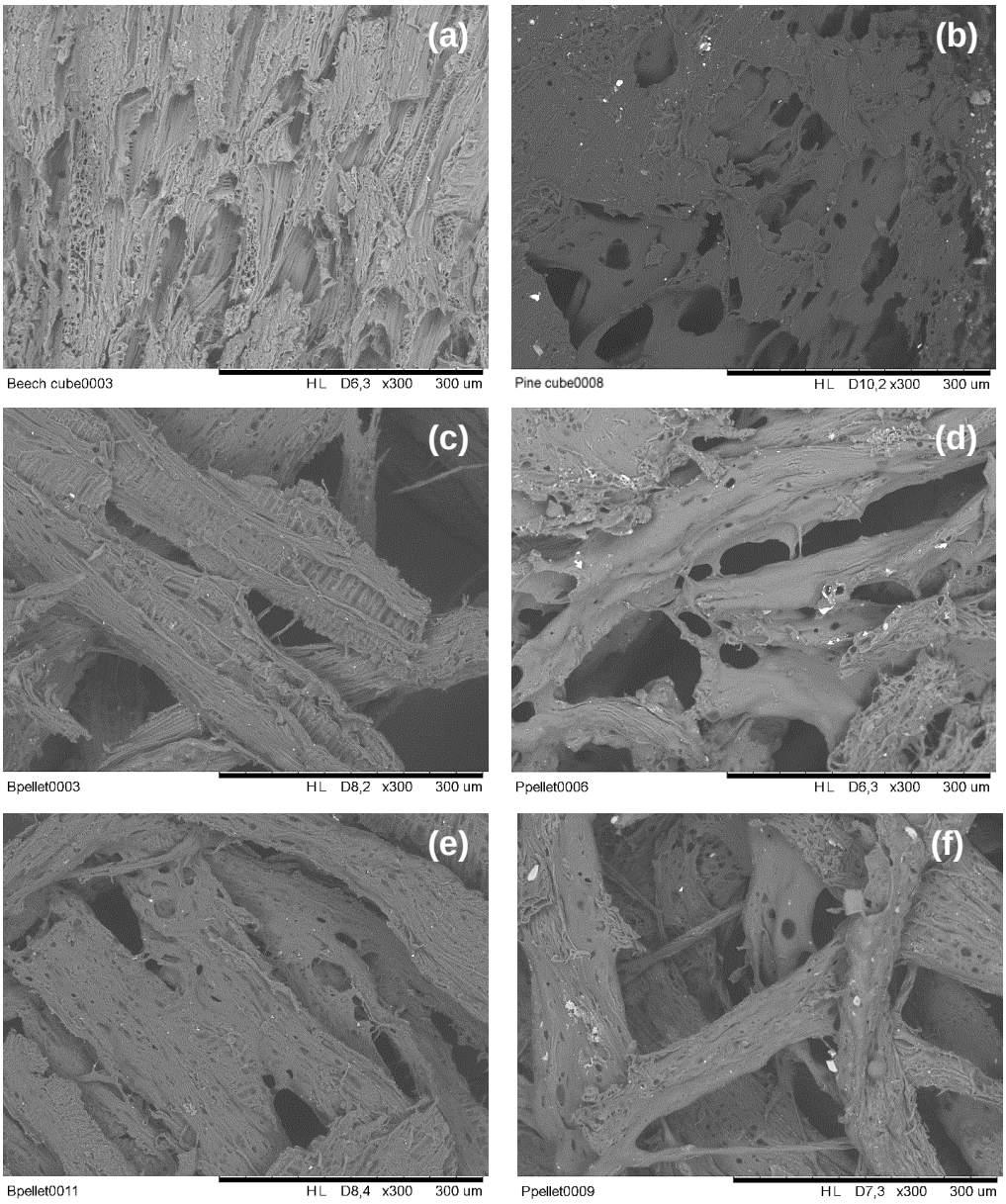

Fig. 23: Scanning electron micrographs of the char structure of (a) raw beech cube, (b) raw pine cube, (c) pelletized beech cube (75°C and 100 MPa), (d) pelletized pine cube (75°C and 100 MPa), (e) pelletized beech cube (125°C and 200 MPa), and (f) pelletized pine cube (125°C and 200 MPa). Raw cubes are shown in tangential section and pellets in radial section.

Based on the SEM analysis, different char structures from the raw pine and beech cubes were observed (Fig. 23a and b). Compared to the parent fuel (Fig. 15b), the char from raw pine cubes tended to develop larger pores formed due to the rapid release of volatile matter. On the other hand, in beech char, the structure of the parent fuel (Fig. 15a) was still recognizable. Knowledge of the wood pore structure is directly linked to the density, stability, permeability, and thermal properties of wood [44]. Hence, the pore structure may affect the combustion process. Detailed knowledge about the char morphology at suspension-fired conditions can improve the understanding and modelling of the particle combustion process.

3.3.3 Swelling behavior of pellets during devolatilization

The swelling of pelletized beech and pine cubes during devolatilization is also shown in Fig. 14. Pellets largely expanded in the longitudinal press direction (ca. 40-80%), while the expansion in tangential direction was rather small (ca. 0-15%), especially for pine pellets. This indicates that the bonding between particles inside the pellet (e.g., by adhesion, mechanical interlocking, and solid bridges) appears to be stronger in tangential (and presumably radial) direction than in longitudinal press direction. The rapid release of gaseous volatile components may cause high mechanical stress (and internal pressure) on the longitudinal direction. Furthermore, the material strength decreases because of the pyrolysis process. As a result, the bonds between internal pellet particles break, leading to the expansion of the pellet structure and subsequent pellet fragmentation during char combustion.

The general trend is that beech pellets swell more than pine pellets during devolatilization, which confirms the weaker inter-particle bonding strengths produced during beech pellet production, as mentioned previously. Moreover, different pelletizing conditions seem to affect the pellet swelling behavior. At the least severe conditions (75°C and 100 MPa), the average swelling in both cube directions was largest for both biomasses, while it was smallest for the most severe conditions (125°C and 200 MPa). The latter conditions seem to produce stronger bonds between particles, which reduces the swelling behavior during pyrolysis.

SEM micrographs of the char of pelletized beech and pine cubes produced at similar conditions are shown in Fig. 23c-f. Pelletized cube chars have lost all features of the parent pellet structure (Fig. 15c-f). The swelling of the pellets during pyrolysis breaks

bonds between wood particles, causing larger inter-particle gaps within the pellet structure. It is also observed that the pyrolysis process causes some plastic deformation due to melting of the wood particles, and this is mostly pronounced for charred pine pellet particles (Fig. 23d and f). However, in some charred beech pellet particles (Fig. 23c), the parent beech wood structure was still recognizable. Moreover, particles in pelletized beech cubes produced at 125°C and 200 MPa seem to be closer attached to each other than at less severe pelletizing conditions (i.e., 75°C and 100 MPa) due to different magnitude of the inter-particle bonding strengths.

3.3.4 Devolatilization time

In Fig. 24A, the devolatilization times of raw wood cubes and wood pellets produced under different conditions are compared. A strong linear correlation between devolatilization time and apparent cube density is shown (R^2=0.87). This concurs well with observations made by Lu et al. [5], who studied the devolatilization of raw and torrefied wood particles of similar sizes, but different apparent densities. They also observed a strong correlation between particle density and devolatilization time. In the present study, the apparent cube density and cube mass are well correlated (r=0.94, $p<0.05$). Different pelletizing conditions had a larger influence on the beech pellet than the pine pellet densities and therefore a larger spread in beech devolatilization times was observed (Fig. 24A).

3.3.5 Fragmentation of pellets during char combustion

Table 15a and b illustrate the char combustion process for a pine pellet (1035 kg/m3) and beech pellet (1030 kg/m3) both produced at 125°C and 200 MPa. Table 15c and d illustrate the char combustion process for a beech pellet (821 kg/m3) produced at 75 °C and 100 MPa and a raw beech cube (811 kg/m3). It is seen that the charred wood pellets underwent some fragmentation, while the charred raw wood showed no fragmentation. Different pelletizing conditions led to different degrees of fragmentation (cf. Table 15b and c). In case of beech, the pellets produced at the least severe conditions (75°C and 100 MPa) showed a higher degree of fragmentation compared to pellets produced at the most severe conditions (125°C and 200 MPa). The latter conditions probably produced stronger inter-particle bonds in pellets, promoting a better dimensional stability during char combustion. Furthermore, differences in the pellet feedstock composition cause different degrees of fragmentation. Although the pine and beech

pellet (Table 15a and b, respectively) were produced under same conditions, the pine pellet showed a lower degree of fragmentation and higher dimensional stability. Thus, pelletizing pine appears to produce stronger inter-particle bonds in pine pellets. Consequently, the weaker inter-particle bonds in beech pellets facilitate a higher degree of fragmentation during char combustion. The different degrees of fragmentation may influence the char combustion time.

3.3.6 Char combustion time

Fig. 24B presents the char combustion times of raw and pelletized wood cubes. It is seen that the char combustion process is the most time-consuming step of the total wood cube conversion process. In the present study, the char combustion is about two to three times the devolatilization time. The experimental results show a weak correlation (R^2=0.53) between the char combustion time and the apparent density of the raw and pelletized wood cubes. Lu et al. [5] reported a strong relationship between mass of char particles (char yield) and the char combustion times for raw and torrefied wood spheres. However, in the present study, it was not possible to determine accurately the char yields after the devolatilization process.

Fig. 24B also shows that beech pellets had shorter char combustion times than pine pellets. As mentioned previously, beech pellets fragmented more during char combustion than pine pellets. The higher degree of fragmentation of beech pellets may considerably decrease the char combustion time. However, currently, it is not clear what causes the differences in char combustion times between the pellets. It may be differences in pellet swelling during devolatilization, the different degree of fragmentation during char combustion, the char yields or differences in the chemical wood composition. Besides the difference in pellet structure, also the higher potassium content in beech may act as a catalyst for the char combustion process [15].

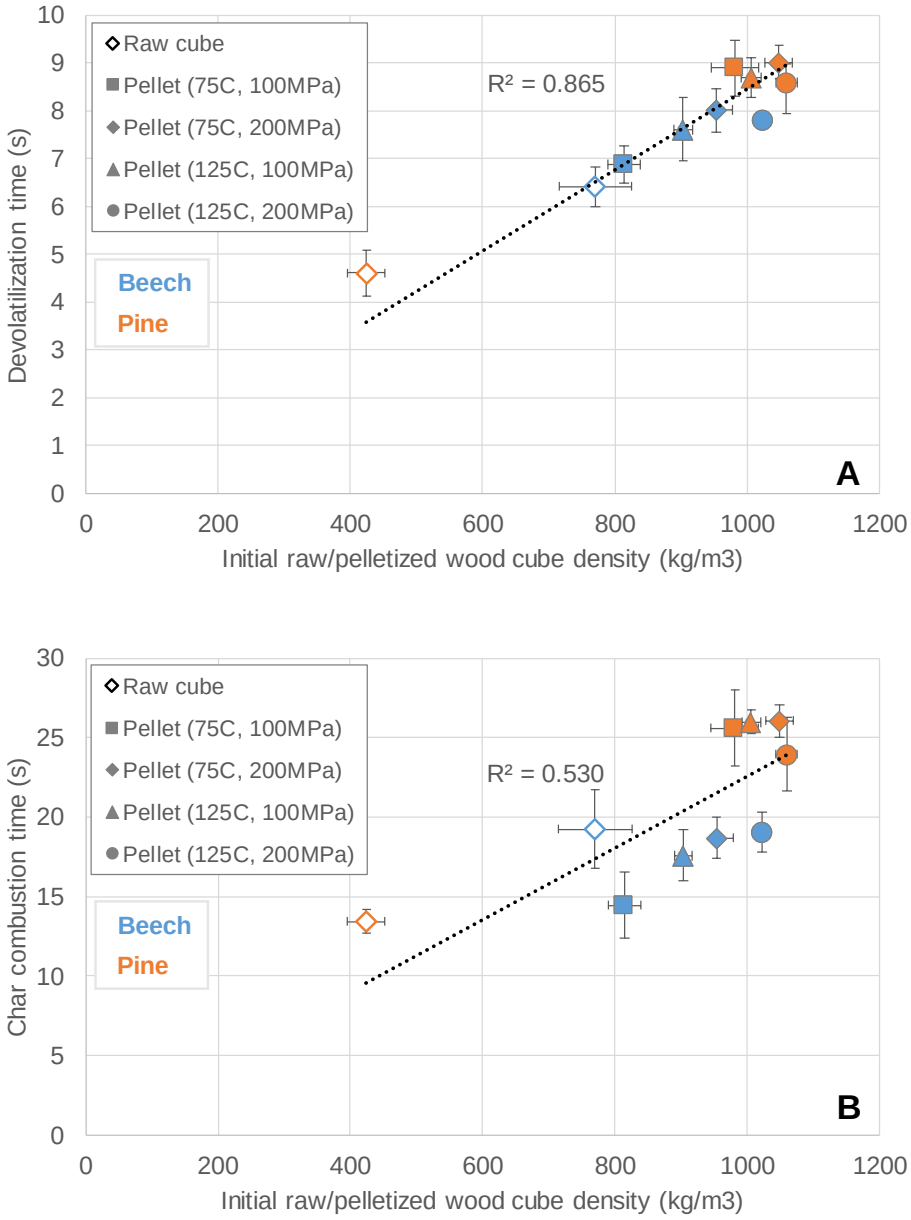

Fig. 24: Devolatilization time (A) and char combustion time (B) of raw and pelletized wood cubes as a function of the initial apparent wood cube density. SPC reactor conditions: 1262°C, 5.0 vol.% O_2, and 1.5 m/s gas velocity.

Table 15: Char combustion process of (a) pelletized pine cube (1035 kg/m3), (b) pelletized beech cube (1030 kg/m3), (c) pelletized beech cube (821 kg/m3), and (d) raw beech cube (811 kg/m3).

Begin of char combustion	5 sec in char combustion	10 sec in char combustion	15 sec in char combustion
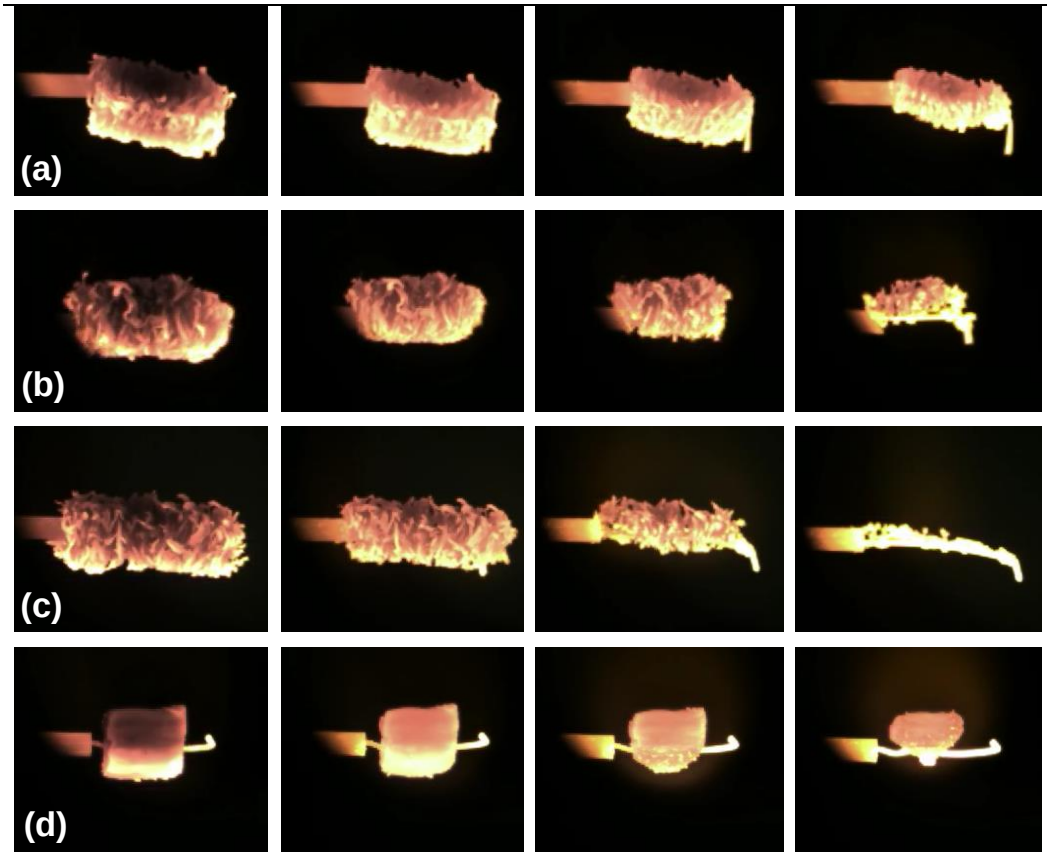			

4. Conclusions

In this paper, the thermal conversion behavior of single particles of raw and pelletized beech and pine wood cubes was investigated in a single particle combustion reactor. This is the first study to describe and compare the combustion behavior of raw and pelletized wood of different apparent densities at suspension-firing conditions. The following conclusions can be drawn from the experimental study:

- Increasing the pelletizing pressure has a stronger effect on the apparent wood density than increasing the pelletizing temperature. Pelletizing pine leads to a better pellet quality than beech indicated by stronger inter-particle bonds that lead to higher dimensional stability and higher apparent densities.
- The apparent density of raw and pelletized wood has a strong influence on the devolatilization times. The char combustion time is the most time-consuming step of the total particle conversion process.
- During devolatilization, raw wood shrinks (especially in tangential direction), while inter-particle bonds in pellets break, causing significant pellet swelling (especially in the press direction).
- Wood pellets fragment during char combustion compared to raw wood. Pellet fragmentation was more pronounced for beech pellets indicating weaker inter-particle bonds in beech pellets. The fragmentation probably has some effect on the char combustion times.
- Further experimental studies are needed to gain knowledge about the char yield and char reactivity, which are important measures for the combustion performance.

Nomenclature

CO_2	carbon dioxide
d.b.	dry basis
H_2	hydrogen
H_20	water
N_2	nitrogen
Nl	normal liter
O_2	oxygen
PSD	particle size distribution
Pt	platinum
Rh	rhodium
SEM	scanning electron microscope
SPC	single particle combustion
STA	simultaneous thermal analysis

T_g	glass transition temperature
TGA	thermogravimetric analysis
w.b.	wet basis
wt.%	weight percent

Acknowledgements

The authors thank Energiteknologiske Udviklings- og Demonstrationsprogram (EUDP) for the financial support received as part of the ForskEL project "AUWP – Advanced Utilization of Wood Pellets" (Project number: 12325).

References

[1] R. Sikkema, M. Steiner, M. Junginger, W. Hiegl, M.T. Hansen, A. Faaij, The European wood pellet markets: current status and prospects for 2020, Biofuels, Bioproducts and Biorefining. 5 (2011) 250–278. doi:10.1002/bbb.277.

[2] C. Verhoest, Y. Ryckmans, Industrial Wood Pellets Report, (2014) 29. doi:IEE/10/463/SI2.592427.

[3] M. Momeni, Fundamental study of single biomass particle combustion (PhD thesis), Aalborg University, Denmark, (2012).

[4] J.R. Gibbins, J. Williamson, Advances in laboratory tests for predicting coal-related combustion problems, Proceedings of the Institution of Mechanical Engineers, Part A: Journal of Power and Energy. 212 (1998) 13–26. doi:10.1243/0957650981536709.

[5] Z. Lu, J. Jian, P.A. Jensen, H. Wu, P. Glarborg, Influence of Torrefaction on Single Particle Combustion of Wood, Energy and Fuels. 30 (2016) 5772–5778. doi:10.1021/acs.energyfuels.6b00806.

[6] A.K. Biswas, M. Rudolfsson, M. Broström, K. Umeki, Effect of pelletizing conditions on combustion behaviour of single wood pellet, Applied Energy. 119 (2014) 79–84. doi:10.1016/j.apenergy.2013.12.070.

[7] C. Rhén, M. Öhman, R. Gref, I. Wästerlund, Effect of raw material composition in woody biomass pellets on combustion characteristics, Biomass and Bioenergy. 31 (2007) 66–72. doi:10.1016/j.biombioe.2006.06.016.

[8] Z. Lu, J. Jian, P. Arendt Jensen, H. Wu, P. Glarborg, Impact of KCl impregnation on single particle combustion of wood and torrefied wood, Fuel. 206 (2017) 684–689. doi:10.1016/j.fuel.2017.05.082.

[9] J. Riaza, R. Khatami, Y.A. Levendis, L. Álvarez, M. V Gil, C. Pevida, F. Rubiera, J.J. Pis, Combustion of single biomass particles in air and in oxy-fuel conditions, Biomass and Bioenergy. 64 (2014) 162–174. doi:10.1016/j.biombioe.2014.03.018.

[10] J. Riaza, J. Gibbins, H. Chalmers, Ignition and combustion of single particles of coal and biomass, Fuel. 202 (2017) 650–655. doi:10.1016/j.fuel.2017.04.011.

[11] C. Yin, M. Momeni, S.K. Kær, P. Due, J. Vej, Physical and combustion characteristics of biomass particles prepared by different milling processes for suspension firing in utility boilers, (2016).

[12] M. Flower, J. Gibbins, A radiant heating wire mesh single-particle biomass combustion apparatus, Fuel. 88 (2009) 2418–2427. doi:10.1016/j.fuel.2009.02.036.

[13] P.E. Mason, L.I. Darvell, J.M. Jones, M. Pourkashanian, A. Williams, Single particle flame-combustion studies on solid biomass fuels, Fuel. 151 (2015) 21–30. doi:10.1016/j.fuel.2014.11.088.

[14] M. Phanphanich, Pelleting Characteristics of Torrefied Forest Biomass (Master's thesis), University of Georgia, USA, (n.d.).

[15] P.E. Mason, L.I. Darvell, J.M. Jones, A. Williams, Observations on the release of gas-phase potassium during the combustion of single particles of biomass, Fuel. 182 (2016) 110–117. doi:10.1016/j.fuel.2016.05.077.

[16] H. Luo, Z. Lu, J. Jian, H. Wu, P.A. Jensen, P. Glarborg, Devolatilization of wood and torrefied wood with different apparent density: Experimental and modelling study, in: The Joint Meeting of the Polish and Scandinavian-Nordic Sections of the Combustion Institute, 2018.

[17] J.M. Johansen, P.A. Jensen, P. Glarborg, M. Mancini, R. Weber, R.E. Mitchell, Extension of apparent devolatilization kinetics from thermally thin to thermally thick particles in zero dimensions for woody biomass, Energy. 95 (2016) 279–

290. doi:10.1016/j.energy.2015.11.025.

[18] C. Branca, C. Di Blasi, Global Kinetics of Wood Char Devolatilization and Combustion, Energy & Fuels. 17 (2003) 1609–1615. doi:10.1021/ef030033a.

[19] B. Yan, Y. Cheng, P. Xu, C. Cao, Y. Cheng, Generalized Model of Heat Transfer and Volatiles Evolution Inside Particles for Coal Devolatilization, American Institute of Chemical Engineers Journal. 60 (2014) 2893–2906. doi:10.1002/aic.

[20] J. Xu, L. Qiao, Mathematical modeling of coal gasification processes in a well-stirred reactor: Effects of devolatilization and moisture content, Energy and Fuels. 26 (2012) 5759–5768. doi:10.1021/ef3008745.

[21] D.G. Roberts, D.J. Harris, A Kinetic Analysis of Coal Char Gasification Reactions at High Pressures, Energy & Fuels. 20 (2006) 2314–2320. doi:10.1021/ef060270o.

[22] N.M. Laurendeau, Heterogeneous kinetics of coal char gasification and combustion, Progress in Energy and Combustion Science. 4 (1978) 221–270. doi:10.1016/0360-1285(78)90008-4.

[23] D. Bergström, S. Israelsson, M. Öhman, S.A. Dahlqvist, R. Gref, C. Boman, I. Wästerlund, Effects of raw material particle size distribution on the characteristics of Scots pine sawdust fuel pellets, Fuel Processing Technology. 89 (2008) 1324–1329. doi:10.1016/j.fuproc.2008.06.001.

[24] M. Masche, M. Puig-Arnavat, P.A. Jensen, J.K. Holm, S. Clausen, J. Ahrenfeldt, U.B. Henriksen, From wood chips to pellets to milled pellets: the mechanical processing pathway of Austrian pine and European beech. Manuscript submitted for publication, (n.d.).

[25] P. Horáček, M. Fajstavr, M. Stojanović, The variability of wood density and compression strength of Norway spruce (Picea abies/L./Karst.) within the stem, Beskydy. 10 (2017) 17–26. doi:10.11118/beskyd201710010017.

[26] J.K. Holm, U.B. Henriksen, J.E. Hustad, L.H. Sørensen, Toward an understanding of controlling parameters in softwood and hardwood pellets production, Energy and Fuels. 20 (2006) 2686–2694. doi:10.1021/ef0503360.

[27] Z. Fang, Pretreatment Techniques for Biofuels and Biorefineries (Green Energy and Technology), Springer, 2013. doi:10.2174/97816080528511060101.

[28] W. Stelte, Fuel pellets from biomass - Processing, bonding, raw materials (PhD thesis), Technical University of Denmark, Denmark, (2011).

[29] J. Utt, R. Giglio, F. Wheeler, Technology comparison of CFB versus pulverized-fuel firing for utility power generation, (2011) 91–99. doi:10.1016/j.medengphy.2011.06.017.

[30] P.C.A. Bergman, H.J. Veringa, Combined torrefaction and pelletisation, ECN Biomass. (2005) 29.

[31] W. Stelte, J.K. Holm, A.R. Sanadi, S. Barsberg, J. Ahrenfeldt, U.B. Henriksen, Fuel pellets from biomass: The importance of the pelletizing pressure and its dependency on the processing conditions, Fuel. 90 (2011) 3285–3290. doi:10.1016/j.fuel.2011.05.011.

[32] G. Prokopski, Investigation of wood fracture toughness using mode II fracture (shearing), Journal of Materials Science. 30 (1995) 4745–4750. doi:10.1007/BF01153088.

[33] P. Križan, L. Šooš, M. Matúš, I. Onderova, D. Vukelic, Difference Between Compacting of Softwood and Hardwood, in: Scientific Proceedings 2009: Faculty of Mechanical Engineering, STU in Bratislava, Slovakia, 2009: pp. 1–7.

[34] N. Kaliyan, R.V. Morey, Natural binders and solid bridge type binding mechanisms in briquettes and pellets made from corn stover and switchgrass, Bioresource Technology. 101 (2010) 1082–1090. doi:10.1016/j.biortech.2009.08.064.

[35] W. Stelte, A.R. Sanadi, L. Shang, J.K. Holm, J. Ahrenfeldt, U.B. Henriksen, Recent developments in biomass pelletization – a review, 7 (2012) 4451–4490.

[36] W. Stelte, J.K. Holm, A.R. Sanadi, S. Barsberg, J. Ahrenfeldt, U.B. Henriksen, A study of bonding and failure mechanisms in fuel pellets from different biomass resources, Biomass and Bioenergy. 35 (2011) 910–918. doi:10.1016/j.biombioe.2010.11.003.

[37] P. Križan, M. Matúš, M. Svátek, J. Beniak, M. Lisý, Determination of Compacting Pressure and Pressing Temperature Impact on Biomass Briquettes Density and Their Mutual Interactions, in: 14th International Multidisciplinary Scientific GeoConference SGEM 2014 on Energy and Clean Technologies, 2014: pp. 133–140. doi:10.5593/SGEM2014/B41/S17.018.

[38] T. Grotkjær, K. Dam-Johansen, A.D. Jensen, P. Glarborg, An experimental study of biomass ignition, Fuel. 82 (2003) 825–833. doi:10.1016/S0016-2361(02)00369-1.

[39] K.O. Davidsson, J.B.C. Pettersson, Birch wood particle shrinkage during rapid pyrolysis, Fuel. 81 (2002) 263–270. doi:10.1016/S0016-2361(01)00169-7.

[40] M. Dall'Ora, A.D. Jensen, P.A. Jensen, Reactivity and burnout of wood fuels (PhD thesis), Technical University of Denmark, Denmark, (2011).

[41] C.E. Byrne, D.C. Nagle, Carbonized wood monoliths characterization, Carbon. 35 (1997) 267–273. doi:10.1016/S0008-6223(96)00135-2.

[42] K. Umeki, K. Kirtania, L. Chen, S. Bhattacharya, Fuel Particle Conversion of Pulverized Biomass during Pyrolysis in an Entrained Flow Reactor, Industrial & Engineering Chemistry Research. 51 (2012) 13973–13979. doi:10.1021/ie301530j.

[43] D.K. Shen, S. Gu, K.H. Luo, A. V. Bridgwater, Analysis of Wood Structural Changes under Thermal Radiation, Energy and Fuels. 23 (2009) 1081–1088. doi:10.1021/ef800873k.

[44] W.D. Ding, A. Koubaa, A. Chaala, T. Belem, C. Krause, Relationship between wood porosity, wood density and methyl methacrylate impregnation rate, Wood Material Science and Engineering. 3 (2008) 62–70. doi:10.1080/17480270802607947.

Department of Chemical and Biochemical Engineering - CHEC
Technical University of Denmark

Søltofts Plads, Building 229
2800 Kgs. Lyngby
Denmark
Phone: +45 45 25 28 00

www.kt.dtu.dk